NOTICE

The quality of this microform is heavily dependent upon the quality of the original thesis submitted for microfilming. Every effort has been made to ensure the highest quality of reproduction possible.

If pages are missing, contact the university which granted the degree.

Some pages may have indistinct print especially if the original pages were typed with a poor typewriter ribbon or if the university sent us an inferior photocopy.

AVIS

La qualité de cette microforme dépend grandement de la qualité de la thèse soumise au microfilmage. Nous avons tout fait pour assurer une qualité supérieure de reproduction.

S'il manque des pages, veuillez communiquer avec l'université qui a conféré le grade.

La qualité d'impression de certaines pages peut laisser à désirer, surtout si les pages originales ont été dactylogra phiées à l'aide d'un ruban usé ou si l'université nous a fait parvenir une photocopie de qualité inférieure.

Canada

THE UNIVERSITY OF ALBERTA

SHEAR STRENGTH OF HYDRAULICALLY PLACED CLAY SHALE

by

DANIEL WAYNE MIMURA $\copyright$

A THESIS

SUBMITTED TO THE FACULTY OF GRADUATE STUDIES AND RESEARCH

IN PARTIAL FULFILMENT OF THE REQUIREMENTS FOR THE DEGREE

OF MASTER OF SCIENCE

DEPARTMENT OF CIVIL ENGINEERING

EDMONTON, ALBERTA

SPRING, 1990

NOTICE

AVIS

The quality of this microform is heavily dependent upon the quality of the original thesis submitted for microfilming. Every effort has been made to ensure the highest quality of reproduction possible.

If pages are missing, contact the university which granted the degree.

Some pages may have indistinct print especially if the original pages were typed with a poor typewriter ribbon or if the university sent us an inferior photocopy.

La qualité de cette microforme dépend grandement de la qualité de la thèse soumise au microfilmage. Nous avons tout fait pour assurer une qualité supérieure de reproduction.

S'il manque des pages, veuillez communiquer avec l'université qui a conféré le grade.

La qualité d'impression de certaines pages peut laisser à désirer, surtout si les pages originales ont été dactylographiées à l'aide d'un ruban usé ou si l'université nous a fait parvenir une photocopie de qualité inférieure.
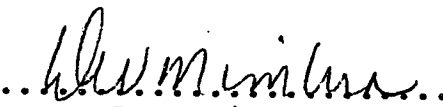
Canada

THE UNIVERSITY OF ALBERTA

RELEASE FORM

NAME OF AUTHOR: DANIEL WAYNE MIMURA

TITLE OF THESIS: SHEAR STRENGTH OF HYDRAULICALLY PLACED CLAY SHALE

DEGREE: MASTER OF SCIENCE

YEAR THIS DEGREE GRANTED: SPRING, 1990

Permission is hereby granted to THE UNIVERSITY OF ALBERTA LIBRARY to reproduce single copies of this thesis and to lend or sell such copies for private, scholarly or scientific research purposes only.

The author reserves other publications rights, and neither the thesis nor extensive extracts from it may be printed or otherwise reproduced without the author's written permission.

..ꓕꓥꓥꓕꓕꓱꓕꓕ..
D.W. Mimura

Permanent Address:

10816 54th Avenue
Edmonton, Alberta
T6H 0T9

Date: April 17, 1990

THE UNIVERSITY OF ALBERTA

FACULTY OF GRADUATE STUDIES AND RESEARCH

The undersigned certify that they have read, and recommend to the Faculty of Graduate Studies and Research, for acceptance, a thesis entitled **SHEAR STRENGTH OF HYDRAULICALLY PLACED CLAY SHALE** submitted by **DANIEL WAYNE MIMURA** in partial fulfilment of the requirements for the degree of **MASTER OF SCIENCE**.

Dr. J.D. Scott   ....
                      (Supervisor)

Dr. D.C. Sego   ....

Dr. N. Rajaratnam   ....

Dr. K. Barron   ....

Date: April 17, 1990

Abstract

In northeastern Alberta, Canada, an open pit oil sands mine, operated by Syncrude Canada Ltd. currently uses a truck/shovel operation to strip and transport their overburden (an overconsolidated Clearwater Formation clay shale). As the mine expands, the overburden thickness will also increase, therefore, there is an economic incentive to hydraulically transport the overburden. Another incentive is to use the abundant quantity of tailings pond water or tailings pond sludge as the transport fluid.

The hydraulically transported clay shale will manifest itself as clay lumps. At the disposal site, whether it is within the mined out pit or independent of it, the clay lump mixture will be used to construct berms or retaining dykes, or simply discharged as backfill.

To investigate the behaviour of hydraulically placed clay shale lumps, six softening tests and forty two consolidated undrained triaxial compression tests were conducted. The softening tests were used to determine the confining stress required for the clay shale lumps to deform into a structure that is no longer free draining. Large diameter triaxial tests were conducted to determine the undrained shear strength of the clay lump structures under varying conditions of lump

size, mixing fluid (tailings pond water or sludge), confining
stress and softening duration. Smaller diameter triaxial
tests were conducted to determine the undrained shear strength
of dispersed clay shale representing the long term condition
of these mixes.

The tests revealed that the clay lump structure compresses
under the application of a low confining stress, with the
structure approaching a constant void ratio of 0.7 to 0.75
under higher stresses. The water trapped in these voids is
all that is available for further lump softening. Triaxial
test results on softened clay lumps revealed that both the
total and effective stress failure envelopes had low angles
of internal friction (less than 8°) and high cohesion
intercepts (up to 62 kPa). The lump structure behaved as an
overconsolidated clay but developed high positive pore
pressures.

Acknowledgements

I owe a special debt of gratitude to my supervisor, Dr. J.D. Scott, for his invaluable guidance, encouragement, and patience throughout this study.

I am also grateful for Syncrude Canada Ltd. for providing me with the incentive for this project and supplying me with the clay shale, pond water and sludge materials. Special thanks to Syncrude personnel, William Shaw, Byron Isaac, Ted Lord and Graham Cuddy, for their assistance and invaluable advice.

I would also like to thank the Civil Engineering technologists, Gerry Cyre and Steve Gamble, for their technical assistance.

Finally, I extend my greatest appreciation to my wife and family for without their patience, motivation and support, this project would not have been completed.

Table of Contents

LIST OF TABLES

LIST OF FIGURES

1.0 Introduction

1.1 Statement of Problem

Todays earth moving projects, whether it is a small excavation or a large mega project, require some means of transporting the excavated material which often determines the economic viability of the project.

In northeastern Alberta, Canada, an open pit oil sands mine, operated by Syncrude Canada Ltd. (Figure 1.1), currently removes over 22 million cubic metres of overburden annually to access the oil sands (Lord and Isaac 1989). As the mine expands towards the west, both the overburden thickness and the haul distance is increasing, therefore, alternatives to their present truck/shovel operation are being sought. One method which is being considered is to hydraulically transport the overburden through a pipeline. The transport medium would be either tailings pond water or tailings pond sludge. These are by-products from the hot water extraction process Syncrude uses to extract the bitumen from the oil sand. Since Syncrude must comply to a 'zero discharge' policy, these wastes are stored in a large tailings pond. The silts and clays that enter the pond slowly settle and consolidate forming a sludge zone with a solids content ranging from 10 to 50%. By utilizing the pond water or pond sludge as the transport

medium, the economic savings are two fold. First, these transport fluids are readily available and in large quantities (in excess of 118×10^6 m^3 per year) and second, by allowing the clay shale overburden to absorb the waste water, particularly from the tailings sludge, the accumulation of tailings water and sludge in the pond is reduced. The overburden is a highly swelling smectitic clay shale with the potential to absorb large volumes of water. The overburden excavation process will produce clay shale lumps which are then pipelined to a disposal site. The most accessible location for the disposal site would be in the mined out pit in which ultimate deposit heights up to 40 m would be required. At the disposal site, whether it is within the pit or independent of it, there is the possibility of using the clay shale lump mixture to construct berms or retaining dykes, or simply being discharged as backfill. The deposits will have to be designed to accommodate the slopes at which the discharged clay lump mixture will form, therefore, the stability of these deposits, which is controlled by the shear strength, must be determined. Since the clay shale easily swells and slakes in the presence of water, the softening duration and the lump size must be considered. In the long term, the clay shale lumps will continue to soften and water contents within the lump structure will equilibrate with the water contained in the interlump voids (macro-voids). Consequently, the shear strength properties of the clay shale lump structure must also

be determined at this ultimate state.

1.2 Objective of Thesis

The main objective of this thesis is to determine the shear strength of a Clearwater clay shale lump structure that has been hydraulically placed using either tailings pond water or tailing pond sludge as the transport fluid. In addition to lower transportation costs, it is desirable to use these waste fluids as the transport fluid so that they too can be disposed of at the same time as the clay shale overburden. As the clay shale lumps will soften, slake and compress with time and load, the change in shear strength from these processes will be determined.

To analyse this problem, it is also necessary to determine the confining stress required for the clay shale lumps to deform into a structure that is no longer free draining. At this stress level, the liquid trapped within the lump structure cannot be recharged or expelled and therefore, the absorption capacity of the lumps will be controlled by the amount of trapped liquid available. Also, when the lump structure is no longer free draining, any change in pore pressure from an increase in fill height or from shearing strains will dissipate slowly. This rate of pore pressure dissipation will determine which shear strength parameters

must be used to evaluate the stability of the fill.

1.3 Scope of Thesis

To investigate the behaviour of hydraulically placed clay shale lumps, six softening tests and forty two consolidated undrained triaxial compression tests were conducted. The softening tests were used to determine the confining stress required for the clay shale lumps to deform into a structure that is no longer free draining. Large diameter (102 mm diameter samples) triaxial tests were conducted to determine the undrained shear strength of the clay lump structures under varying conditions of lump size, mixing fluid, confining stress and softening duration. Smaller diameter (38 mm diameter samples) triaxial tests were conducted to determine the undrained shear strength of clay shale homogenized with pond water and with sludge which represents approximately the ultimate or long term condition of these mixes.

1.4 Organization of Thesis

Throughout the body of this thesis, all corresponding Figures and Tables are presented at the end of each individual Chapter.

The eight case histories in Chapter Two provide some valuable information and insight into the behaviour of hydraulically placed deposits of clay or clay shale material. In addition, a description of some relevant research work that has been done is presented. Some background information on the materials; that is, the Clearwater clay shale, tailings pond water, and tailings pond sludge, is also presented.

A description of the experimental apparatus fabricated and used in the tests and the test procedures that were followed are presented in Chapter Three.

The results are presented in Chapter Four. For brevity, only the Figures for one triaxial test from each of the test series is included in this Chapter. The complete set of Figures are presented in Appendix B.

Chapter Five is a discussion of the experimental results with the conclusions and recommendations in Chapter Six.
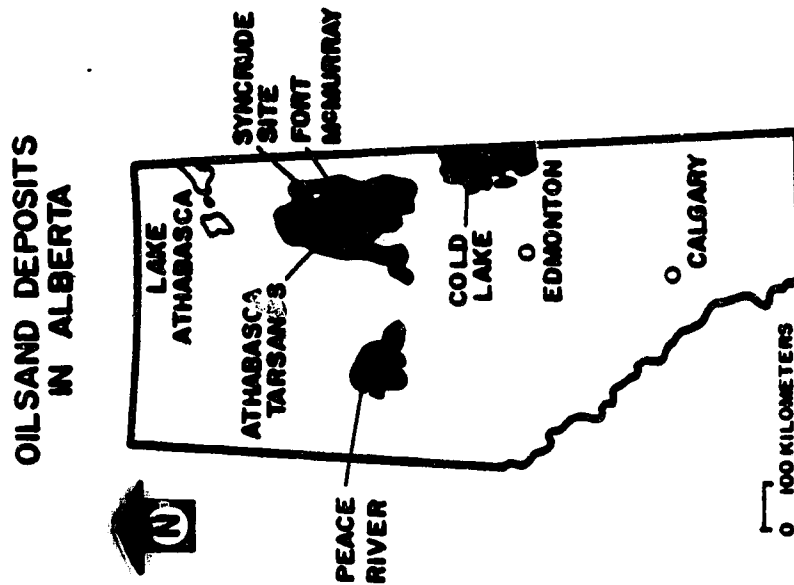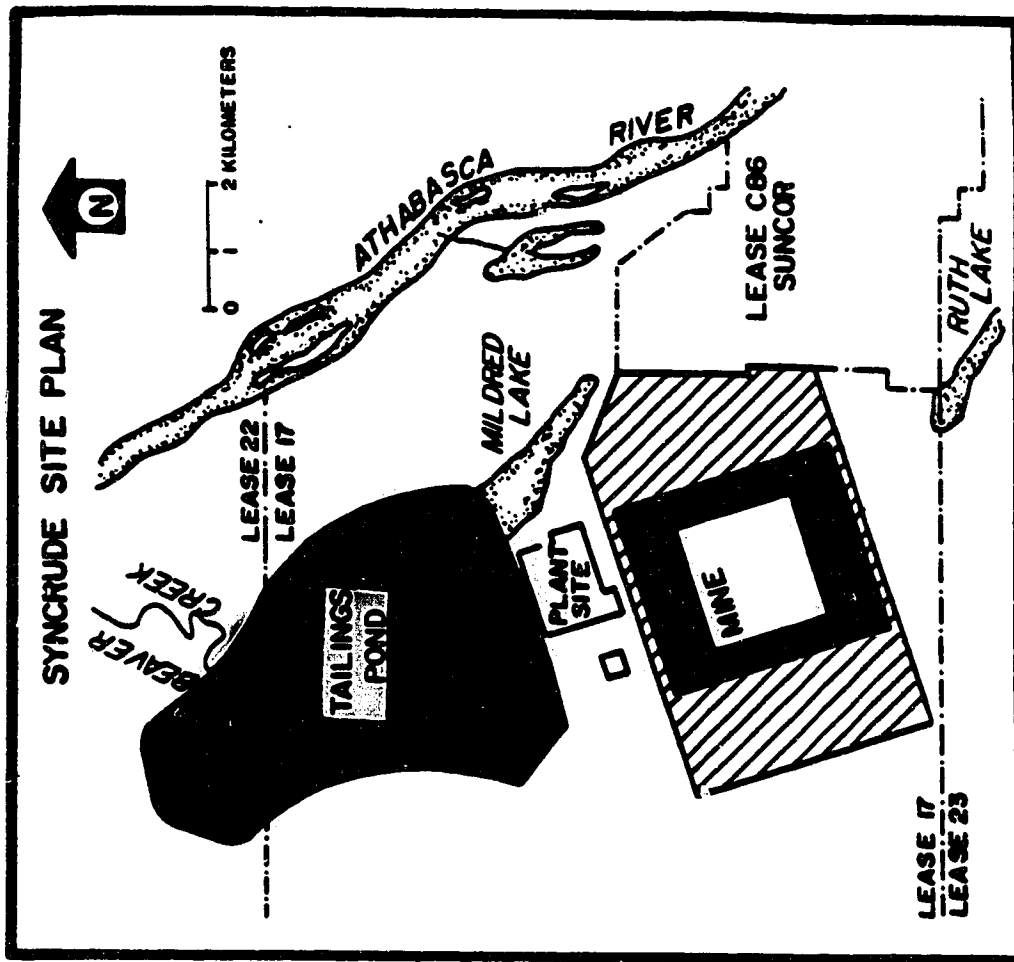
Figure 1.1   Syncrude Mine Site Plan

2.0 Background

2.1 Previous Hydraulically Placed Deposits

There are numerous examples of hydraulically placed deposits, however, almost all of the cases reported in the literature are of granular fill. The usual practice when dredging clay is to fully disperse the clay so that it will flow away from the discharge end of the pipeline eliminating the need to rehandle it. Environmental constraints today, however, require much of this dispersed material to be confined within dikes. Unfortunately, very little information has been documented regarding hydraulically filled deposits using clay lumps as the construction medium.

The following is an account of some case histories that have utilized hydraulically placed clay lumps.

2.1.1 Syncrude Canada, Fort McMurray, Alberta

The most recently documented hydraulically placed clay lump ... were reported by Lord and Isaac (1989). Syncrude ... Ltd. located near Fort McMurray, Alberta, initiated a pilot field experiment which involved dredging approximately 12,100 m^3 of Pleistocene lacustrine clay and till and 13,600 m^3 of Clearwater Formation clay shale. The clay was deposited

into test cells for geotechnical evaluation. Shallow deposits were formed ranging in height from 1.5 to 6 m (average of 3.2 m).

The Pleistocene lacustrine clay is a pink-grey to brown sandy silty glacial clay. The typical liquid limit and plastic limit is 37 and 19%, respectively. The Pleistocene till, underlying the lacustrine clay, has liquid and plastic limits of 22 and 10%, respectively. The dredged Kcc unit of the Clearwater Formation is an overconsolidated dark grey silty clay to clayey silt. Typical liquid and plastic limits range between 47 to 53% and 18 to 22%, respectively. The dredged Kcc clay shale formed deposits with an average dry density of 1,592 kg/m^3.

The field test layout and organization enabled either tailings pond water or tailings pond sludge to be used as the transport medium. Tailings pond water is a by-product of the hot water extraction process Syncrude utilizes to separate the bitumen from the oil sand. Tailings sludge is formed from the fines fraction of the tailings stream that has slowly settled and consolidated in the bottom of the tailings pond. The fines are mainly kaolinite and illite clays, fine sand, and silt. The sludge also contains 3 to 5% bitumen by weight.

The field test determined that Pleistocene lacustrine clays

can be successfully dredged with tailings pond water and deposited as a stable clay lump deposit.

The deposit of clay shale dredged with tailings sludge was unstable and exhibited very slow dissipation of pore pressures. Field vane and static cone testing classified the deposit as very soft to soft. The average deposit depths were less than 3.5 m and exhibited shallow side slopes of less than $9°$. The clay shale lump deposits exhibited steeper side slopes when dredged and transported with tailings pond water, ranging from 6° to 40°.

Undrained shear strengths of the deposited Clearwater clay shale that were measured with a hand vane on shelby tube samples revealed a range from 5 to 62 kPa. Bulk water contents of the clay shale in the dredged deposit ranged from 30 to 40%. The deposits were not measured for settlement.

2.1.2 Logan Airport, Boston, Massachusetts, USA

Between 1943 and 1949, Logan Airport in Boston was constructed in the Boston Harbour (Casagrande 1953; Carrier and Bromwell 1983). Thirty million cubic metres of hydraulically placed Boston blue clay formed the foundation. Approximately 6.5 m of clay fill was placed on top of 1.5 m to 3 m of soft organic silt-clay overlying a typical Boston

clay. The deposit consisted of clay lumps of varying sizes or as Arthur Casagrande described it, "varying in size from pebbles to head size". Although Casagrande did not report any characterization of the Boston blue clay, Carrier and Bromwell (1983) have reported typical Boston blue clay as having a range of 35 to 60% for the liquid limit and 20 to 25% for the plastic limit. The Boston blue clay exhibits lower plasticity indices than other dredged clays, therefore, it yielded better consolidation properties.

Casagrande theorized that since the base clay was overconsolidated, most of the compression would result from the plastic deformation of the clay balls rather than through consolidation. This did not occur; instead, the clay matrix between the clay balls controlled the majority of the rate and amount of consolidation. Carrier and Bromwell (1983) confirms this with calculations based on the finite strain consolidation theory. The strength in the fill could not be developed by the dried crust, but instead, the pavement and base loading caused consolidation which developed the strength required. Consolidation here refers to the drainage of excess pore water pressures from the soft matrix between the clay lumps.

Piezometers revealed that the pore pressure rose during construction and then very slowly dissipated. After 3.7 years

excess pore pressures were still recorded in both the fill and the underlying foundation clay. Settlements were measured at 46 cm after one year and 52 cm after two years, which represents a 15% change in height based on a 6.5 m high fill. Sideslopes of the fill were anticipated at 20(H):1(V) but actually developed at 50(H):1(V) resulting in more material dredged than estimated.

2.1.3 Lacustre Marine Terminal, Lake Maracaibo, Venezuela

In 1956 a fill island for a marine terminal was constructed in Lake Maracaibo, Venezuela (Whitman 1970). It was used for storage tanks (exerting about 139 kPa on the ground surface) to supply tankers docked at the piers which were opened in 1959. Stiff dredged clay was pipelined to an area, enclosed by a wall of driven concrete piles, to a height of approximately 2 m above the lake level. The clay lumps dredged were about the size of man's fist and were rounded and abraded. Some of the sand and clay occupied the open voids between the lumps. Settlements from preloading (60 kPa) and dewatering measured up to 440 mm with differential settlements up to 200 mm. Based on a 2 m high fill, a 22% change in height occurred. Excess pore pressures dissipated within about 60 days.

The project determined that the compressibility resulted

from the deformation of the clay lumps with the rate of
consolidation being controlled by the matrix characteristics.
Preloading was an effective means for preparing the fill to
adequately support the structures.

2.1.4 East Atchafalaya Basin Protection Levee,
Louisiana, USA

In 1961 and 1964 hydraulically filled berms were constructed
against an existing levee (Kemp 1967). The levee was required
for the protection against the Atchafalaya Basin Floodway.
The berms were approximately 2 m high and 60 m long. They
were composed of soft clay lumps within a clay matrix.
Plastic and liquid limits averaged 42 and 96 percent, respec-
tively.

The geotechnical investigation into the strength of the fill
was initiated in 1964 and completed in 1966. The average
strength increased from 5.8 kPa to 19.5 kPa two years after
placement, which represents a significant increase. Water
contents decreased from an average of 103 to 59% (a reduction
of 43%), and bulk densities increased to an average of 1,530
to 1,795 kg/m3 (an increase of 17%). The study predicted that
the deposit would attain a shear strength of about 24 kPa in
five years. There was a gain in strength, density, and a
reduction in water content the longer the deposit was allowed

to set, with the greatest change occurring in the first year.

2.1.5 Industrial Area, Halmstad Harbour, Sweden

A reclamation project on Halmstad Harbour, Sweden (Hartlen and Ingers 1981), utilized a bucket dredge to excavate a stiff overconsolidated silty clay. The excavation process formed clay blocks that were up to 1 m^3 which were deposited as a 3 m high fill. At a later date, a cutter suction dredge excavated more stiff clay. This clay was discharged as well rounded lumps up to 300 mm in diameter. Approximately 3.4 m was deposited giving a total fill thickness of 6.4 m.

Vane tests exhibited a large scatter of shear strengths, even after an homogenization period of 14 months. Undrained shear strengths derived from the vane and unconfined compression tests averaged between 25 to 50 kPa. Pore pressure dissipation in the lower fill was considerably slower than in the upper fill.

A preload embankment placed on top of the fill resulted in 210 mm of settlement and occurred mainly in the fill deposited by the bucket dredge (lower fill). It is believed that the large settlements were caused by the large blocky nature of the clay deforming by plastic deformation and by creep at the contact points. The smaller lumps deposited by the cutter

suction could support the applied stresses better. Based on a fill height of 3 m, a 7% change in height took place in the lower fill deposited by the bucket dredge.

2.1.6 Gaillard Island, Mobile Bay, Alabama, USA

In Mobile Bay, Alabama, a disposal island and a containment dyke were hydraulically constructed for the disposal of maintenance dredged material (Fowler and Hayden 1986; Fowler et al. 1986). The perimeter dyke was constructed to a height of about 5.2 m with a crest width of about 12 m. Approximately half of the dredged material was sand and silt while the other was a soft to stiff clay. The clay formed clay balls while being transported through 11 km of 0.7 m diameter pipeline. The sizes of clay balls formed ranged from 50 to 100 mm in diameter. The deposit consisted of clay balls within a silt, sand, and shell matrix. The trafficability of the clay lump deposits depended upon the location from where it was dredged. Generally, light equipment could work on the deposit either immediately after placement or after several days of drying. At the immediate discharge end of the pipeline, the clay balls formed piles with 45 degree side slopes. Overall sideslopes of the deposit ranged from 1(V):32(H) to 1(V):45(H). Triaxial tests were conducted on samples collected from 75 mm diameter shelby tubes. Cohesion values of 0 to 9.6 kPa and effective friction angles of 20.5

to 24 degrees were determined. Field vane shear strength data revealed strengths ranging from 2 to 30 kPa. The average settlement was 0.2 m which represents a 4% change in height of the 5.2 m high fill.

2.1.7 Hydraulic Earth Structures, USSR

Three construction sites utilizing hydraulically placed clay lumps as the construction medium are discussed (Lutovinov et al. 1975). The authors stated that the optimal construction conditions were accomplished when the maximum possible size of clay lumps or clods were delivered to the deposit. By using large size lumps, fill densities were closer to the in situ state. The problem they recognized was in transporting the large lumps without causing much dispersion to occur.

At the three sites utilizing clay lumps, lump dispersion was monitored through field observations and the lumps size distribution was determined. The soil from the floodplain of the Byk River was a soft black, brown, and grey silty clay with a plasticity index of 25 to 30%. Average water contents were 26%. The North Crimean irrigation canal consisted of a diverse range of soils of the Quaternary age. Plasticity indices range from 5 to 32%. The Kiliya irrigation canal is also of Quaternary age and consists of silty loam soils. Plasticity indices range from 11 to 14 in the upper portion

of the canal and 8 to 10 in the lower part.   Natural water contents are between 25 to 30%.

The clay lumps formed slopes between 1(V):11(H) and 1(V):20(H).   The sand flowed out forming shallower slopes between 1(V):50(H) and 1(V):100(H).   The amount of sand captured within the clay lump structure was not a function of the slurry sand content but of the available void spaces. Within four months, the clay lumps and sand matrix below a 2 m depth became completely monolithic. Permeability, density, shear strength, and compressibility were very low and similar to in situ conditions.

2.1.8 Vesta Mine, Forestburg, Alberta

Dusseault et al. (1984) has investigated coal mining spoil pile subsidence constructed of overconsolidated overburden of the Cretaceous and early Tertiary age.   The smectitic clay shales investigated are similar to the Clearwater clay shale overburden found at the Syncrude site in Fort McMurray, Alberta.   Unlike the previous case histories, the excavated overburden was not hydraulically placed but instead, was placed at its natural water content by dragline as backfill in the mine pit. The clay shale lumps are uncompacted and up to 10 to 15 cm in diameter. Through time, the surface water from precipitation and the natural ground water slowly

percolated into the fill softening and slaking it which has manifested itself as large settlement bowls.

Total settlement is the settlement due to gravitational loading and saturation. Settlements measured in the field have been up to 1 m for a 6 to 8 m fill depth (17 to 13% strain) resulting in an overall average strain of 10%. Upon saturation, the majority of the strains occur quickly and with time, due to swelling, slaking and consolidation, the macro porosity of the lump structure decreases. Oedometer tests indicated that total stains up to 45% can be expected.

2.1.9 Overview of the Case Histories

The case histories reveal that hydraulically placed fills composed of clay lumps or balls exhibit slow pore pressure dissipation and experience settlements of notable magnitude. The amount of settlement or volume change ranged from 3 to 22%. In many cases, the strength of the deposit improved with time. The volume change, whether it is plastic deformation without pore pressure dissipation (compression) or with pore pressure dissipation (consolidation), is controlled by the interstitial material between the clay lumps.

2.2 Previous Research Work and Experiments

In the past, only limited research on the shear strength properties of a Clearwater Formation clay shale lump structure has been conducted. The most comprehensive has been a field program initiated by Syncrude Canada Ltd. in 1985 and 1986 (Lord and Isaac 1989). This was discussed in the previous Section.

The aspect of dispersion and shear strength was investigated by Owen Ash (Ash 1985; Dusseault et al. 1988). He concluded that the Clearwater clay shale can dewater significant volumes of tailings pond sludge. The moisture uptake is dependent on the hydraulic conductivity and the diffusivity of ions through the material. The blended sludge and overburden mixture was analysed with the Swedish drop cone and determined to behave as a soft clay. Average undrained shear strengths were 30 kPa after 24 hours and 33 kPa after 72 hours. The measurements were preferentially conducted on the softer zones between the lumps.

The shear strength of an unsaturated Clearwater clay shale lump structure was investigated by Hilliard et al. (1988; 1989). The results from this study are discussed in Section 5.2.4.

2.3 Geology and Material Characteristics

2.3.1 Geological History

To better understand the subsurface stratigraphy of the Clearwater Formation clay shale, the following section will describe the geological history in the Athabasca region.

The subsurface stratigraphy in the Athabasca region located in northeastern Alberta can be subdivided into four separate periods or ages. The oldest being the Pre-cambrian, then the Devonian, Cretaceous, and lastly the Quaternary period.

The formation of the deposits in the Pre-cambrian and Devonian periods are not of significance to this study and will not be discussed except to say that they underlie the unconformably deposited Cretaceous McMurray Formation.

The Cretaceous deposits found in the basin are the result of a series of transgressive and regressive episodes of the Lower Cretaceous epicontinental sea. Within this period, the McMurray and Clearwater Formation deposits were formed. The McMurray Formation experienced three main environmental sequences during these episodes; the marsh environment, estuarine environment and the marine environment (O'Donnell and Jodrey 1984).

As the sea transgressed over the area again, it put an end to the McMurray sand deposition. The Clearwater Formation was deposited as parallel beds sedimented from the mixed marine and continental environment. It consists of some beach and shoreface sands, but mainly of muds, silts, and marine off-shore shales. The Clearwater Formation in the Athabasca region averages 76 m thick, but in the mineable regions, glaciation and post glacial meltwater channels have scoured away much of this deposit making the oil sand deposits more readily accessible for open pit mining.

The Clearwater Formation can be further broken down into units based upon borehole geophysical characteristics (Isaac et al. 1982). Natural radioactivity is measured with the gamma ray and used to empirically define the clay minerals. Geophysical bulk density logs help to the define low and high density zones (Figure 2.1). Figure 2.2 illustrates the Clearwater Formation stratigraphy in a cross section of Syncrude Canada Ltd. leases. These are labelled Kca to Kcf overlying Kcw. Generally, the Clearwater Formation is composed of uncemented clay shales, clay silts, fine grained sand, and thin indurated silt stones (Isaac et al. 1982). Table 2.1 summarizes the index properties of the Clearwater Formation.

The mineralogy of the clay size fraction indicates the Clearwater Formation is dominantly illite and smectite (average of 44 and 34% respectively) with lesser fractions of chlorite and kaolinite (11% each). The presence of smectite increases in the lower units while kaolinite and chlorite tend to increase in the upper units. Liquid and plastic limits vary between 46 to 156% and 19 to 37%, respectively.

During the Quaternary period, Pleistocene and Holocene deposits were formed. Repeated glaciations, producing up to 2,000 m to 3,000 m of ice, reworked the surface of the Cretaceous Formation. Debris that was deposited by the melting ice was also worked by the post glacial meltwaters. The deposit is generally sand, silt, and gravel. As a result of the glaciation and other rock formations up to 2,000 m thick which have since been eroded away, the Clearwater Formation is an overconsolidated clay shale.

The Clearwater Formation and Pleistocene deposits form the major constituents of the overburden required for removal prior to mining the McMurray oil sands.

2.3.2 Material Characteristics

2.3.2.1 Clearwater Formation Clay Shale (Kcc Unit)

The Clearwater Formation clay shale is subdivided into units Kca to Kcf and Kcw as mentioned in the previous section. The Kcc unit was chosen for the investigation in this thesis because it is the thickest unit in the formation, varying in thickness up to 21 to 23 m (Isaac et al. 1982). Therefore, prior to mining the oil sands, the Kcc unit will be the main overburden unit removed. Because of the sheer volume of this material, transportation costs can be significantly reduced if this unit can be hydraulically transported and disposed.

The Clearwater clay shale is usually dark grey with zones of clay rich strata, low density, and silt stones. The clay fraction is composed of mainly illite, with lesser amounts of kaolinite, smectite, and chlorite. Based on the clay shale's liquid limit to dry density or clay size to activity relationships, the clay shale is classified as having a very high potential for expansion and swelling potential (Holtz and Kovaks 1981). Geotechnical characterization of the clay shale used in this thesis is presented in Section 4.2.

2.3.2.2 Tailings Pond Water

At Syncrude's oil sands plant, bitumen is stripped from the sand utilizing the hot water extraction process. About 15 m^3 of water is required per cubic metre of synthetic crude oil produced. This results in about 120×10^6 m^3 of tailings water going to the tailings pond every year (MacKinnon 1989).

The tailings coming from the plant contains approximately 55% solids, 45% water, and 0.5% bitumen by weight. The solids are composed of sands, silts, and clays (mean particle size is about 150 μm). At the tailings pond, the coarse fraction readily settles out forming the beach while the finer fraction continues to the pond. Upon reaching the pond, the fines settle and consolidate slowly forming the sludge zone. Figure 2.3 illustrates the stratification in the tailings pond. The "free" water zone is approximately 7 to 8 m in depth. It is from this zone that the tailings water was collected for the experiments.

The major components of the dissolved mineral fraction in the tailings pond water includes cations (Na^+, Mg^{++}, Ca^{++}), anions ($Cl^-, SO_4^=, HCO_3^-$), and nutrients ($NO_2^-, NO_3^-, NH_3, PO_4^-$). The cations and anions make up the majority of the dissolved fraction. Of the cation equivalents, 95% is sodium giving the water a hardness of less than 40 mg/l (soft water). Of the anions,

50 to 75% is bicarbonate resulting in a pH of 8 to 8.6.

2.3.2.3 Tailings Pond Sludge

Within the oil sand strata, clay minerals are present in the form of interstitial fillings or clayey seams. The oil sand feed is sent to the extraction plant where 15 to 25% of the fines are removed as extraction rejects (MacKinnon 1989). The remaining fines go through the hot water extraction process with the oil sand feed. Factors such as agitation, pH of 8.5, addition of NaOH, and warm temperatures (85°C) help to disperse this clay into the waste waters (Dusseault et al. 1989).

The waste slurry or tailings consist of approximately 55% solids, 45% water, and 0.5% bitumen by weight. Of the solids fraction, most of the coarse fraction (>22 μm) and half the fines (<22 μm) as well as 15% of the bitumen readily settles out or is trapped on the beach at the discharge end (MacKinnon 1989). The rest of the fines and bitumen is carried towards the centre of the tailings pond.

The fines initially settle to a concentration of about 20% fines by weight within three to nine months. Some factors affecting further consolidation are one dimensional upwards drainage (resulting in an increasing drainage path with time),

hydraulic conductivity, and the presence of bitumen. In 5 to 10 years concentrations of 25 to 30% develop (Mackinnon 1989). These consolidated fines are labelled "tailings sludge". The sludge can be subdivided into an immature and mature sludge zone depending upon its solids concentrations (Figure 2.3).

The fines in Syncrude's sludge are mainly kaolinite (55-65%) and illite (30-40%). A typical x-ray diffraction trace is shown in Figure 2.4 (Dusseault et al. 1989). Traces of smectitic and chloritic clays, ferric oxide, and feldspar silts are also present. Typical concentrations of bitumen in the sludge range from less than 1% to over 5% by weight (MacKinnon 1989).

2.3.2.4 Materials Used in the Testing Program

The overburden to be stripped prior to mining the oil sand consists of mainly the Clearwater Formation. Within the Clearwater Formation, the Kcc clay shale unit dominates this sequence. Therefore, this thesis investigated the hydraulically placed characteristics of the Kcc clay shale.

The clay minerals, specifically illite, kaolinite, smectite and chlorite, gives the Kcc clay shale its highly swelling character. This characteristic is beneficial because it gives the clay shale the potential to absorb large volumes of water.

A disadvantage is that the clay shale swells and slakes forming a low permeable structure that does not dissipate pore pressures readily. If effective stresses are reduced between the clay shale lumps, large volume changes and low shear strengths will result.

In a hydraulic scheme, it is economically desirable to use either tailings pond water or sludge as the transport fluid. The water transfer and dispersion of the clay shale lumps transported with tailings pond water is much greater than with tailings pond sludge. This occurs because the pond water has a pH of 8 (which is optimal for dispersion), increased NaOH concentration (which reduces the interplatelet bonding allowing the clay to disperse more readily), lack of fines (from the sludge) that form a low permeable film around the clay lump, and provides more agitation in the pipeline than with sludge (in which the sludge solids dampens the agitation effect).

To determine the shear strength of a hydraulically placed deposit of Kcc clay shale, a series of softening and triaxial tests were conducted to determine the effects of softening duration, lump size, transport fluid (tailing pond water or tailings sludge), and confining stress.

GEOLOGIC UNIT	GRAIN SIZES % SAND/SILT/CLAY			CLAY FRACTION MINERALOGY % CHLORITE/ILLITE/KAOLINITE/SMECTITE				ATTERBERG LIMITS $W_L\%$ $W_P\%$ $I_P\%$			NATURAL MOISTURE $W_N\%$	LIQUIDITY INDEX	ACTIVITY $I_P/\%$CLAY
Kcd	20	53	27	21	39	28	12	56	19	37	20.5	0.04	1.37
Kcc	2	53	45										
	1	61	38	15	50	15	20	61	22	39	18.0	-0.10	0.94
	0	50	50	15	40	10	35	101	31	70	22.7	-0.12	1.40
	0	60	40	15	50	20	15	74	23	51		-0.01	1.28
Kcb	7	47	46	15	55	15	15	58	22	36	16.6	-0.15	0.78
	4	37	59	5	30	0	65	156	37	119	33.3	-0.03	2.02
	8	46	46	10	45	10	35	76	22	54	18.4	-0.07	1.17
Kca	2	45	53	5	45	10	40	122	30	92	20.9	-0.10	1.74
	0	56	44					92	27	65	18.5	-0.13	1.48
Kcw	30	47	23	5	50	5	40	46	21	25	14.3	-0.27	1.09
				10	50	0	40						
				5	30	10	55						

Table 2.1   Clearwater Formation Index Properties

(after Isaac et al. 1982)

GAMMA RAY LOG
API UNITS
20 40 60 80 100 120

BULK DENSITY LOG
2.1 2.2 2.3 2.4 2.5 2.6 gm/cc

PHYSICAL CHARACTERISTICS

INDURATED ZONES	THICKNESS (mm)	CLAY RICH ZONES	LITHOLOGY
XXXX - Siltstones			
XXXX	800-1200		Grey to grey-green, fine- to medium-grained glauconitic sandstone with shaly interbeds
XXXX	150-400		
		High smectite	Predominantly grey-black shale with thin interbedded stringers of silt and sand
XXXX	200-400	Low density	
XXXX	100-200		
XXXX	300-800		
XXXX	30-300		
XXXX	100-200		
XXXX	150-300	Low density High smectite	Grey to grey green, very fine- to fine-grained glauconitic sandstone
XXXX	150-300		Grey-black, fissile, silty clay shale
XXXX	150-200 DISCONTINUOUS		
XXXX	250-600		Grey-green, fine- to medium-grained glauconitic sandstone

(after Isaac et al. 1982)

DEPTH IN METRES
10 20 30 40 50

HIGH DENSITY LINE 2.4 gm/cc
SAND LINE 20 API UNITS

RECENT AND GLACIAL — QUATERNARY

Kcd
Kcc
Kcb
Kca
Kcw
Km
CLEARWATER FORMATION
CRETACEOUS

Figure 2.1   Geophysical Signatures of the Clearwater Formation
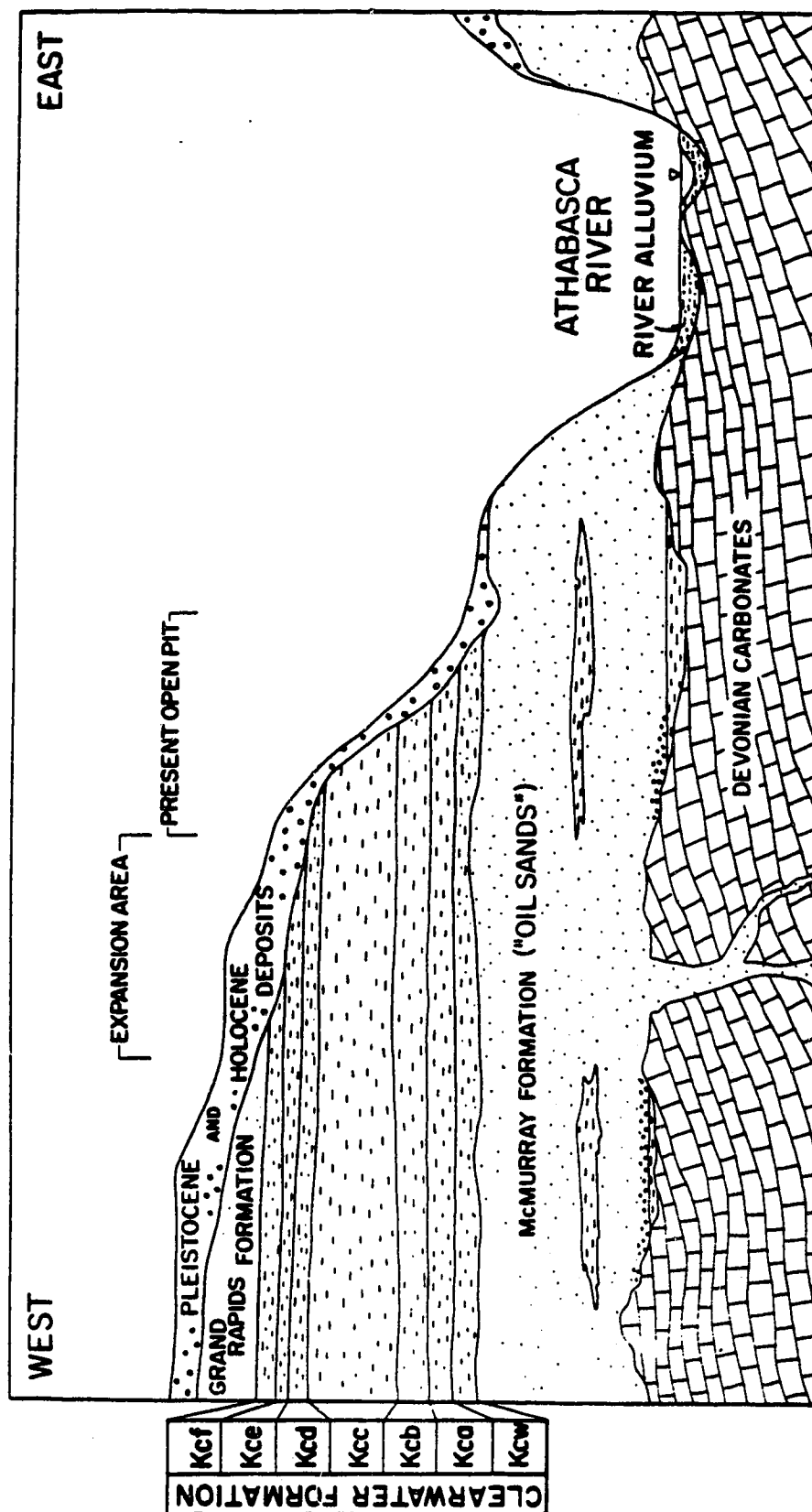
Figure 2.2   Geologic Cross-Section, Syncrude Canada

(after Isaac et al. 1982)

29

FIGURE 2.4 X-ray Diffraction Trace of Tailings Sludge Clay Minerals (Dusseault et al. 1989)
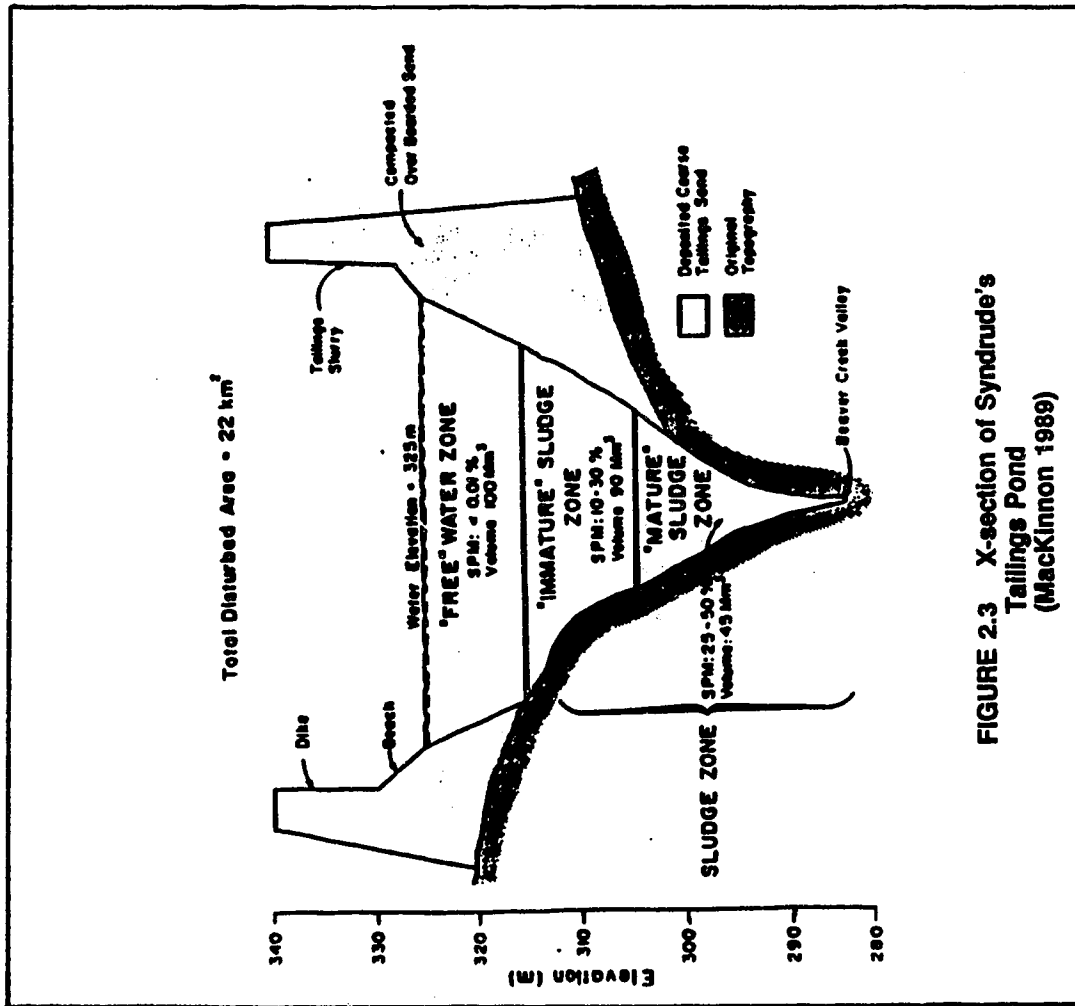
FIGURE 2.3 X-section of Syncrude's Tailings Pond (MacKinnon 1989)
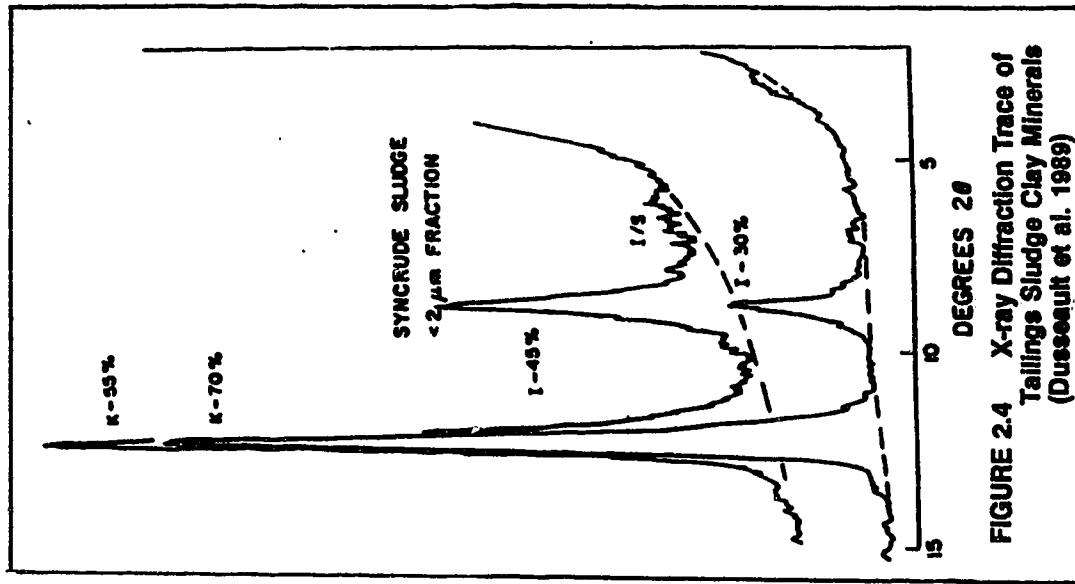
3.0 Laboratory Apparatus and Procedures

Clearwater Formation clay shale was collected from Syncrude's Oil Sands Lease property located in Fort McMurray, Alberta. This clay shale is typical of the overburden that will have to be removed as the mine progresses to the northwest. The clay shale was delivered in the form of large lumps varying in size from 150 mm to 300 mm in diameter. The lumps were subsequently broken down manually and sampled to obtain similar gradations for each test.

The following is a description of the testing program using some standard and some non-standard test procedures and equipment.

3.1 Index Tests

The index tests performed on the Clearwater Formation clay shale lumps consisted of water content determination, Atterberg limits, grain size analysis, lump size analysis, and relative density. The bitumen content of the tailings pond sludge was also determined.

3.1.1 Water Content

The water content of the clay shale is defined as the weight

of water divided by the weight of the dry soil solids. The procedure followed is in accordance to ASTM D2216 "Laboratory Determination of Water (Moisture) Content of Soil, Rock, and Soil-Aggregate Mixtures". To ensure that an overall water content was determined that represented the whole sample, approximately half of the triaxial sample was utilized for the water content determination.

3.1.2 Atterberg Limits

Test procedures to determine the liquid and plastic limit of the clay shale followed standard ASTM D4318 practices. The Atterberg limits of the clay shale were determined from samples at their natural water content, not oven dried samples. Distilled water was used to mix with the clay shale and then allowed to saturate overnight prior to testing.

3.1.3 Grain Size and Lump Size Analysis

The grain size distribution of the Clearwater clay shale was determined using the hydrometer method in accordance to ASTM D422 "Particle-Size Analysis of Soils".

The soil sample of clay shale was initially soaked for 16 hours and then further dispersed using a mechanical mixer. A 4% solution (by weight) of dispersing agent (Calgon) was

used as a deflocculating agent. A standard hydrometer and a 1,000 ml graduated cylinder was used for the test.

For the lump size analysis, the Clearwater clay shale was manually broken down into smaller lumps. The lumps were representatively sampled using a splitter box. For the tests requiring 12.7 mm maximum size lumps, only the lump size fraction retained between the 12.7 mm and the 0.84 mm sieve was used. For tests requiring 19 mm maximum size lumps, the lump size fraction retained between the 19 mm and the 2 mm sieve was used. A representative sample of these lumps were examined for their lump size gradation using standard sieves with openings of 19 mm, 12.7 mm, 9.42 mm, 6.68 mm, 4.76 mm, 2 mm, and 0.84 mm, respectively. The standard method of shaking the sieves was not administered since the mechanical action of the sieve shaker would break the lumps up further. To alleviate this problem, the sieves were manually shaken in an up, down, and rolling motion for a period between 5 to 10 minutes. Visual examination of the lumps left on the sieves determined that this length of shaking time was sufficient to ensure that all of the smaller lumps had passed through the sieves.

The lump gradation is plotted on a modified grain size curve presented in Figure 4.2.

3.1.4 Relative Density

The Clearwater clay shale was prepared and tested in accordance to the procedure outlined in ASTM D854 "Standard Test Method for Specific Gravity of Soils". A dried sample of clay shale was broken up using a rubber pestle. The test was performed using distilled water and then performed again using methanol as the fluid. Methanol was used as it is a better wetting agent than distilled water for oven dried samples.

3.1.5 Bitumen Content of the Tailings Pond Sludge

The method for determining the bitumen content of the tailings sludge is in accordance with the standard practice used by Syncrude Research in Edmonton. The process is called "The Determination of Bitumen, Water, and Solids content of Oil Sands Reject and Slurry Samples, Syncrude Analytical Method #27". Toluene was used for the extraction solvent. A detailed account of the test procedure and equipment is described in the reference "Syncrude Analytical Methods for Oil Sand and Bitumen Processing", published by AOSTRA (Bulmer and Starr 1979).

3.2 One Dimensional Compression/Softening Tests

The objective of the compression/softening tests was to determine the confining stress required for the clay shale lumps to deform into a structure that is no longer free draining. Throughout the compression stage, the lumps will be softening; that is, the lumps will be absorbing water, swelling, and slaking.

To simulate hydraulically placed clay shale lumps, 12.7 mm maximum size lumps were mixed with tailings pond water within the modified consolidation cell. Table 3.1 summarizes the six compression/softening tests performed. The following is a description of the test apparatus and procedure used.

3.2.1 Apparatus

A testing device was required in which the clay shale lumps could be introduced to a fluid (tailings pond water) and subjected to a confining stress. Double drainage (top and bottom) was required for the sample to consolidate. To accommodate these requirements, a 305 mm diameter consolidation cell was modified for this purpose (Figure 3.1). Modifications included manufacturing a top and bottom platen with holes large enough for unimpeded flow yet small enough to prevent the smaller lumps from passing through. This was

achieved by drilling 12.7 mm diameter holes through a 25 mm
thick aluminum circular plate and then covering the holes with
a number 10 wire mesh (2 mm opening). A loading ram was
welded to the top platen so that the confining stress could
be applied through a bellofram controlled by compressed air.
A drainage hole was drilled through the bottom and fitted with
a valve so that hydraulic conductivity measurements could be
taken at appropriate time intervals. Details of the modified
consolidation cell are presented in Appendix A.

3.2.2 Testing Procedure

The Clearwater clay shale was prepared by manually breaking
up the larger lumps into smaller lumps. Only the clay shale
lumps passing a 12.7 mm sieve and retained on a 0.84 mm sieve
were used for the tests.

The bottom platen was put into position while the valve on
the bottom of the cell was kept open. The drainage tube,
connected to the valve, was elevated so that an equal head was
applied to both the top and bottom of the sample. Tailings
pond water was poured into the cell until it was about half
full. The clay shale lumps were slowly poured into the cell
in a uniform manner to prevent large cavities or voids in the
lump structure. Keeping the water level above the lumps at
all times ensured that the lump structure would be saturated.

This was accomplished by pouring tailings water into the cell as the lumps were dropped in.

Once all of the clay lumps were introduced into the cell, the top surface was levelled and the top platen positioned. Care was taken to ensure that all of the modified consolidation cell components were properly aligned so that the top platen would not tilt and bind against the sides of the cell. Additional tailings pond water was poured into the cell up to the top rim. This level was continually maintained to sustain a constant head. Two dial gauges were fastened to the testing frame to measure the vertical displacement of the top platen. A predetermined confining stress was applied to the top platen by a bellofram. The clay lumps were allowed to compress and consolidate while dial gauges recorded the volume change.

On completion of the consolidation/compression stage, a constant head permeability test was performed. This was achieved by lowering the drainage tube to a graduated cylinder where the drainage was collected and measured. The cell was continually supplied with tailings pond water to maintain the constant head. Consecutive readings were taken until a consistent set of readings were attained. After determining the hydraulic conductivity, the drainage tube was repositioned and the clay lumps were allowed to soften further.

Permeability tests were taken at regular time intervals until a trend was established; that is, the hydraulic conductivity either increased, remained constant, or decreased.

On completion of the test, the sample was broken apart and water contents were taken of the clay lump structure (bulk water content). Water contents were taken of the individual clay lumps if they could be delineated. This was only possible for confining stresses below 100 kPa.

3.3 Consolidated Undrained Triaxial Compression Tests

The objective of the consolidated undrained triaxial tests was to determine the shear strength of a clay shale lump structure mixed with either tailings pond water or tailings sludge. Parameters that were investigated included the mixing fluid, lump size, softening duration and confining stress.

The triaxial test program was divided into two parts. The first part investigated the shear strength of the clay shale lump structure while the second part investigated the shear strength of a homogenized clay shale, which represents a fully softened state. The testing program consisted of 42 triaxial tests which were subdivided into 7 test series (Table 3.2).

3.3.1 Clay Shale Lump Triaxial Tests

3.3.1.1 Apparatus

A large triaxial cell was used to test samples with dimensions of up to 102 mm in diameter by 203 mm high. The base of the cell incorporated four ports; one for measuring pore pressure, one for the cell pressure, one for the back pressure and saturation, and an additional port for drainage if it was required. Pressure transducers with a range of 0 to 2,070 kPa and 0 to 1,720 kPa were used to measure the pore pressure and the cell/back pressure, respectively. Volume change was determined by measuring the level in a 25 ml capacity manometer. An elevated reservoir, approximately 1 m above the height of the triaxial cell, supplied the tailings pond water for saturating the sample. Tailings pond water was not used in the pressure system because any fines and impurities, intrinsic to the pond water, could contaminate the system.

To support the clay shale lumps prior to the application of a confining stress, an aluminum split mold former was manufactured (Figure 3.2). The former consisted of two halves fastened together by six cap screws. The base of the former was recessed to accept the pedestal base of the triaxial cell. At midheight, a connection allowed a vacuum line to be

attached to deliver a small vacuum to hold the rubber membrane tight against the sides of the former. The rubber membrane was 0.375 mm thick and was long enough to stretch over the top of the former. Number 2 filter paper was used for the top and bottom, as well as the 12.7 mm wide filter strips used for radial drainage. Porous stones were also required on the top and bottom of the sample.

To prevent the sample from failing under the weight of the top platen, a lighter platen was machined from perspex. The platen incorporated a drainage port so that the back pressure could be delivered to the top of the sample.

The clay lump samples in the triaxial cell were tested on a W᛫ ᛫ham Farrance 10,000 kg capacity controlled strain compression frame.

3.3.1.2 Test Procedure - Clay Shale mixed with Pond Water

Setting up the clay lump samples and saturating them is unique to this testing program. The following is a description of the procedure used for testing the clay shale lumps mixed with tailings pond water.

The first step was to position the deaired porous stone and filter paper on top of the pedestal base. A 0.375 mm thick

102 mm diameter rubber membrane was stretched over the base and secured with two rubber o-rings. The split mold former was clamped onto the base and the rubber membrane was stretched over the top. A small vacuum was applied to hold the membrane tight against the former. Radial drainage filter paper strips were placed inside the mold (against the membrane) and the lumps were slowly poured into the split mold former being careful not to leave any large voids. The top filter paper, porous stone, and top platen was placed into position so that the rubber membrane could be stretched over the top platen and secured with two rubber o-rings. A vacuum of 20 kPa was applied through the top platen to provide enough support to the clay lump structure so that the split mold could be removed. The outer casing of the triaxial cell was positioned and fastened in place. The cell was filled with water and a small confining stress of 10 kPa was applied as the vacuum was released.

To saturate the sample, tailings pond water, which was stored in an elevated reservoir, was allowed to percolate from the bottom to the top of the clay lump sample. The lumps were permitted to soften under the small confining stress of 10 kPa while the saturation line, supplying the pond water, remained open. Following the softening period, a B-test determined the back pressure required for complete saturation. Standard testing procedures were followed for consolidating and

shearing the sample. The samples were sheared in an undrained manner with pore pressure measurements.

The preceding apparatus and test procedure was used for triaxial test series 1 and 2. Examination of the pore pressure measurements taken during the consolidation stage revealed that the side drains were not working effectively. That is, the pore pressure transducer, measuring the pore pressures at the base of the sample, was not readily tracking the applied back pressure at the top of the sample during consolidation. To alleviate this problem, another drainage line was connected to the additional port at the base of the cell. The two drainage lines, one from the top and the other from the bottom of the sample, were joined together with a Y connection to form a common line to the volume change manometer.

Identical procedures were followed for testing both sizes of clay shale lumps (12.7 mm and 19 mm maximum size lumps). The confining stresses used for the triaxial tests ranged from 150 to 550 kPa. This stress range represents clay shale deposits between 8.5 m to 31 m in depth (based on a bulk density of 1800 kg/m^3). The strain rate used throughout test series 1 to 5 was 0.034% per minute which resulted in shearing times up to 8 hours.

3.3.1.3 Test Procedure - Clay Shale mixed with Pond Sludge

The tailings pond sludge has a solids concentration of 30% by weight of the total solids and contains about 6% bitumen (by weight of solids). Unlike tailings pond water, the fines and bitumen within the sludge cannot pass through the porous stone nor the filter paper to saturate the clay lump sample; therefore, the clay lumps that were tested with sludge were prepared differently.

Saturation was accomplished by pouring the sludge into the mold first and then the clay lumps were dropped in. This is similar to the procedure utilized for the compression/softening tests. The remainder of the test was identical to the triaxial tests using tailings pond water. The samples were sheared in an undrained manner with pore pressure measurements.

Sludge was used for test series 5 in which 19 mm maximum diameter clay shale lumps were used.

3.3.2 Homogenized Clay Shale Triaxial Tests

Hydraulically placed clay shale lumps will absorb water, swell, slake, and eventually soften into a homogeneous clay mass depending on the amount of water (tailings pond water or

tailings sludge) available. To determine the shear strength of the clay at this ultimate or fully softened state, thirteen 38 mm diameter by 76 mm high triaxial samples of homogenized clay shale were tested. The consolidated undrained triaxial compression tests were subdivided into three test series; 6, 6A and 7. The clay shale in test series 6 and 6A was homogenized with tailings pond water while test series 7 used tailings sludge. Table 3.2 summarizes the test parameters for each of the test series. The homogenized clay shale samples were tested on a Wykeham Farrance 1,000 kg capacity controlled strain compression frame.

3.3.2.1 Test Procedure

To homogenize the clay shale, the clay lumps were broken down into a powder with a rubber pestle. Depending on the test series, the clay shale was mixed with tailings pond water or tailings sludge (30% solids content). The amount of fluid was predetermined so that the resulting mixture would have a water content of about 30%. A water content of 30% was chosen because previous experience using clay shale lumps revealed the final bulk water contents were consistently around 30%. Therefore, whether the water is in the macro-voids or in the micro-voids, this is the amount of water available to the lumps for softening. The mixture was allowed to saturate overnight and then compacted into a 102 mm diameter compaction

mold. Steel tubes with an inside diameter of 38 mm were pushed into the compacted sample to attain the samples. The samples were extruded and trimmed to length.

Radial drainage was used in conjunction with a porous stone and number 2 filter paper on the top and bottom of the sample. A rubber membrane was used to encapsulate the sample. A B-test determined the back pressure required to achieve complete saturation. The sample was consolidated and sheared in an undrained manner with pore pressure measurements. Test series 6 was sheared at a rate of 0.13% per minute while test series 6A and 7 were sheared at a rate of 0.028% per minute.

Table 3.1   1D Compression/Softening Tests

Test No.	WMC1	WMC2	WMC3	WMC4	WMC5	WMC6
CONFINING STRESS (kPa)	250	3.7	100	41	57.5	65.7
MAX LUMP SIZE (mm)	12.7	12.7	12.7	12.7	12.7	12.7
MIXING FLUID	water*	water*	water*	water*	water*	water*

* tailings pond water

Table 3.2   Consolidated Undrained Triaxial Compression Tests

	Test Series 1	Test Series 2	Test Series 3	Test Series 4	Test Series 5	Test Series 6	Test Series 6A	Test Series 7
CONFINING STRESS RANGE (kPa):	182-298	199-434	179-428	283-505	257-541	150-550	150-500	157-544
MAXIMUM LUMP SIZE (mm) :	12.7	12.7	12.7	19	19	Homo	Homo	Homo
MIXING FLUID:	water*	water*	water*	water*	sludge	Homo	water*	sludge
NO. OF TESTS:	5	6	4	9	5	5	3	5

* tailings pond water

Figure 3.1 Modified Consolidation Cell

Loading Ram

Perspex Top Platen

O rings

Porous Stones

Vacuum Port

Aluminum
Split Mold Former

Pedestal

Pore Pressure

Extra Port

Back Pressure

Cell Pressure
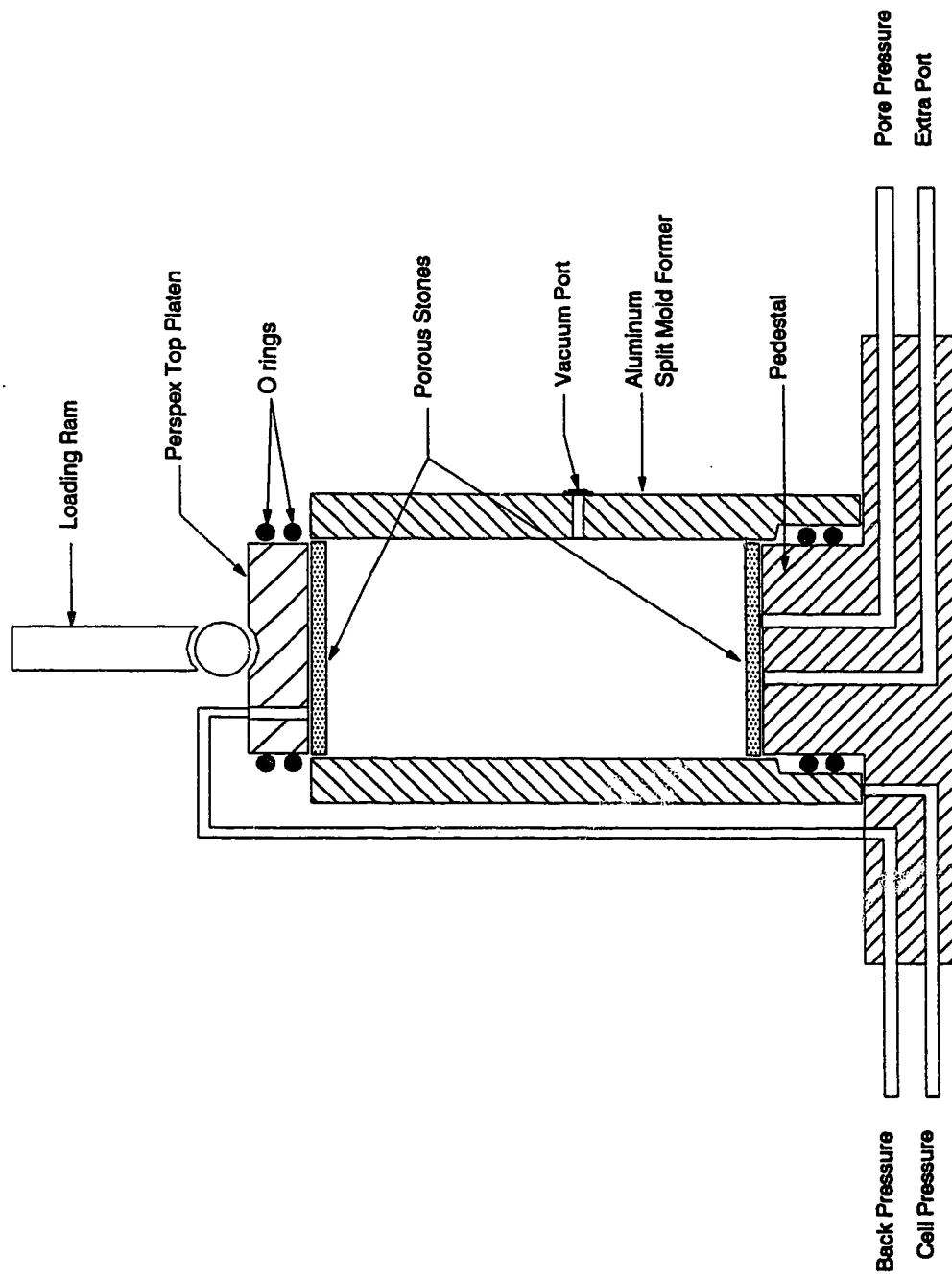
Figure 3.2   Equipment for Preparing Triaxial Cell Specimens

4.0 Experimental Results

4.1 Introduction

The laboratory testing program was separated into two parts. The first part investigated the softening stage while the last part investigated the strength characteristics.

Syncrude's Clearwater Formation clay shale overburden is subdivided into sub-units labelled Kca to Kcf and Kcw. The Kcc Clearwater Formation unit was chosen because it is the thickest of the units that will be encountered as mining progresses towards the northwest of their present mine. The Kcc clay shale collected for the softening stage tests was excavated from the northwest corner of Syncrude's lease property, near the test site of the field pilot dredging operation (Lord and Isaac 1988). Additional Kcc clay shale, required for the strength tests, was excavated from a site close to the first location.

The following section characterizes the clay shale used for the testing program as well as summarizes the results from the softening and strength tests.

4.2 Index Tests

Index tests were performed on the two separate batches of Kcc clay shale collected for the softening stage tests and the strength tests. The first lot was used for the softening stage tests while the second lot was used for the triaxial shear strength tests. Since the Kcc clay shale was obtained at two separate times, representative samples were taken from each lot and characterized separately.

4.2.1 Atterberg Limits

The representative samples that were collected have been characterized by their Atterberg Limits. The results are presented in Table 4.1. The second lot of Kcc clay shale has higher Atterberg limits than the first lot. The difference in plasticity of these two lots of clay shale did not appear to have any significant effect.

4.2.2 Relative Density

Representative samples from each of the two clay shale lots were analysed for their relative density. Both samples were analysed using typical ASTM test methods. The first lot was tested using methanol as the wetting agent while the second lot of clay shale was tested two ways; one using water and the

other using methanol as the wetting agent. Methanol, similar to kerosine, is a better wetting agent than water (ASTM D854-83). The first lot of clay shale has a slightly lower relative density than the second lot (Table 4.2).

Relative densities were not conducted on the sludge solids. For calculations requiring the relative density of the sludge solids, a value of 2.4 was used. This value is within the range reported by Dusseault et al. (1989).

4.2.3 Grain Size Distribution

Representative samples of clay shale were analysed for grain size distribution using the standard ASTM hydrometer test method. The first and second lot of clay shale were analysed separately (Figure 4.1). The first lot of clay shale is siltier, with a smaller percentage of clay size particles (33% clay size) than the second lot (41% clay size). The grain size distribution of the tailing pond sludge was not investigated but it has been reported by Scott and Chichak (1985) (see Section 4.2.5).

4.2.4 Lump Size Distribution

The testing program required the clay shale lumps to be broken up into sizes that were manageable and small enough for

the size of the testing apparatus. For the softening tests, the clay shale lumps were broken up by hand and sieved. Only the lumps passing the 12.7 mm sieve and retained on the 0.84 mm sieve were used. The strength tests utilized 102 mm diameter by 203 mm high samples made up of two sets of lump sizes. The first set consisted of 12.7 mm maximum diameter lumps with a lump gradation identical to that used for the softening tests. The second set consisted of 19 mm maximum diameter lumps. These were clay shale lumps passing the 19 mm sieve and retained on the 2 mm sieve. The maximum size lumps acceptable for a 102 mm diameter triaxial test sample is 19 mm (Bishop and Henkel 1962). Typical lump size distributions for the two sets of lump sizes are presented in Figure 4.2.

The coefficient of uniformity is a numerical measure of the uniformity of a soil. Values less than 5 indicate that the particle size of the soil is uniform. The coefficient of uniformity is 2.6 and 2.1 for the 12.7 mm and 19 mm lump size distributions, respectively. This demonstrates that both lump size distributions are proportionally similar and very uniform.

4.2.5 Tailing Pond Sludge

Tailings pond sludge was collected from Syncrude's tailings

pond and analysed for its solids content concentration. Typical solids content concentrations of the tailings sludge, which is defined as the weight of the sludge solids over the total weight, was 30%. The grain size of the sludge solids was not analysed but it has been reported by Scott and Chichak (1985) (Figure 4.3). Bitumen, extracted using the standard practice followed by Syncrude Research and conducted at the University of Alberta, was 6.6% by weight of the total solids. No tailings water was added to the sludge to dilute it to a lower solids content fluid.

4.3 One Dimensional Compression Softening Tests

Six softening tests were conducted using a range of vertical confining stresses from 3.7 kPa to 250 kPa. This represents deposit depths of less than 1 m to 14 m. Clay lumps with a 12.7 mm maximum lump size gradation were used and mixed with tailings pond water.

A summary of the density, void ratio and water content that has been calculated for the condition before softening and after the compression is presented in Table 4.3 for each of the softening tests labelled WMC1 to WMC5. The stress level and test duration is also presented for each of the softening tests.

Vertical displacements of the top platen were measured as the sample compressed and softened. Volume change, which is directly proportional to the change in sample height, is plotted against time in Figures 4.4 to 4.9. Also shown on the plots are the results of hydraulic conductivity measurements conducted at selected times throughout the test.

The test results are analysed and discussed in Chapter 5.

4.4 Consolidated Undrained Triaxial Compression Tests

A total of 29 consolidated undrained triaxial compression tests were conducted using 102 mm diameter by 203 mm high samples made up of prepared clay shale lumps. An additional 13 consolidated undrained triaxial compression tests were conducted on 38 mm diameter by 76 mm high samples made up of homogenized clay shale.

4.4.1 Clay Shale Lump Triaxial Tests

Five test series of consolidated undrained triaxial compression tests investigated combinations of maximum lump size, testing time, pore mixing fluid and confining stress (Table 4.4). Test series one, consisting of 5 tests, utilized clay shale lumps with a maximum size of 12.7 mm mixed with tailings pond water. These tests were labelled PWA2 to PWA6.

Test series two, consisting of 6 tests, analysed the effect of increasing the softening period from an average of 3 to 6 hours. These tests were labelled PWA7 to PWA12. Test series three, consisting of 4 tests, analysed the effect of increasing the softening period further, to an average of 25 hours. These tests were labelled PWA13 to PWA16. The next two test series analysed the effect of using a larger size clay shale lump (19 mm maximum size). Test series 4, consisting of 9 tests, utilized tailings pond water as the mixing fluid. These tests were labelled PWA1A to PWA9A. Test series 5, consisting of 5 tests, utilized tailings pond sludge as the mixing fluid. These tests were labelled PSA1 to PSA5.

The total testing time can be separated into three stages; softening, consolidation, and shearing. The softening stage differs from the consolidation and shearing stage in that the clay shale is allowed to soften under a low confining stress of 10 kPa. The small confining stress was required to provide support to the sample. Since the Kcc clay shale has an affinity to water, the softening period time should impact on its strength behaviour. The softening fluid is either tailings pond water or tailings sludge. Tailings sludge is a clay-silt suspension which exhibits low hydraulic conductivities into Kcc clay shale. This property makes the sludge a unique medium to hydraulically transport Kcc clay shale lumps. Tailings pond water, also a by-product of the

extraction process, is the clarified water above the sludge in the tailings pond.

The large diameter triaxial test apparatus, which has the capacity to test up to 102 mm diameter by 203 mm high samples, was required to accommodate the 19 mm maximum diameter clay shale lumps.

The density, void ratio and water content of the clay lump structure was determined before saturating the sample, after saturation and softening, and after consolidation. These measurements, as well as the stress levels and test duration times, are presented for each of the triaxial tests of test series 1 to 5 in Tables 4.5 to 4.9.

A load cell, LVDT, and pore pressure transducers measured the response of the sample during consolidation and shearing. The volume change during the consolidation/softening period for each of the triaxial tests of test series 1 to 5 are presented in Figures B1 to B29 (Appendix B). During shear, the deviator stress and pore pressure were measured and the pore pressure parameter A-bar was calculated for each of the triaxial tests. These parameters are plotted against axial shear strain in Figures B43 to B71 (Appendix B). For brevity, representative test results from one triaxial test of each test series is presented in this chapter. Figures 4.10 to

4.14 are the consolidation/softening plots for triaxial tests PWA3, PWA7, PWA13, PWA6A and PSA3. Similarly, Figures 4.18 to 4.22 show the parameters measured during shear for the respective triaxial tests.

The test results are analysed and discussed in Chapter 5.

4.4.2   Homogenized Clay Shale Triaxial Tests

To simulate the ultimate or fully softened state of the clay shale, 13 consolidated undrained triaxial compression tests were conducted on homogenized clay shale samples. The 13 tests are divided into three test series (series 6, 6a, and 7). Test series 6, consisting of 5 tests, were conducted on clay shale homogenized with tailing pond water. For these tests, labelled PWMS1 to PWMS5, the back pressure was inadvertently lowered prior to consolidation and shearing, so the samples may not have been fully saturated. Three more tests, labelled PWMS6 to PWMS8 (test series 6A), were conducted to substantiate the results from test series 6. Test series 7, consisting of 5 tests, were conducted on clay shale homogenized with tailings pond sludge. These tests are labelled PSMS1 to PSMS5.

The density, void ratio and water content of the homogenized test samples were determined before softening, after

saturation and softening, and after consolidation. These values, as well as the stress levels and test duration times, are presented for each of the test series 6, 6A and 7 in Tables 4.10 to 4.12.

The volume change during consolidation was plotted for each of the homogenized triaxial tests and are presented in Figures B30 to B42 (Appendix B). The deviator stress, pore pressure and pore pressure parameter A-bar for each of the homogenized triaxial tests are presented in Figures B72 to B84 (Appendix B).

For brevity, representative test results from one triaxial test of each homogenized clay shale test series is presented in this chapter. Figures 4.15 to 4.17 are the consolidation plots for triaxial tests PWMS2, PWMS6 and PSMS4. Similarly, Figures 4.23 to 4.25 show the parameters measured during shear for the respective triaxial tests.

The test results are analysed and discussed in Chapter 5.

	Softening Tests (Lot 1)		Strength Tests (Lot 2)	
Table 4.1 **Atterberg Limits**				
	mean	range	mean	range
Liquid Limit	52%	50.7-53.0	82%	78.0-89.0
Plastic Limit	20%	20.0-20.3	24%	-
Plasticity Index	32%	30.4-34.1	58%	-
Liquidity Index	-.03	-.034--.031	-.05	-
Natural Water %	19%	18.9-19.3	21%	17.0-22.5

	Softening Tests (Lot 1)	Strength Tests (Lot 2)
Table 4.2 **Relative Density**		
with water	--	2.75
with methanol	2.69	2.72

Table 4.3	1D Compression/Softening Test Results					

Test No.	WMC1	WMC2	WMC3	WMC4	WMC5	WMC6
Confining						
Stress (kPa)	250.0	3.7	100.0	41.0	57.5	65.7
Max Lump Size (mm)	12.7	12.7	12.7	12.7	12.7	12.7
Mixing Fluid	water*	water*	water*	water*	water*	water*
BEFORE SOFTENING:						
Density (kg/m3)						
dry density	892.0	1226.8	1072.4	1071.3	1208.0	1072.0
bulk density	1560.4	1770.7	1673.7	1673.1	1758.9	1673.5
Void Ratio						
initial ei	2.016	1.193	1.508	1.511	1.227	1.509
macro eM	1.462	0.690	0.997	0.994	0.716	0.998
micro em	0.554	0.503	0.511	0.516	0.511	0.511
Water Content %	20.6	18.7	19.0	19.2	19.0	19.0
AFTER COMPRESSION:						
Density (kg/m3)						
dry density	1577.9	1383.6	1543.8	1511.2	1522.7	1534.3
bulk density	1991.3	1869.3	1969.9	1949.4	1956.6	1964.0
Void Ratio						
final ef	0.705	0.944	0.742	0.780	0.767	0.753
Water Content %						
lumps	--	28.5	--	22.0	23.5	21.6
bulk	26.2	35.1	27.6	29.0	28.5	28.0
TEST DURATION:						
(hrs)	1.1	95.1	2.6	119.7	122	142.4

* Tailings pond water

Table 4.4   Consolidated Undrained Triaxial Compression Test Series

	Test Series 1	Test Series 2	Test Series 3	Test Series 4	Test Series 5	Test Series 6	Test Series 6A	Test Series 7
CONFINING STRESS RANGE (kPa):	182-298	199-434	179-428	283-505	257-541	150-550	150-500	157-544
MAXIMUM LUMP SIZE (mm) :	12.7	12.7	12.7	19	19	Homo	Homo	Homo
TIME: (hrs)								
Softening	3	6	25	24-64	63	2	15	7
Consolidation	23	46	34	24	82	30	105	24
Shearing	8	7	8	9	8	3	8	9
Total	34	59	66	57-96	153	35	128	31
MIXING FLUID:	water*	water*	water*	water*	sludge	water*	water**	sludge
NO. OF TESTS:	5	6	4	9	5	5	3	5

* tailings pond water

Table 4.5		Clay Shale Lump Triaxial Tests - Series 1			
Test No.	PWA2	PWA3	PWA4	PWA5	PWA6
Effect Confining					
Stress (kPa)	264.6	288.8	240.6	181.6	297.6
Back Pressure	162.1	220.3	234.4	143.3	248.6
Max Lump Size (mm)	12.7	12.7	12.7	12.7	12.7
Mixing Fluid	water*	water*	water*	water*	water*
BEFORE SOFTENING:					
Density (kg/m3)					
dry density	891.5	860.1	882.0	948.9	986.9
bulk density	1078.7	1040.7	1074.3	1147.3	1195.2
Void Ratio					
initial ei	2.051	2.162	2.084	1.866	1.756
macro eM	1.480	1.591	1.491	1.298	1.182
micro em	0.571	0.571	0.593	0.568	0.754
Water Content %	21.0	21.0	21.8	20.9	21.1
AFTER SATURATION & SOFTENING:					
Density (kg/m3)					
dry density	1233.5	1249.8	1313.7	1154.9	1296.2
bulk density	1780	1790.3	1830.7	1730.3	1819.7
Void Ratio ein	1.205	1.176	1.070	1.355	1.098
Water Content %	44.3	43.3	39.4	49.8	40.4
AFTER CONSOLIDATION:					
Density (kg/m3)					
dry density	1502.3	1522	1522.9	1504.6	1532.2
bulk density	1950	1962.4	1963	1951.4	1968.9
Void Ratio ef	0.811	0.787	0.786	0.808	0.775
Water Content %	29.8	28.9	28.9	29.7	28.5
TEST DURATION (hrs):					
softening	3.5	3.8	3.7	2.2	3.3
consolidation	21.5	24.1	19.5	22.6	25.8
shear	8.4	8.1	9.5	7.6	7.5
total	33.4	36	32.7	32.4	36.6

* Tailings pond water
** Side drains used

| Table 4.6 | Clay Shale Lump Triaxial Tests - Series 2 | | | | | |

Test No.	PWA7	PWA8	PWA9	PWA10	PWA11	PWA12
Effect Confining						
Stress (kPa)	370.6	434.4	288.5	199.0	339.5	398.5
Back Pressure	246.0	288.6	211.7	210.9	213.0	212.9
Max Lump Size (mm)	12.7	12.7	12.7	12.7	12.7	12.7
Mixing Fluid	water*	water*	water*	water*	water*	water*
BEFORE SOFTENING:						
Density (kg/m3)						
dry density	969.8	1005.9	1083.5	999.7	972.7	957.4
bulk density	1166.7	1221.2	1299.2	1206.7	1175.0	1162.3
Void Ratio						
initial ei	1.805	1.704	1.510	1.721	1.796	1.841
macro eM	1.252	1.122	0.969	1.158	1.231	1.259
micro em	0.552	0.582	0.541	0.563	0.566	0.582
Water Content %	20.3	21.4	19.9	20.7	20.8	21.4
AFTER SATURATION & SOFTENING:						
Density (kg/m3)						
dry density	1263.48	1273.9	1175.9	1058.1	1063.4	1117.7
bulk density	1798.96	1805.6	1743.6	1669.1	1672.4	1706.8
Void Ratio ein	1.153	1.135	1.313	1.571	1.558	1.433
Water Content %	42.4	41.7	48.3	57.8	57.3	52.7
AFTER CONSOLIDATION:						
Density (kg/m3)						
dry density	1548.8	1570.7	1529.9	1473.5	1509.1	1506.8
bulk density	1979.4	1993.3	1967.4	1931.8	1954.3	1952.9
Void Ratio ef	0.756	0.732	0.778	0.846	0.802	0.805
Water Content %	27.8	26.9	28.6	31.1	29.5	29.6
TEST DURATION (hrs):						
softening	1.7	4.6	6.3	7.7	7.8	8
consolidation	49.9	50.5	49.3	44.6	39.8	38.6
shear	7	6.3	7	7.8	7.8	7.9
total	58.6	61.4	62.6	60.1	55.4	54.5

* Tailings pond water
** Side drains used

Table 4.7   Clay Shale Lump Triaxial Tests - Series 3

Test No.	PWA13	PWA14	PWA15	PWA16
Effect Confining				
Stress (kPa)	288.2	427.6	178.7	355.8
Back Pressure	213.0	213.3	212.6	214.1
Max Lump Size (mm)	12.7	12.7	12.7	12.7
Mixing Fluid	water*	water*	water*	water*
BEFORE SOFTENING:				
Density (kg/m3)				
dry density	988.3	1129.8	998.8	1027.5
bulk density	1201.8	13.....	1201.6	1225.7
Void Ratio				
initial ei	1.752	1....	1.723	1.647
macro eM	1.165	0.85:	1.171	1.122
micro em	0.588	0....	0.552	0.525
Water Content %	21.6	...4	20.3	19.3
AFTER SATURATION & SOFTENING:				
Density (kg/m3)				
dry density	1005.2	1230.2	1186.7	1221.2
bulk density	1635.6	1777.9	1750.4	1772.3
Void Ratio ein	1.706	1.211	1.292	1.227
Water Content %	62.7	44.5	47.5	45.1
AFTER CONSOLIDATION:				
Density (kg/m3)				
dry density	1421.2	1518.3	1450.0	1488.9
bulk density	1698.7	1960.1	1916.9	1941.5
Void Ratio ef	0.914	0.792	0.876	0.827
Water Content %	33.6	29.1	32.2	30.4
TEST DURATION (hrs):				
softening	24.5	24.7	24	24.8
consolidation	40.1	47.1	24.3	22.8
shear	7.5	8	7.8	8.5
total	72.1	79.8	56.1	56.1

* Tailings pond water
** Double drainage (top and bottom)

Table 4.8		Clay Shale Lump Triaxial Tests - Series 4				
Test No.	PWA1A	PWA2A	PWA3A	PWA4A	PWA5A	PWA6A
Effect Confining						
Stress (kPa)	358.5	426.9	300.8	359.0	356.2	425.0
Back Pressure	213.8	212.7	211.4	210.9	213.8	216.7
Max Lump Size (mm)	19	19	19	19	19	19
Mixing Fluid	water*	water*	water*	water*	water*	water*
BEFORE SOFTENING:						
Density (kg/m3)						
dry density	1220.0	1029.0	1040.8	1043.4	1003.3	1049.6
bulk density	1465.2	1237.9	1253.1	1250.0	1222.0	1266.9
Void Ratio						
initial ei	1.229	1.643	1.613	1.607	1.711	1.591
macro eM	0.683	1.091	1.059	1.068	1.118	1.028
micro em	0.547	0.552	0.555	0.539	0.593	0.563
Water Content %	20.1	20.3	20.4	19.8	21.8	20.7
AFTER SATURATION & SOFTENING:						
Density (kg/m3)						
dry density	1295.7	1286.9	1299.1	1229.8	1238.4	1256.7
bulk density	1819.3	1813.8	1821.5	1777.7	1783.1	1794.68
Void Ratio ein	1.099	1.114	1.094	1.212	1.196	1.164
Water Content %	40.4	40.9	40.2	44.6	44.0	42.8
AFTER CONSOLIDATION:						
Density (kg/m3)						
dry density	1539.3	1967.4	1544.1	1529.9	1509.1	1544.1
bulk density	1973.4	1529.9	1976.4	1967.4	1954.3	1976.4
Void Ratio ef	0.767	0.778	0.762	0.778	0.802	0.762
Water Content %	28.2	28.6	28	28.6	29.5	28
TEST DURATION (hrs):						
softening	24.8	24.6	24.3	24	61.7	60.5
consolidation	22.9	24.4	23.9	23.7	23.8	25
shear	8.5	8.5	9	8.3	8.3	8.5
total	56.2	57.4	57.2	56	93.8	94

* Tailings pond water
** Double drainage (top and bottom)

Table 4.8 (cont)   Clay Shale Lump Triaxial Tests - Series 4

Test No.	PWA7A	PWA8A	PWA9A
Effect Confining			
Stress (kPa)	283.4	504.6	496.1
Back Pressure	216.9	220.7	215.1
Max Lump Size (mm)	19	19	19
Mixing Fluid	water*	water*	water*
BEFORE SOFTENING:			
Density (kg/m3)			
dry density	1046.7	946.8	1007.4
bulk density	1268.6	1144.7	1228.1
Void Ratio			
initial ei	1.599	1.873	1.700
macro eM	1.022	1.304	1.104
micro em	0.577	0.568	0.596
Water Content %	21.2	20.9	21.9
AFTER SATURATION & SOFTENING:			
Density (kg/m3)			
dry density	1311.41	1158.7	1164.6
bulk density	1829.3	1732.7	1736.5
Void Ratio ein	1.074	1.347	1.335
Water Content %	39.5	49.5	49.1
AFTER CONSOLIDATION:			
Density (kg/m3)			
dry density	1575.7	1529.9	1529.9
bulk density	1996.4	1967.4	1967.4
Void Ratio ef	0.726	0.778	0.778
Water Content %	26.7	28.6	28.6
TEST DURATION (hrs):			
softening	61.6	60.5	73.9
consolidation	23.2	23.4	22.8
shear	9.1	8.8	8.5
total	93.9	92.7	105.2

* Tailings pond water
** Double drainage (top and bottom)

Table 4.9	Clay Shale Lump Triaxial Tests - Series 5				

Test No.	PSA1	PSA2	PSA3	PSA4	PSA5
Effect Confining					
Stress (kPa)	360.7	428.9	257.3	432.1	541.0
Back Pressure	201.3	201.7	199.5	198.0	200.1
Max Lump Size (mm)	19	19	19	19	19
Mixing Fluid	sludge	sludge	sludge	sludge	sludge
%solids	29.5	27.7	29.0	35.3	30.2
BEFORE SOFTENING:					
Density (kg/m3)					
dry density	1179.0	1143.3	1188.7	1063.6	1038.1
bulk density	1377.1	1400.5	1456.1	1300.8	1257.1
Void Ratio					
initial ei	1.307	1.379	1.288	1.557	1.620
macro eM	0.850	0.767	0.676	0.951	1.046
micro em	0.457	0.612	0.612	0.607	0.574
Water Content %	16.8	22.5	22.5	22.3	21.1
AFTER SATURATION & SOFTENING:					
Density (kg/m3)					
dry density	1230.9	1098.6	1098.9	1185.3	1152.7
bulk density	1773.5	1690.0	1683.5	1743.6	1723.9
Void Ratio ein	1.186	1.448	1.467	1.264	1.332
Water Content %	44.1	53.8	54.6	47.1	49.6
AFTER CONSOLIDATION:					
Density (kg/m3)					
dry density	1456.4	1453.7	1476.4	1563.4	1555.1
bulk density	1915.2	1913.1	1926.7	1980.8	1976.6
Void Ratio ef	0.848	0.85	0.819	0.717	0.728
Water Content %	31.5	31.6	30.5	26.7	27.1
TEST DURATION (hrs):					
softening	63.9	62.8	61.8	63	62.8
consolidation	23.7	24.8	114.1	135.7	111.1
shear	8.5	8.3	8.3	8.3	8.1
total	96.1	95.9	184.2	207	182

** Double drainage (top and bottom)

Table 4.10   Homogenized Clay Shale Triaxial Tests - Series 6

Test No.	PWMS1	PWMS2	PWMS3	PWMS4	PWMS5
Effect Confining					
Stress (kPa)	150	250	350	450	550
Back Pressure	50	50	50	50	50
Mixing Fluid	water*	water*	water*	water*	water*
BEFORE SOFTENING:					
Density (kg/m3)					
dry density	1470.0	1470.0	1470.0	1470.0	1470.0
bulk density	1911.0	1911.0	1911.0	1911.0	1911.0
Void Ratio					
initial ei	0.850	0.850	0.850	0.850	0.850
air ea	0.034	0.034	0.034	0.034	0.034
micro em	0.816	0.816	0.816	0.816	0.816
Water Content %	30.0	30.0	30.0	30.0	30.0
AFTER SATURATION & SOFTENING:					
Density (kg/m3)					
dry density	1409.1	1395.7	1396.9	1408.5	1391.5
bulk density	1891.0	1844.6	1845.4	1890.7	1879.9
Void Ratio ein	0.930	1.036	1.035	0.931	0.955
Water Content %	34.2	38.1	38.0	34.2	35.1
AFTER CONSOLIDATION:					
Density (kg/m3)					
dry density	1460.6	1464.9	1477.9	1493.1	1532.2
bulk density	1923.6	1926.3	1934.5	1944.2	1968.9
Void Ratio ef	0.862	0.857	0.840	0.822	0.775
Water Content %	31.7	31.5	30.9	30.21	28.5
TEST DURATION (hrs):					
softening***	2	2	2	2	2
consolidation	17	21	18	72	24
shear	2	2.9	2.6	3	2.1
total	21	25.9	22.6	77	28.1

* Tailings pond water
** Side drains used
*** Estimated

Table 4.11   Homogenized Clay Shale Triaxial Tests - Series 6A

Test No.	PWMS6	PWMS7	PWMS8
Effect Confining Stress (kPa)	336.8	149.9	499.8
Back Pressure	590.0	190.3	290.1
Mixing Fluid	water*	water*	water*
BEFORE SOFTENING:			
Density (kg/m3)			
dry density	1311.0	1324.5	1291.8
bulk density	1800.1	1815.0	1782.6
Void Ratio			
initial ei	1.075	1.054	1.106
air ea	0.060	0.046	0.072
micro em	1.015	1.007	1.033
Water Content %	37.3	37.0	38.0
AFTER SATURATION & SOFTENING:			
Density (kg/m3)			
dry density	1298.7	1289.6	1269.9
bulk density	1821.2	1815.5	1803.0
Void Ratio ein	1.094	1.109	1.142
Water Content %	40.2	40.8	42.0
AFTER CONSOLIDATION:			
Density (kg/m3)			
dry density	1425.2	1374.3	1464.9
bulk density	1901.2	1869.0	1926.3
Void Ratio ef	0.908	0.979	0.857
Water Content %	33.4	36.0	31.5
TEST DURATION (hrs):			
softening	4	20.5	21
consolidation	31.8	142.1	142.3
shear	8.7	6.9	6.9
total	44.5	169.5	170.2

* Tailings pond water
** Side drains used

Table 4.12   Homogenized Clay Shale Triaxial Tests - Series 7

Test No.	PSMS1	PSMS2	PSMS3	PSMS4	PSMS5
Effect Confining					
Stress (kPa)	156.9	349.8	252.3	543.9	447.3
Back Pressure	690.0	892.4	490.2	689.8	590.2
Mixing Fluid	sludge	sludge	sludge	sludge	sludge
%solids	28	28	28	28	28
BEFORE SOFTENING:					
Density (kg/m3)					
dry density	1425.6	1452.3	1395.5	1375.6	1417.6
bulk density	1864.0	1874.3	1846.4	1833.5	1872.3
Void Ratio					
initial ei	0.908	0.873	0.949	0.977	0.919
air ea	0.072	0.083	0.070	0.072	0.046
micro em	0.836	0.790	0.879	0.906	0.873
Water Content %	30.7	29.1	32.3	33.3	32.1
AFTER SATURATION & SOFTENING:					
Density (kg/m3)					
dry density	1443.3	1451.7	1386.4	1388.0	1409.5
bulk density	1912.7	1918.0	1876.7	1877.7	1891.3
Void Ratio ein	0.885	0.874	0.962	0.960	0.930
Water Content %	32.5	32.1	35.4	35.3	34.2
AFTER CONSOLIDATION:					
Density (kg/m3)					
dry density	1480.1	1529.9	1471.4	1518.3	1513.7
bulk density	1935.9	1967.4	1930.4	1960.1	1957.2
Void Ratio ef	0.838	0.778	0.849	0.792	0.797
Water Content %	30.8	28.6	31.2	29.1	29.3
TEST DURATION (hrs):					
softening	5.5	6	7.7	12.6	4
consolidation	23.8	22.7	21	21	32.1
shear	7.8	9.2	8.8	8.8	8.7
total	29.3	28.7	28.7	33.6	36.1

** Side drains used
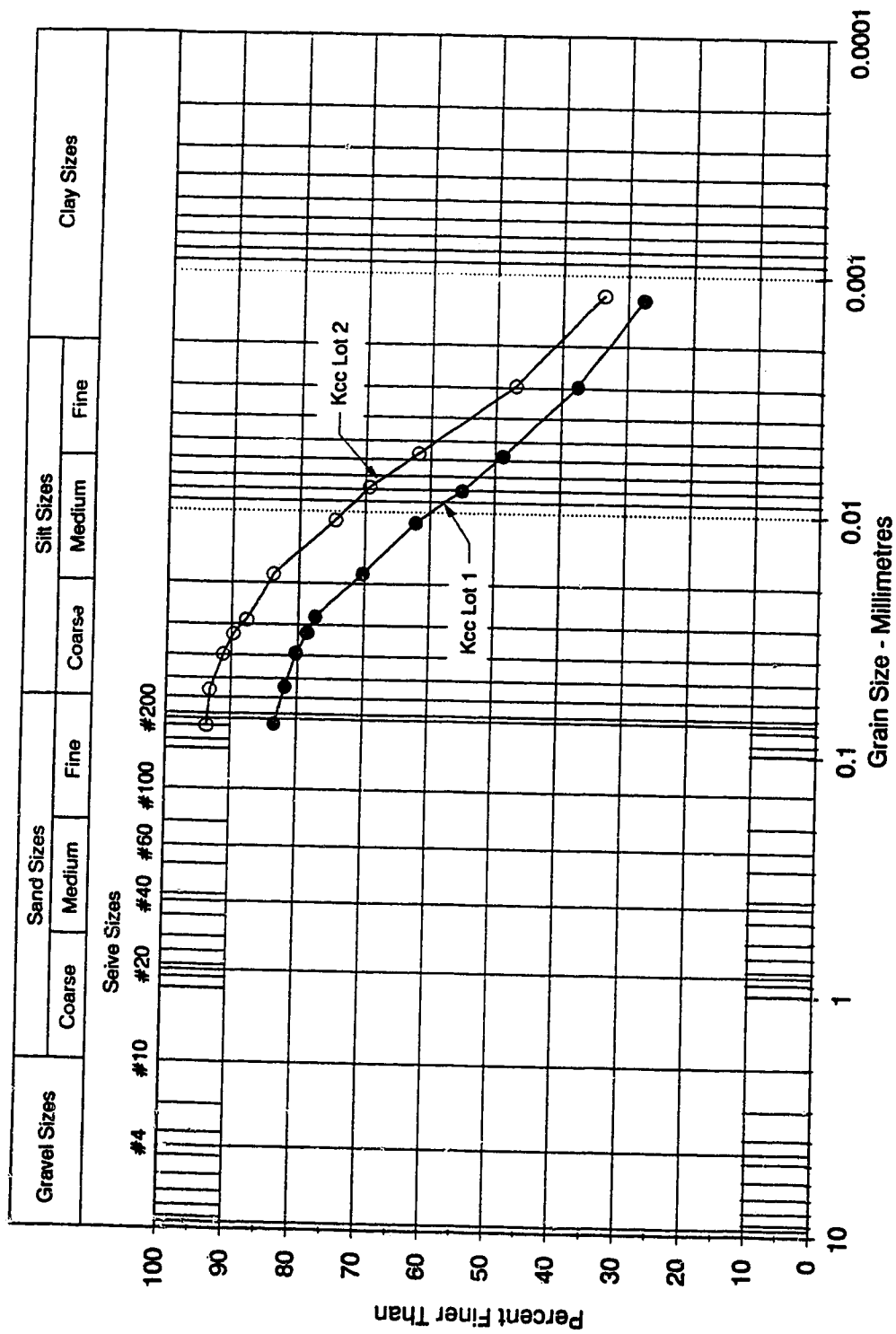
Figure 4.1   Grain Size Curve for Kcc Overburden (Lot 1 & 2)

72
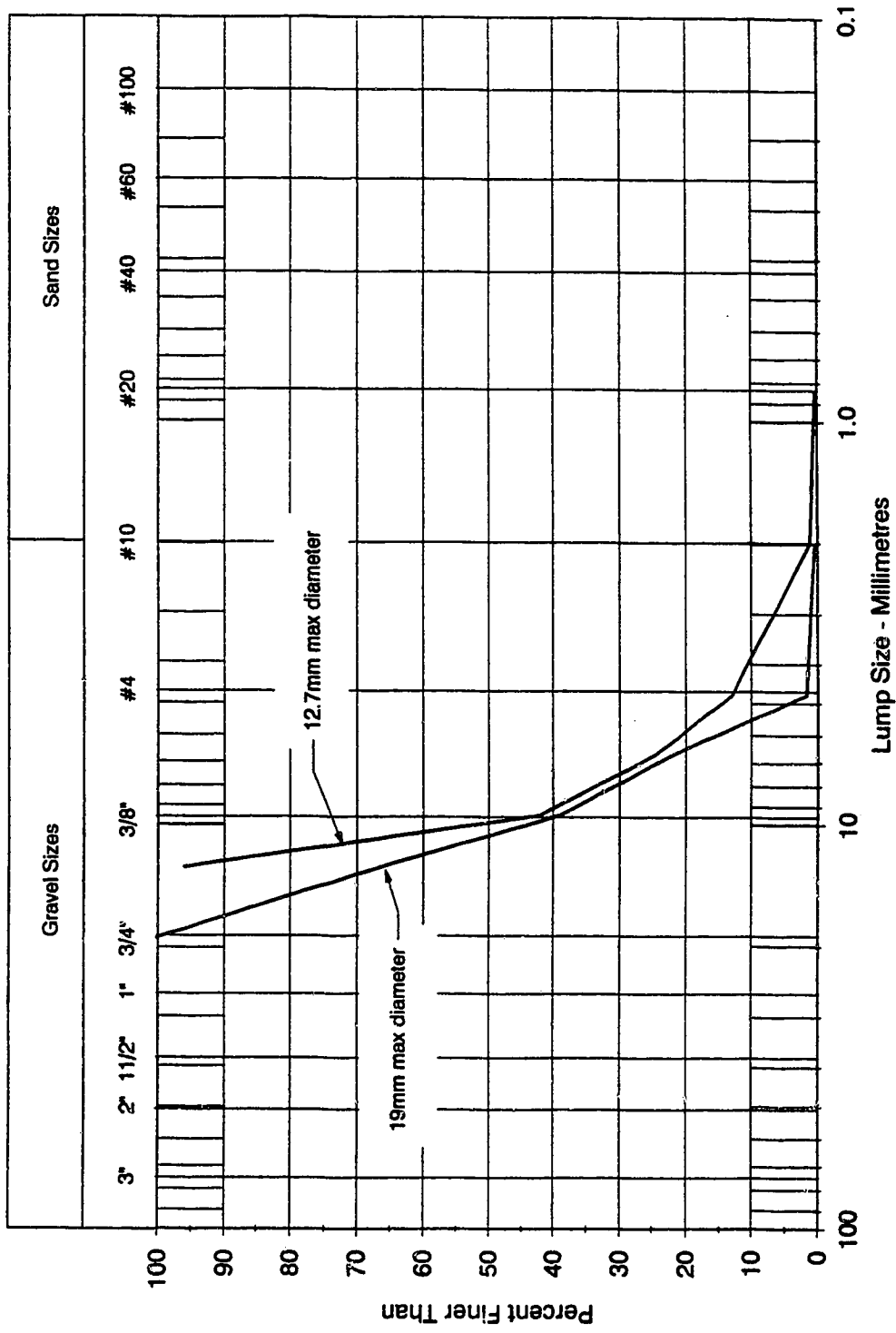
Figure 4.2 Lump Size Distribution of Kcc Clay-shale Lumps

73

Figure 4.3   Grain Size Curve for Tailings Sludge
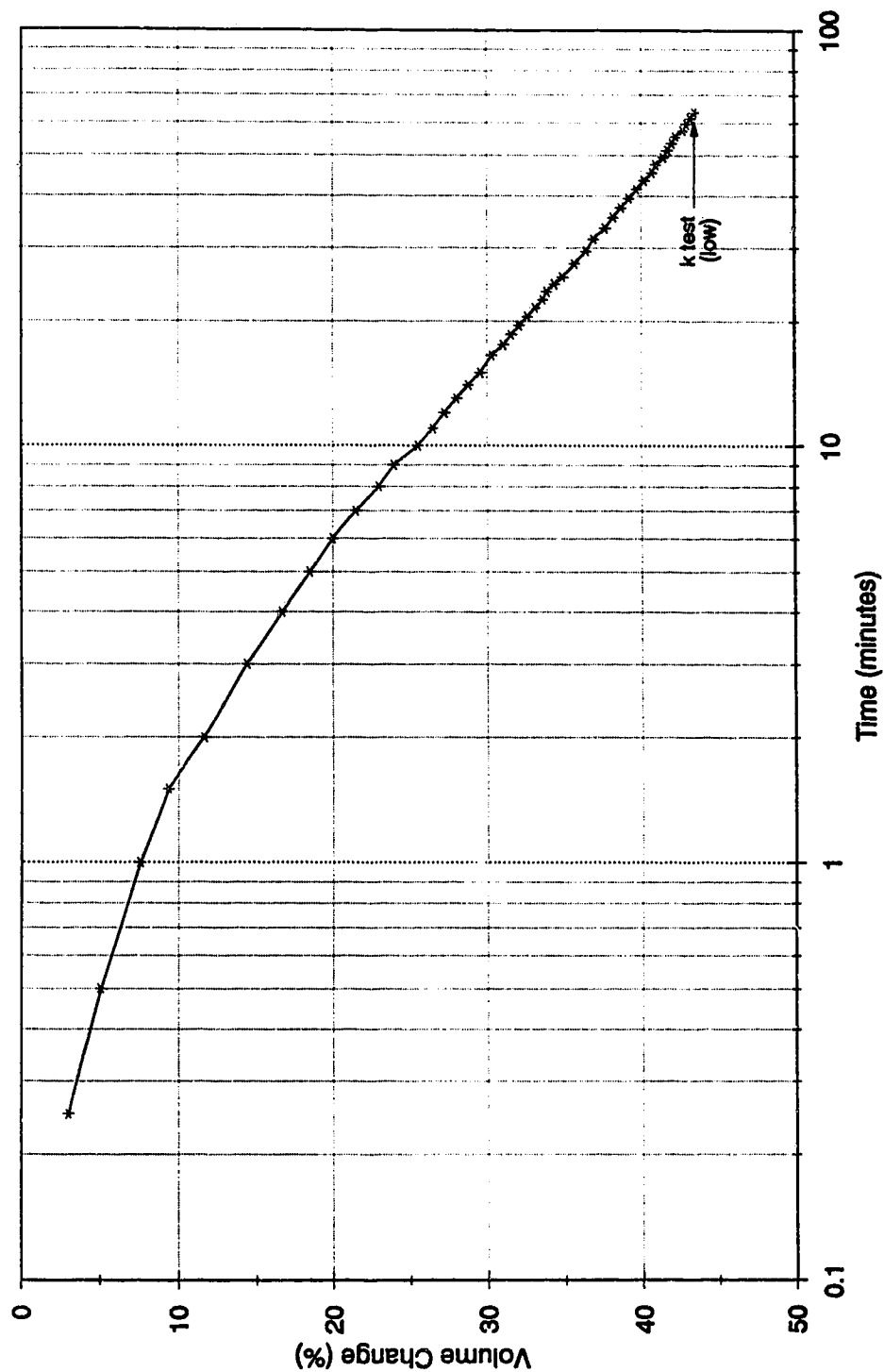
Figure 4.4   Test WMC1
Volume Change during Compression
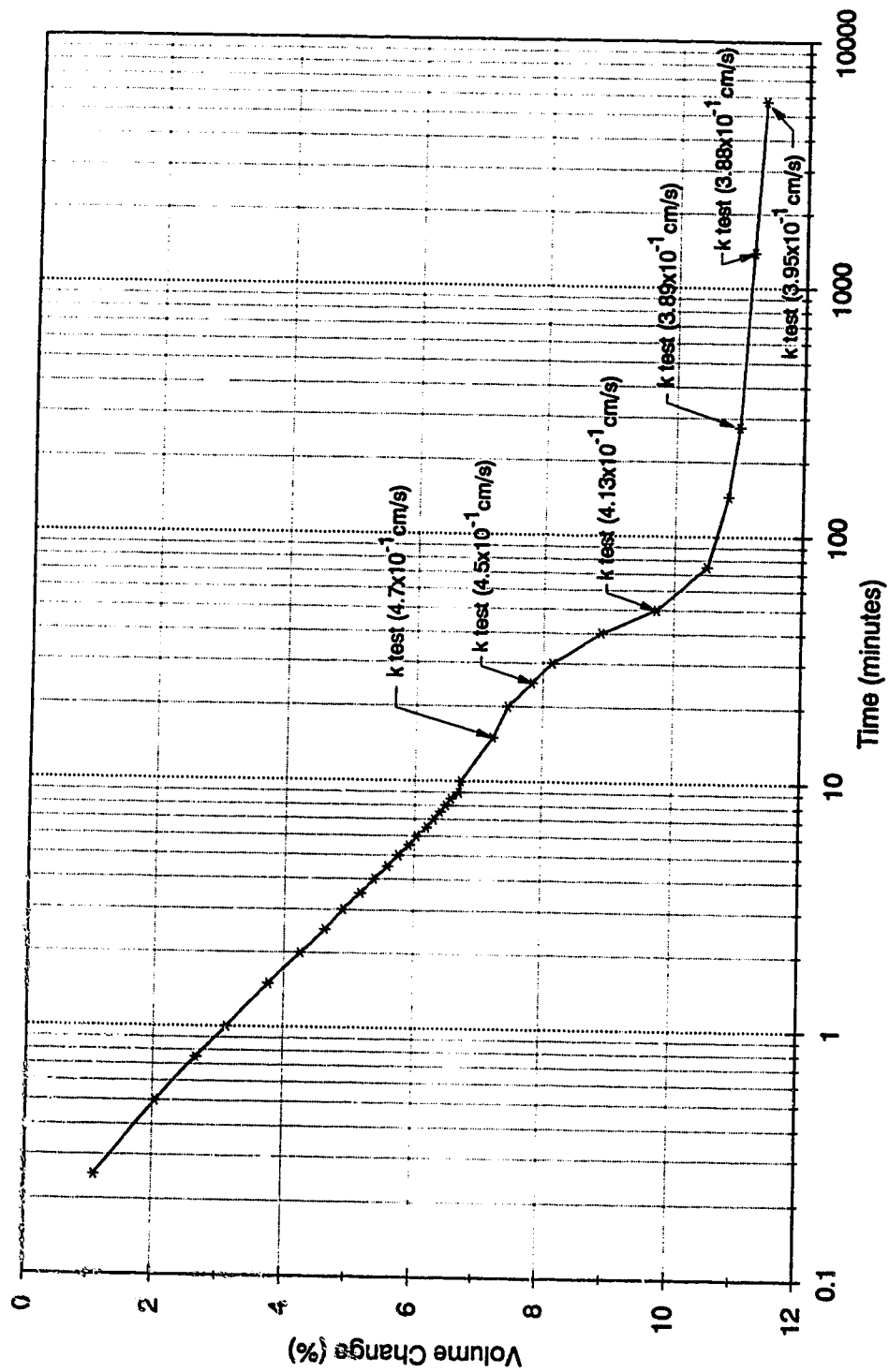
Figure 4.5   Test WMC2
Volume Change during Compression
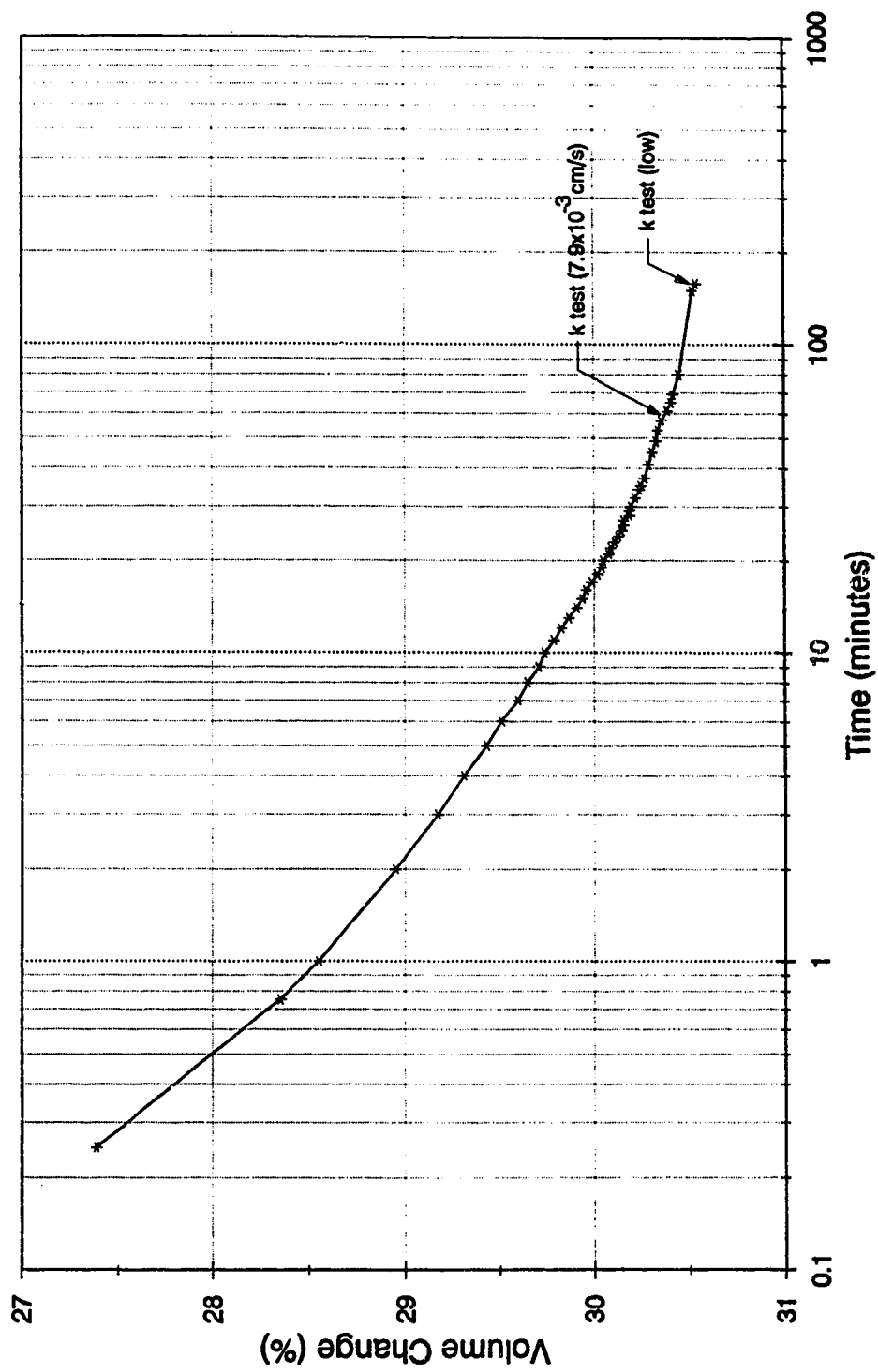
Figure 4.6   Test WMC3
Volume Change during Compression
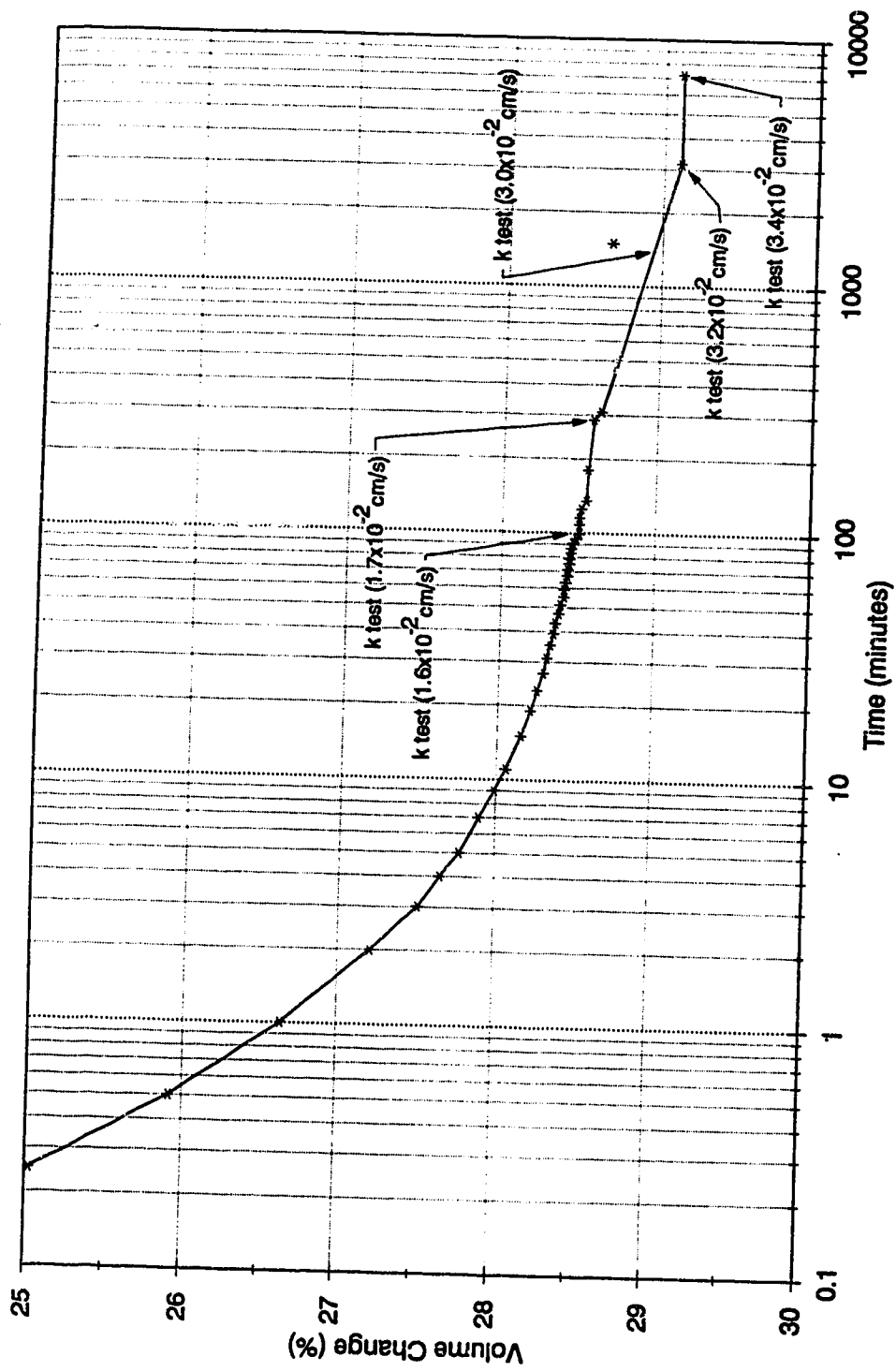
Figure 4.7   Test WMC4
Volume Change during Compression
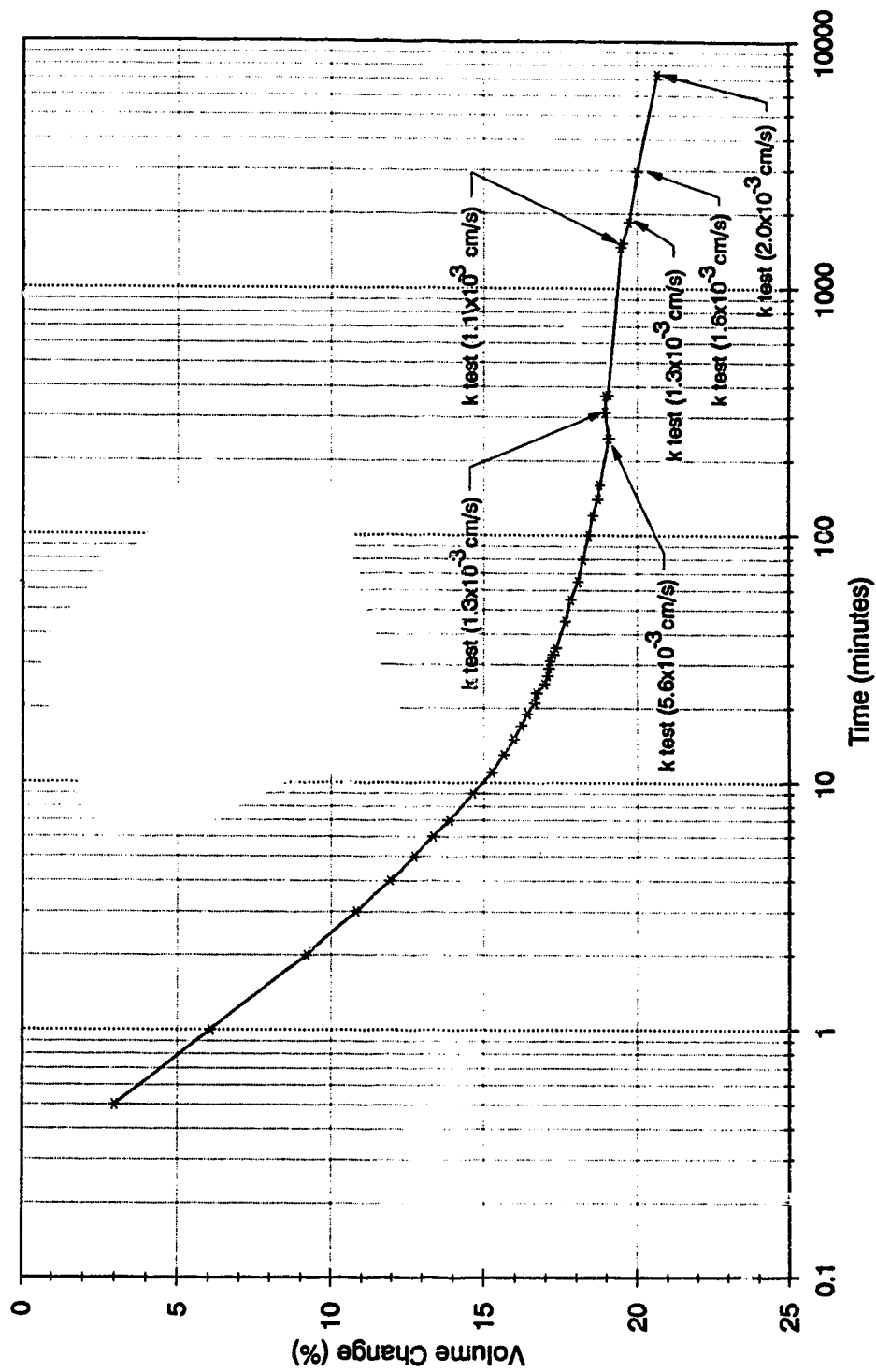
Figure 4.8   Test WMC5
Volume Change during Compression
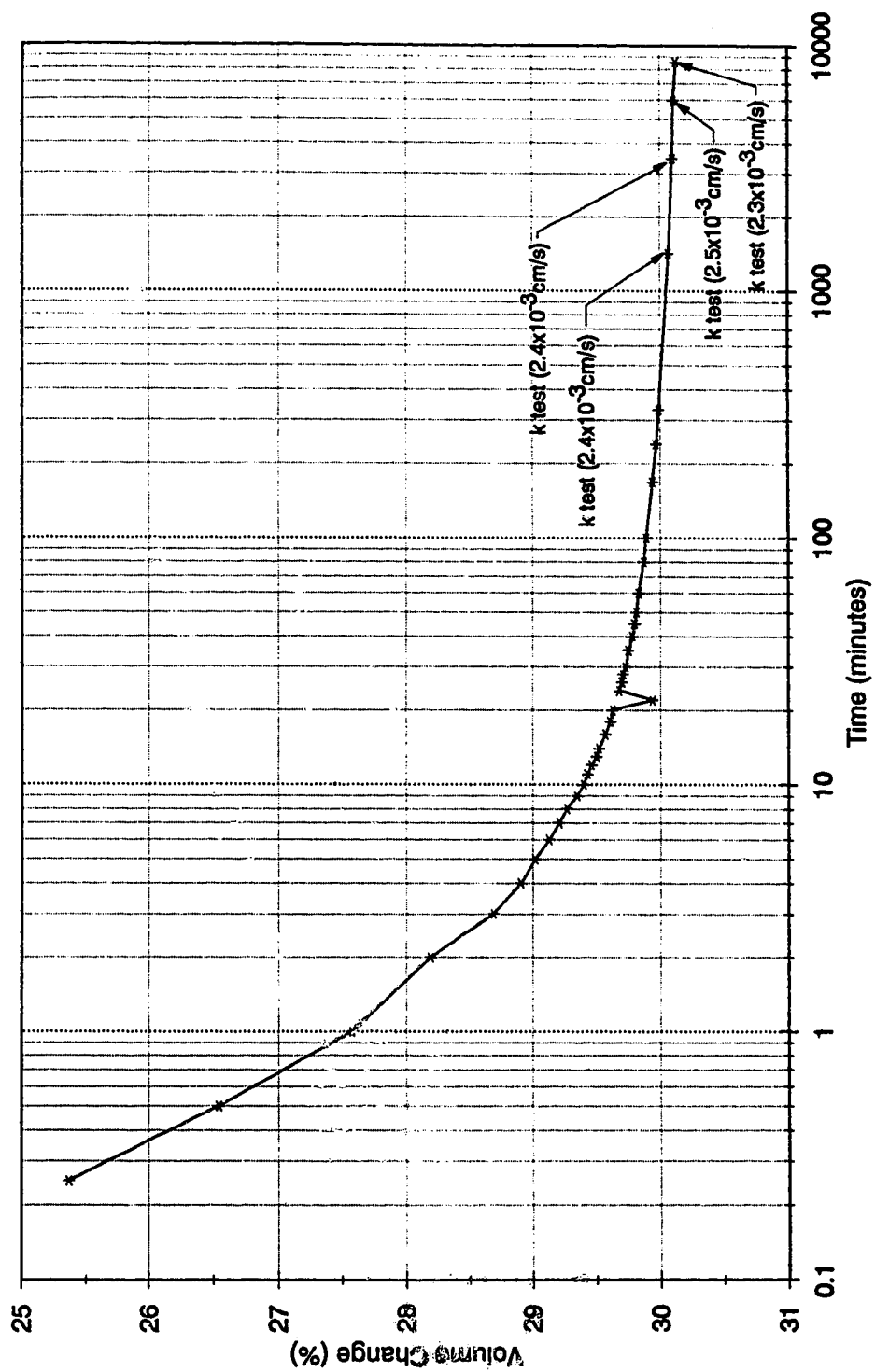
Figure 4.9   Test WMC6
Volume Change during Compression
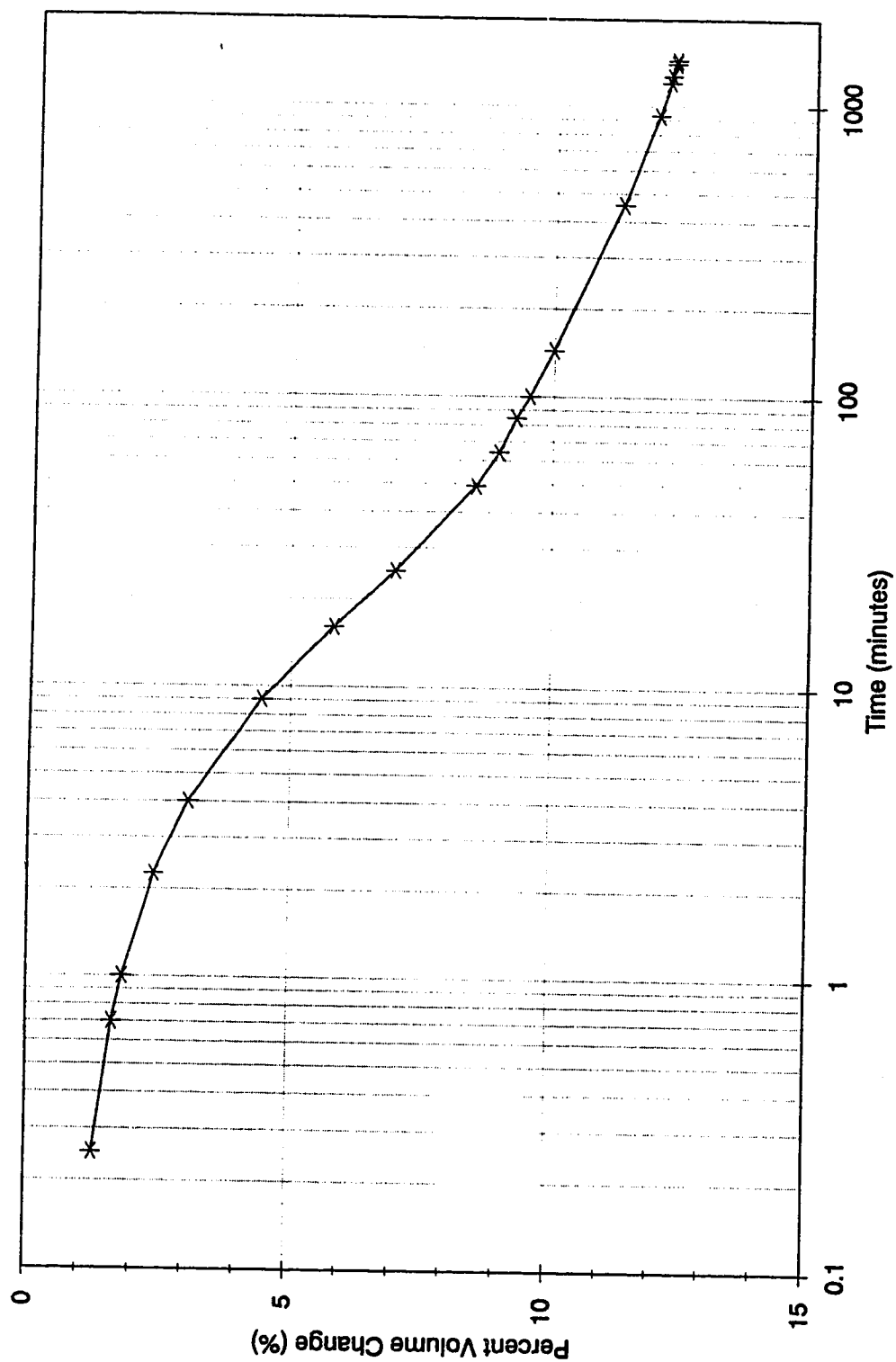
Figure 4.10   Consolidation/Softening - Test PWA3   Series 1
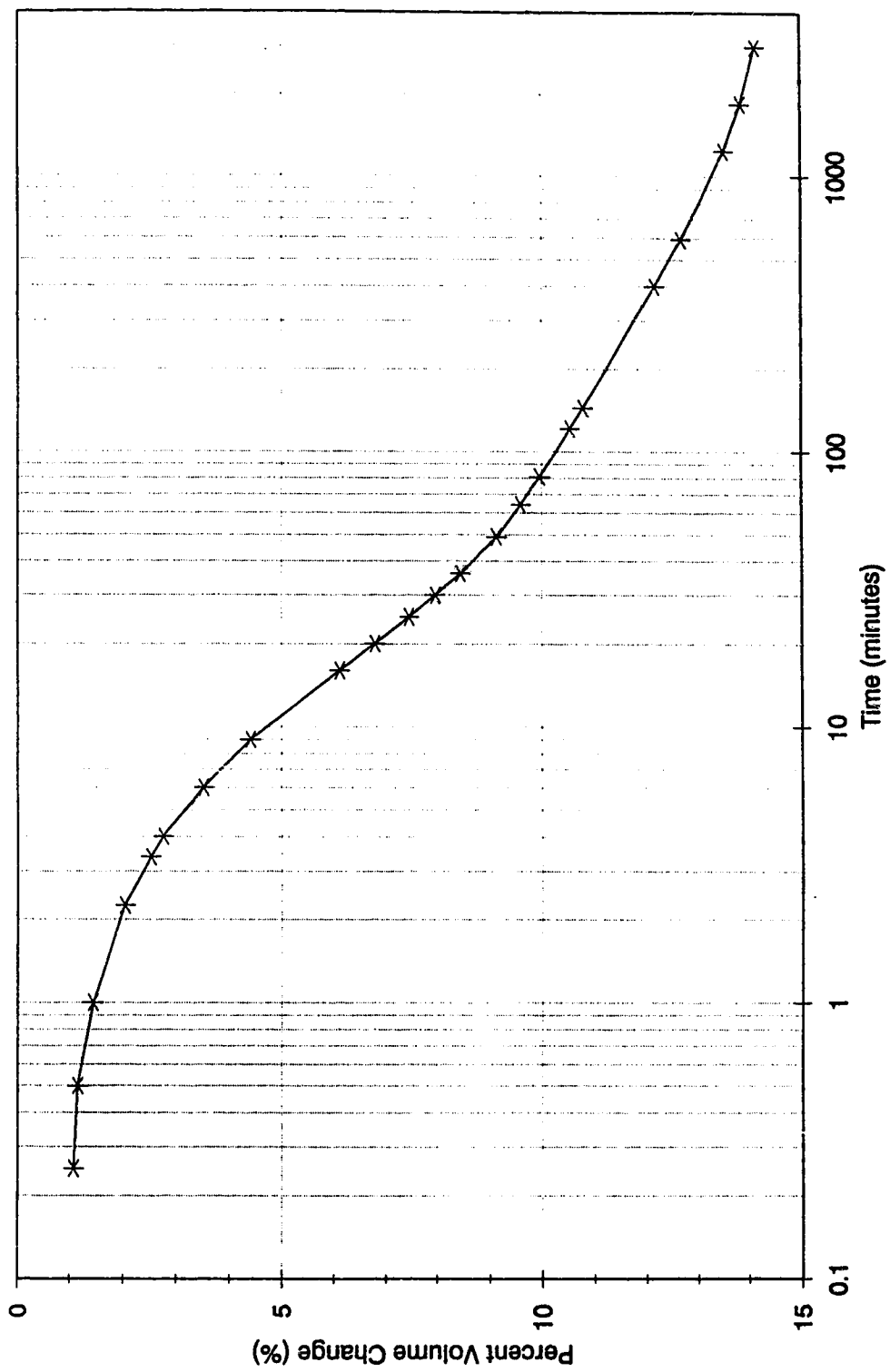
Figure 4.11   Consolidation/Softening - Test PWA7   Series 2
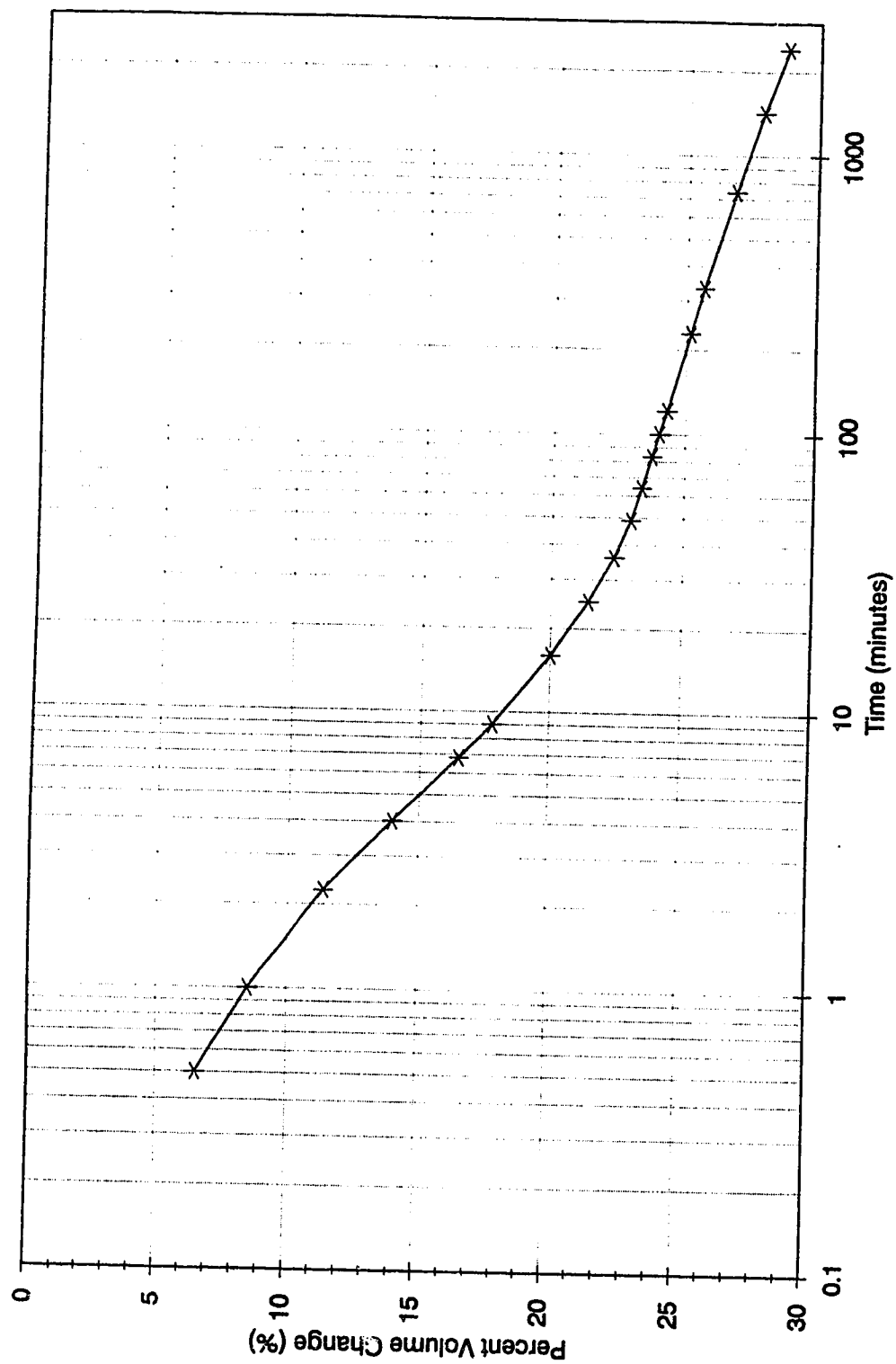
Figure 4.12 Consolidation/Softening - Test PWA13 Series 3
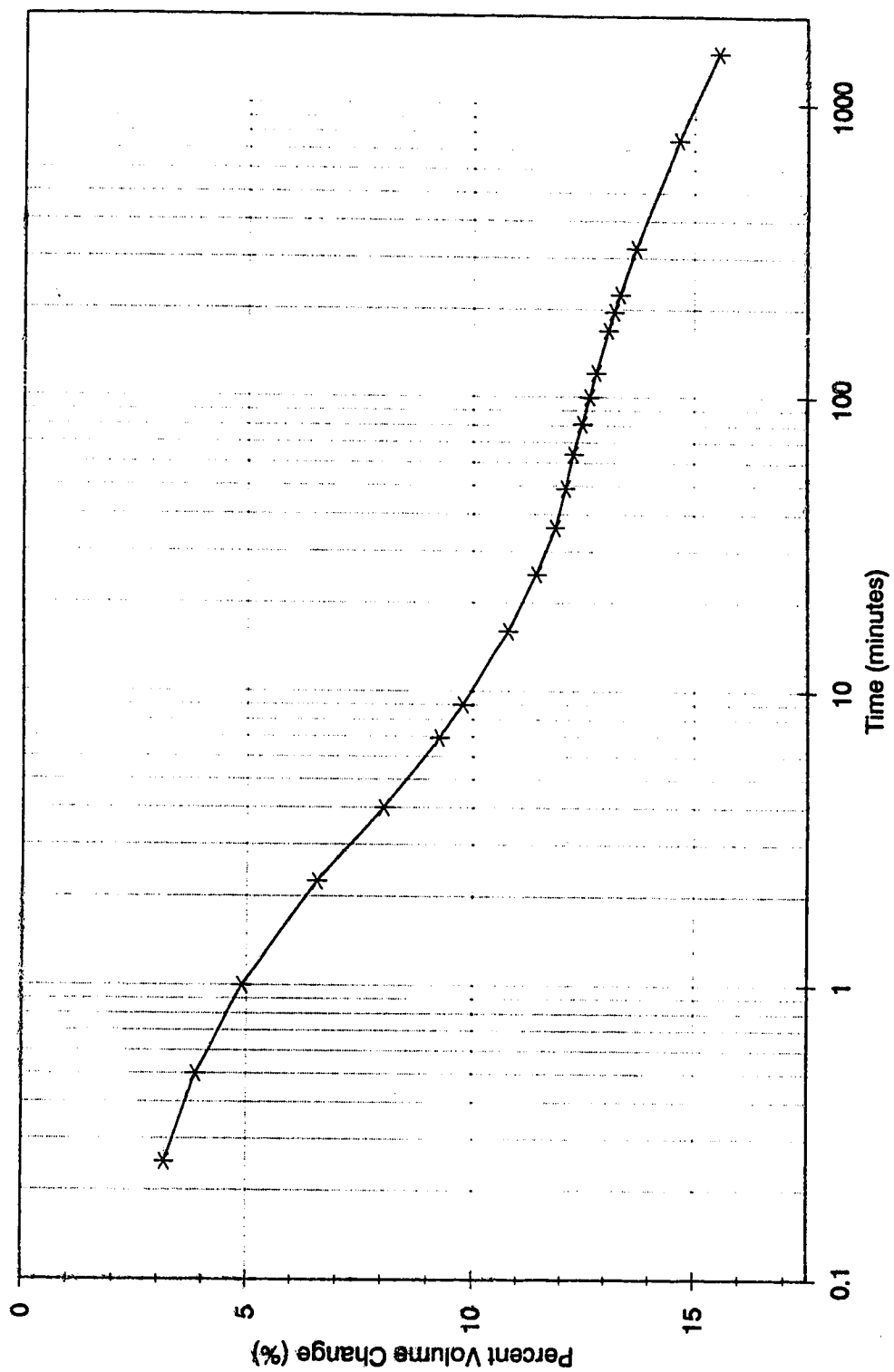
Figure 4.13 Consolidation/Softening - Test PWA6A Series 4

83
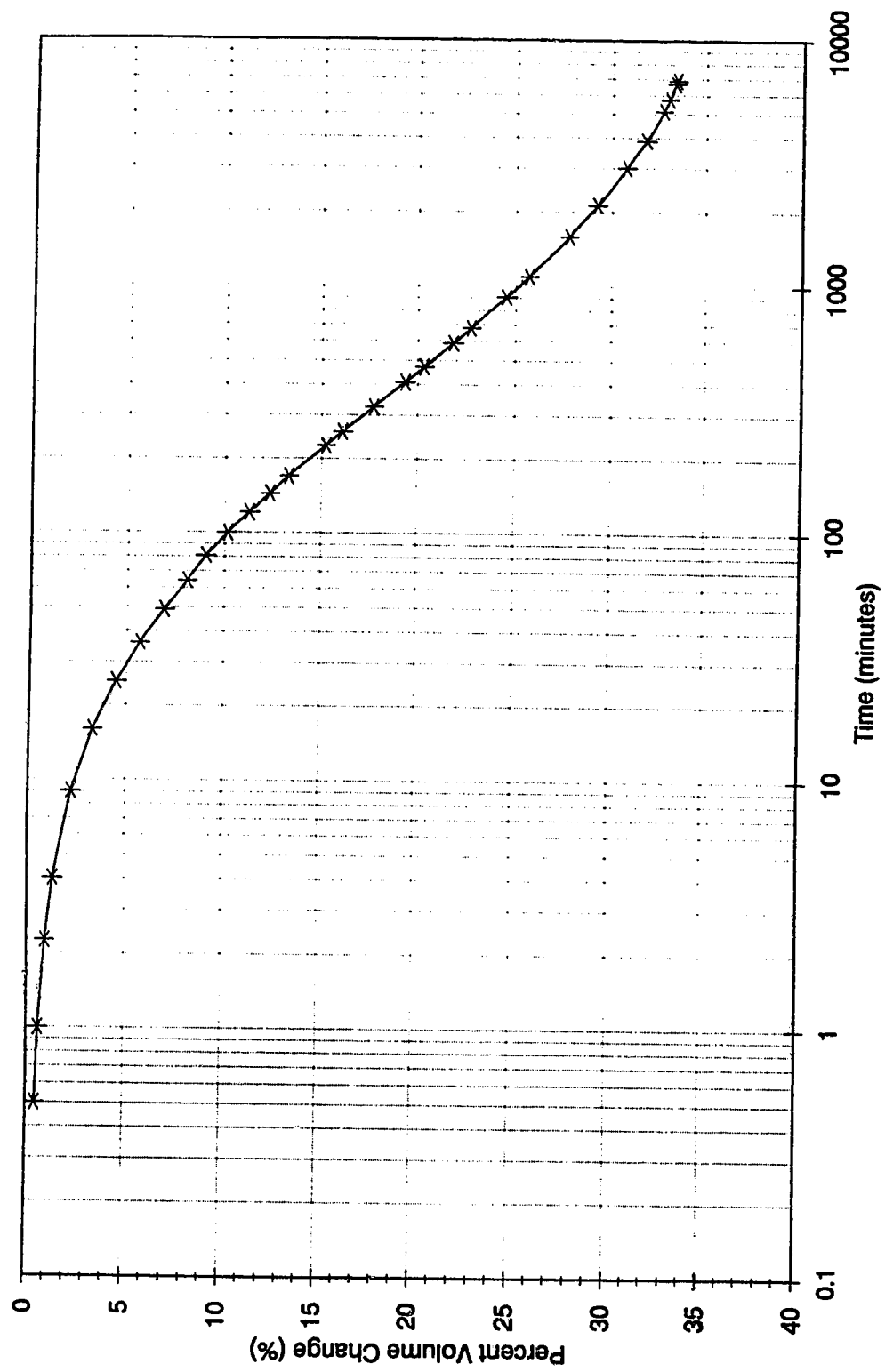
Figure 4.14 Consolidation/Softening - Test PSA3 Series 5
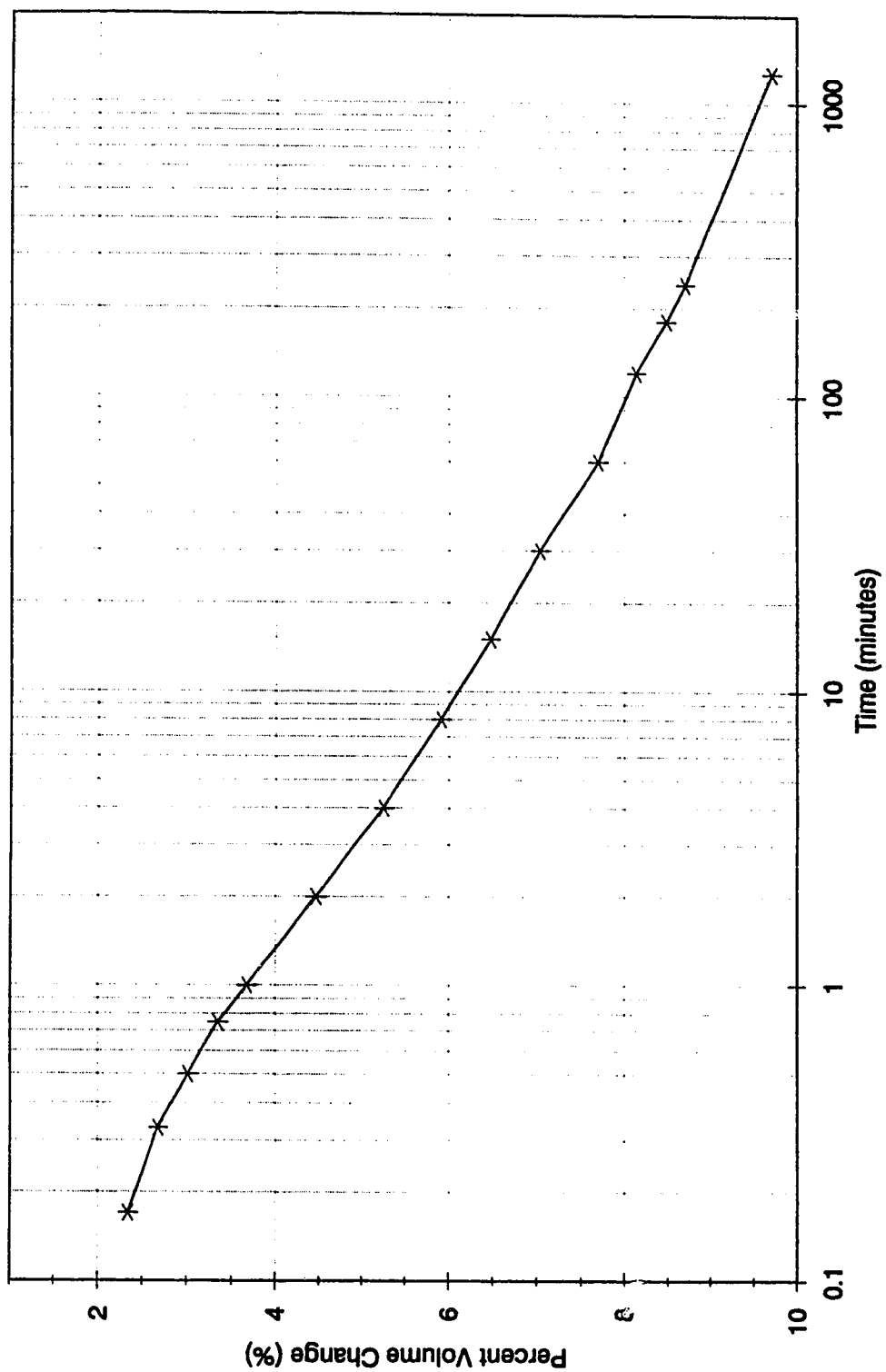
Figure 4.15 Consolidation/Softening - Test PWMS2 Series 6
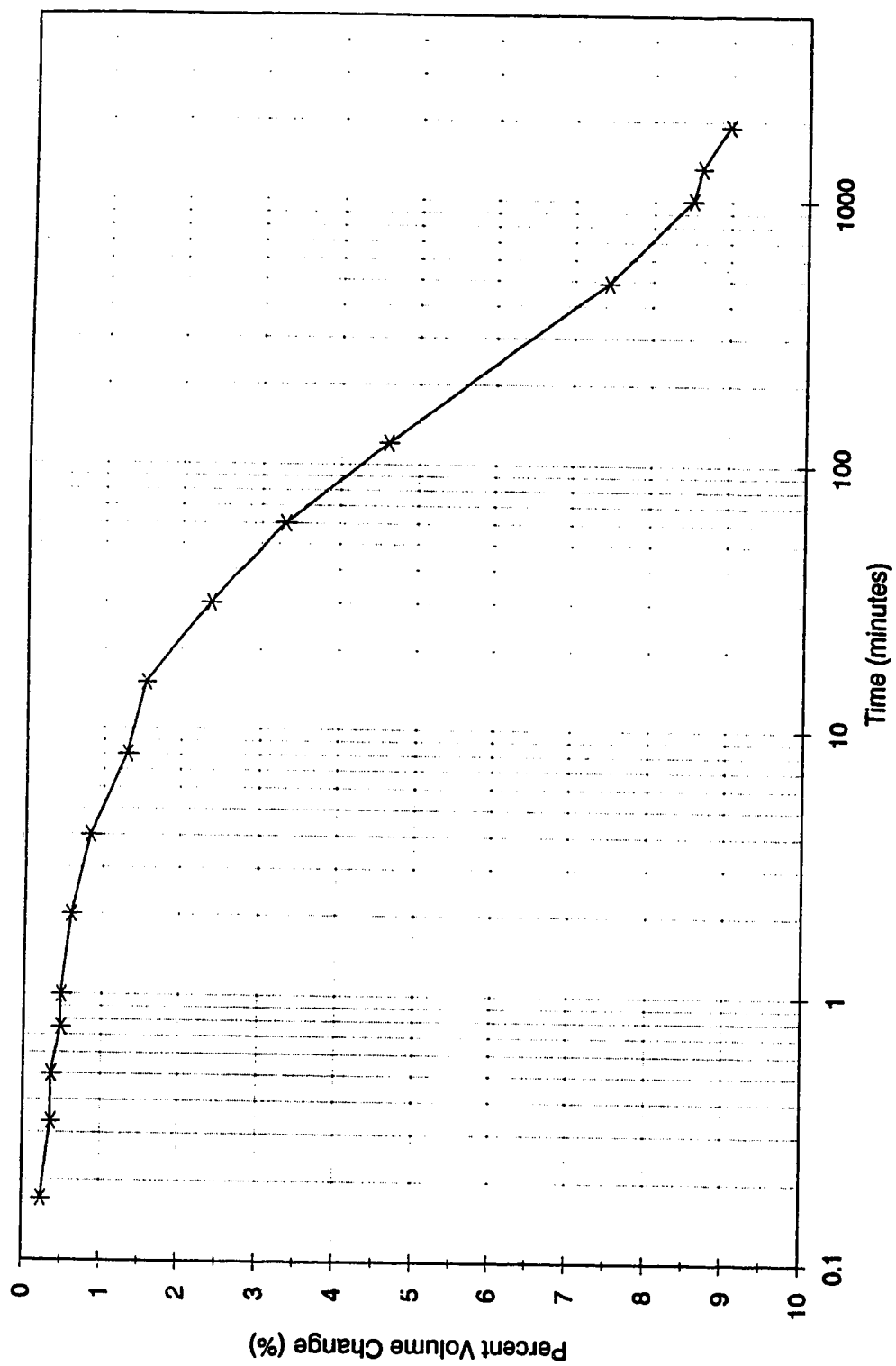
Figure 4.16 Consolidation/Softening - Test PWMS6 Series 6A
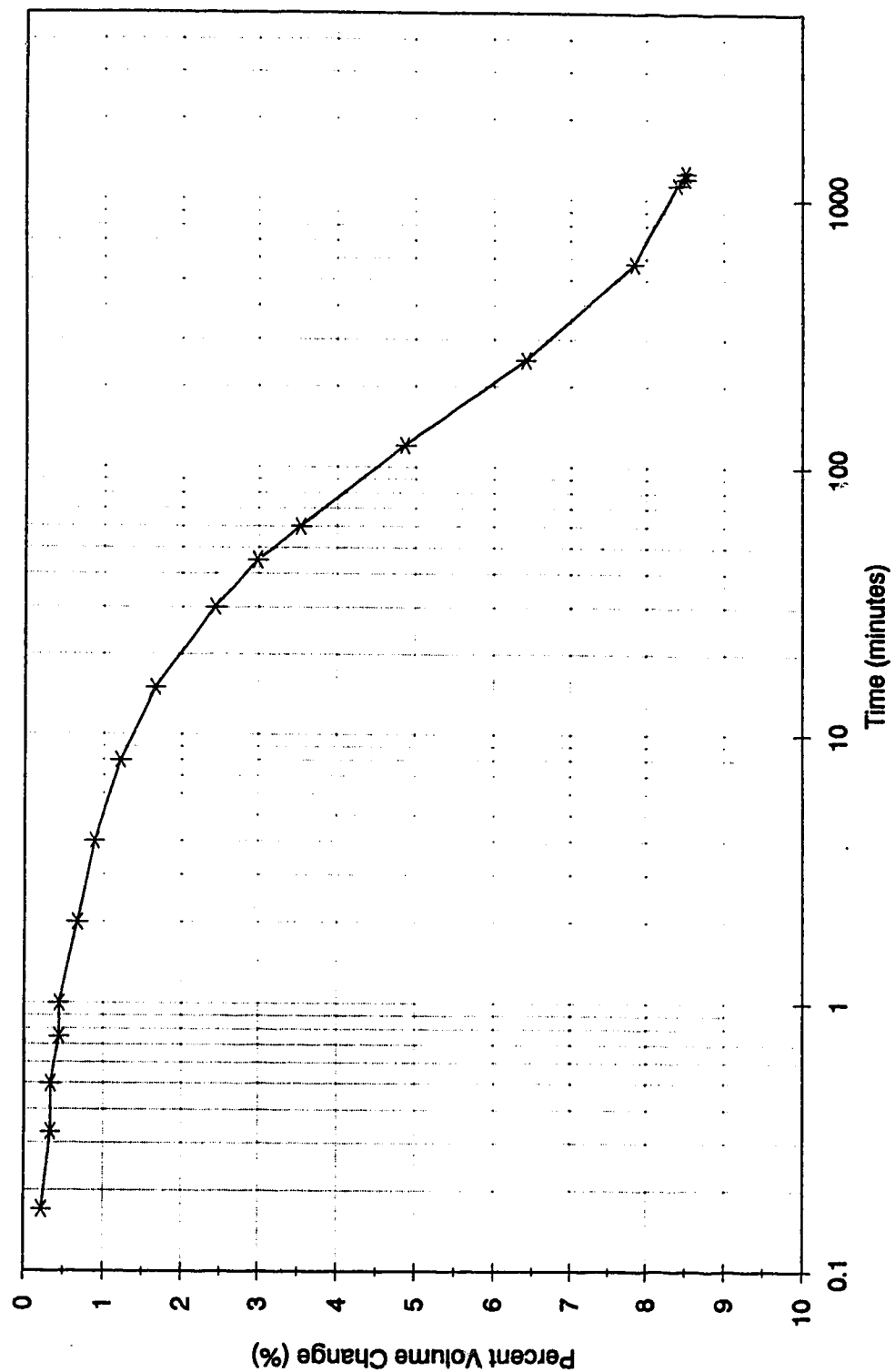
Figure 4.17 Consolidation/Softening - Test PSMS4 Series 7

STRESS-STRAIN RESPONSE

Deviator Stress (kPa)

Axial Strain (%)

PORE PRESSURE RESPONSE

Pore Pressure (kPa)

Axial Strain (%)

PARAMETER A-BAR RESPONSE

A-Bar

Axial Strain (%)
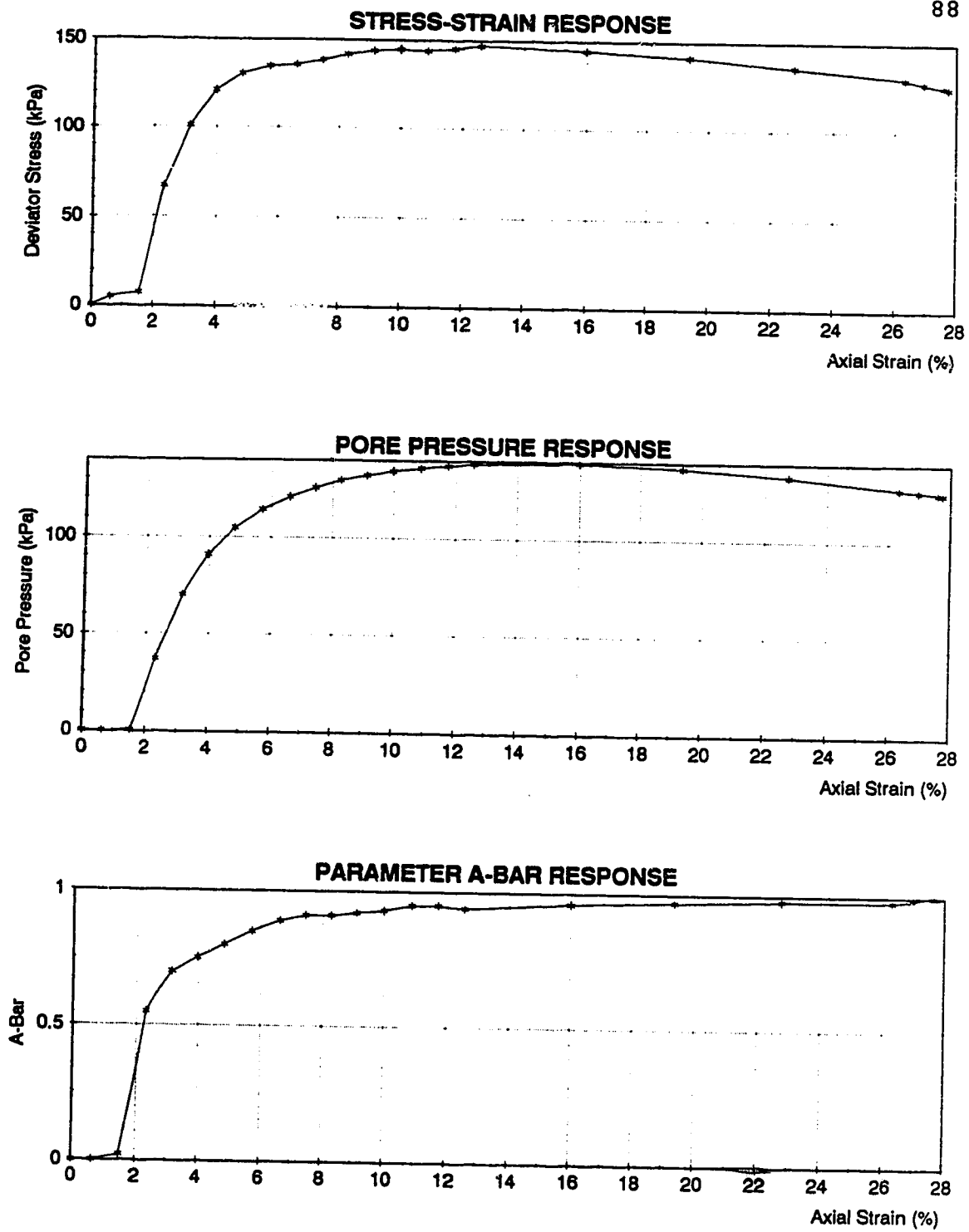
Figure 4.18   Triaxial Test PWA3   Series 1

STRESS-STRAIN RESPONSE

PORE PRESSURE RESPONSE

PARAMETER A-BAR RESPONSE
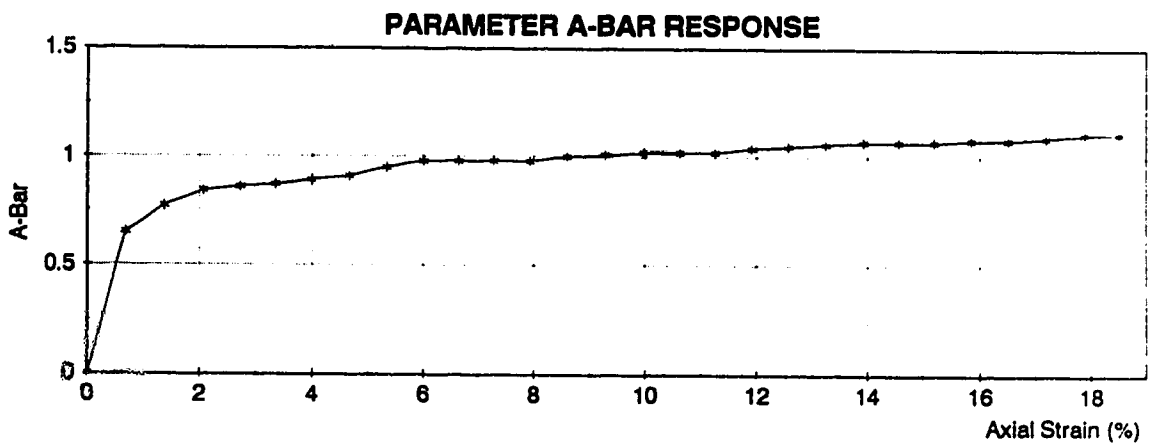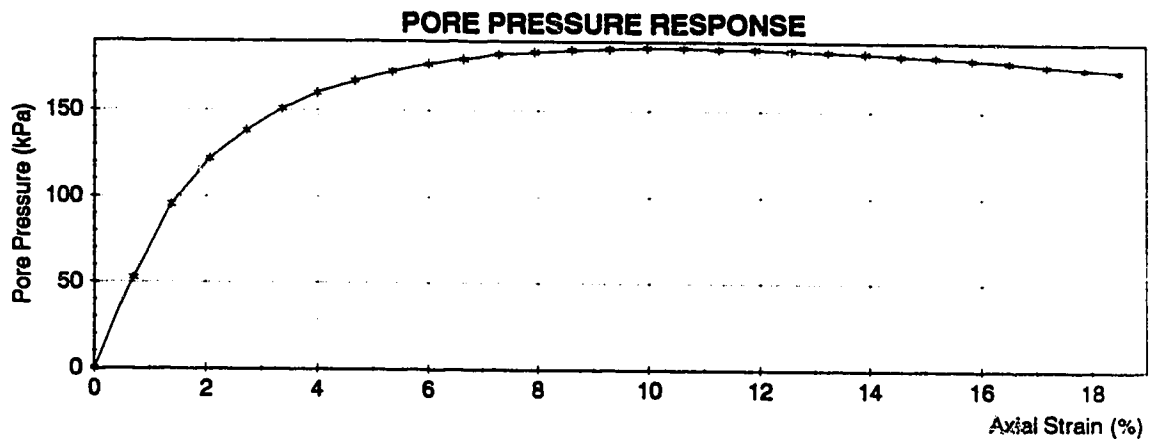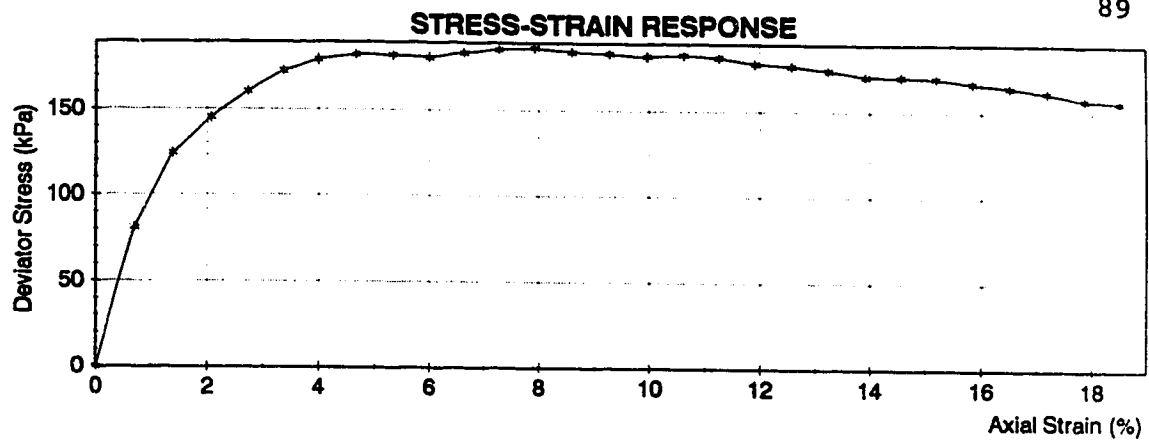
Figure 4.19   Triaxial Test PWA7   Series 2

STRESS-STRAIN RESPONSE

PORE PRESSURE RESPONSE

PARAMETER A-BAR RESPONSE
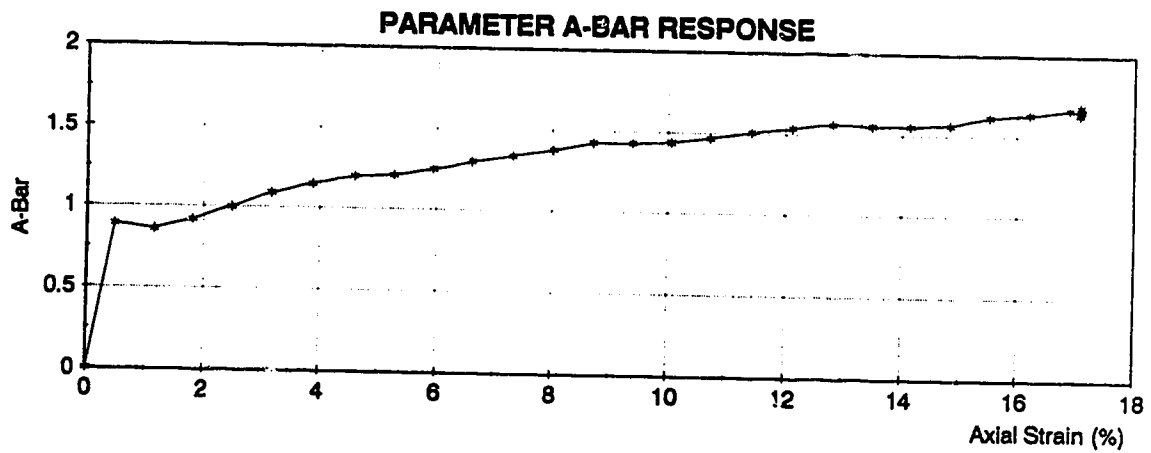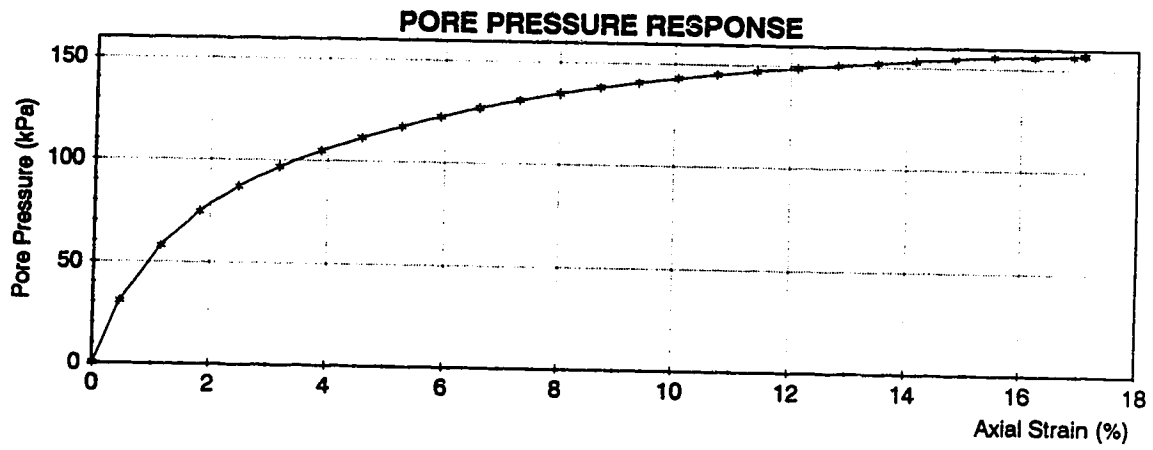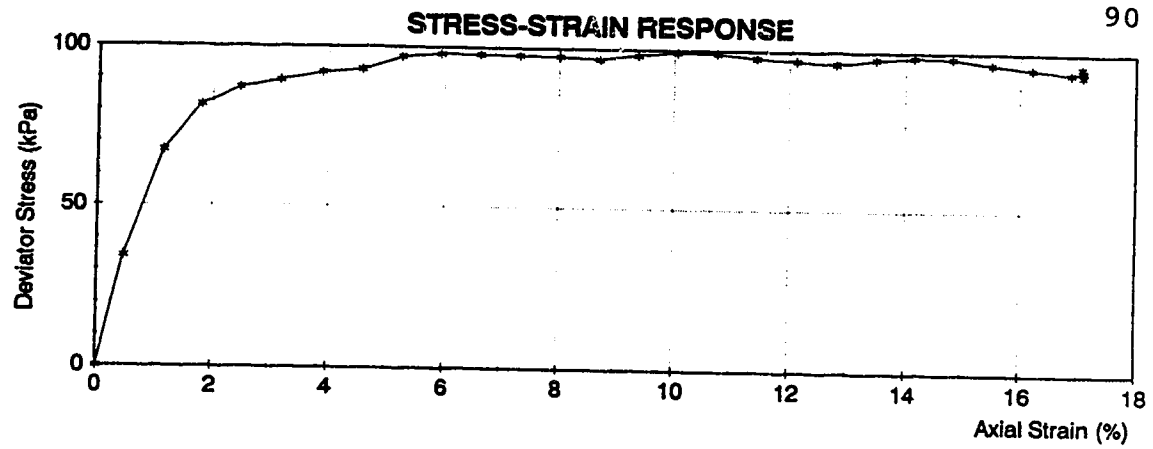
Figure 4.20   Triaxial Test PWA13 Series 3
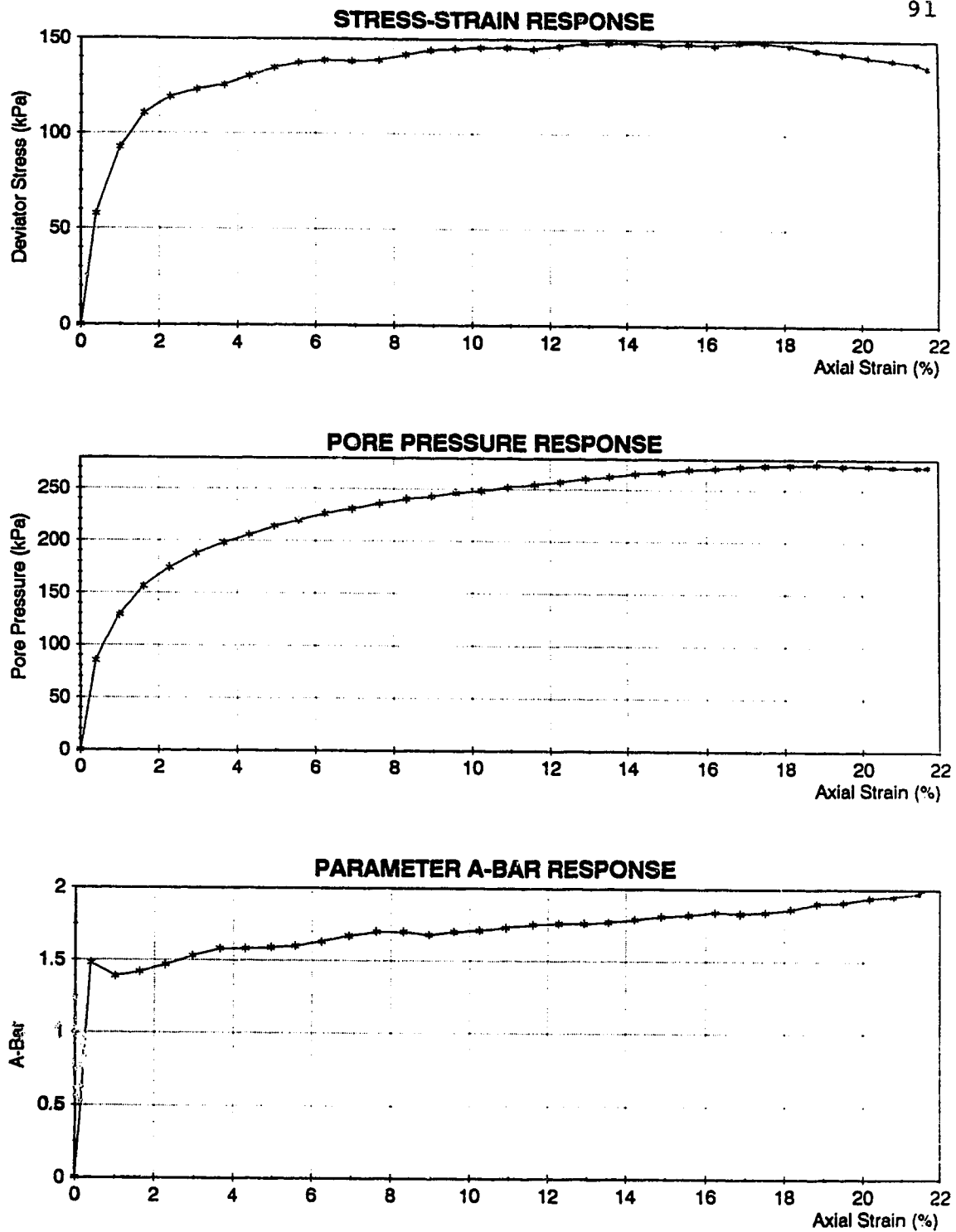
Figure 4.21 Triaxial Test PWA6A Series 4

STRESS-STRAIN RESPONSE

PORE PRESSURE RESPONSE

PARAMETER A-BAR RESPONSE
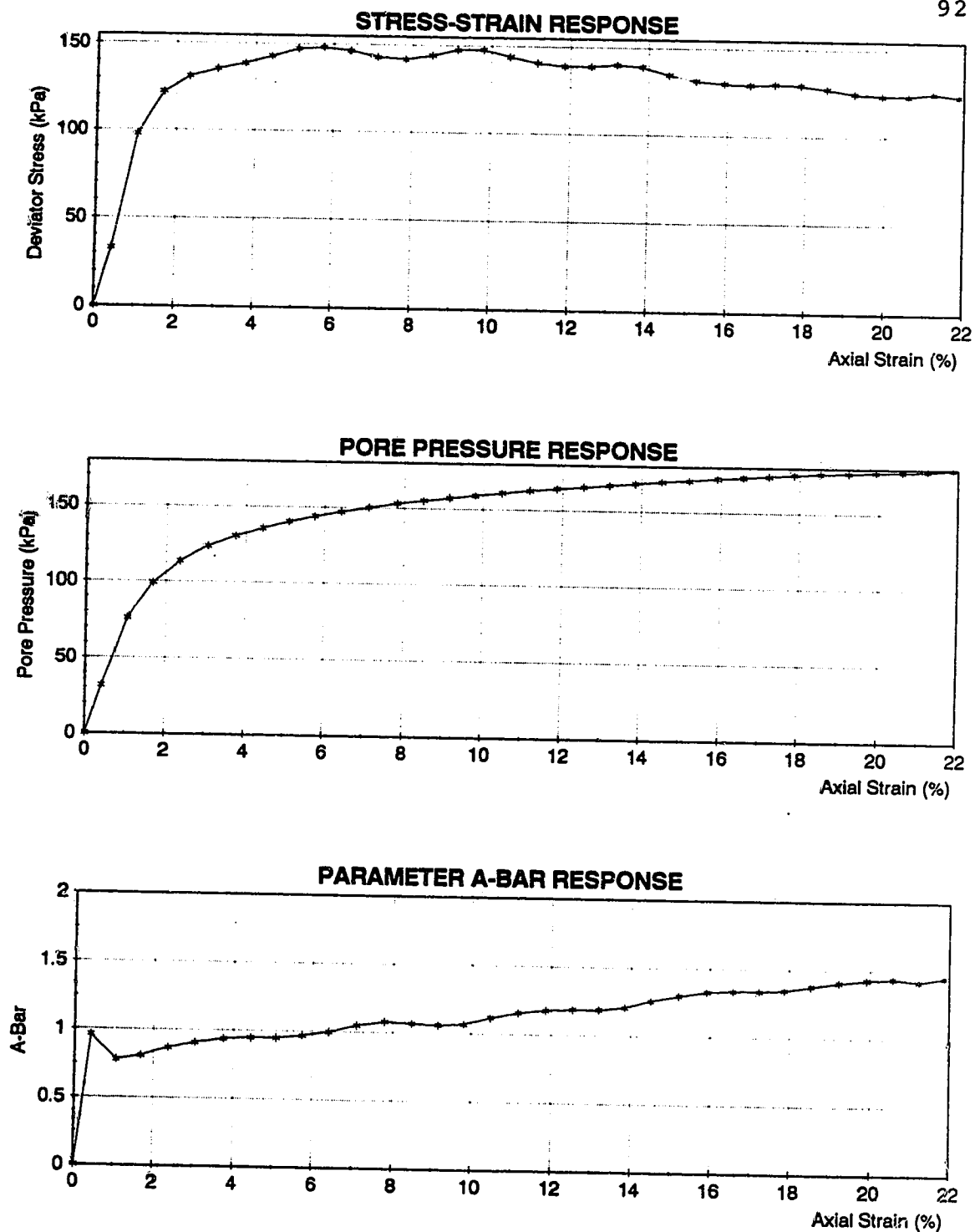
Figure 4.22   Triaxial Test PSA3 Series 5

STRESS-STRAIN RESPONSE

PORE PRESSURE RESPONSE

PARAMETER A-BAR RESPONSE
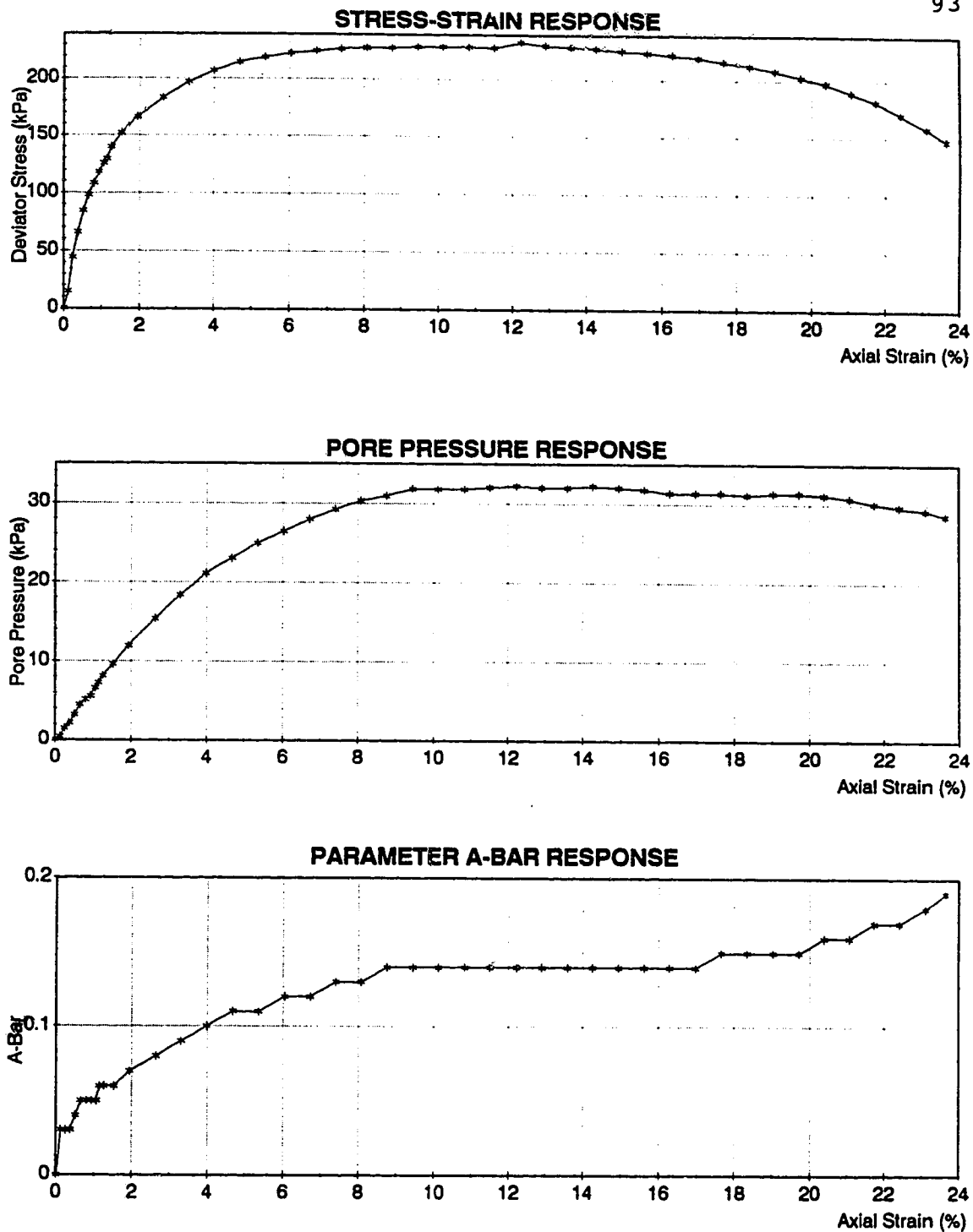
Figure 4.23 Triaxial Test PWMS2 Series 6

STRESS-STRAIN RESPONSE

PORE PRESSURE RESPONSE

PARAMETER A-BAR RESPONSE
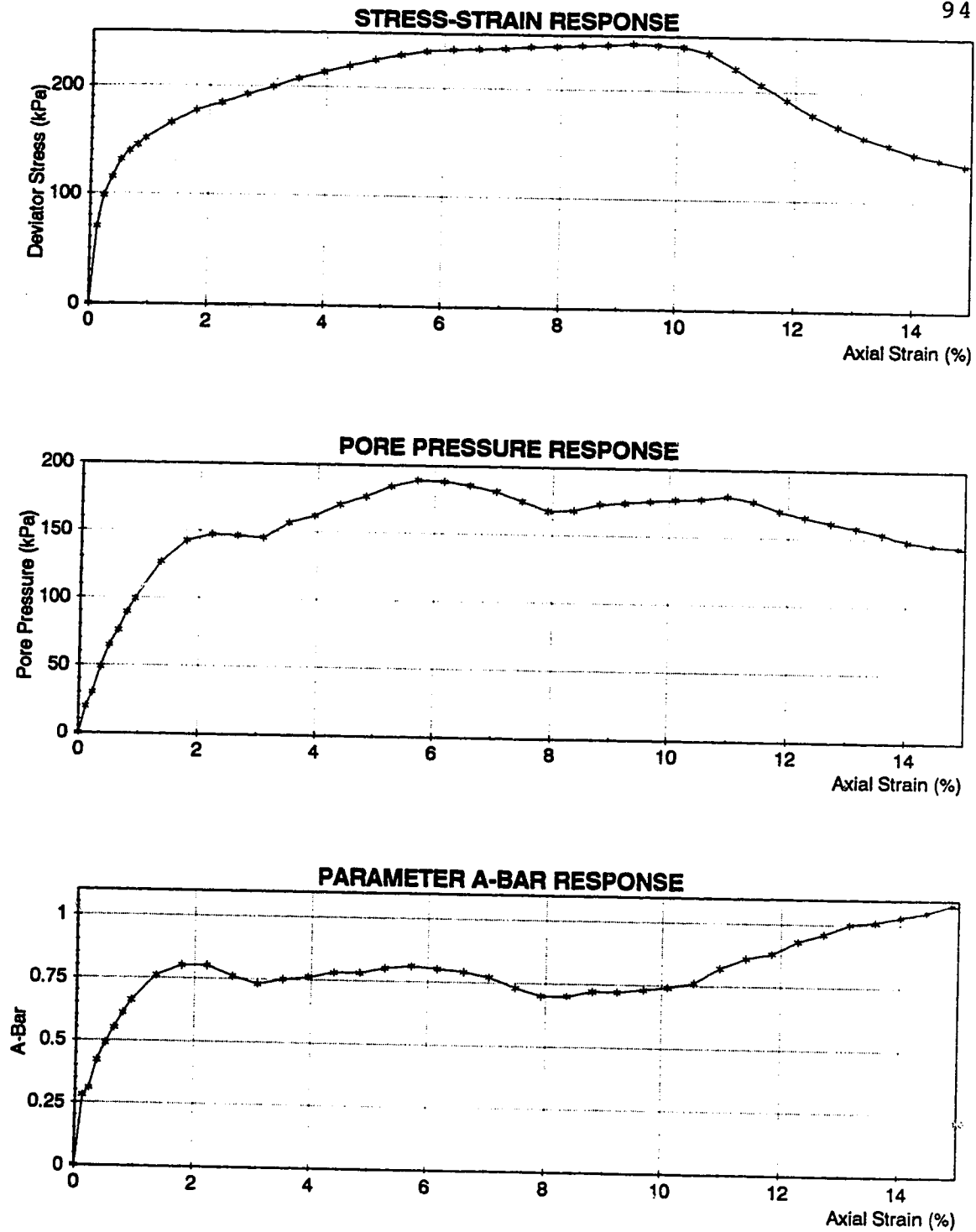
Figure 4.24 Triaxial Test PWMS6 Series 6A

STRESS-STRAIN RESPONSE

PORE PRESSURE RESPONSE

PARAMETER A-BAR RESPONSE
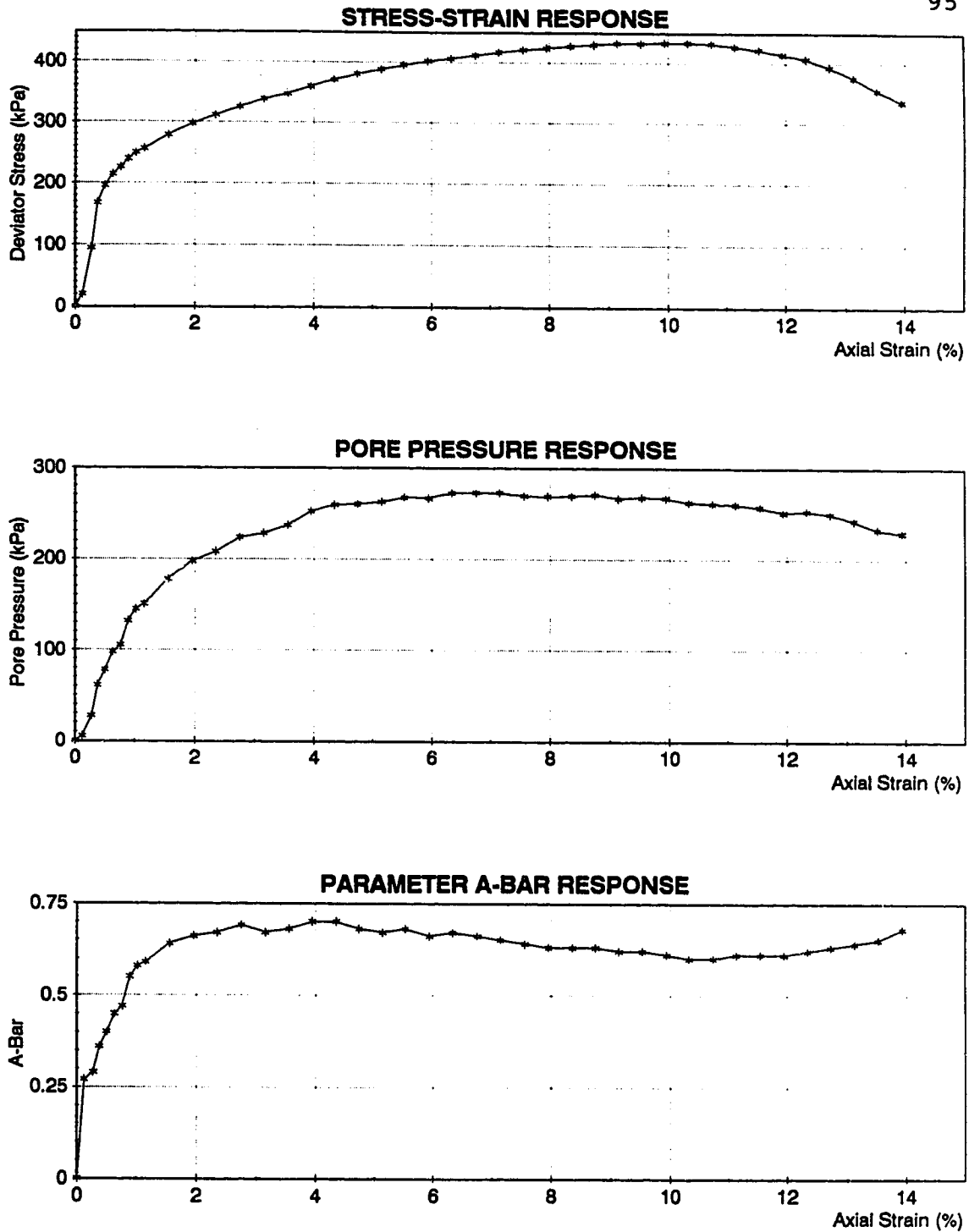
Figure 4.25 Triaxial Test PSMS4 Series 7

5.0 Discussion of Experimental Results

5.1 One Dimensional Compression Softening Tests

The objective of the softening tests was to determine the confining stress required to sufficiently compress the clay shale lumps into a mass that is no longer free draining. That is, at what stress will the lumps form a structure in which the fluid, either tailings pond water or tailings sludge, will not freely flow into or out of but remain within the voids of the clay shale lump structure. Throughout the compression stage, the lumps will be absorbing water, swelling and slaking.

Six tests were conducted under vertical confining stresses that ranged from 3.7 to 250 kPa. The 3.7 kPa confining stress represents a shallow deposit (less than 1 m in depth) while the 250 kPa confining stress represents a deposit up to 14 m in depth. Tailings pond water was used as the only mixing fluid for these experiments.

5.1.1 Water Content

Figure 5.1 shows that the water content of the clay shale, both lump and bulk, reaches a limiting lower value with increasing confining stresses. At low confining stresses the

lumps are able to absorb more water. At higher confining stresses the individual lumps could not be extracted for water content determination. The bulk water contents decrease at an attenuating rate with confining stress. The relationship demonstrates that the clay lumps will absorb little water at higher confining stresses because the higher stresses do not allow the lumps to slake and swell as easily. The lump structure compresses into a tighter packing arrangement decreasing the macro-void space available for free water. This relationship shows that for confining stresses over 50 kPa, the bulk water content should approach 26%. A vertical confining stress of 50 kPa represents a depth of only 2.5 m.

5.1.2 Density

A plot of the dry density and bulk density for both the initial and final conditions are presented in Figures 5.2 and 5.3, respectively. Both plots demonstrate the variation in initial densities. As the clay shale samples are allowed to soften and compress under a confining stress, the densities reach a limiting upper value. Dry densities approach 1,600 kg/m^3 while the bulk densities approach 2,000 kg/m^3. This demonstrates the consistency at which the lump structure compresses. The lumps appear to approach a maximum packing arrangement under a confining stress of 50 kPa up to the maximum stress used of 250 kPa.

5.1.3 Volume Change

The percent maximum volume change is defined as the volume change that occurs during the compression/softening stage compared to the initial volume (Figure 5.4). Even though the amount of volume change increases with confining stress, the magnitude of this volume change is more dependent on the initial density or void ratio of the sample. The volume change measurements demonstrate that large settlements, up to 30% to 40%, would take place as the fill height is increased. Calculation of potential fill volumes should be based on volume change up to a bulk density of 2,000 kg/m^3.

5.1.4 Void Ratio

Void ratios can be calculated for different stages of the test and can be subdivided into two parts. The void volumes within the individual lumps are defined as the micro-void ratio (e_m) while the void volumes between the lumps are defined as the macro-void ratio (e_M). Bulk void ratio refers to the total voids both within and between the lumps.

e_m = volume voids within the lumps / volume of soil solids

e_M = volume voids between the lumps / volume of soil solids

e = bulk or total void ratio = $e_m + e_M$

Both the macro and micro-void ratio, of which the sum is the total or bulk void ratio, can be calculated for the initial conditions. It cannot be calculated for the final conditions (after shearing) since the integrity of the individual lumps, specifically around the edges, have been altered through the softening and slaking process.

Typically, initial micro-void ratios average 0.52 while macro-void ratios vary from 0.7 to 1.5. The major change in void ratio during the compression/softening stage occurs within the macro-voids. The final void ratio appears to be independent of the initial void ratio of the sample. The lump structure compresses under a low confining stress and approaches a minimum bulk void ratio of 0.7 (Figure 5.5). Further softening of the clay shale allows the clay to slake off of the lumps filling the macro-voids. As this process continues, it obstructs the flow of water reducing the hydraulic conductivity of the lump structure to small values.

5.1.5 Hydraulic Conductivity

Permeability measurements show that the lump structure will behave as a well drained medium with a hydraulic conductivity of 4.0×10^{-1} cm/s. As the confining stress increases, the hydraulic conductivity decreases (Figure 5.6). At a confining

stress between 66 kPa and 100 kPa, the hydraulic conductivity decreases dramatically. Permeability flow measurements at the 100 kPa stress level were too small to be measured with the apparatus. Figure 5.7 indicates that the hydraulic conductivity values will be considerably smaller than 1×10^{-4} cm/s for confining stresses greater than 100 kPa.

The dramatic decrease in hydraulic conductivity between confining stresses of 66 and 100 kPa demonstrates that the lump structure has broken down and that the lumps have compressed to form a mixture exhibiting very low drainage capabilities. This stress range would be reached at a depth of 3 m to 5 m below the fill surface.

5.1.6 Visual Description

The individual clay lumps subjected to low confining stresses (less than 100 kPa) could be extracted from the sample for water content determination. The lumps were clearly visible with the surrounding voids filled with soft wet clay. Only the outer surface of the lumps had been penetrated by the water. At higher confining stresses, the lumps could not be extracted for study. The lump structure was still visible but delineating the boundaries of the lumps was difficult. The hard lumps could be felt by hand when pressing the lump matrix.

5.1.7 Summary of One Dimensional Compression Softening Tests

One dimensional compression softening tests reveal a characteristic that may only be seen with lumpy clay deposits. The lumps form a structure that is initially free draining. As the confining stress increases, the structure quickly compresses and continues to compress, but at an attenuating rate. The lumps reach a maximum packing arrangement which is able to sustain the applied confining stress. This is demonstrated by both the final void ratios and final densities whose calculated values approach a limiting lower (0.7) and upper bound (2,000 kg/m^3), respectively.

Water contents also reach a limiting lower value (26%) which is consistent with the void ratio and density response. Once the lump structure has compressed to its limiting lower bound, the only water available to the lumps for further softening will come from the macro-voids. However, the low hydraulic conductivities do not readily allow the ingress of more water to replenish these macro-voids.

Unlike the trends found with the density, void ratio and water contents, the hydraulic conductivity continues to decrease. This is the result of the lump structure quickly compressing to its maximum packing arrangement. The macro-voids formed between the lumps are sealed off by the swelling

and slaking action of the clay. The limiting values of water content, density and void ratio would be reached at a depth of 2.5 m to 3 m below the surface of a hydraulically placed fill while the free draining structure of a clay lump fill would become sealed at a depth of 3 m to 5 m.

5.2 Consolidated Undrained Triaxial Compression Tests

The objective of the clay shale triaxial test program was to determine the strength developed in a clay shale lump deposit saturated with either tailings pond water or tailings sludge.

Since the clay shale has an affinity for water uptake, the effect of softening duration time and lump size was analysed. The conditions under which the triaxial test samples saturate and soften are unlike that for the one dimensional compression softening tests samples (Section 5.1). The triaxial test samples were allowed to saturate and soften under a small confining stress of about 10 kPa whereas with the softening tests, the clay lumps softened under the full confining stress. This softening process continues throughout the consolidation and shearing stages of the triaxial tests, but under the full confining stress.

The testing program was divided into seven test series, with

each series analysing a specific parameter (Table 4.4). Test series 1 through 3 utilized 12.7 mm maximum size clay shale lumps. Within these test series, series 2 analysed the effect of increasing the softening duration time (under low confining stresses) from 3 to 6 hours. Test series 3 studied the influence of a considerably longer softening duration time , averaging 25 hours. The effect of lump size was studied in test series 4. The maximum clay lump size was increased to 19 mm, the maximum size allowable for a 102 mm diameter triaxial test sample. Test series 5 studied the influence of using tailings pond sludge as the mixing fluid instead of tailings pond water. Finally, test series 6, 6A and 7 represented the clay shale in the fully softened state or long term condition, with the clay being homogenized with tailings pond water in test series 6 and 6A, and tailings pond sludge in test series 7.

After softening, the shape of the lumps (subangular) that were used in the laboratory experiments were similar to those found in the pilot field dredging experiment (section 2.1.1). The angle of internal friction is affected to some extent by the size of the particles in the test specimens. Marachi et al. (1972) found that for rock fill materials, that at any given confining stress, the angle of internal friction for 100 mm diameter specimens was about 2° lower than that of 15 mm diameter specimens. This trend seemed to be unaffected by the

confining stress or the material type. The particle shape and gradation, however, had to be similar.

Within each test series a number of consolidated undrained triaxial compression tests were conducted with pore pressure measurements to determine the effective and total strength parameters.

A very slow rate of shear strain was chosen to ensure that pore pressure equalization occurred throughout the entire sample. The average duration for shearing was 8 hours at an axial strain rate of 0.034% per minute.

5.2.1 p-q Stress Paths

Triaxial test results from each test series one through seven are plotted on p'-q and p-q plots showing the effective and total stress paths, respectively. These parameters are defined as $p = (\sigma_1+\sigma_3)/2$, $p' = (\sigma_1'+\sigma_3')/2$, and $q = (\sigma_1-\sigma_3)/2$. A linear regression analysis through the peak strengths is used to derive the strength parameters. The p-q plots for test series are presented in Figures 5.8 to 5.15. Shear parameters, both total and effective, are derived the plots and are presented in Table 5.1.

5.2.2 Saturated Clay Shale Lump Triaxial Test Series

In order to model a deposit of clay shale lumps, a large diameter triaxial cell was chosen to test 102 mm diameter triaxial samples with clay lumps up to 19 mm in diameter. The twenty-nine triaxial tests conducted on the saturated clay shale lumps are subdivided into five test series. Each test series studied the effects of lump size, softening duration, and mixing fluid.

During the consolidation/softening stage, the clay lump structure is consolidating on a macro scale; that is, the lumps are moving into a tighter packing arrangement expelling the fluid out of the macro-voids as the confining stress is applied. The softened clay around the lumps is also consolidating, forcing water out of its micro-voids as with traditional soft clay soil. The lump micro-voids are probably not consolidating and may even be swelling. This heterogeneity in volume change as well as other factors such as, large volume changes or strains and non-uniform hydraulic conductivities, make the calculation of a coefficient of consolidation from the consolidation curve invalid. For this reason, the coefficient of consolidation is not reported.

Test series 1 through 3 were tested using 12.7 mm maximum diameter clay shale lumps mixed with tailings pond water.

Test series 1 and 2 display essentially the same strength parameters. Therefore, increasing the initial softening period (under a low confining stress) from 3 to 6 hours has little influence. The softening process continues throughout the consolidation and shearing stage, but under the full confining stress. The total softening time is therefore the test duration time. The test duration time for test series 2 was 25 hours longer than test series 1, yet no difference in strength is seen. This indicates that the full confining stress restricts the degree of softening that occurs at the contact points between the clay lumps. It is likely though, the softening process (swelling and slaking) is continuing to occur along the lump surfaces that are not in contact with each other, filling the macro-voids.

Test series 3 was allowed to soften for a considerably longer period of time (average 25 hours) under a low confining stress. The total test duration averaged only 7 hours more than series 2 yet the strength parameters are significantly different. The low angle of friction, high cohesion intercept, and stress paths shown in Figure 5.10 shows that the clay lump structure is behaving as an overconsolidated clay but is exhibiting very high positive pore pressures.

The wavy behaviour of the stress strain curve in Figure B58 is typical of all the lump triaxial tests and became more

pronounced when the larger size clay lumps were tested. This may be an indication that the individual clay shale lumps are being sheared through. Since these are overconsolidated clay shale lumps, negative pore pressures may be developing within the individual lumps being sheared. However, the pore pressure transducers reveal high positive pore pressures. This is displayed by the large pore pressure parameter A value which develops under low confining stresses. Figure B43 is a typical example of the test results that was observed in all of the lump triaxial tests. The high pore pressure parameter A value demonstrates the collapsible nature of the lump structure caused by the shear strains. As the lump structure collapses, the confining stresses are transferred to the pore water contained within the softened clay of the macro-voids.

Therefore, the high positive pore pressures in the macro-voids will attempt to dissipate into the clay shale lumps where negative pore pressures may be attempting to develop. Effective stresses within the individual clay lumps are reduced which reduces the shear strength of the lumps. This pore pressure development reduces the effectiveness of the confining stress which manifests itself as a shallow failure envelope (low angle of internal friction).

To investigate the influence of lump size, larger lumps with a maximum diameter of 19 mm were used for test series 4 and

5. The softening time under a low confining stress for the samples in series 4 ranged from 24 to 64 hours. Within this softening duration time, there is little difference in the shear strength. The strength envelope is very shallow with a high cohesion intercept. The same process is occurring as was seen in test series 3. The clay lump structure is as well, behaving as an overconsolidated clay but exhibiting high positive pore pressures. The pore pressures are attributed to the stress being transferred to the pore water in the macro-voids as the lump structure collapses during shear.

The effect of tailings pond sludge as the mixing fluid was investigated in test series 5. The clay lumps were allowed to soften under a low confining stress for a duration similar to that used in test series 4. Time for consolidation using sludge was significantly longer, taking four to six times longer than lumps mixed with tailings pond water. It is attributed to the slow rate of softening of shale lumps in sludge (Ash 1986) and to the low permeability characteristics of the mixture of softened clay and tailings sludge in the macro-voids. This demonstrates that clay shale lumps mixed with tailings sludge will consolidate much slower and high pore pressures will take a long time to dissipate. The strength envelope again reveals a low friction angle with a high cohesion intercept. The reasoning for this was discussed in the previous paragraphs.

Since softening of the clay shale occurs at such a slow rate, especially in the presence of sludge, a clay shale lump deposit will consolidate for a very long time. This consolidation rate will inhibit rapid construction as high pore pressures that develop readily throughout the deposit from shearing strains will dissipate very slowly.

5.2.2.1 Water Content

A plot showing the water contents with confining stress is presented in Figure 5.16. The water contents can be divided into three regions: the initial water content of the clay shale, the water content immediately after saturation, and the water content of the total sample after consolidation (bulk water content). Both the water contents after saturation and after consolidation are a measure of the water within the micro and macro-voids.

The results in Figure 5.16 clearly demonstrate that the final bulk water content is independent of the mixing fluid. After saturation, the clay lump samples display a wide range of water contents ranging from 38% to 63%. After consolidation, a very consistent bulk water content emerged. Similar to that discovered with the softening tests, the bulk water contents approach a limiting lower bound of 28%. The

bulk water content is almost independent of the confining stress applied. The lump structure reaches a maximum packing arrangement under low confining stresses. The lower bound of 26% found in the softening tests is slightly lower and is likely a reflection of the lower plastic clay shale used for those tests.

5.2.2.2 Density

Figures 5.17 and 5.18 display the dry and bulk density relationship with confining stress. The initial density is defined as the density of the clay shale lump sample including the air in the micro-voids. The large scatter in the initial densities is a function of the sample assembly and preparation.

The densities calculated for the triaxial tests closely correlate with the densities calculated for the softening tests. The final densities after consolidation again approach a limiting upper value; dry densities approach 1,550 kg/m^3 while bulk densities approach 2,000 kg/m^3.

The final densities are independent of the size of clay lumps, the amount of softening time that the clay shale lumps are subjected to and the type of mixing fluid; that is, tailings pond water or tailings sludge. Over the stress range

used, there is very little dependency on confining stress. The clay lumps approach their final densities or maximum packing arrangement under a low confining stress.

5.2.2.3 Volume Change

A plot of the volume change with confining stress, presented in Figure 5.19, illustrates the total volume change and the volume change that the clay lump structure has undergone as a result of the softening and consolidation stage. The wide range of volume change is a reflection of the initial density of the samples before testing. There is no distinct difference in the amount of volume change whether pond water or tailings sludge is used as the mixing fluid. Although consolidation with tailings sludge was much slower, the final amount of softening and slaking with both fluids appears to be similar.

The range in total volume change was between 30 and 44% which is consistent with that observed with the softening tests.

5.2.2.4 Void Ratio

Void ratio, plotted against confining stress in Figure 5.20, displays a very distinct trend. Although there is a large

variation in the initial void ratios, the final void ratio, regardless of the mixing fluid or the length of softening duration, approaches a limiting lower value of 0.75. This is very consistent to that found with the softening tests.

The clay lumps form a structure with a maximum packing arrangement very quickly under confining stresses lower than 150 kPa. Once this void ratio is achieved, the lump to lump contact is strong enough to sustain confining stresses up to 550 kPa. A vertical confining pressure of 550 kPa represents a depth of fill of 50 m assuming a water table at a depth of 3 m to 5 m below the surface.

5.2.2.5 Visual Description

Similar to the softening tests, the clay lump structure could still be visually identified even with the samples that were allowed to soften for extended periods of time. The lumps had absorbed some water making the individual lumps slightly softer. On a few occasions there were small voids that were filled with very wet softened clay or sludge and clay.

The clay lumps could be defined on the exterior surface of the samples as the rubber membrane stretched around the lumps and pushed into the softened clay or voids between the lumps

(Figure 5.21a). Figure 5.21b shows the sample with the rubber membrane removed. A definite shearing plane developed through the lump structure. Figure 5.22 is a clay shale lump sample that has been mixed with tailings sludge. The black spots on the lumps are the bitumen that is present in the sludge. All the figures clearly show that the interlump voids have been filled by the softened clay.

5.2.3 Saturated Homogenized Clay Shale Triaxial Tests

The preceding section describes the behaviour of a clay shale lump deposit immediately after mixing and deposition. To gain further insight into the ultimate behaviour of the clay shale, thirteen triaxial tests were conducted on homogenized clay shale. Homogenized clay shale may represent the long term and consolidated state of a lump deposit where the macro-voids and the micro-voids contained an amount of water equivalent to a bulk water content of 30%. This long term condition may never be reached in the field as the water available in the macro-voids does not appear to be enough to fully homogenize the clay shale.

5.2.3.1 Triaxial Test Series

The first set of tests, Series 6, were conducted on clay shale homogenized with tailings pond water. Prior to

consolidation and shearing, the back pressure was reduced inadvertently leaving the saturation level questionable. An additional three tests (Series 6A) were conducted to substantiate the previous results. Comparing the effective stress parameters in the two sets of tests, the friction angle is lower and the cohesion intercept is considerably higher for the possible unsaturated test samples. High positive pore pressures were not measured throughout the shearing stage for any of these samples. It, therefore, appears that these samples were unsaturated and the compression of the air bubbles prevented the development of or measurement of pore pressures. If high positive pore pressures had been measured, the effective stress failure envelopes would have been more similar for the two test series. Test series 6 will not be considered further although it is an example of shear strength parameters for a lump structure which may not become saturated during deposition.

Triaxial tests were also conducted on samples homogenized with tailings pond sludge as the mixing fluid in test series 7. The higher cohesion intercept may be a reflection of the increased fines from the tailings sludge resulting in a stiffer macro-void material.

The triaxial tests on homogenized clay shale revealed that when a water content of 30% in a saturated lump structure

fully disperses and softens the clay shale lumps into a homogeneous mass, the ultimate strength of the deposit will improve. A fully softened state, however, may never be reached as the water available in the macro-voids may not be enough to fully homogenize the clay shale. Test series 6A and 7, therefore, will represent an upper bound on the long term shear strength of a lump structure.

5.2.3.2 Water Content

The water content of the test samples after consolidation, presented in Figure 5.23, shows that they approach a limiting lower value with increasing confining stress. The samples homogenized with tailings sludge display slightly lower water contents which is attributed to the suspended fines intrinsic to the tailings sludge. The pond water samples approach water contents of 30% while the sludge samples approach 29%. This trend in approaching a limiting lower water content is similar to the trend found with the triaxial tests using clay shale lumps. This shows that the clay lump structure compresses and consolidates into a dense state so that the average water content is similar to the homogenized clay shale water content.

5.2.3.3 Density

The densities, both dry and bulk density, also approach a limiting upper value. Figure 5.24 reveals that the densities reach a maximum value with increasing confining stress. This maximum is about 1,550 kg/m^3 and 2,000 kg/m^3 for the dry and bulk densities, respectively. The bulk densities are approaching the bulk density of in situ Clearwater Formation Kcc clay shale which is approximately 2,100 kg/m^3 (Lord and Isaac 1989).

The triaxial test specimens of clay shale lumps also approach densities very similar to homogenized clay shale values; however, the higher density (2,100 kg/m^3) of the clay lumps within the matrix increases the overall average density. More importantly, what this does show is that the tailings pond water or tailings sludge softens the contact points of the lumps so that the lump structure can compress into a dense state under a low confining stress.

5.2.3.4 Void Ratio

The void ratio's also show a trend similar to that found with the triaxial tests using clay lumps (Figure 5.25). The samples homogenized with tailings water approach a void ratio of 0.85 while the sludge samples approach a void ratio of

0.78. The fines in the sludge occupy some of the void space reducing the void ratio compared to those samples mixed with tailings water. The void ratios are slightly higher than those recorded with the lump triaxial tests. This is attributed to the dense overconsolidated nature of the clay shale lumps, which exhibit void ratios of about 0.5, resulting in a lower average void ratio.

5.2.4 Unsaturated Clay Shale Lump Triaxial Tests

Twenty-one triaxial tests on unsaturated clay shale lumps have been conducted by the Department of Earth Sciences at the University of Waterloo for the Alberta Oil Sands Technology and Research Authority (AOSTRA) (Hilliard et al. 1988; Hilliard et al. 1989).

The clay shale was acquired from undisturbed cores taken in the Clearwater Formation unit. Liquid limits and water contents ranged from 33 to 110% and 11 to 35%, respectively. The clay shale was manually broken down into 9.5 mm lumps and, using a high compactive effort, compacted into a 102 mm diameter three piece compaction mold. This gave approximate dry densities of 1,700 kg/m^3, about 300 to 400 kg/m^3 greater than the samples prepared for this thesis. At this compaction level, it is unknown whether the lump structure remaining was as obvious as in the specimens in this work. Quick undrained

triaxial tests without pore pressure measurements using 102 mm diameter triaxial samples were used.

The unsaturated clay shale triaxial tests display a similar stress-strain response of an elastic-plastic nature with the transition at approximately 5% strain. The tests were also sheared at a considerably faster rate, ranging from a strain rate of 1.5% to 2.5% per minute over a range of confining stresses from 170 to 310 kPa. Even though the sample was unsaturated, at this strain rate, the lumps would have still been sheared in an undrained manner.

A linear regression analysis of the results from the triaxial tests conducted by Hilliard et al. (1989) plotted on a p-q plot (Figure 5.26) indicates that the angle of friction is $34°$ with a cohesion intercept of 40.9 kPa. Since the clay lumps are overconsolidated and the lump structure is unsaturated, negative pore pressures may be developing within the lumps being sheared. These negative pore pressures are not being equilibrated by any high positive pore pressures in the macro-voids as was observed with the triaxial tests on saturated clay shale lumps. Therefore, it is logical that the friction angle calculated for the triaxial tests on the unsaturated clay shale lump structure is higher.

The high cohesion intercept illustrates that the failure

mechanism was dominated by shear through the overconsolidated clay shale lumps.

5.2.5 Summary of Shear Strength Tests

The results from the consolidated undrained tests on clay shale lumps are very consistent with the results discovered from the softening tests. Water contents approach a limiting lower value of between 26 to 28%, depending on the plasticity of the clay shale. This is a reflection of the limiting lower void ratio of 0.75 and the limiting upper bulk density o. 2,000 kg/m^3 which the clay lumps approach under the applied confining stress. This demonstrates the ability of the lump structure to densify under the application of a low confining stress and then resist further consolidation under higher confining stresses.

The triaxial test results from the homogenized clay shale specimens show similar final density results compared to the lump triaxial test results (approaching 2,000 kg/m^3). The densities calculated from the clay shale lump specimens are an average of the higher density lumps (with densities close to in situ) and the softened clay within the macro-voids. Therefore, the lumps bias the calculation to give a higher overall density. This does, however, show that the lumps are able to compress into a packing arrangement that is quite

dense.

The large volume change measured during consolidation is a reflection of the lump structure. The clay lump specimens consolidate on two scales; a micro scale where the lumps act as individual compressible grains, and on a macro scale, where the softened clay within the macro-voids consolidates. The lump micro-voids are probably not consolidating and may even be swelling. The volume changes from consolidation in the softening tests and in the triaxial tests on clay lumps average approximately 30%.

The stress-strain response from all of the clay shale lump samples are quite similar, displaying an elastic-plastic response. A typical example is Test PWA2, Figure B43. Throughout all of the tests, large positive pore pressures developed very quickly which resulted in very high pore parameter A-bar values. These test results indicate that the clay lump structure becomes stable under a confining stress, but after it is subjected to a shear stress, a small shear strain causes the lump structure to collapse, transferring the confining stress to the pore water contained within the macro-voids. The clay lumps are able to move under a small shear stress because the softening process at the contact points reduces the interlump effective shear strength. The lumps continue to soften at their contact points throughout the

consolidation and shearing stage. This mechanism contributes to the development of the large positive pore pressures and pore pressure parameter A values (up to 2.6). Skempton (1954) indicates that a pore pressure parameter A value greater than 0.75 is an indication that the soil structure is highly sensitive.

The stress-strain curves plotted from the triaxial tests on clay shale lumps display a wavy behaviour (Figure B58). This behaviour was more pronounced when the larger clay shale lumps were tested (19 mm maximum size). The wavy behaviour may be an indication that the individual clay lumps are being sheared through. Since the clay shale lumps are overconsolidated, negative pore pressures may be attempting to develop within the sheared lumps. However, with the application of the shear stress, high pore pressures develop within the macro-voids of the lump structure. This is caused by the collapse of the lump structure during shear, thereby transferring some of the confining and shearing stress to the pore water within the saturated softened clay in the macro-voids. With high pore pressures in the macro-voids and negative pore pressures that may be attempting to develop within the clay lump, pore pressures will attempt to equilibrate. That is, the high pore pressures will partially dissipate into the clay shale lumps. This pore pressure equilibration dampens the influence of the confining stress which results in the shallow failure

envelopes. Unlike typical overconsolidated clay soil, the development of a positive pore pressure shifts the effective stress failure envelope to the left of the total stress failure envelope. The cohesion intercept is a reflection of the overconsolidated nature of the intact clay shale lumps.

The pore pressure transducers on the triaxial cell measure the average or equilibrated pore pressure which should be representative of the pore pressures that would develop in the field.

In a clay lump deposit, shear stresses, caused by subsequent construction lifts, may cause shear strains within the lump deposit, triggering the development of high pore pressures. The pore pressures will dissipate very slowly due to the low permeable nature of the softened clay shale in the macro-voids. Therefore, the failure of a clay shale lump deposit in an undrained manner is influenced by the amount of softening at the lump contact points and the shearing rate. Slow shear rates, which may be in the order of days or weeks, will allow the high positive pore pressures to equilibrate throughout the deposit and into the individual clay shale lumps. This reduces the effective strength within the clay lumps reducing the overall shear strength. The shear strength will improve as the clay lump deposit consolidates.

For rapid construction of a clay lump deposit, the unconsolidated undrained shear strength (c_u) should be used for design calculations. For stage construction, the effective angle of friction (ϕ'), cohesion intercept (c'), and an estimation of the pore pressure could be used for design. Estimating the pore pressure is difficult since the coefficient of consolidation calculated from the consolidation curve of triaxial tests is invalid (see Section 5.2.2).

The unconsolidated undrained shear strength (c_u) can be extrapolated (to σ_3 equal to zero) from each of the test series (from stress path plots in Figures 5.8 to 5.15). Table 5.1 lists the undrained shear strengths from each of the test series. A simple calculation using Taylor's slope stability design chart indicates that a 15 m high deposit of clay shale lumps with an undrained shear strength of 30 kPa would be stable with 18° slopes. Therefore, it appears that free standing deposits of clay shale lumps can be designed and do not necessarily have to be contained as concluded by Lord and Isaac (1989).

Changing the mixing fluid from tailings water to sludge does not influence the strength significantly but it does influence the rate of consolidation and moisture transfer into the lumps. Therefore, a deposit of clay lumps mixed with sludge has the potential to develop high pore pressures which will

dissipate very slowly.

The tests representing the ultimate or long term condition of the clay shale (homogenized clay) reveal that a deposit of clay lumps will become more stable. The clay mineral content is dominating the shear strength behaviour of the homogenized clay, whereas, the lump structure is dominating the behaviour in a clay lump deposit.

The homogenized clay shale is behaving as a lightly overconsolidated clay. The p-q plots (Figures 5.13 to 5.15) reveal that the clay is exhibiting a cohesion intercept with some development of positive pore pressure during shear (average pore pressure parameter A of 0.5).

5.3 Comparison to Case Histories

Previous research on hydraulically placed fills that have been documented are presented in Section 2.1. Most of the cases report large volume changes ranging from a low of 4% to as much as 22%. The sites reporting the smaller volume changes also report that fines such as sand, silt and sometimes shell fragments infilled the interlump void spaces. If these sites are eliminated, then the average volume change reported is 15%. This is within the range of volume change determined from the softening and consolidated undrained

triaxial tests (10% to 40%). The field volume change measurements in the case histories were probably higher than that reported since the clay lumps, upon deposition, will very quickly settle into a denser structure.

Dusseault et al. (1984) reported on a clay lump spoil backfill that was subsequently saturated after being placed. The lump to lump contact points soften, reducing the effective strength between the lumps, which allows the lumps to manoeuvre into a denser arrangement. This can account for the large consolidation volume changes that occur during the softening tests and the triaxial compression tests with clay shale lumps. The samples reach a limiting lower void ratio under a low confining stress. As the lumps continue to absorb water and the clay shale swells and slakes into the macro-voids, further volume change (consolidation) is dependent on the interlump material characteristics. This interlump material, which is essentially the same material as the clay shale lumps and therefore has inherited the same properties, exhibits low hydraulic conductivities. This was also found by Carrier and Bromwell (1983) and Whitman (1970) who determined that the amount and rate of compression was controlled by the clay matrix between the clay balls. Pore pressure dissipation was also noted to be very slow in many of the cases discussed.

Many of the sites also reported that after a period of time the fill developed enough strength for it to be put into its design use. During this time period, the water contents have presumably equilibrated throughout the clay lump structure. Consolidated undrained triaxial compression tests on the homogenized clay shale also revealed that the ultimate or long term condition would exhibit higher strengths.

Syncrude has reported that their hydraulically placed clay shale lump fill exhibited water contents with a range between 25 to 40%, or an average of 30 to 35% (Lord and Isaac 1989). The fill heights averaged 3.2 m which represents a confining stress between 55 to 60 kPa. Figure 5.1 and 5.5 shows that at low confining stresses (low fill heights), the bulk water contents are within this range. The figures also demonstrate that as higher lifts are constructed, the ability of the clay shale lump structure to absorb large volumes of water decreases. Their conclusion was that the hydraulically placed clay shale deposits were unstable and must be contained. This is valid for the fill heights that they constructed but at higher fill heights (greater than 3 m), the confining stress compresses (lump movement without the dissipation of pore pressure) and consolidates (pore pressure dissipation) the clay shale lump structure to form a deposit that can be free standing.

5.4 Volume of Transporting Liquid Trapped in Clay Lump Deposit

Although it is not within the scope of this thesis, it is important to realize the implications of the test results with respect to the amount of fluid that can be trapped within the clay lump void volumes and ultimately absorbed by the clay shale.

For every cubic metre of clay shale excavated, the volume of tailings pond water or sludge trapped in the voids can be estimated from the void ratios.

In situ clay shale has a void ratio (e_s) of 0.5, and the deposited clay shale lump structure has a void ratio (e_l) of 0.7, therefore:

$e_s = 0.5 = V_{vs} / V_s$

$e_l = 0.7 = V_{vl} / V_s$

where: V_{vs} = in situ void volume

V_s = volume of the solids

V_{vl} = lump structure void volume

(Assuming that the volume of solids (V_s) does not change, which is true for pond water and approximate for sludge, as sludge solids are small)

The difference in volume is therefore:

$$V_{vl} - V_{vs} = 0.7V_s - 0.5V_s = 0.2V_s$$

In 1 m^3 of in situ clay shale, V_s = 0.667 m^3, therefore, the difference in volume is 0.2 x 0.667 = 0.13 m^3.

Therefore, for every 1 m^3 of clay shale excavated, 0.13 m^3 of liquid can be disposed, or, for 22x10^6 m^3 of excavated overburden, 2.9x10^6 m^3 of liquid waste can be disposed of annually.

Table 5.1   Shear Strength Parameters*

Triaxial Test Series	Effective ϕ' (deg)	Effective c' (kPa)	Total ϕ (deg)	Total c (kPa)	Undrained c_u (kPa)
Series 1	21.7	9	11.8	8	10
Series 2	20.2	9	12.4	6	7
Series 3	7.8	38	5.3	29	32
Series 4	2.4	62	1.6	58	59
Series 5	8.2	50	5.3	44	48
Series 6	13.6	63	12.7	58	75
Series 6A	21.9	16	13.7	15	20
Series 7	21.1	29	11.7	57	73

* Derived from p-q plots:
  $\sin\phi = \tan\psi$ $c = a / \cos\phi$
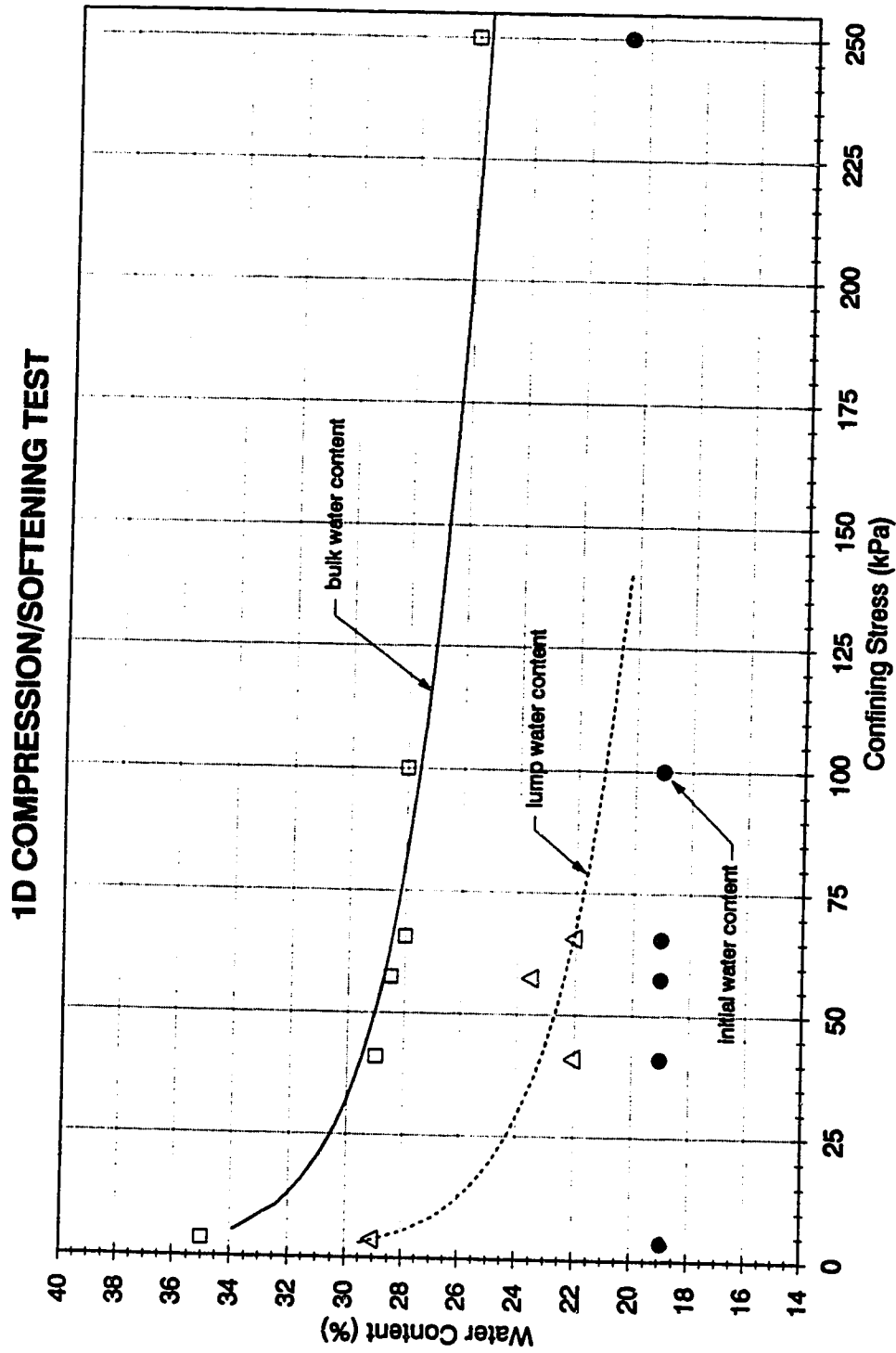
Figure 5.1   Water Content with Confining Stress

131
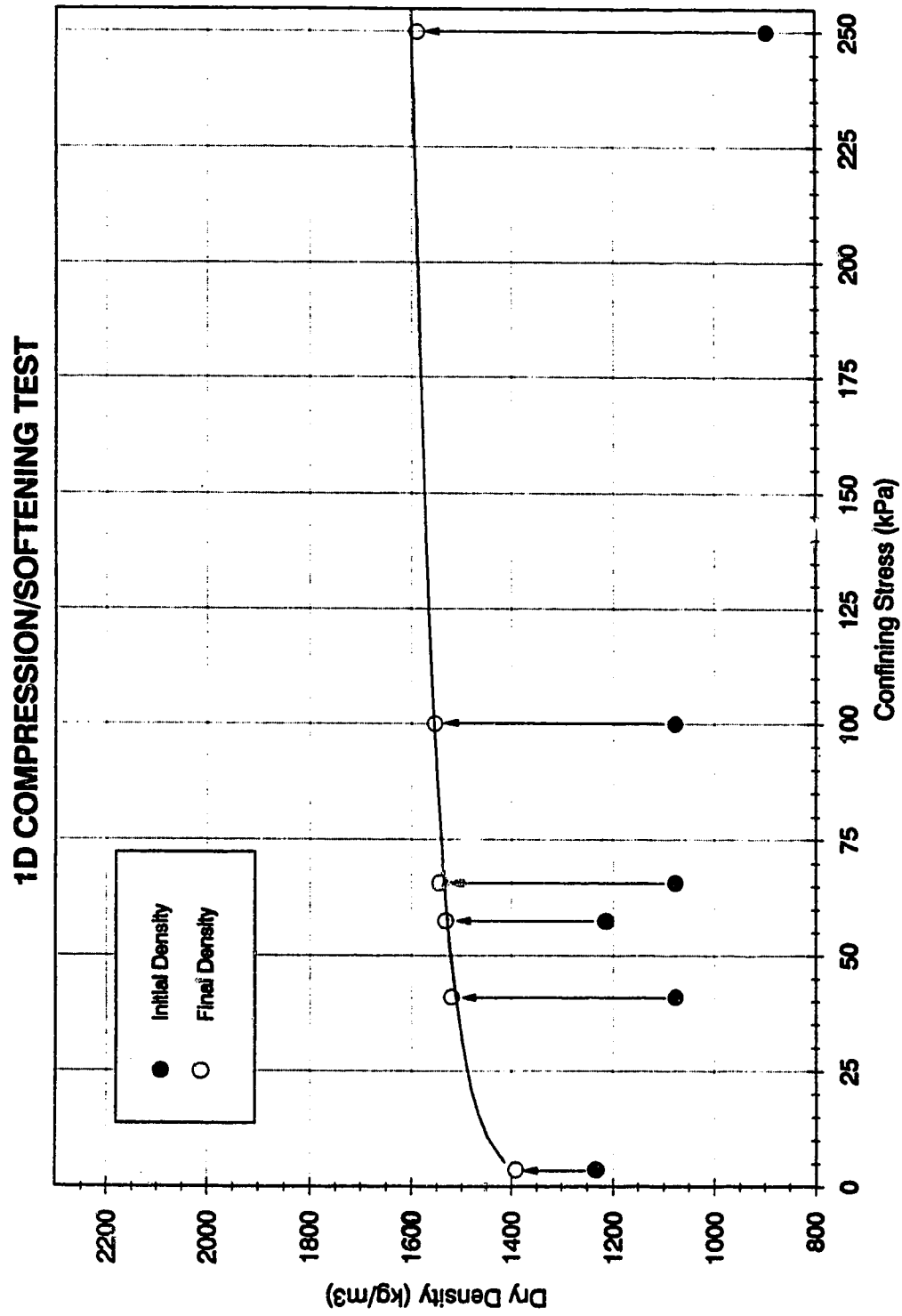
Figure 5.2   Dry Density with Confining Stress
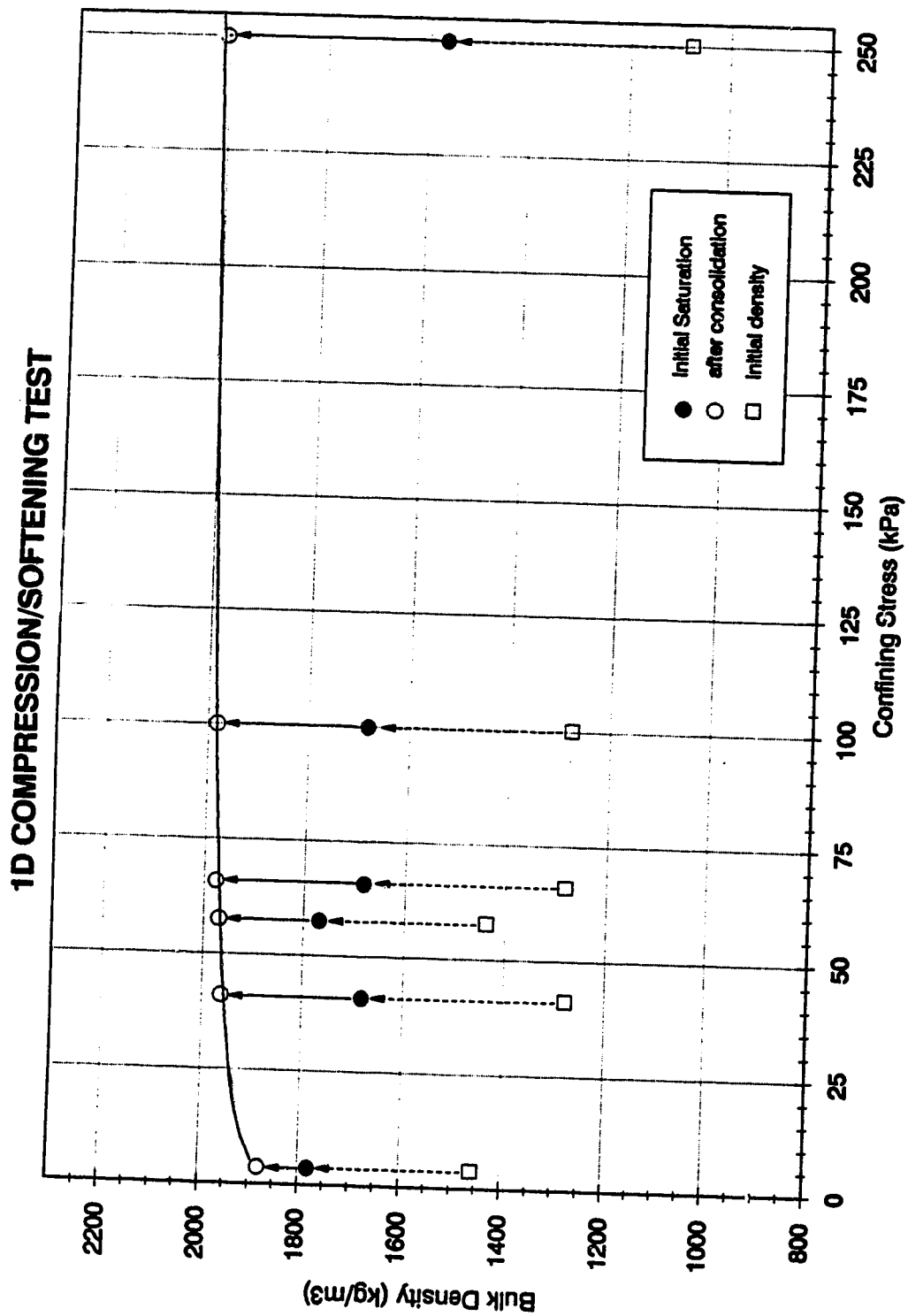
Figure 5.3   Bulk Density with Confining Stress

1D COMPRESSION/SOFTENING TEST

Confining Stress (kPa)

Maximum Volume Change (%)
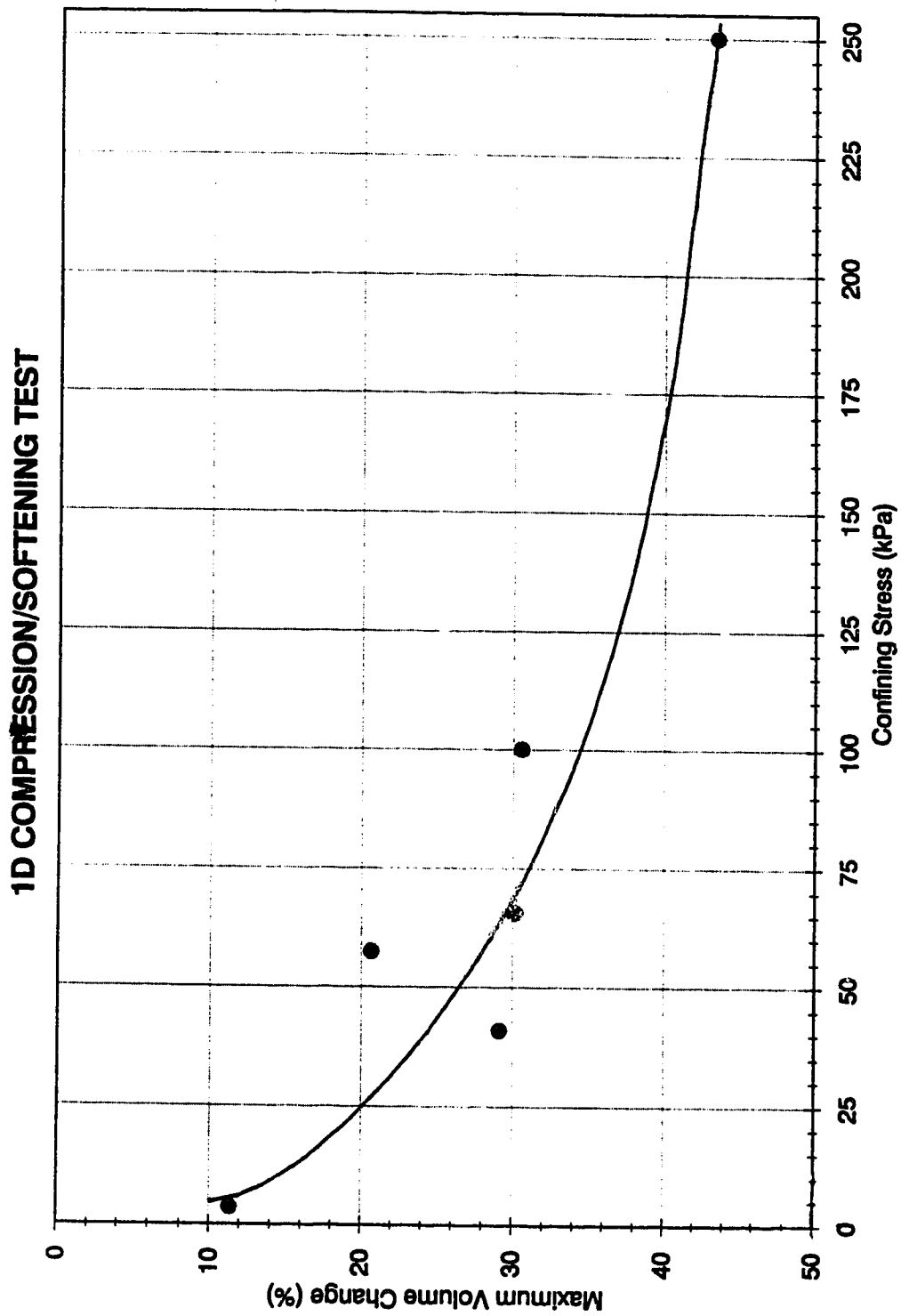
Figure 5.4   Maximum Volume Change during Compression

134
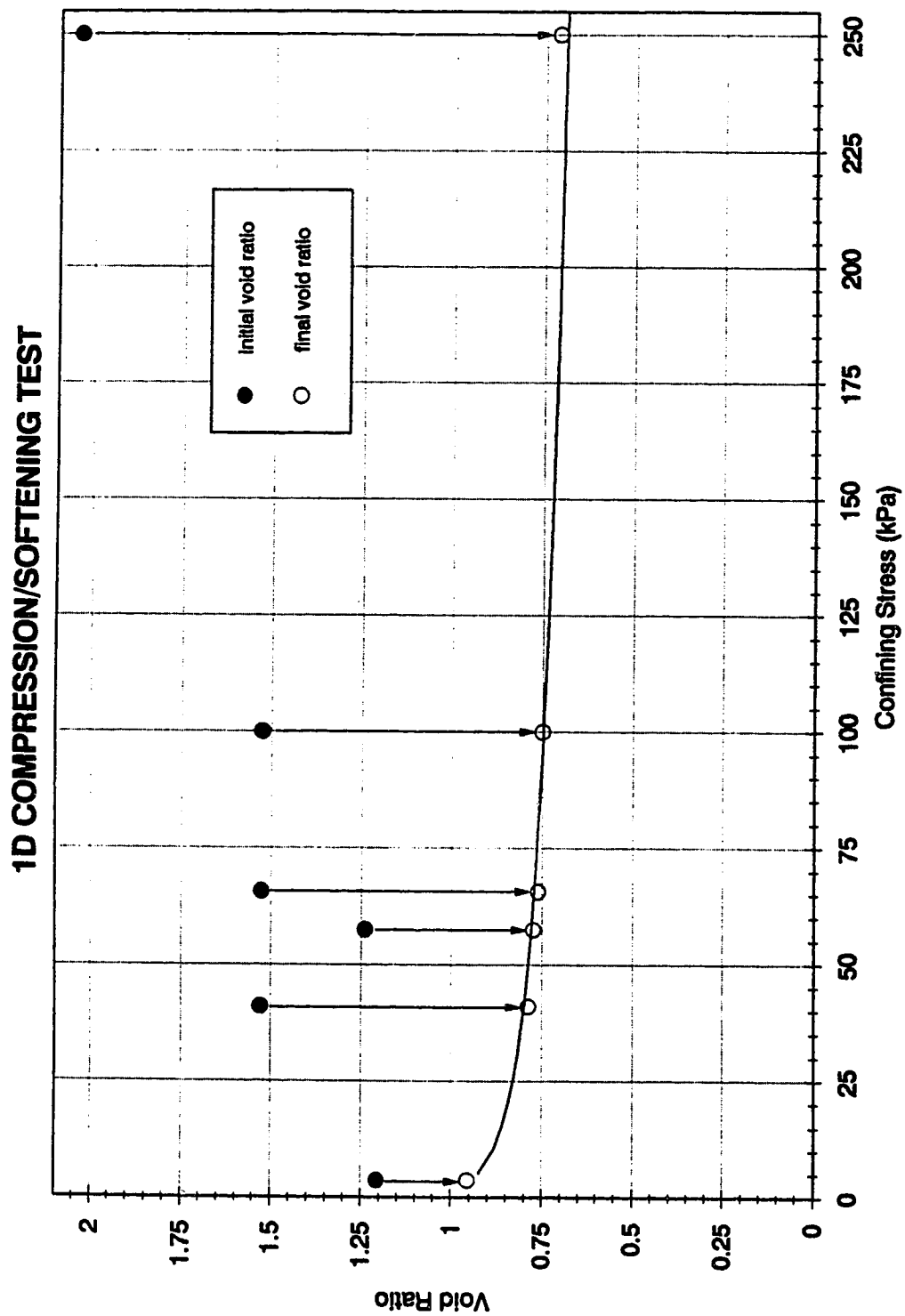
Figure 5.5   Void Ratio with Confining Stress
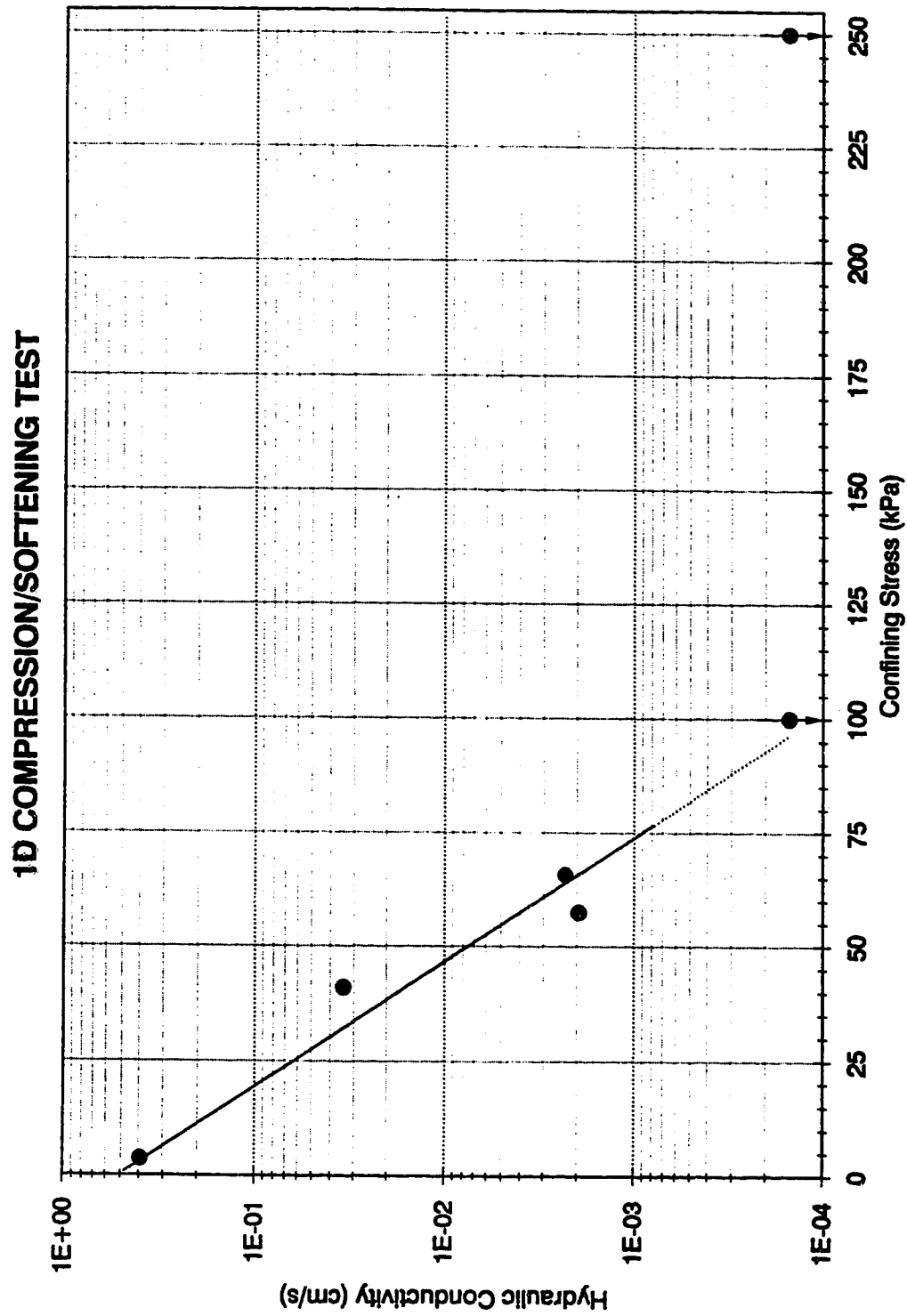
Figure 5.6   Hydraulic Conductivity with Confining Stress
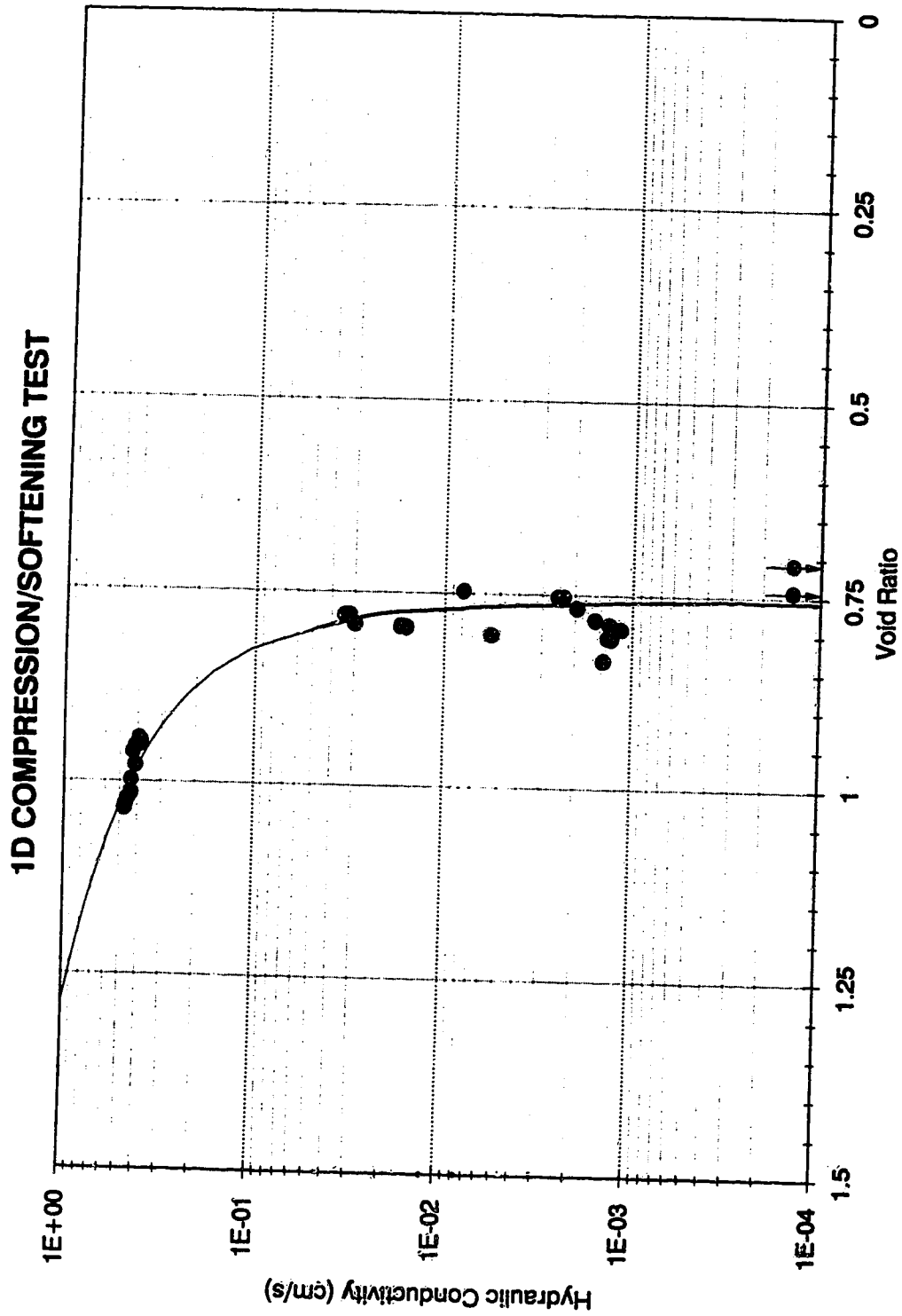
Figure 5.7 Hydraulic Conductivity with Void Ratio
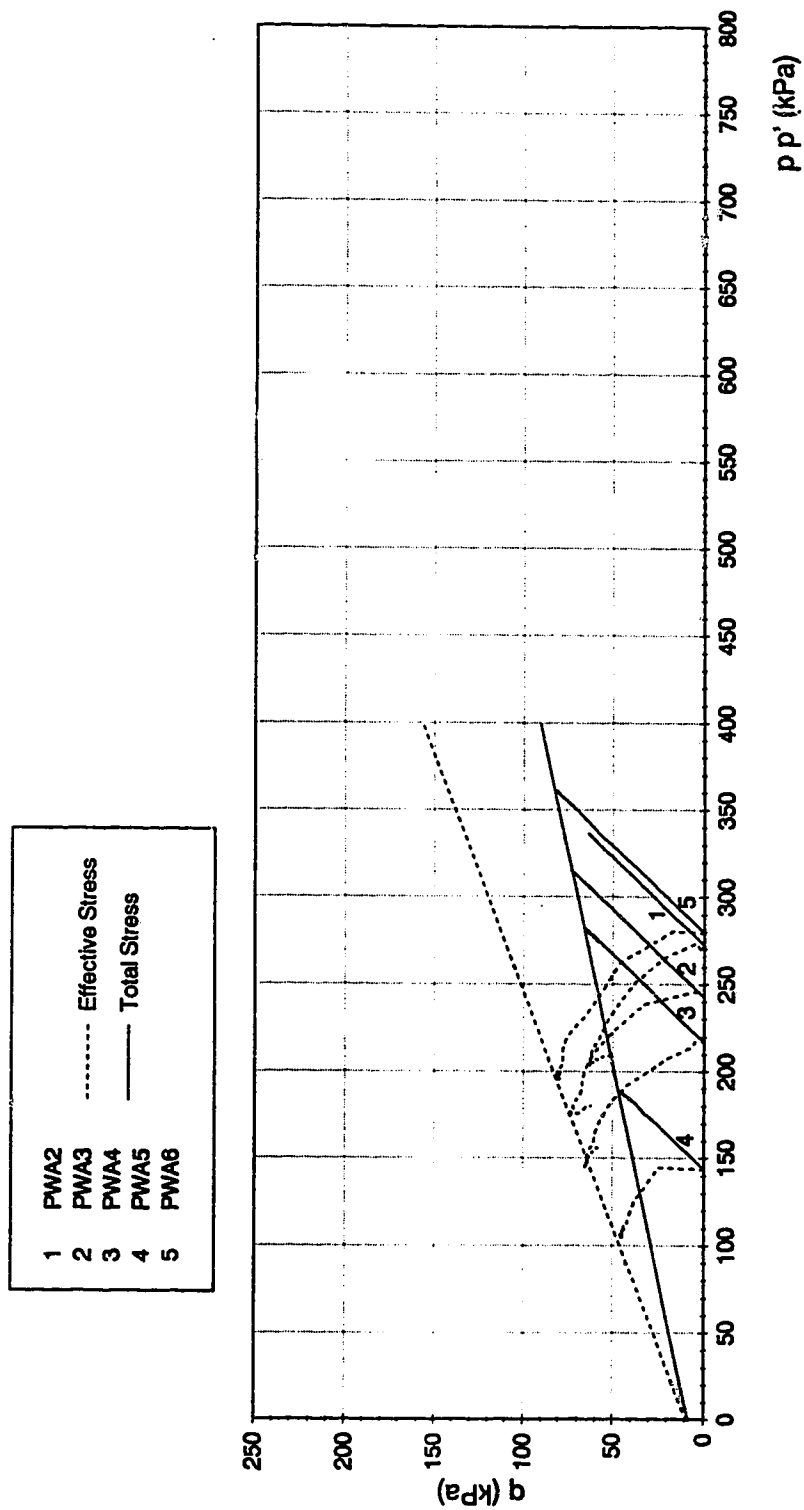
Figure 5.8   Stress Path - Triaxial Test Series 1
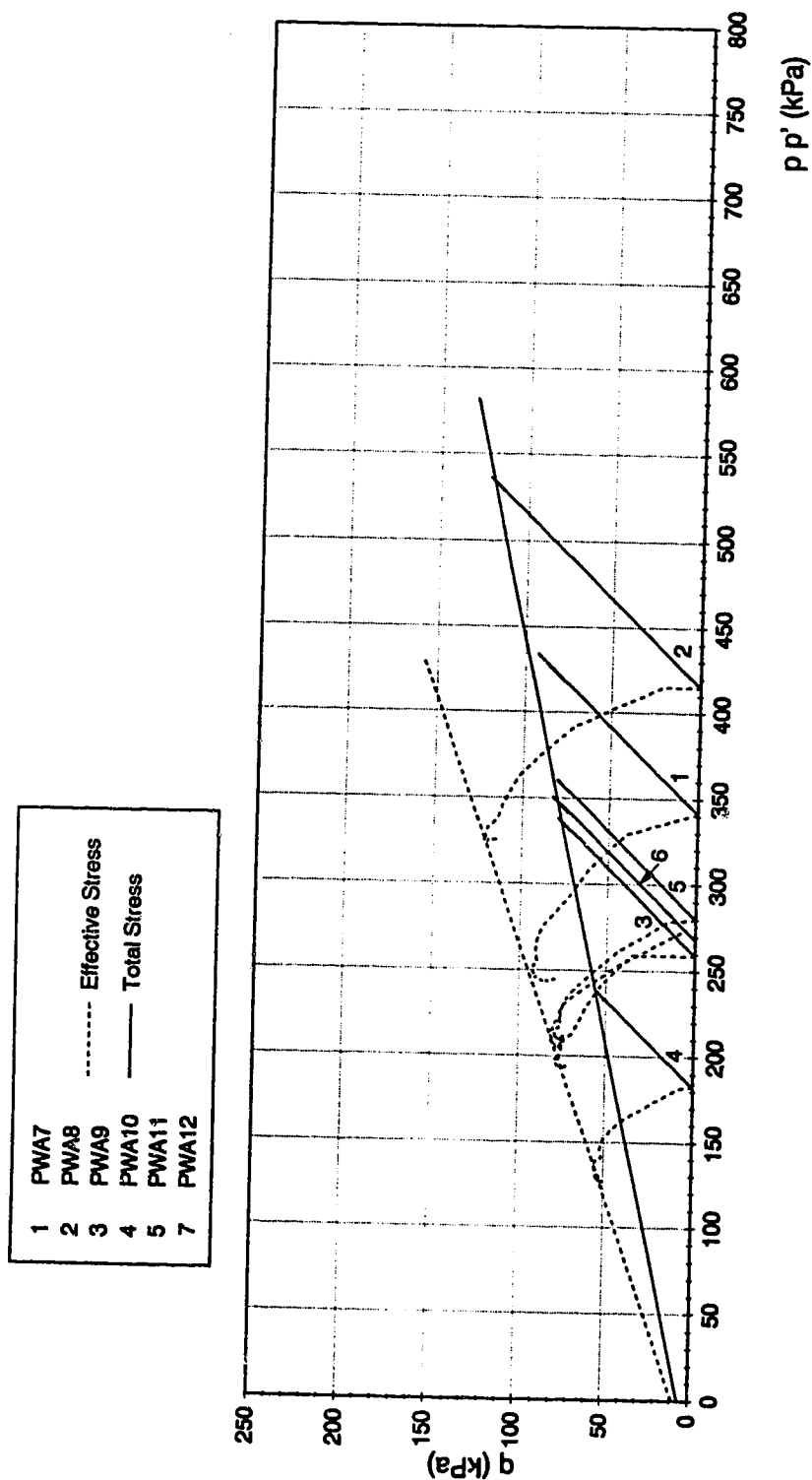
Figure 5.9   Stress Path - Triaxial Test Series 2
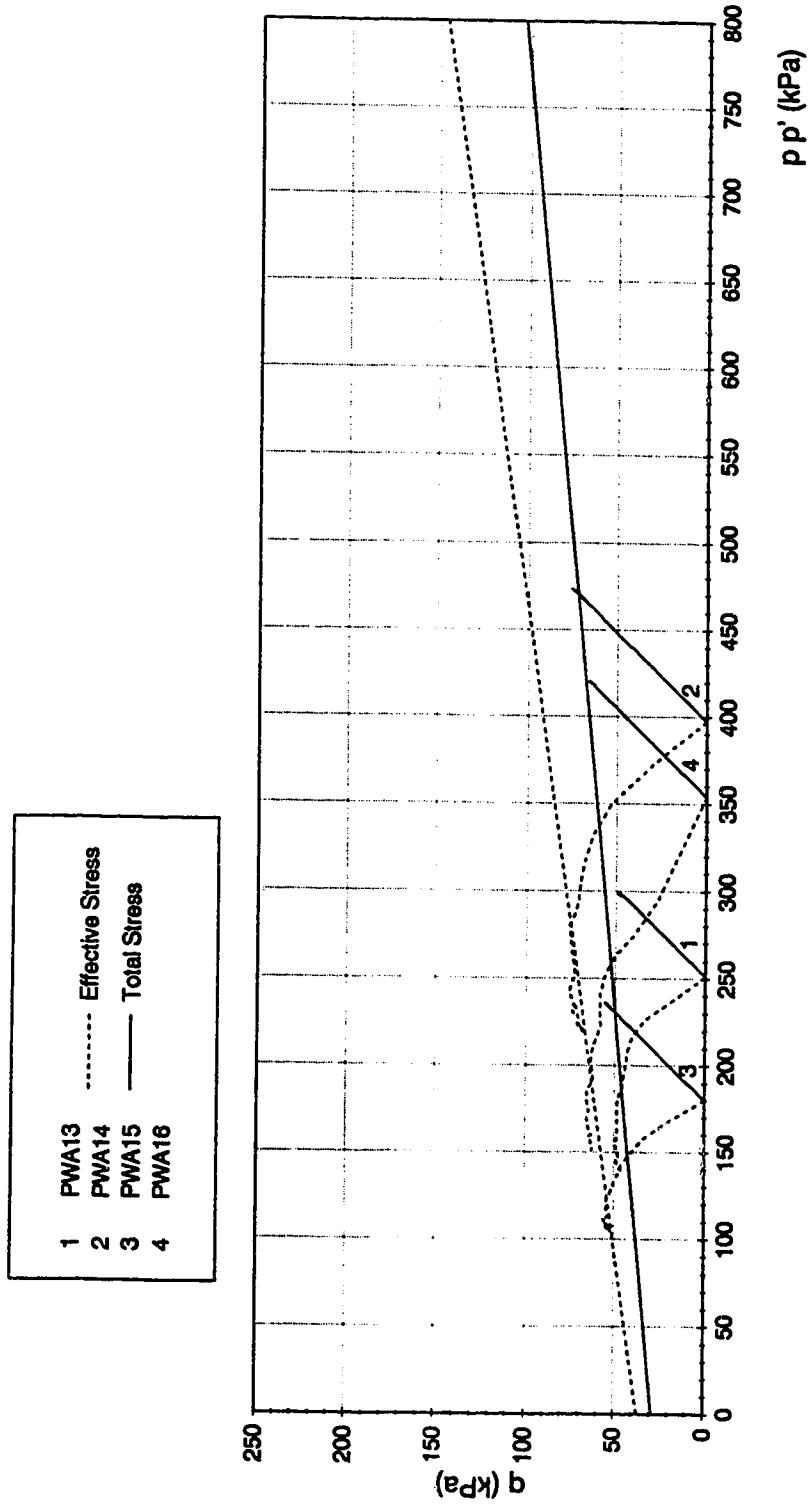
Figure 5.10   Stress Path - Triaxial Test Series 3
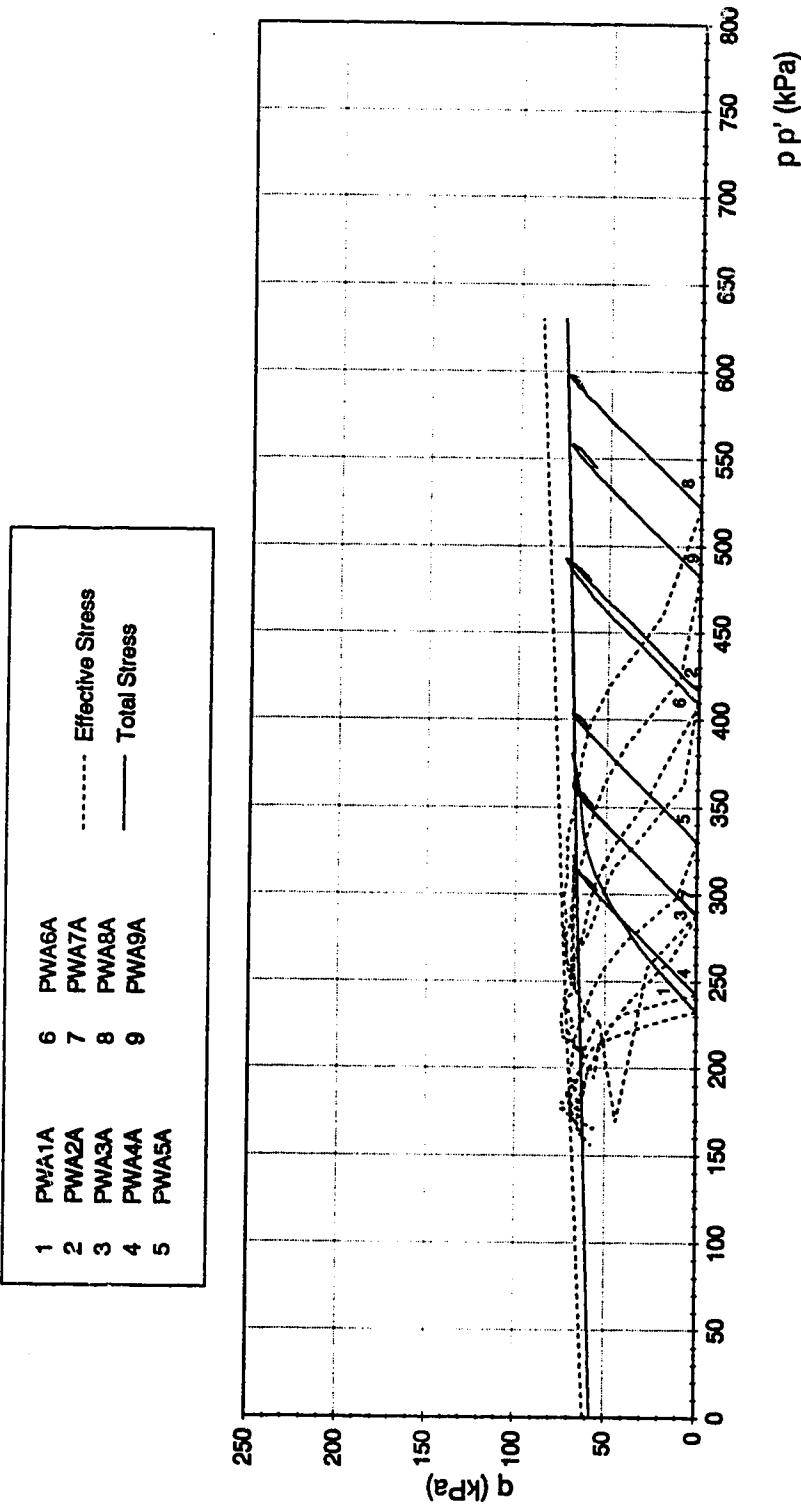
Figure 5.11   Stress Path - Triaxial Test Series 4
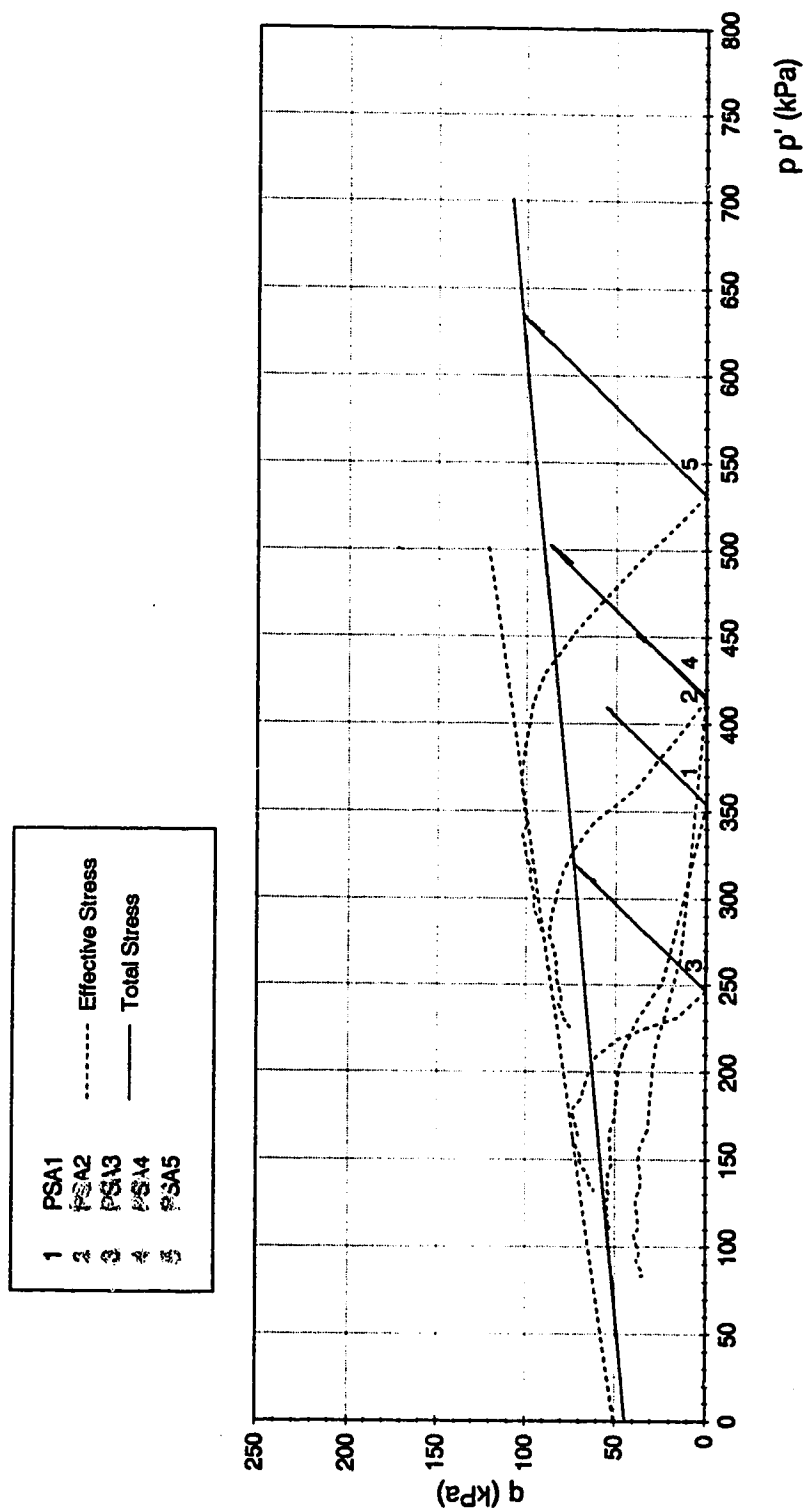
Figure 5.12   Stress Path - Triaxial Test Series 5
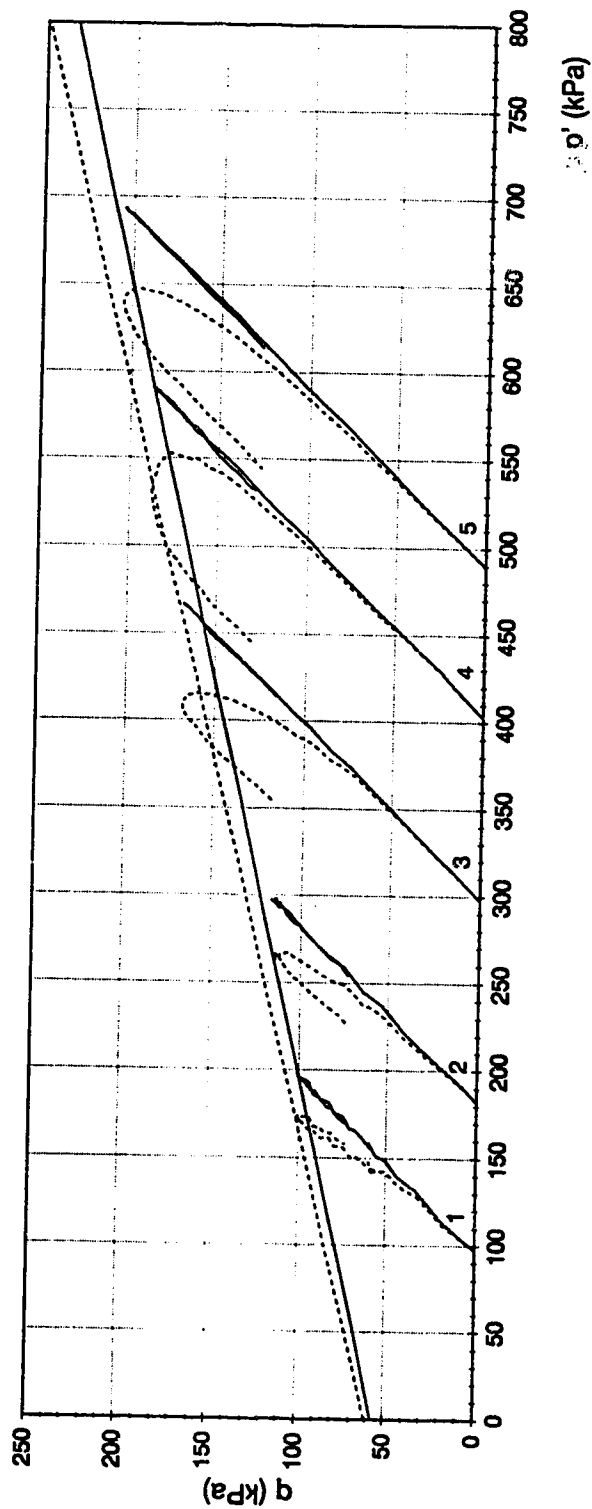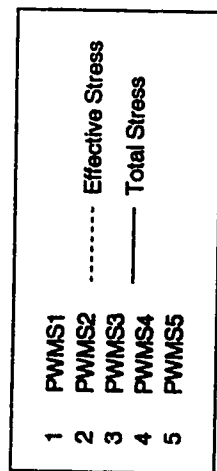
Figure 5.13   Stress Path - Triaxial Test Series 6
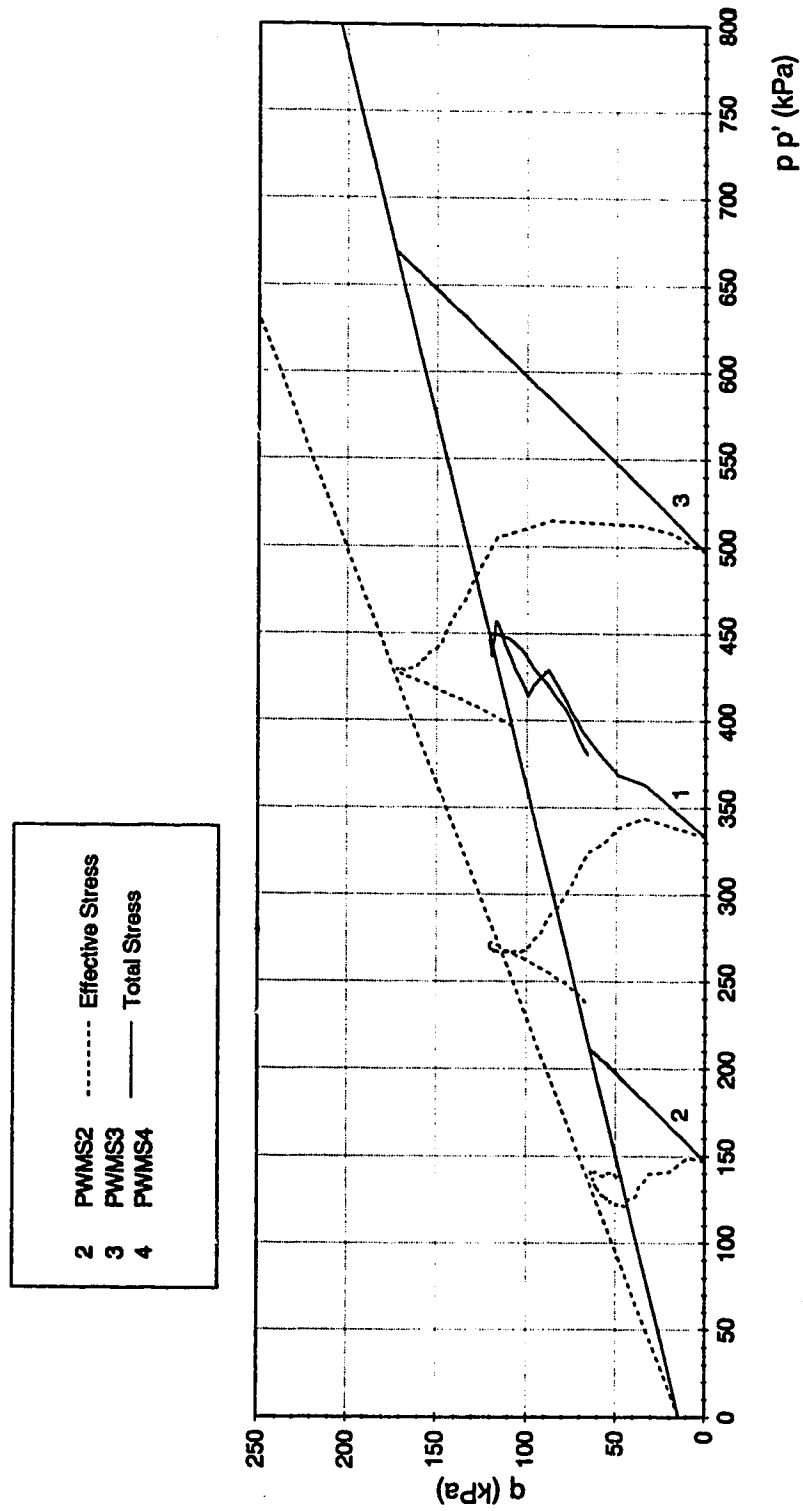
Figure 5.14   Stress Path - Triaxial Test Series 6A
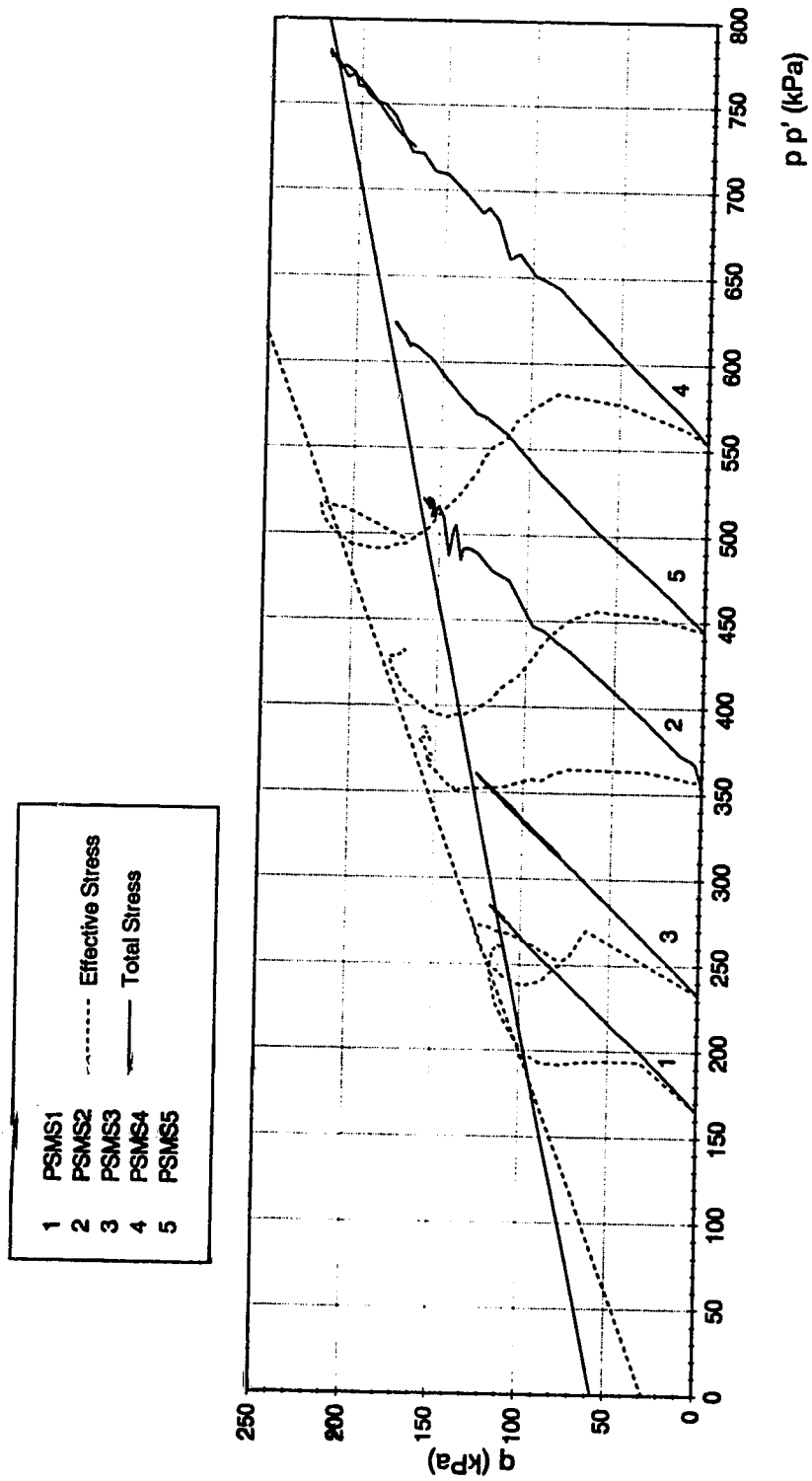
Figure 5.15   Stress Path - Triaxial Test Series 7

TRIAXIAL COMPRESSION TESTS (102mm dia)
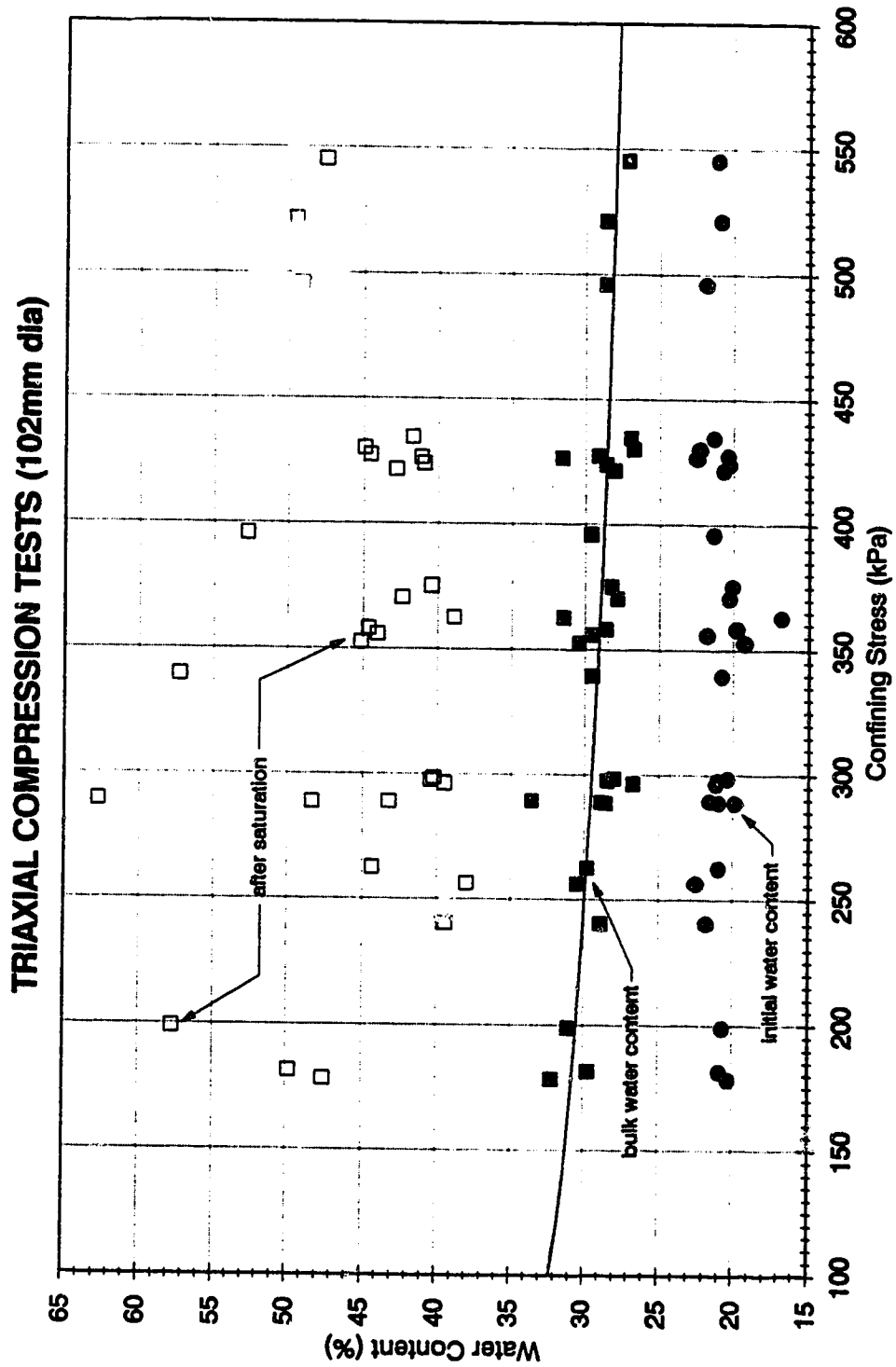
Figure 5.16   Water Content with Confining Stress
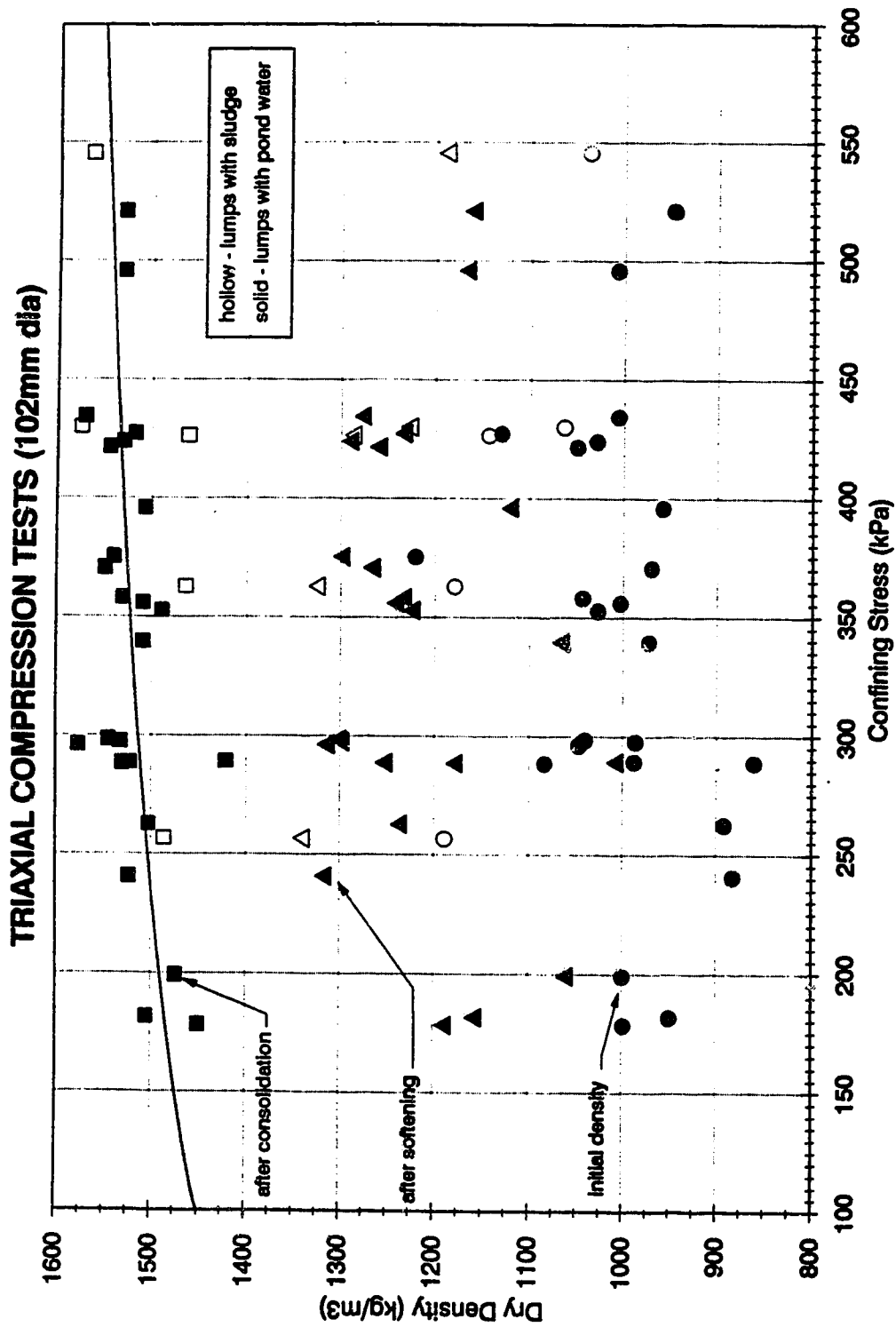
Figure 5.17   Dry Density with Confining Stress
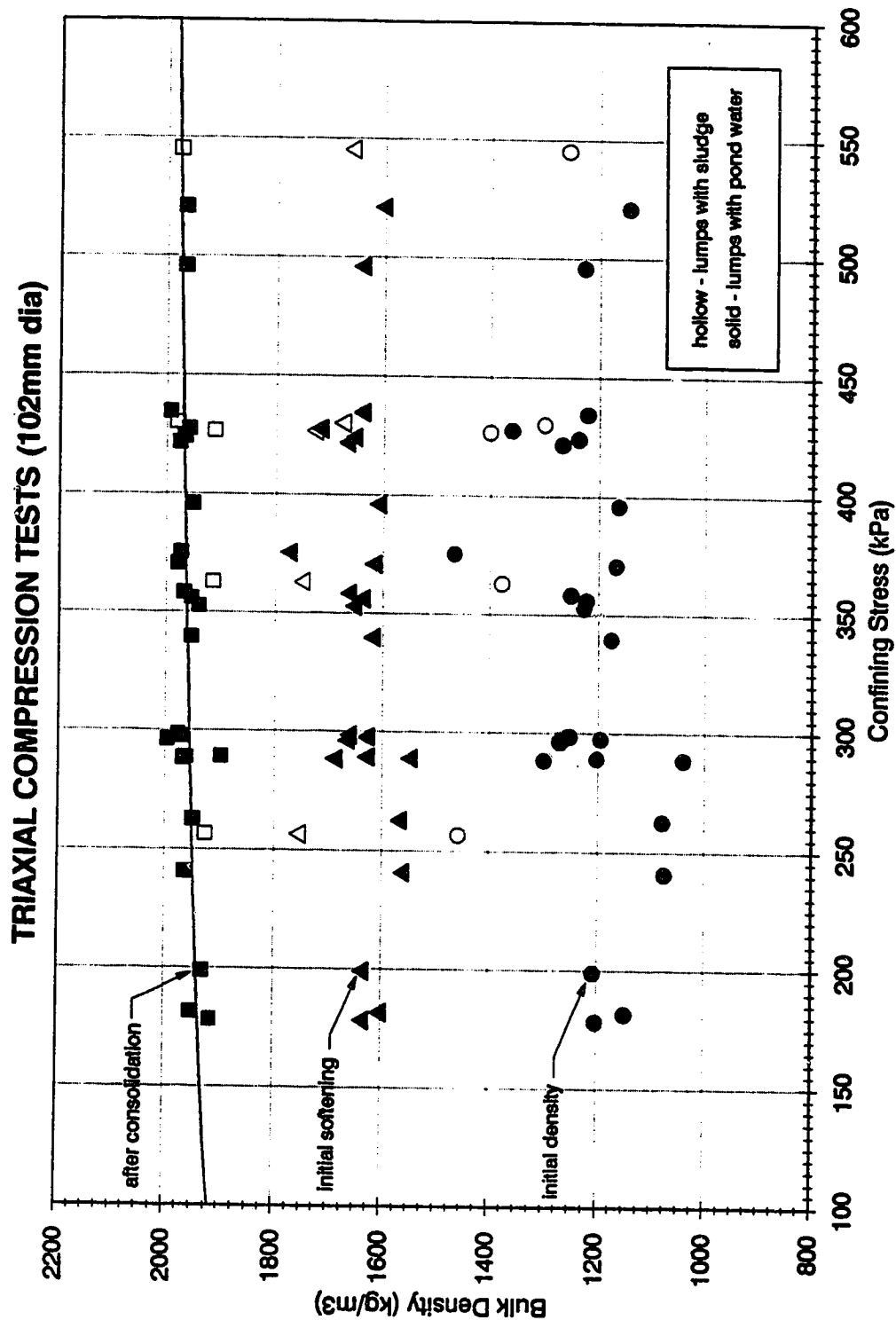
Figure 5.18   Bulk Density with Confining Stress
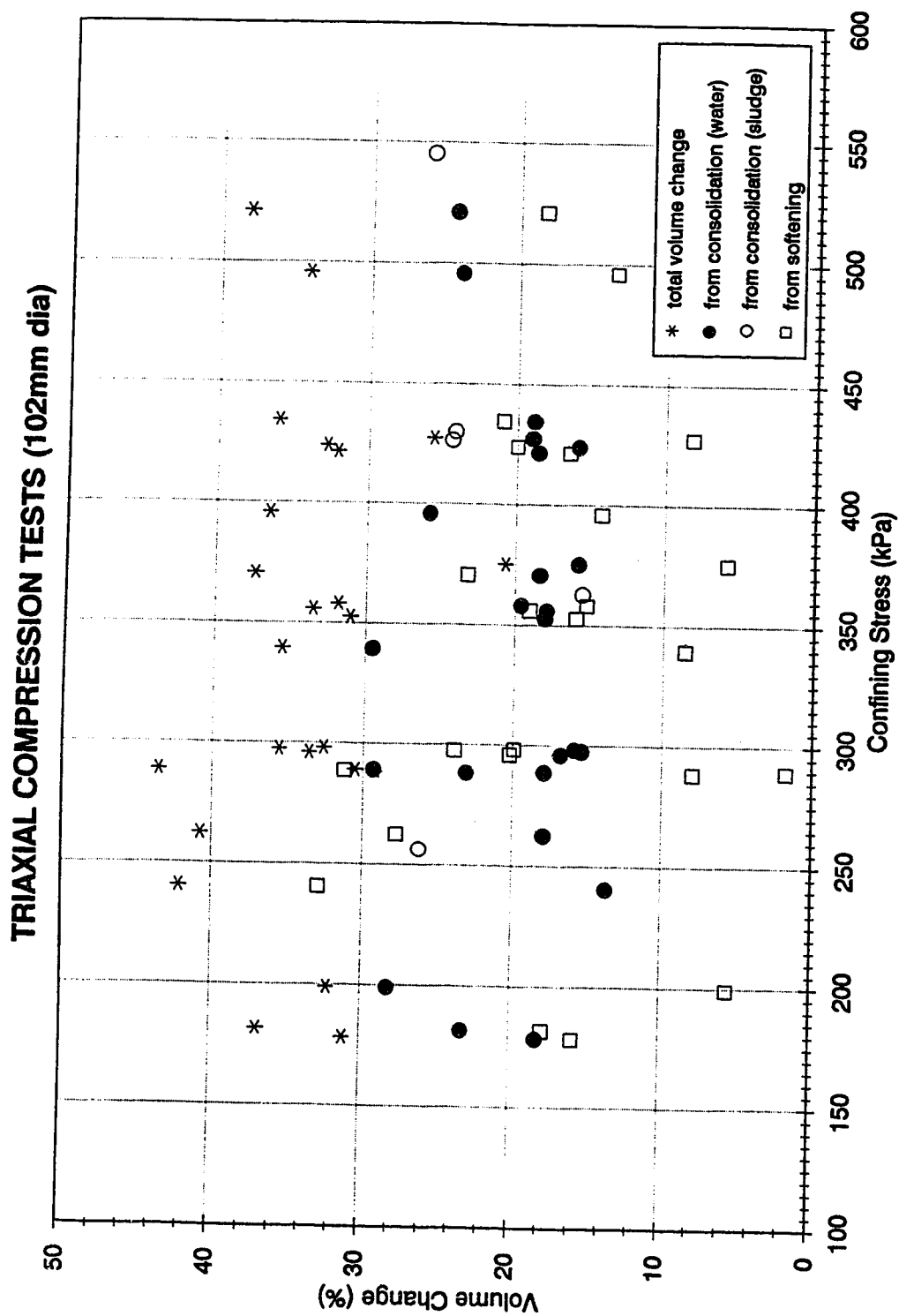
Figure 5.19   Volume Change with Confining Stress

TRIAXIAL COMPRESSION TESTS (102mm dia)

Void Ratio

Confining Stress (kPa)

initial void ratio

final void ratio
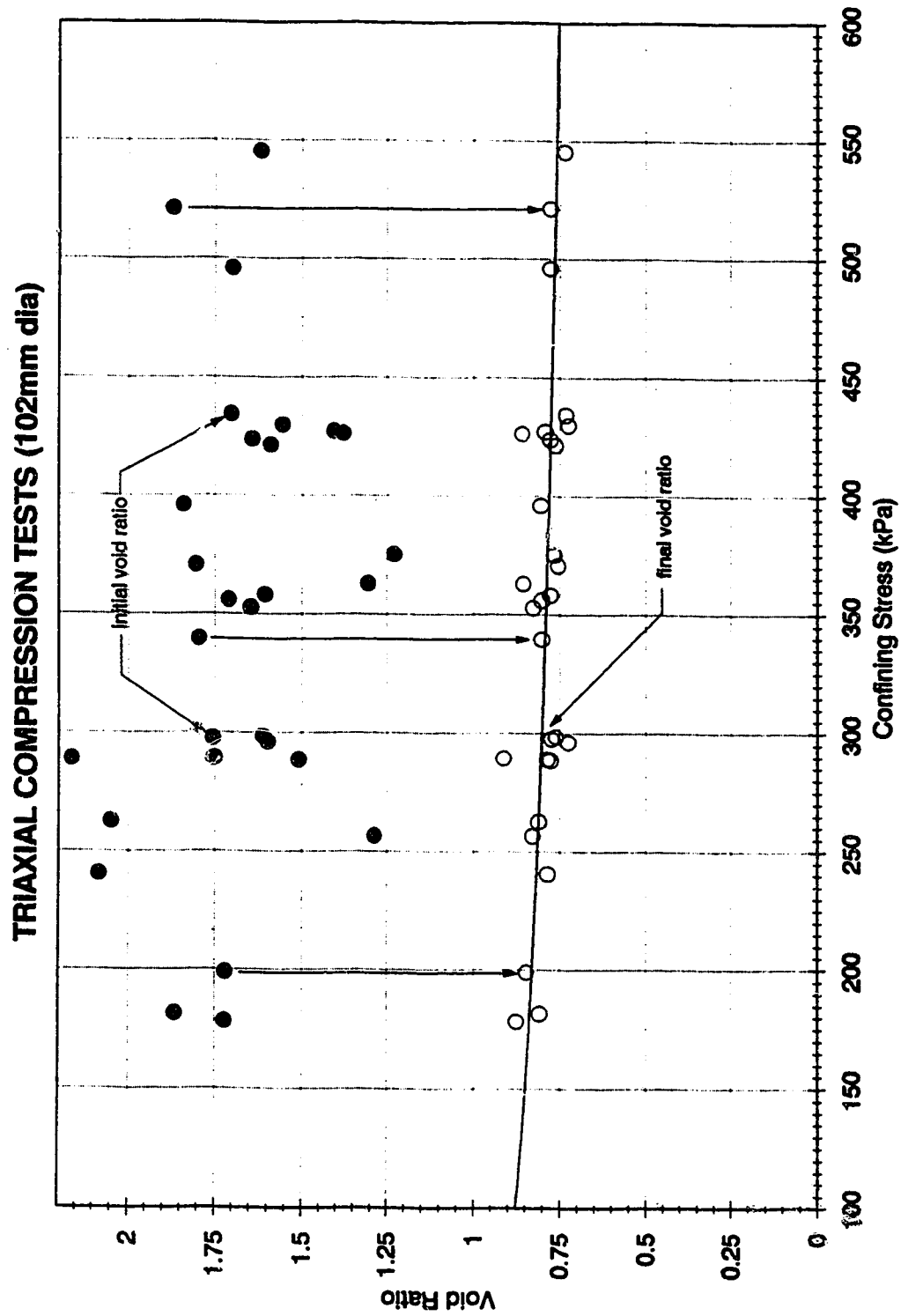
Figure 5.20   Void Ratio with Confining Stress

Figure 5.21b Clay Shale Lump - Pond Water Specimen after Shearing (rubber membrane removed)
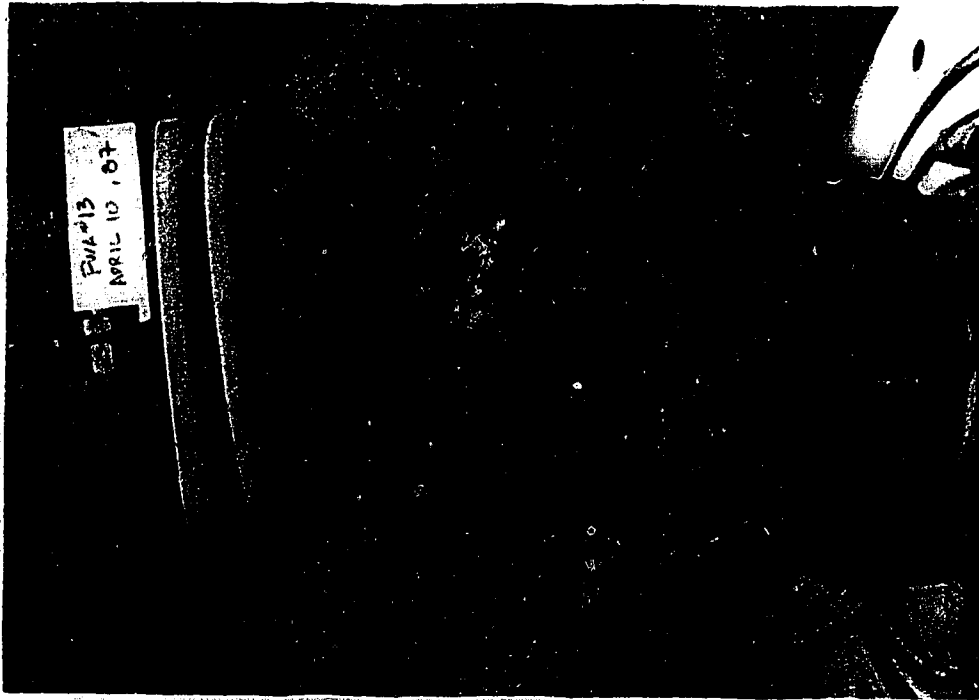
Figure 5.21a Clay Shale Lump - Pond Water Specimen after Shearing (in rubber membrane)
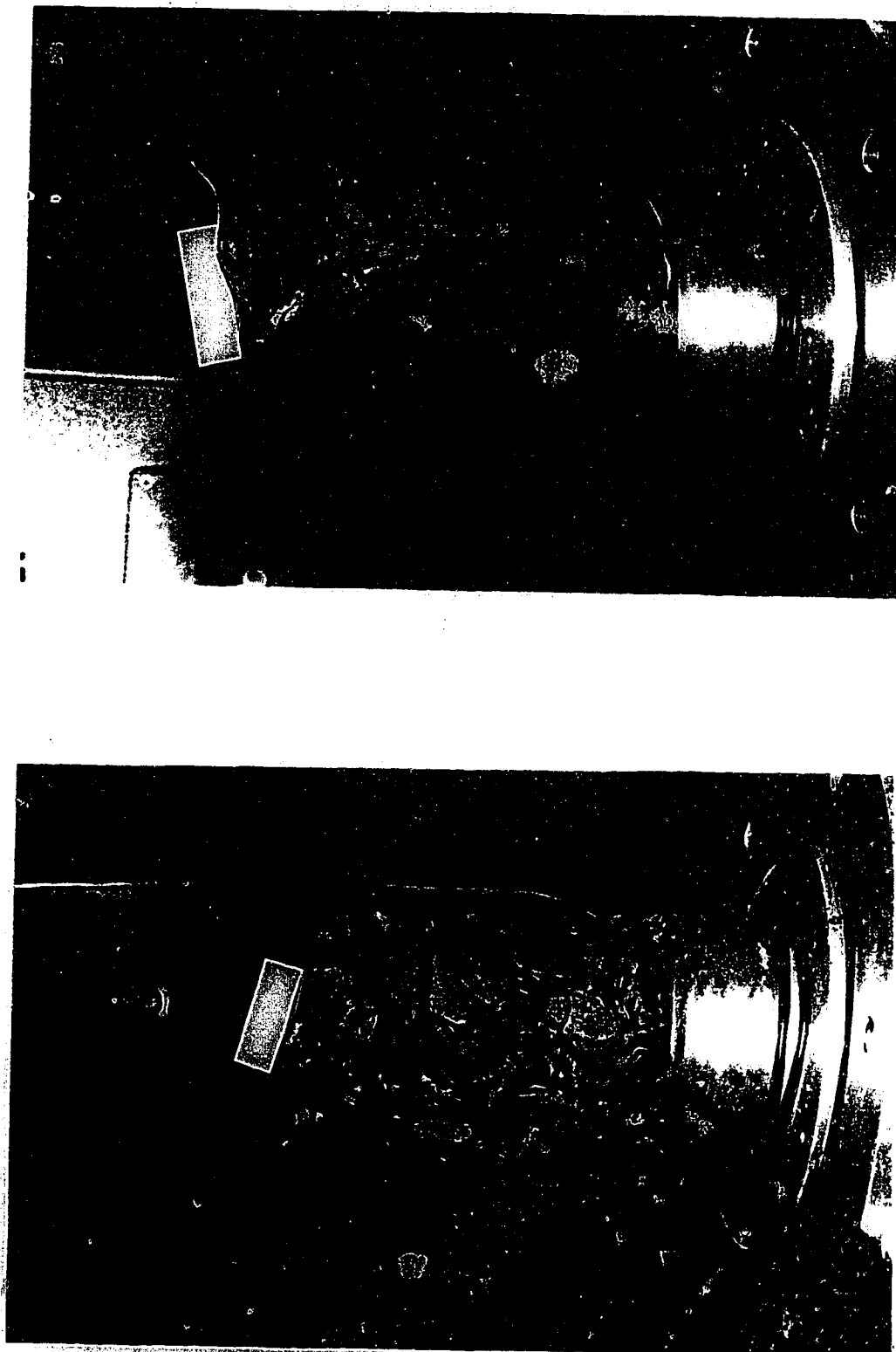
Figure 5.22   Clay Shale Lump - Sludge Specimens after Shearing
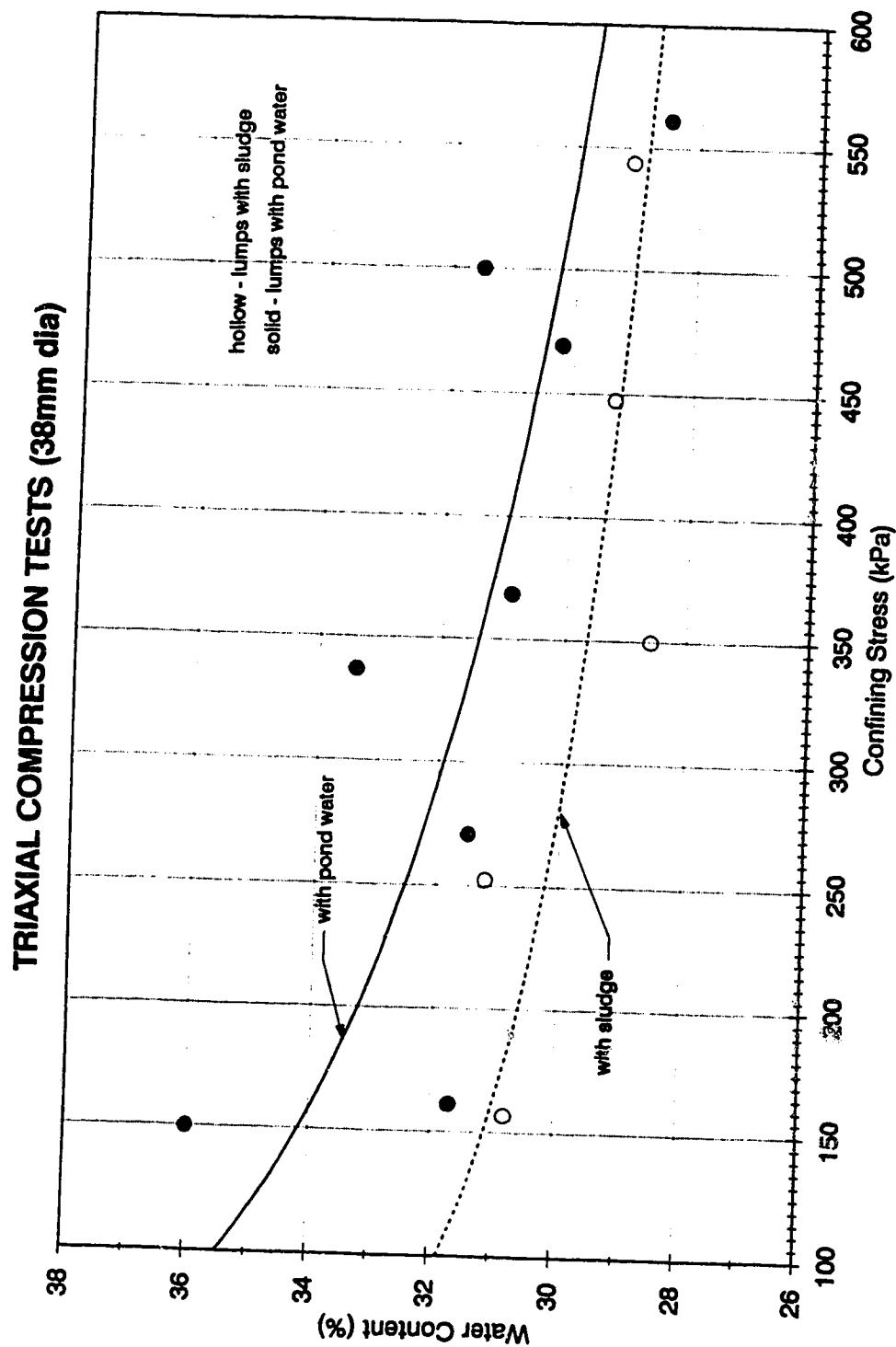
Figure 5.23   Water Content after Consolidation
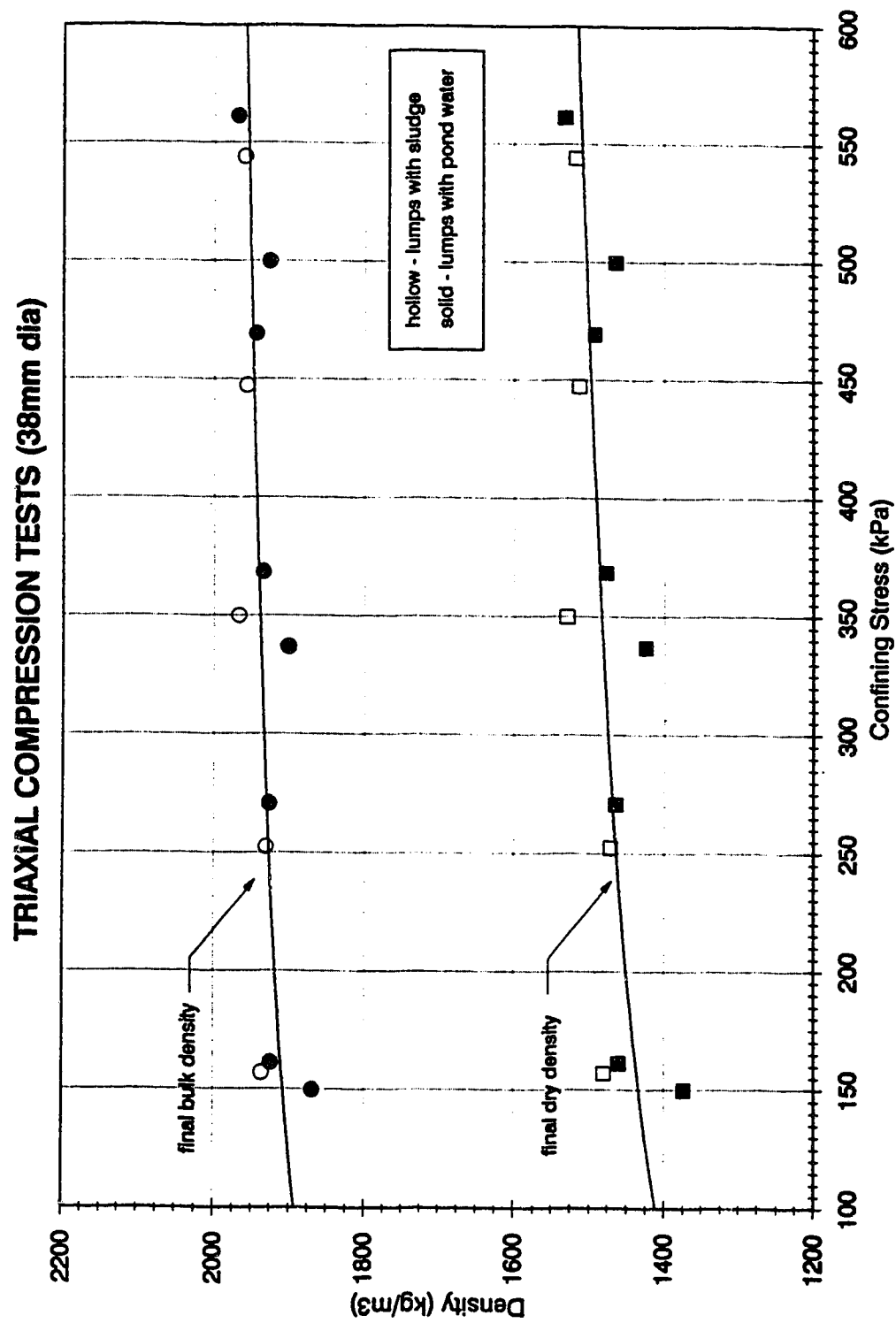
Figure 5.24   Bulk and Dry Density after Consolidation

154

TRIAXIAL COMPRESSION TESTS (38mm dia)
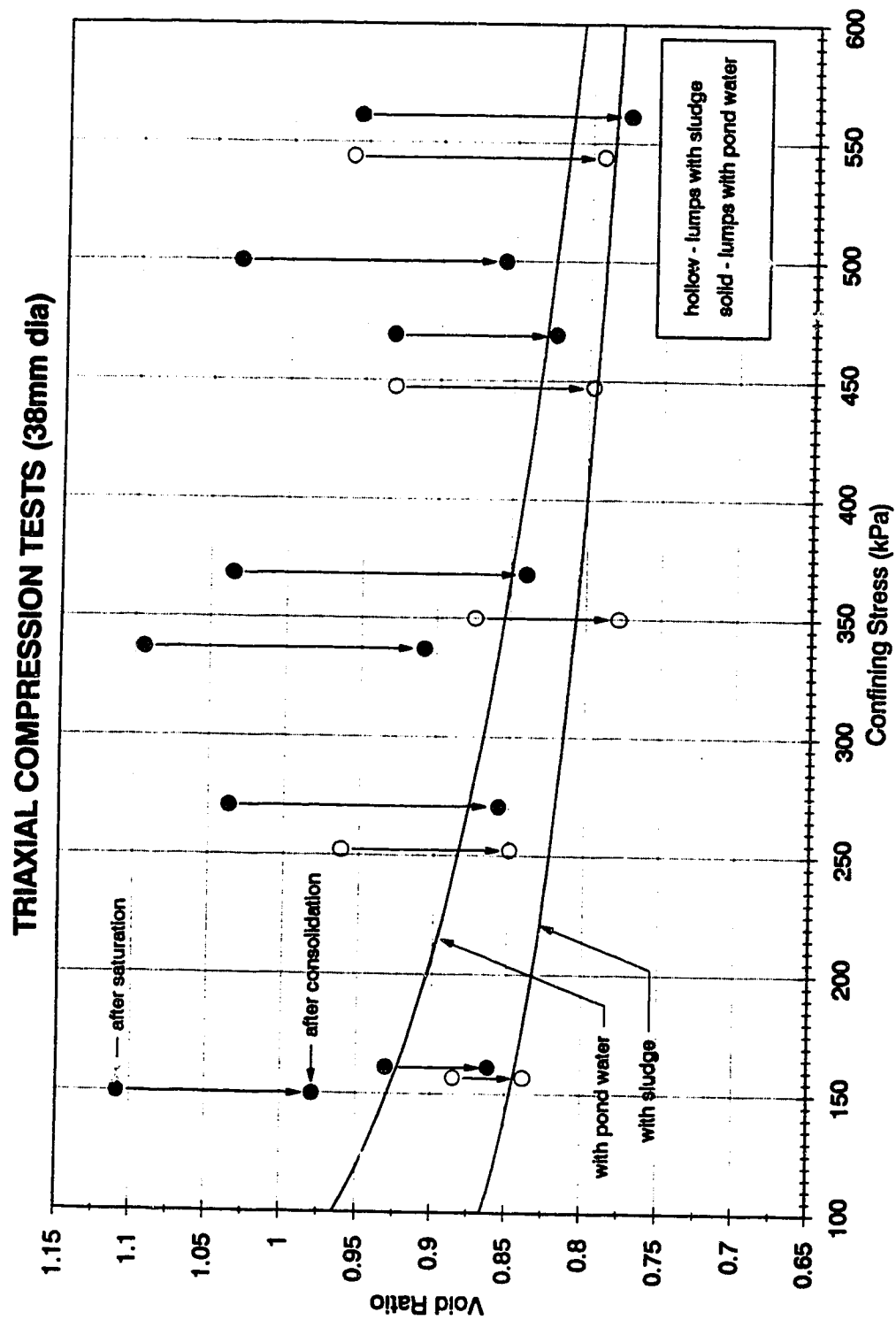
Figure 5.25   Void Ratio with Confining Stress
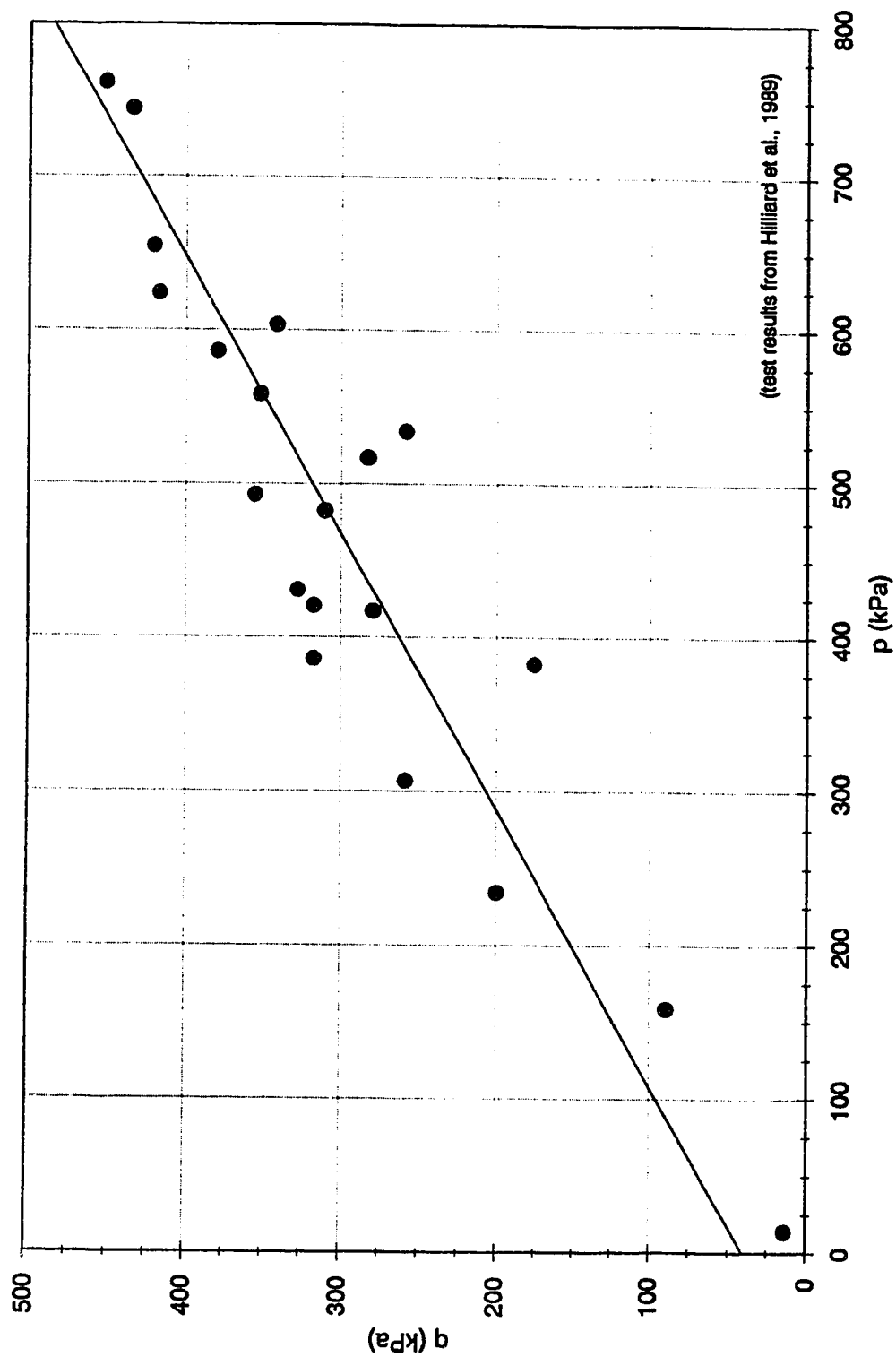
Figure 5.26 Unsaturated Clay Shale Lump Triaxial Test Results

(test results from Hilliard et al., 1989)

6.0 Conclusions and Recommendations

6.1 Conclusions

The work in this thesis investigated how the confining stress, softening duration, lump size and mixing fluid influences the shear strength of a hydraulically placed clay shale deposit. The results are as follows:

1. The softening tests revealed that the lumps form a structure that is initially free draining (confining stresses less than 66 kPa). At a confining stress between 66 and 100 kPa, the lump structure compresses to form a mixture exhibiting very low drainage capabilities. This stress range would be reached at a depth of 3 m to 5 m below the fill surface. The only water available to the lumps for further softening will come from the macro-voids. The low hydraulic conductivity of the mixture does not readily allow the ingress of more water to the macro-voids to continue the lump softening process.

2. Increasing the softening period (under a low confining stress of 10 kPa) from 3 to 6 hours has little influence on the shear strength. Effective and total shear strength parameters are $\phi'=21°$, $c'=9$ kPa and $\phi=12.1°$, $c=7$ kPa, respectively.

Increasing the softening period (under a low confining stress of 10 kPa) to an average of 25 hours results in a lower friction angle and a higher cohesion intercept. Effective and total shear strength parameters are $\phi'=7.8°$, $c'=38$ kPa and $\phi=5.3°$, $c=29$ kPa, respectively.

3. The lump structure is behaving as an overconsolidated clay soil but exhibiting very high positive pore pressure development (reflected by the large pore pressure parameter A values).

4. The wavy nature of the stress strain curve, which became more pronounced when the larger size clay lumps were tested, may be an indication that the individual clay shale lumps are being sheared through. Since the clay shale lumps are overconsolidated, negative pore pressures may be attempting to develop within the individual lumps being sheared, however, large positive pore pressures are measured. This high pore pressure (or high pore pressure parameter A) demonstrates the collapsible nature of the lump structure caused by the shear strains. The clay lumps are able to move under a small shear stress because of the softening process at the contact points. As the lump structure collapses, the confining stresses are transferred to the pore water

contained within the softened clay of the macro-voids. The sample is then sheared in a partially unconsolidated undrained manner. Therefore, the influence of the confining stress on the shearing strength is reduced.

5. The pore pressures measured in the triaxial tests on the more softened lumps are very high over the entire range of confining stresses. The high pore pressures are caused by the collapse of the lump structure from shear strains. As the magnitude of the pore pressure was not strongly affected by the magnitude of the confining stress, the effective stress and total stress shear strength envelopes are similar. The lump structure is still able to sustain some confining stress that is likely provided by the unsoftened clay shale lumps. The pore pressures measured during the triaxial test should be representative of the pore pressures that would develop in the field from shearing strains and therefore, these shear strength envelopes should be applicable to field conditions.

6. The size of lumps (12.7 mm versus 19 mm maximum size) has some influence on the shear strength, particularly the cohesion intercept. Effective and total shear strength parameters for the larger size clay lump specimens are $\phi'=2.4°$, $c'=62$ kPa and $\phi=1.6°$, $c=58$ kPa,

respectively. The friction angles are low because of the explanation in point 4. The higher cohesion intercept is from the larger size lump that has to be sheared through.

7. The mixing fluid (tailings pond water versus tailings sludge) has little influence on the shear strength. A low friction angle and high cohesion intercept was determined. Effective and total shear strength parameters are $\phi'=8.2°$, $c'=50$ kPa and $\phi=5.3°$, $c=44$ kPa, respectively.

8. Using tailings sludge in lieu of tailings water influences the rate of consolidation and moisture transfer into the lumps. The softening process, which controls the consolidation rate, is continuing to occur during the consolidation stage but at a slower rate since the sludge solids form a low permeable film around the lumps. Therefore, a deposit of clay lumps mixed with sludge has the potential to develop high pore pressures which will dissipate very slowly.

9. The results show that the final water content, whether tailings pond water or sludge was used, is consistently around 28%. Therefore, the amount of water available and ultimately, the degree of softening of the clay shale

lumps is approximately the same. The difference is in the rate of softening.

10. The tests representing the ultimate or long term condition of the clay shale (homogenized clay) reveal a deposit of clay lumps will become more stable. The clay mineral content is dominating the shear strength behaviour of the homogenized clay, whereas, the lump structure is dominating the behaviour in a clay lump deposit. Effective and total shear strength parameters are $\phi'=21.5°$, $c'=22$ kPa and $\phi=12.7°$, $c=36$ kPa, respectively.

11. The long term condition as represented by the homogenized specimens may never be reached in the field as the water available in the macro-voids does not appear to be enough to fully homogenize the clay shale.

12. In a clay lump deposit, shear stresses, caused by subsequent construction lifts, may cause shear strains within the lump deposit, triggering the development of high pore pressures. The pore pressures will dissipate very slowly due to the low permeable nature of the softened clay shale in the macro-voids. Therefore, the failure of a clay shale lump deposit in an undrained manner is influenced by the amount of softening at the

lump contact points and the shearing rate. Slow shear rates, which may be in the order of days or weeks, will allow the high positive pore pressures to equilibrate throughout the deposit and into the individual clay shale lumps. This reduces the effective stresses within the clay lumps reducing the shear strength within the lumps. The shear strength will improve as the clay lump deposit consolidates.

13.   For rapid construction of a clay lump deposit, the unconsolidated undrained shear strength (c_u) should be used for design calculations. For stage construction, the effective angle of friction (ϕ'), cohesion intercept (c'), and an estimation of the pore pressure could be used for design. Estimating the pore pressure is difficult since the coefficient of consolidation calculated from the consolidation curve of triaxial tests is invalid.

14.   A simple calculation using Taylor's slope stability design chart indicates that a 15 m high deposit of clay shale lumps with an undrained shear strength of 30 kPa would be stable with $18°$ slopes. Therefore, it appears that free standing deposits of clay shale lumps can be designed and do not necessarily have to be contained.

15. Large consolidation volume changes up to 30% to 40% can occur. Calculation of potential fill volumes should be based on volume change up to a maximum bulk density of 2,000 kg/m3.

16. Water contents of the lump structure approach a limiting lower value of between 26% to 28%, depending on the plasticity of the clay shale . This is a reflection of the limiting lower void ratio of 0.75 and the limiting upper bulk density of 2,000 kg/m3 which the clay lumps approach under the applied confining stress. This demonstrates the ability of the lump structure to densify under the application of a low confining stress and then resist further consolidation under higher confining stresses.

17. Dry and bulk densities approach a limiting upper value of 1,600 kg/m3 and 2,000 kg/m3 with confining stress, respectively. This demonstrates the consistency at which the lump structure densifies to under confining stresses over 50 kPa.

18. The major change in void ratio during the compression/softening stage occurs within the macro-voids. The final void ratio appears to be independent of the initial void ratio of the lump structure. The lump

structure compresses under a low confining stress and approaches a minimum bulk void ratio between 0.7 and 0.75.

19.   The volume change occurring in the individual lumps (micro scale) and in the lump structure (macro scale), as well as, the non-uniform hydraulic conductivities make the calculation of a coefficient of consolidation from the consolidation curves invalid.

20.   A definite shearing plane developed through the lump structure. Visually, all the interlump voids were filled with the softened clay.

21.   Using a split mold former, successful preparation of the clay shale lump specimens was accomplished. Providing a small vacuum was adequate to support the sample until the triaxial cell was assembled and a confining stress applied.

22.   The volume of tailings pond water or sludge trapped in the voids can be estimated from the void ratios. For every 1 m^3 of clay shale excavated, 0.13 m^3 of liquid can be disposed. For 22×10^6 m^3 of overburden excavated annually, 2.9×10^6 m^3 of liquid waste can be disposed.

6.2 Recommendations

The test results show that a confining stress greater than approximately 100 kPa is required for the clay lump structure to compress to a minimum packing arrangement and cease to be free draining. This represents a fill height of about 5 m. Previous field studies have been conducted at or below these fill heights, therefore, to fully understand the consequence of higher fills or larger confining stresses, future field studies should be conducted using a minimum fill height of 5 m.

Using a larger testing apparatus would enable larger and possible more representative (rounded lumps) clay shale lumps to be tested. This may be accomplished in a very large consolidometer type of apparatus. The lumps and mixing fluid could be introduced and a confining stress applied in stages. During each stage, hydraulic conductivity measurements could be taken to determine the confining stress at which the lump structure ceases to be free draining.

Laboratory or field trials could be conducted to determine the strength of a clay shale lump deposit that has been deposited utilizing different placement techniques, specifically, placement techniques to enhance absorption capacity. For example, Syncrude has experimented with pushing

overburden clay shale into a sludge pool with a dozer to create a polder, dropped the overburden into the sludge simulating a spreader, and sprayed sludge onto an advancing face of overburden. Other methods may involve slurrying and transporting the overburden in a pipeline.

A sensitive hydraulic conductivity measuring system would be beneficial in a testing program since the hydraulic conductivities approach very low values.

When conducting the triaxial tests on the clay shale lump structure, a pore pressure measuring device could be developed to measure the pore pressures within the individual clay lumps to verify whether or not negative pore pressures are attempting to developing during shear.

REFERENCES

ASH, P.O. 1986. Improvement of Oil Sands Tailings Sludge Disposal Behaviour With Overburden Material. M.Sc. thesis, University of Waterloo, Waterloo, Ontario, 107 p.

BISHOP, A.W., and HENKEL, D.J. 1962. The Measurement of Soil Properties in the Triaxial Test. Edward Arnold (Publishers) Ltd., London, 227 p.

BULMER, J.T., and STARR, J. 1979. Syncrude Analytical Method for Oil Sand and Bitumen Processing. Published by AOSTRA, Edmonton, Alberta, 173 p.

CARRIER, W.D.,III, and BROMWELL, L.G. 1983. Logan Airport Revisited. ASCE Journal of Geotechnical Engineering, vol. 109, pp 344-355.

CASAGRANDE, A. 1953. Soil Mechanics in the Design and Construction of the Logan Airport. Contributions to Soil Mechanics, 1941-1953, Boston Society of Civil Engineers, pp 176-205.

DUSSEAULT, M.B., SCAFE, D.W., and SCOTT, J.D. 1989. Oil Sands Mine Waste Management: Clay Mineralogy, Moisture Transfer and Disposal Technology. AOSTRA Journal of Research, vol. 5, no. 4, pp 303-320.

DUSSEAULT, M.B., SCOTT, J.D., and ASH, P.O. 1988. The Development of Shear Strength in the Sludge/Clay Shale Mixes for Oil Sands Tailings Disposal. Proc. 4th UNITAR/UNDA Conference on Heavy Crude and Tar Sands, Edmonton, Alta., AOSTRA vol. 1, 161 p.

DUSSEAULT, M.B.,SCOTT, J.D., ZINTER, G., and MORAN, S. 1984. Simulation of Spoil Pile Subsidence. Fourth Australia - New Zealand Conference on Geomechanics, Perth, The Institute of Engineers, Australia, 7 p.

FOWLER, J., and HAYDEN, M.L. 1986. Verification of Design and Construction Techniques for Gaillard Island Dredged Material Disposal Area. Mobile, Alabama, US Army Engineer Waterways Experiments Station, Vicksburg, Mississippi, rpt no. 39180-0631, 96 p.

FOWLER, J., BLAXNEY, H.N., and HAYDEN, M.L. 1986. Verification of Design and Construction Techniques Gaillard Dredged Material Disposal Island. Mobile, Alabama, 11th World Dredging Congress, Brighton, U.K., Central Dredging Association, pp 627-633.

HARTLEN, J., and INGERS, C. 1981. Land Reclamation Using Fine-Grained Dredged Material. Proceedings of the 10th International Conference on Soil Mechanics and Foundation Engineering, Stockholm, vol. 1, pp 145-148.

HILLIARD, T., DAVIDSON, B., FORDHAM, C., and DUSSEAULT, M. 1988. Progress Report on Laboratory Testing of the Clearwater Clay shale. AOSTRA Agreement #626 Part 1, Dept. of Earth Sciences, University of Waterloo, Waterloo, Ontario. 150 p.

HILLIARD, T., FORDHAM, C., and DUSSEAULT, M.B. 1989. Report on Triaxial Testing of the Clearwater Clay shale. AOSTRA Agreement #626, Dept. of Earth Sciences, University of Waterloo, Waterloo, Ontario, 81 p.

HOLTZ, R.D., and KOVAKS, W.D. 1981. An Introduction to Geotechnical Engineering. Prentice-Hall, Inc., New Jersey. pp 733.

ISAAC, B.A., DUSSEAULT, M.B., LOBB, G.D., and ROOT, J.D. 1982. Characterization of the Lower Cretaceous Overburden for Oil Sand Surface Mining Within Syncrude Canada Ltd. Leases, Northeast Alberta, Canada. Proceedings 4th Congress International Association of Engineering Geology. New Delhi 1982, 14 p.

KEMP, E.B. 1967. East Atchafalaya Basin Protection Levee, Louisiana. United States Army, Corps of Engineers, Office of the District Engineer, New Orleans, Louisiana, 27 p.

LORD, E.R.F., and ISAAC, B.A.A. 1989. Geotechnical Investigations of Dredged Overburden at the Syncrude Oil Sand Mine in Northern Alberta, Canada. Canadian Geotechnical Journal, vol. 26, no. 1, pp 132-153.

LUTOVINOV, A.G., TERENT'EV, V.G., and SHIPKO, I.I. 1975. Hydraulic Filling of Earth Structures using a Mixture of Lumpy Clays and Sand. Hydrotechnical Construction, no. 6, pp 531-535.

MACKINNON, M.D. 1989. Development of the Tailings Pond at Syncrude's Oil Sands Plant: 1978-1987. AOSTRA Journal of Research, vol. 5, no. 2, pp 109-134.

MARACHI, N.D., CHAN, C.K., and SEED, H.B. 1972. ASCE Journal of the Soil Mechanics and Foundations Division, vol. 98, no. SM1, pp 95-114.

MOSSOP, G.D. 1980. Geology of the Athabasca Oil Sands. Science, vol. 207, American Association for the Advancement of Science, pp 145-152.

O'DONNELL, N.D., and JODREY, F.M. 1984. Geology of the Syncrude Mine Site and its Application to Sampling and Grade Control. Society of Mining Engineers of AIME, Denver Colorado, 19 p.

SCOTT, J.D., and CHICHAK, M.F. 1985. Large Sludge Stand Pipe Consolidation Test 1. Progress Report, Agreement C2919-55, University of Alberta, Edmonton, Alberta, 58 p.

SCOTT, J.D., and DUSSEAULT, M.B. 1982. Behaviour of Oil Sand Tailings Sludge. Proc. Petroleum Society of CIM, Paper 82-33-85, Calgary, Alberta, 19 p.

STEWART, G.A., and MacCALLUM, H.T. 1978. Athabasca Oil Sands Guide Book. International Conference Facts and Principles of Geologists, Canadian Society of Petroleum Geologists, Calgary, Alberta, 30 p.

VIGRASS, L.W. 1968. Geology of Canadian Heavy Oil Sands. The American Association of Petroleum Geologists Bulletin, vol. 52, no. 10, pp 1984-1999.

WHITMAN, R.V. 1970. Hydraulic Fills to Support Structural Loads. Proceedings of the American Society of Civil Engineers, ASCE Journal of the Soil Mechanics and Foundations Division, vol. 96, pp 23-47.

APPENDIX A

169
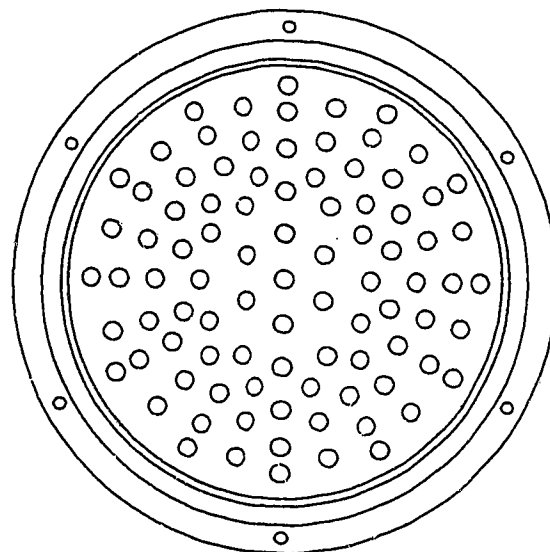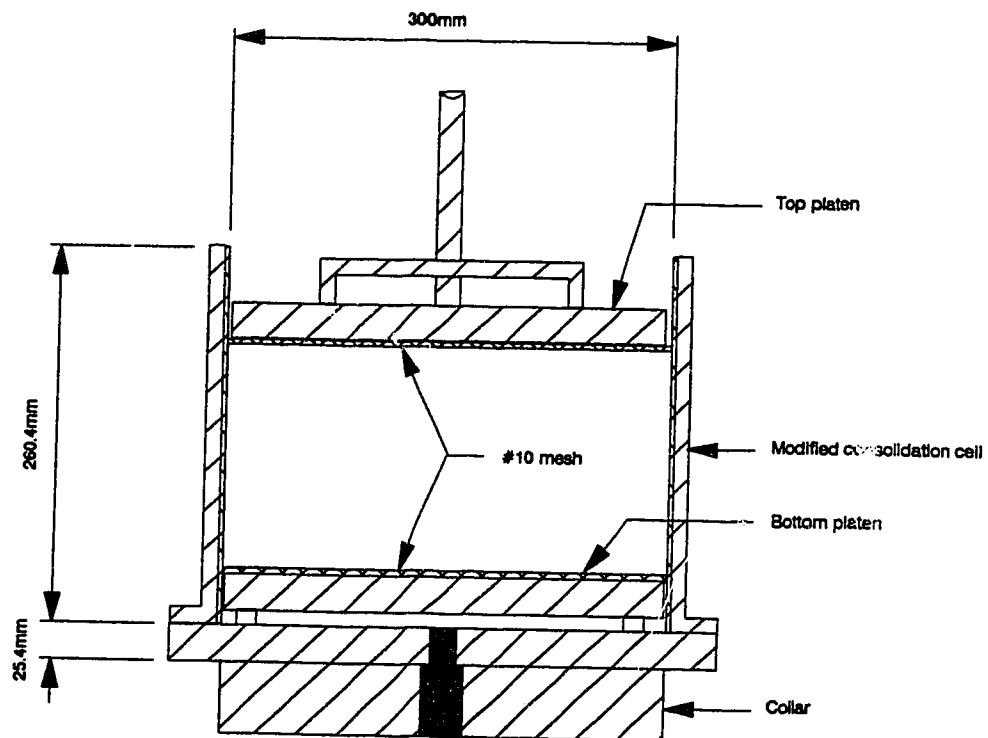
TOP VIEW

Figure A1

MODIFIED CONSOLIDATION CELL

171

consolidation cell wall

teflon liner plate

#10 mesh

NTS

Aluminum piston arm (38mm ø)

welded

Stiffening collar

30mm

SECTION C-C

Collar

Hole spacing similar to bottom plate

25mm aluminum plate with #10 mesh below

295mm

C

C

TOP VIEW

Figure A2
TOP PLATEN

300mm

25mm
10mm

118mm   118mm

30mm

30mm

#10 Mesh

Aluminum Plate

Alum. Leg Supports

SECTION D-D

D

D

Leg Supports

Aluminum Plate

#10 Mesh
(typical)

TOP VIEW

Figure A3

Bottom Platen

APPENDIX B

174
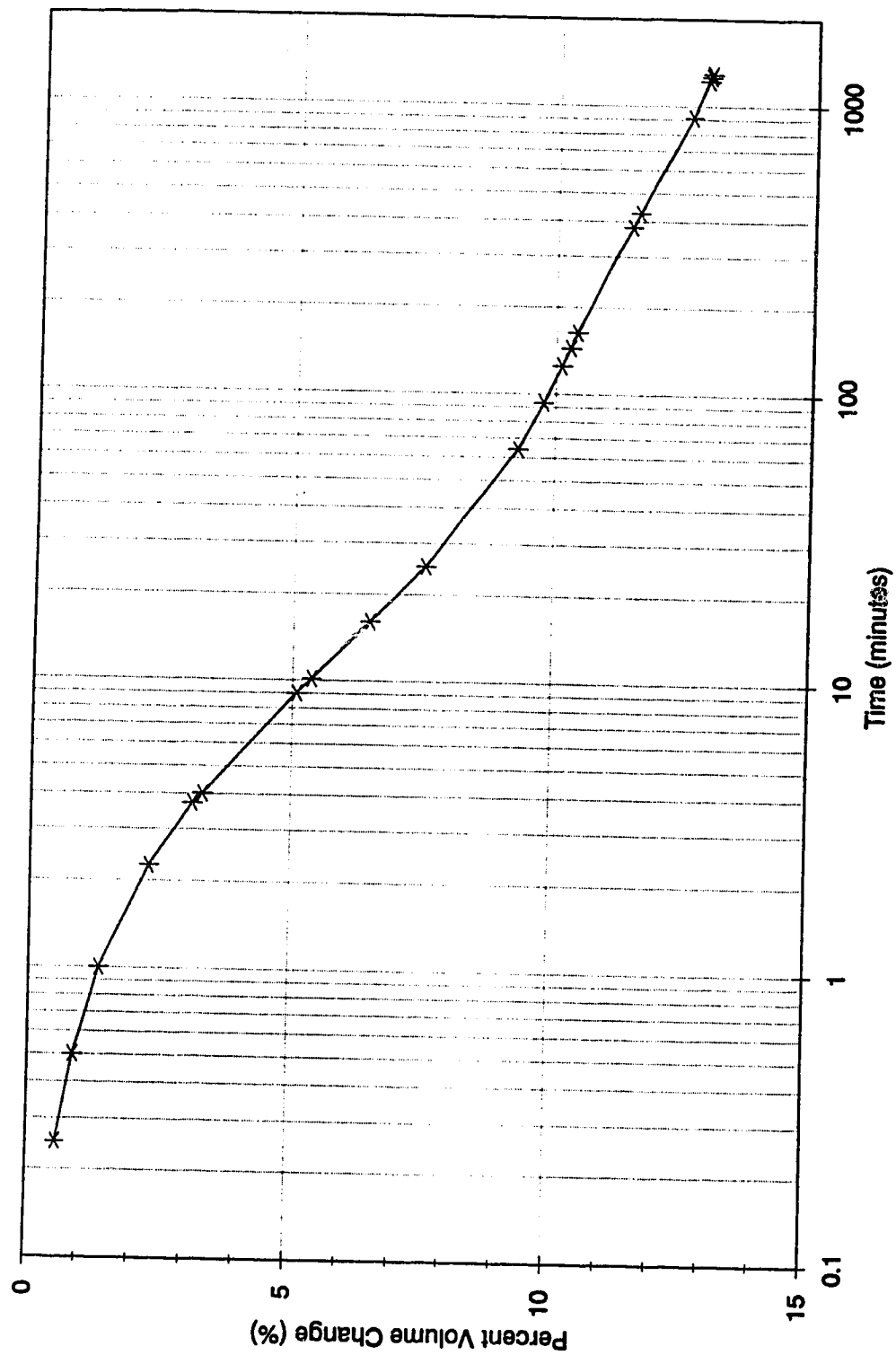
Figure B1   Consolidation/Softening - Test PWA2   Series 1
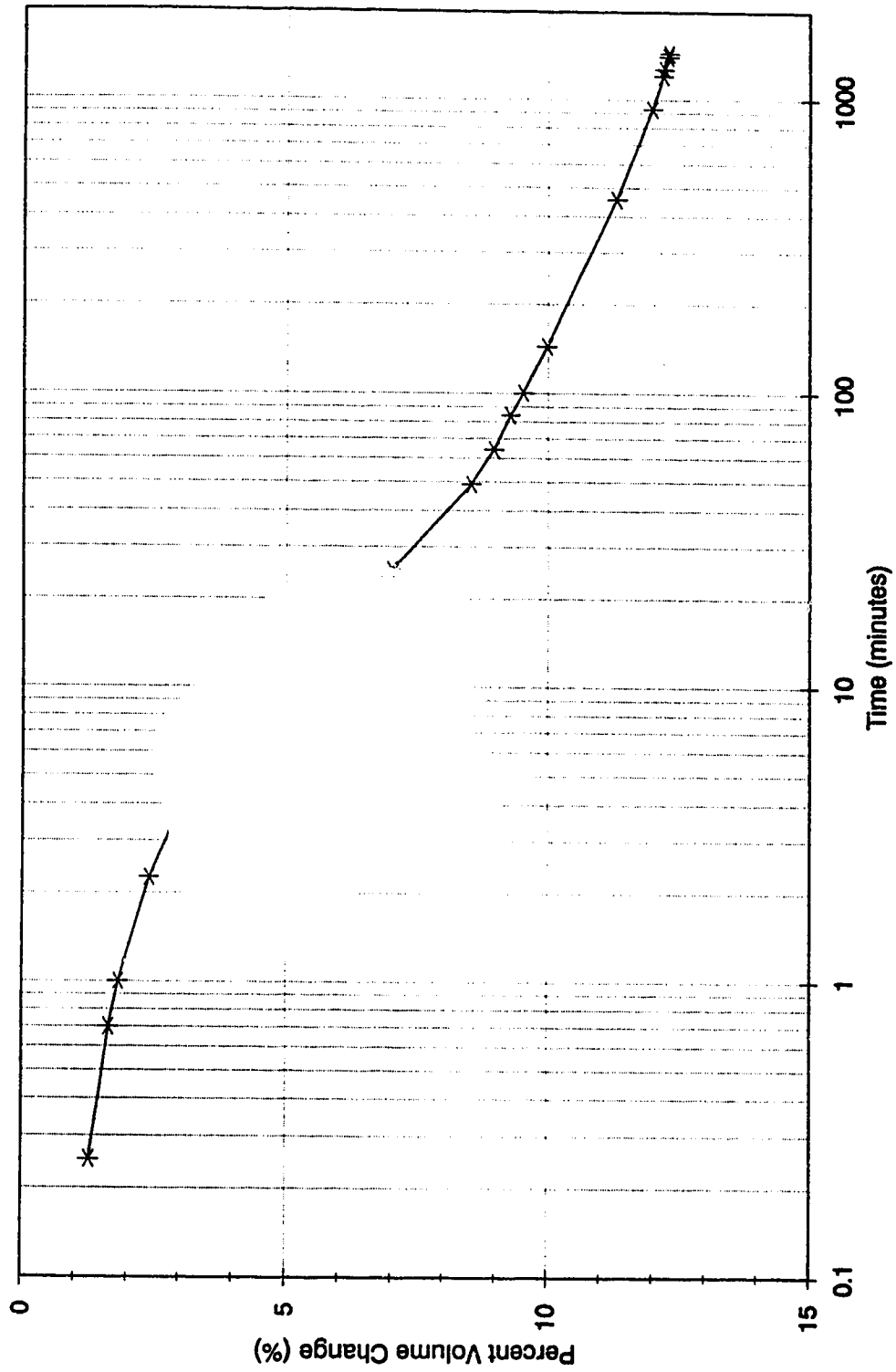
Figure B2   Consolidation/Softening - Test PWA3 Series 1
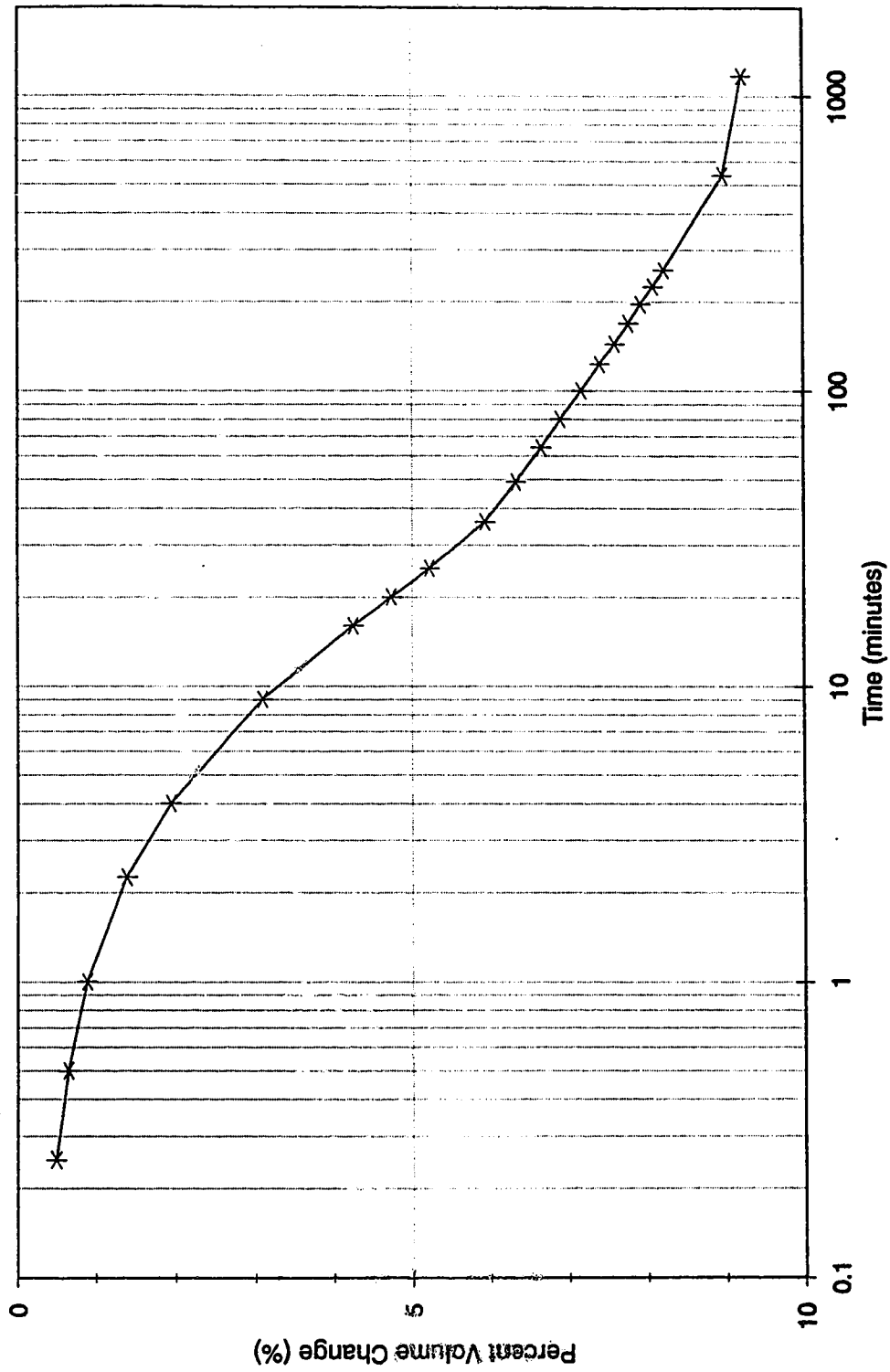
Figure B3   Consolidation/Softening - Test PWA4   Series 1

177
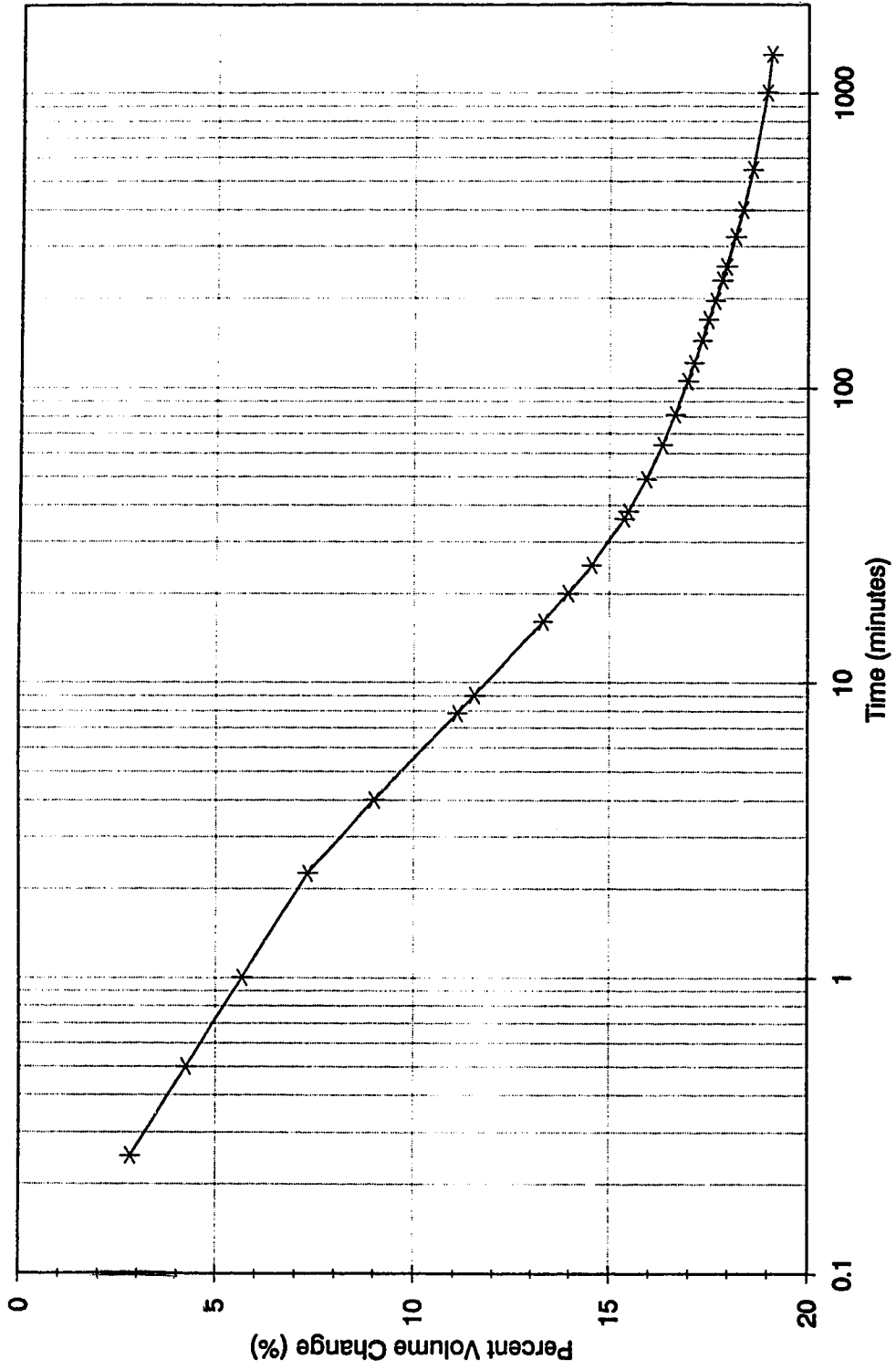
Figure B4 Consolidation/Softening - Test PWA5 Series 1
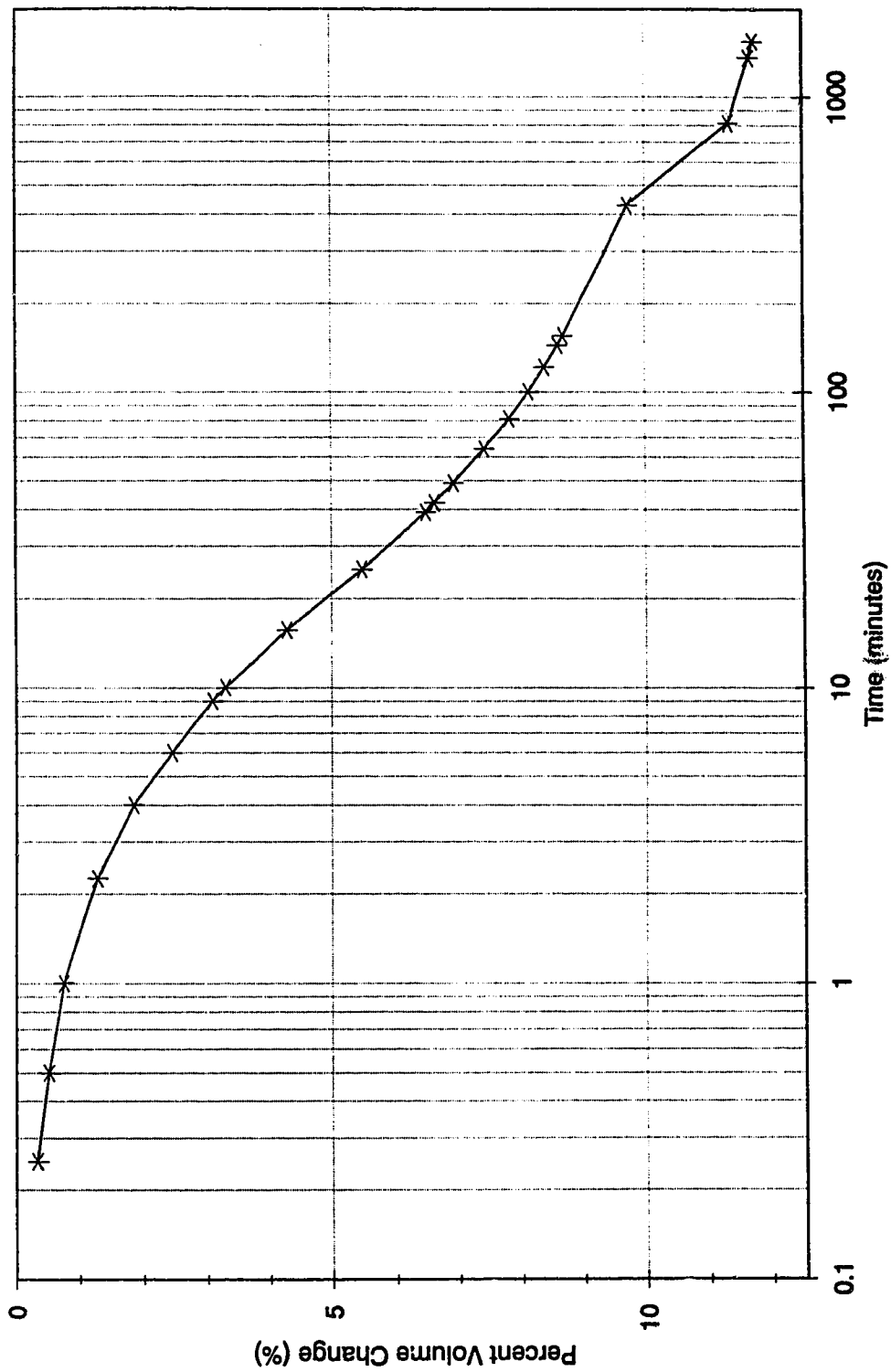
Figure B5 Consolidation/Softening - Test PWA6 Series 1
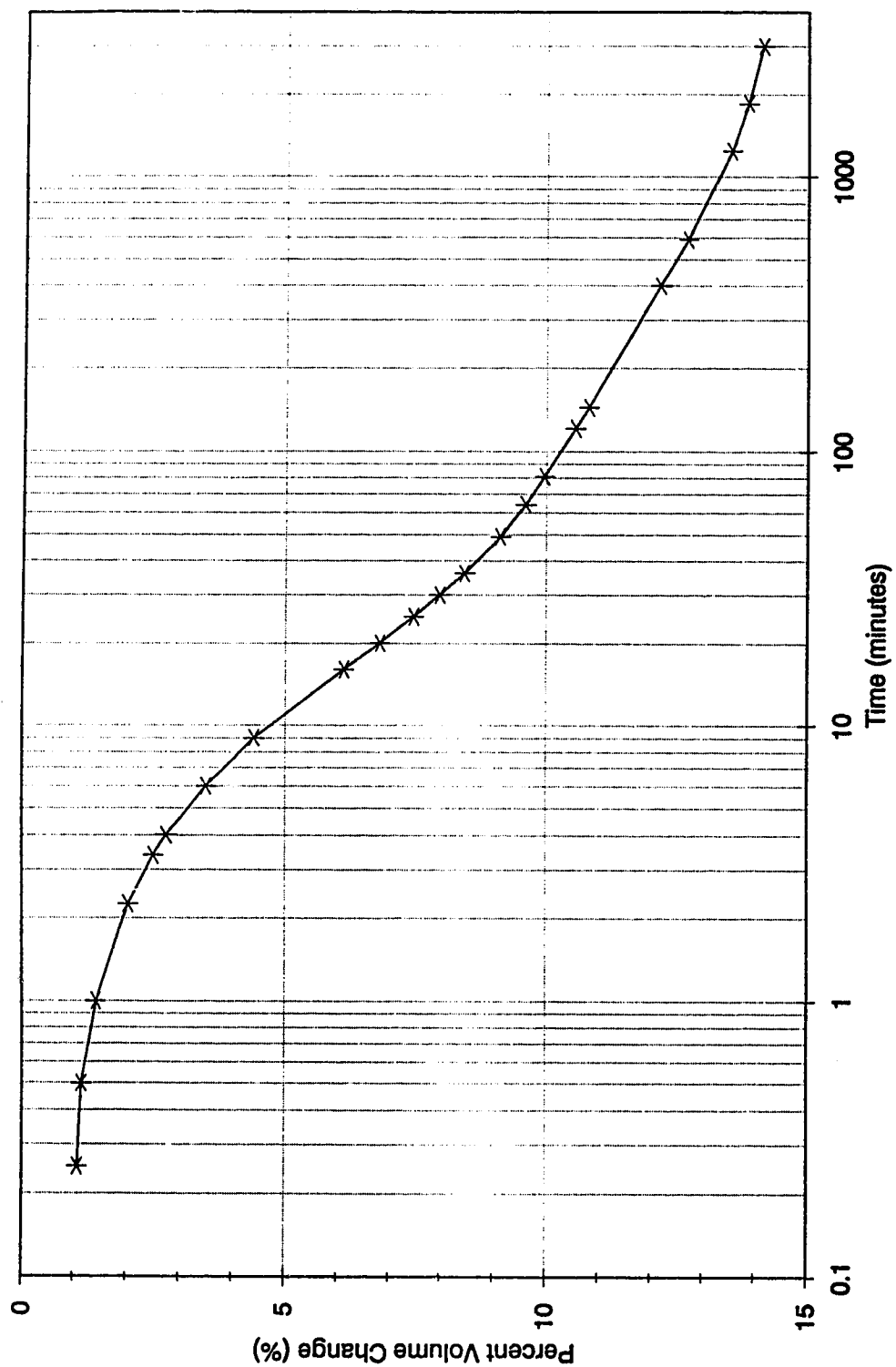
Figure B6   Consolidation/Softening - Test PWA7   Series 2

180
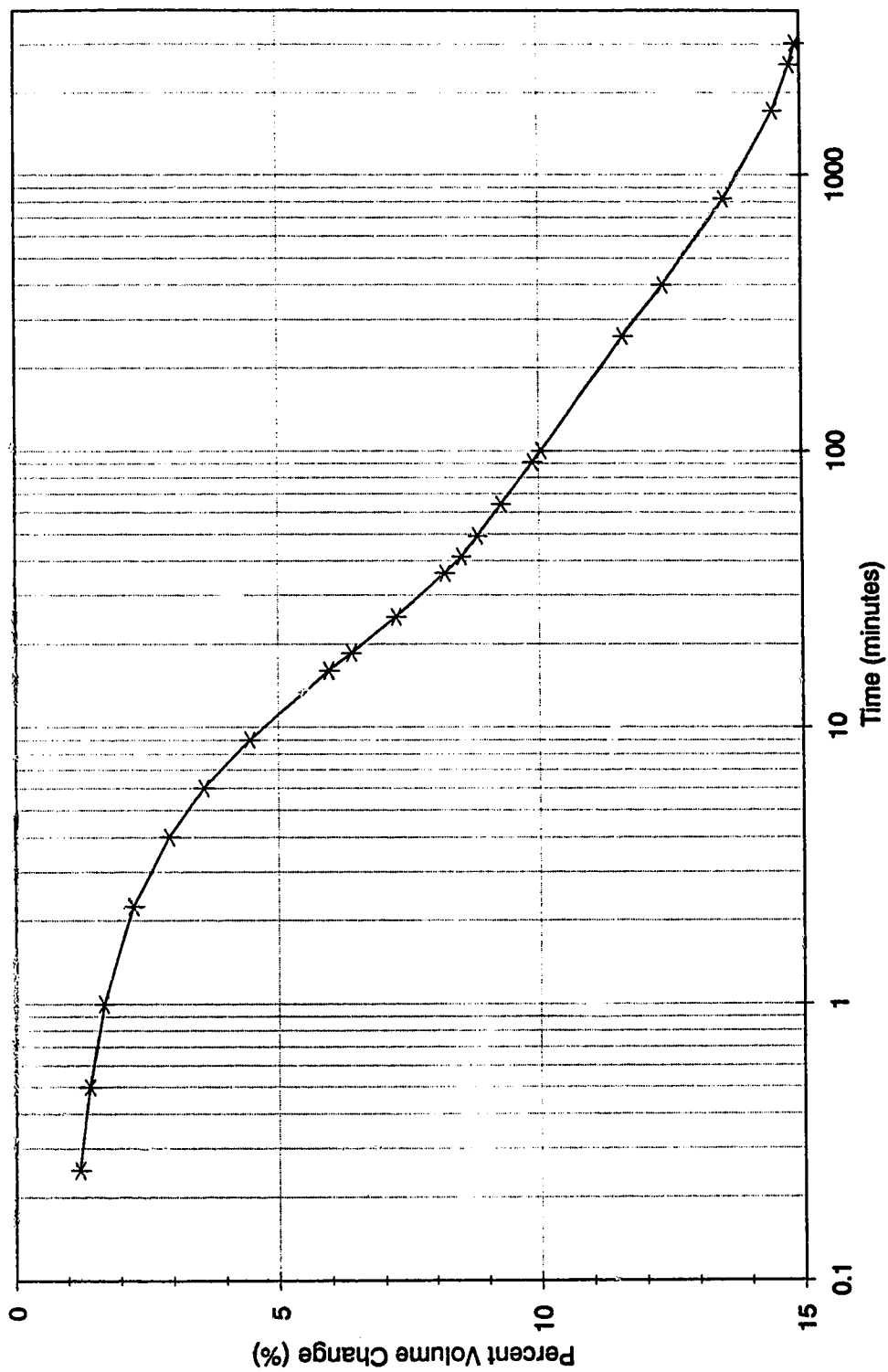
Figure B7   Consolidation/Softening - Test PWA8   Series 2
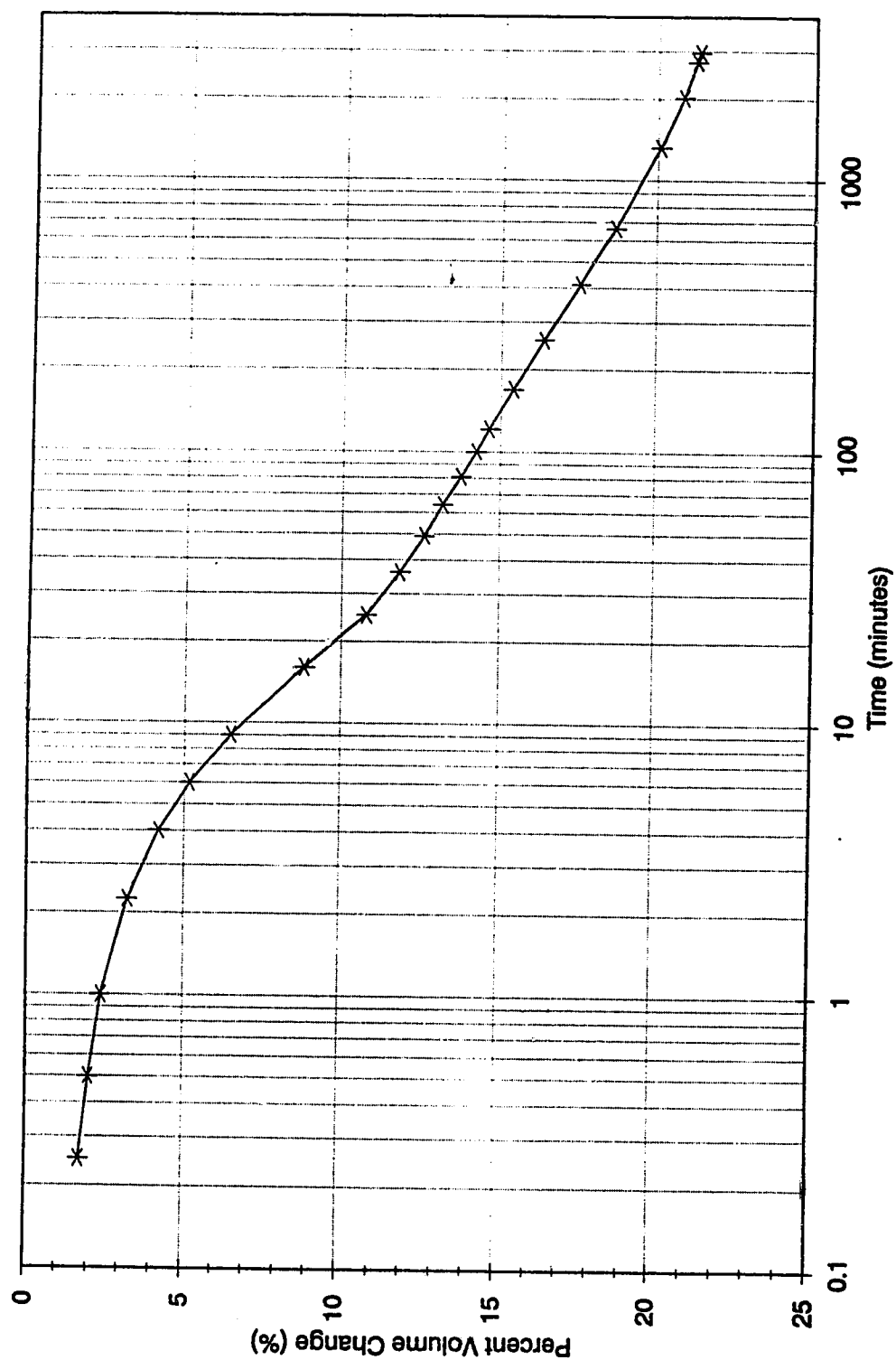
Figure B8 Consolidation/Softening - Test PWA9 Series 2
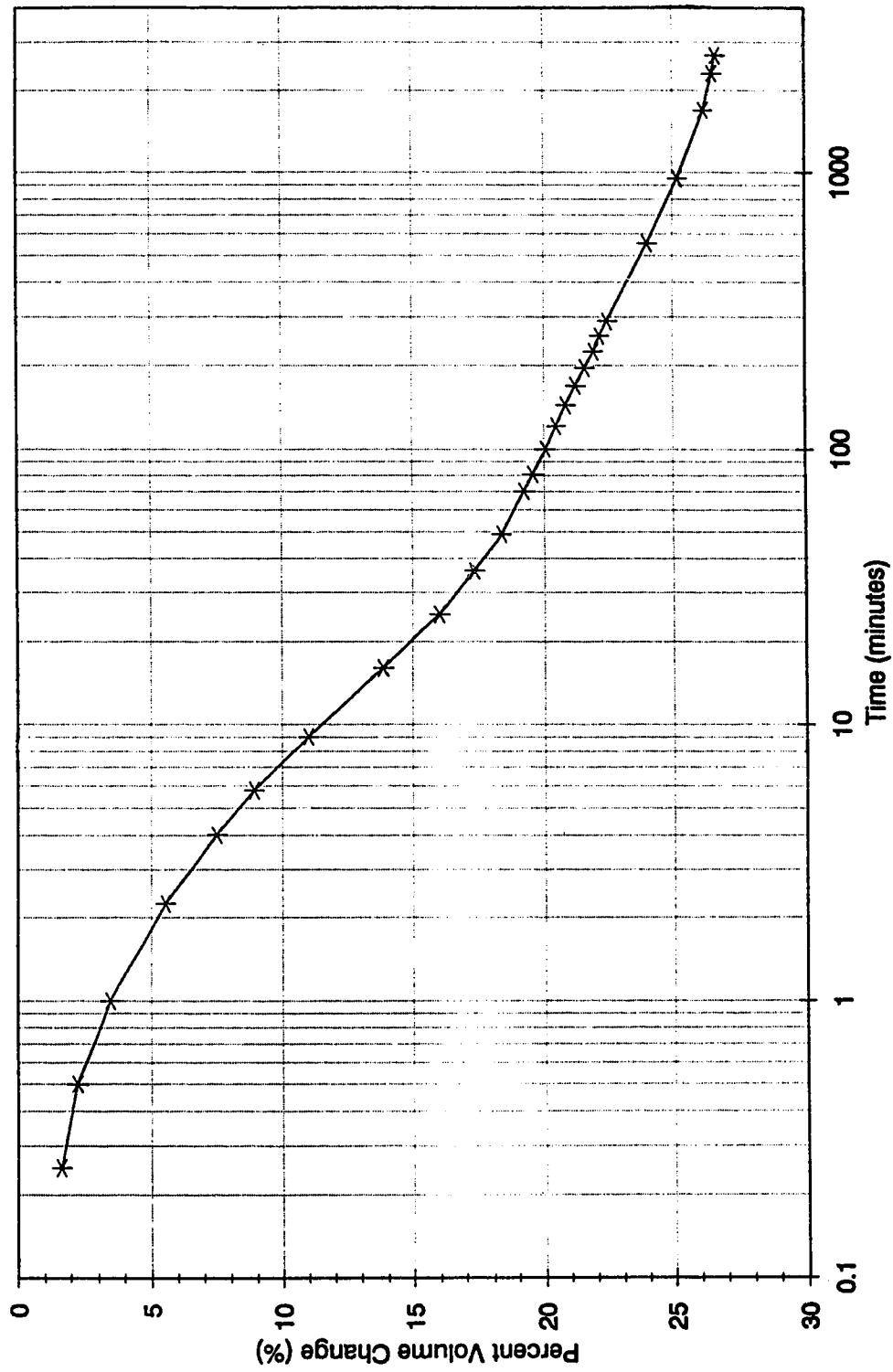
Figure B9   Consolidation/Softening - Test PWA10   Series 2
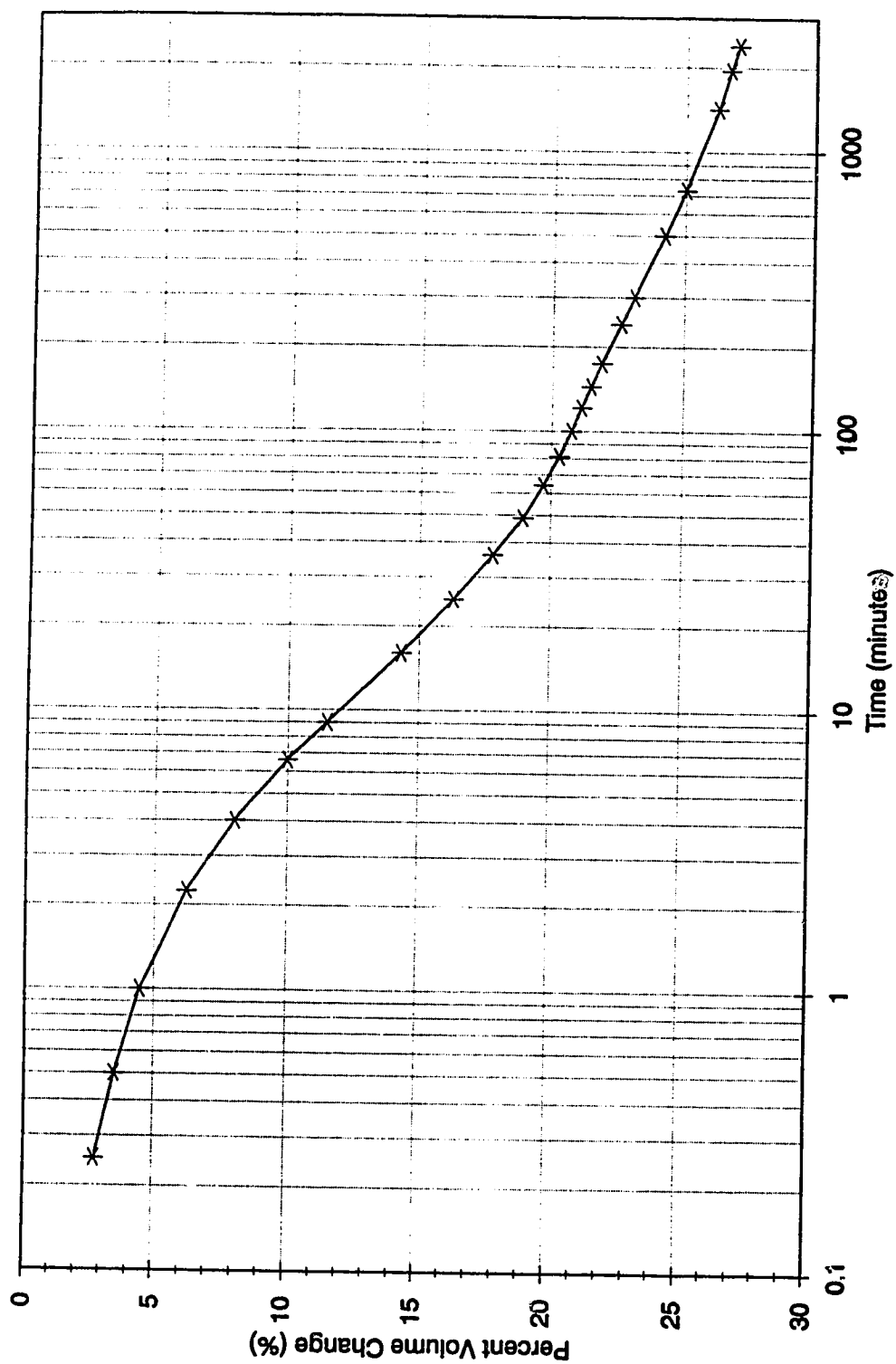
Figure B10 Consolidation/Softening - Test PWA11 Series 2
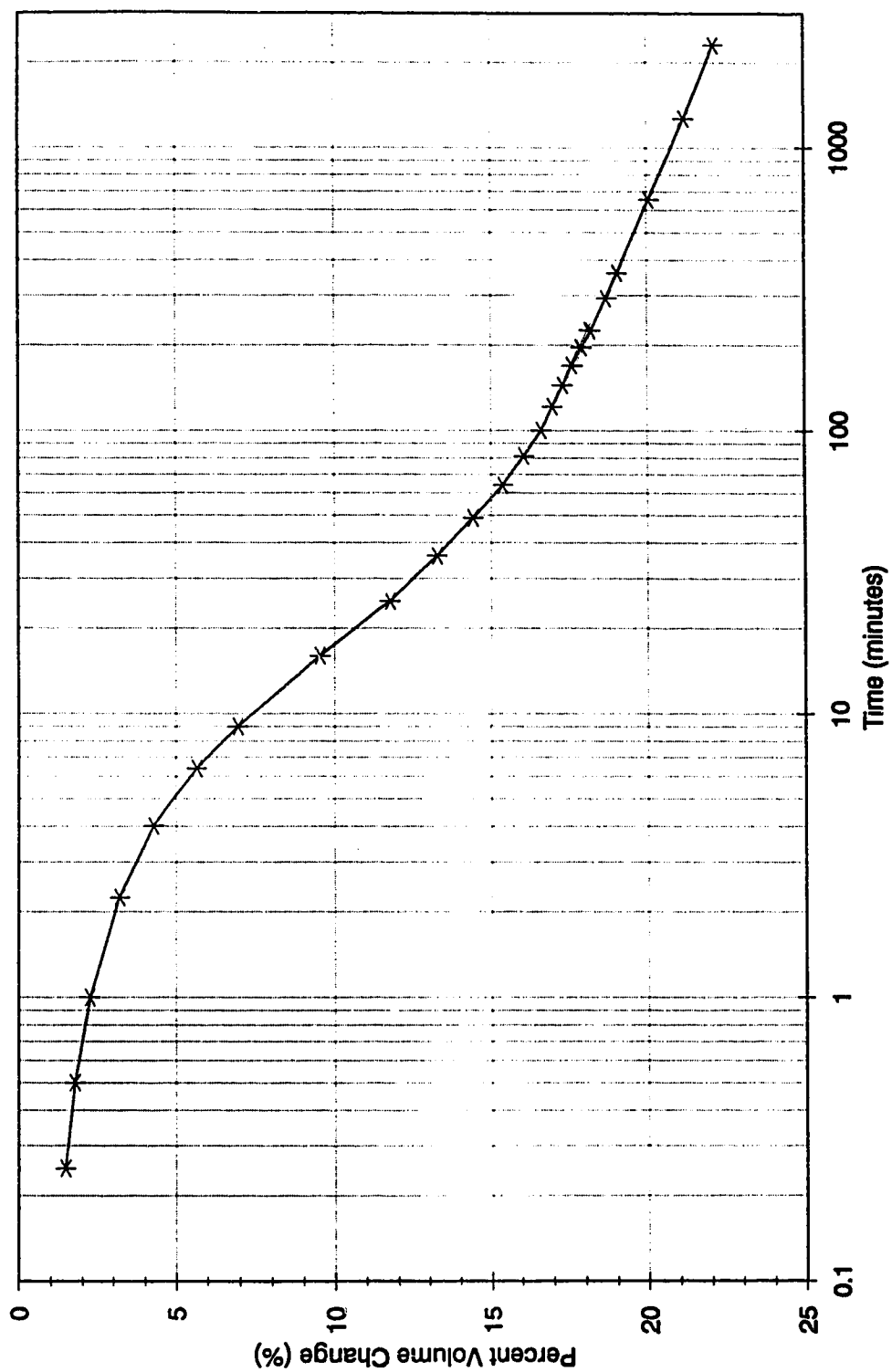
Figure B11   Consolidation/Softening - Test PWA12   Series 2

184
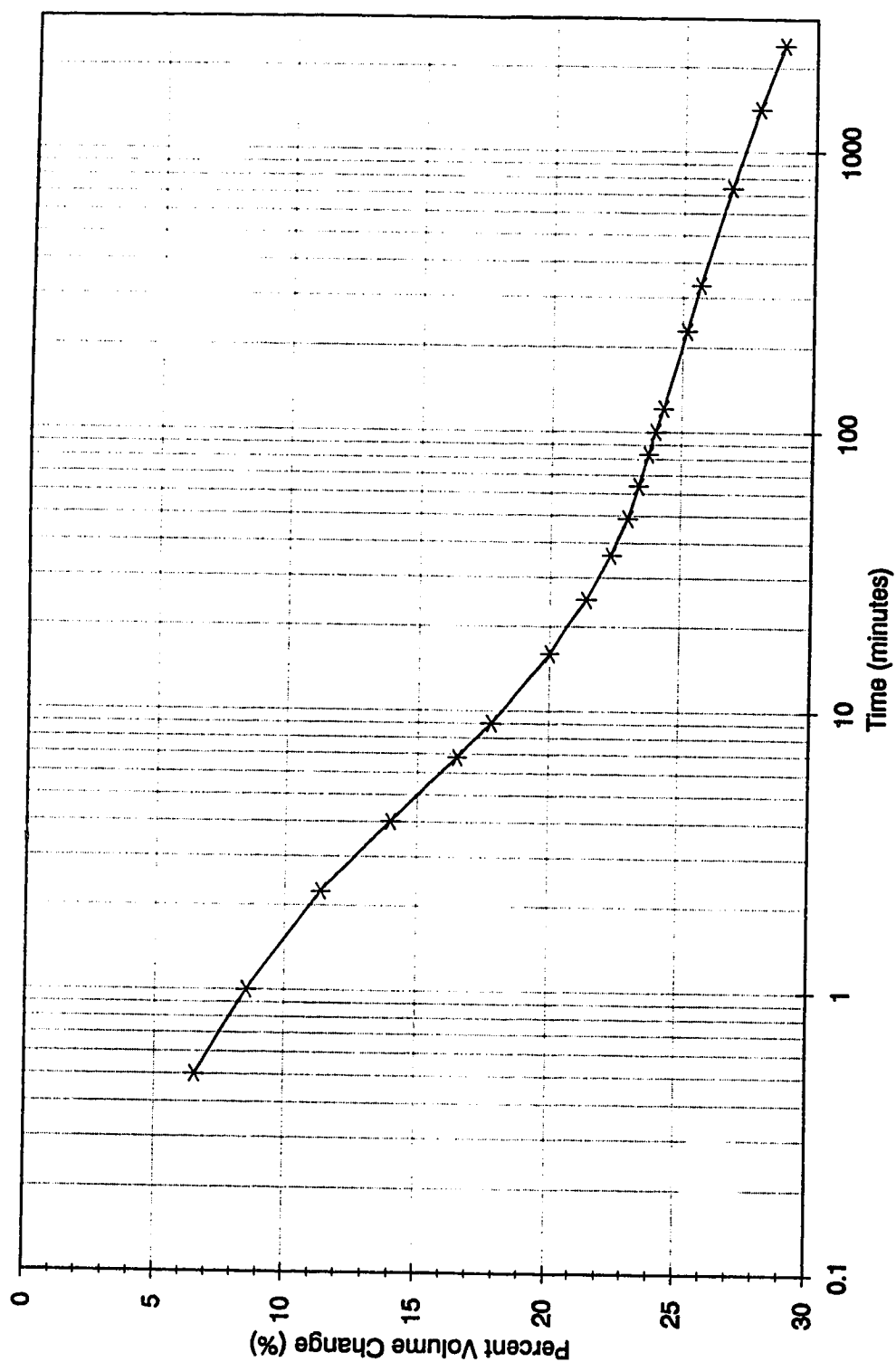
Figure B12   Consolidation/Softening - Test PWA13 Series 3
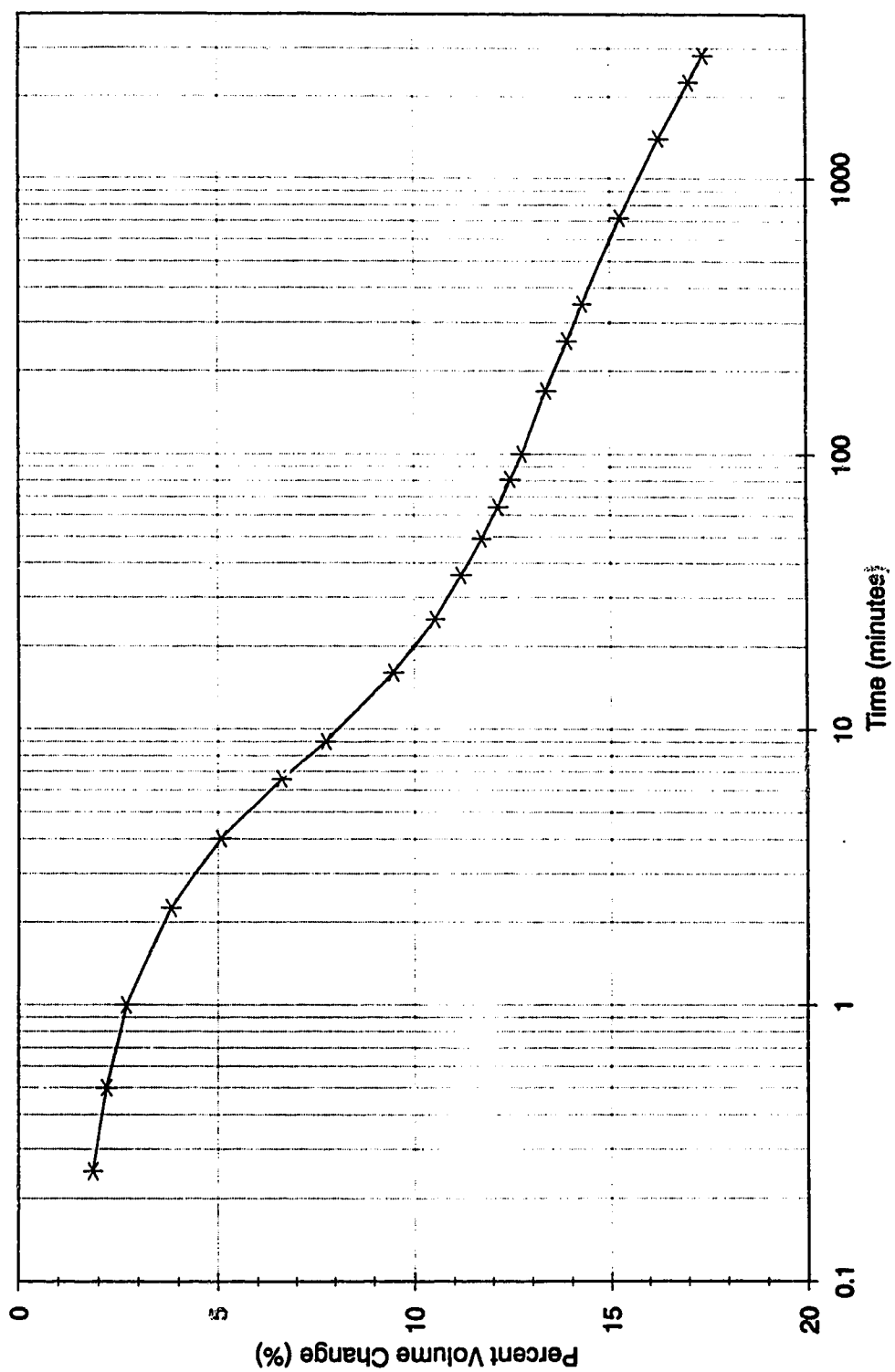
Figure B13 Consolidation/Softening - Test PWA14 Series 3
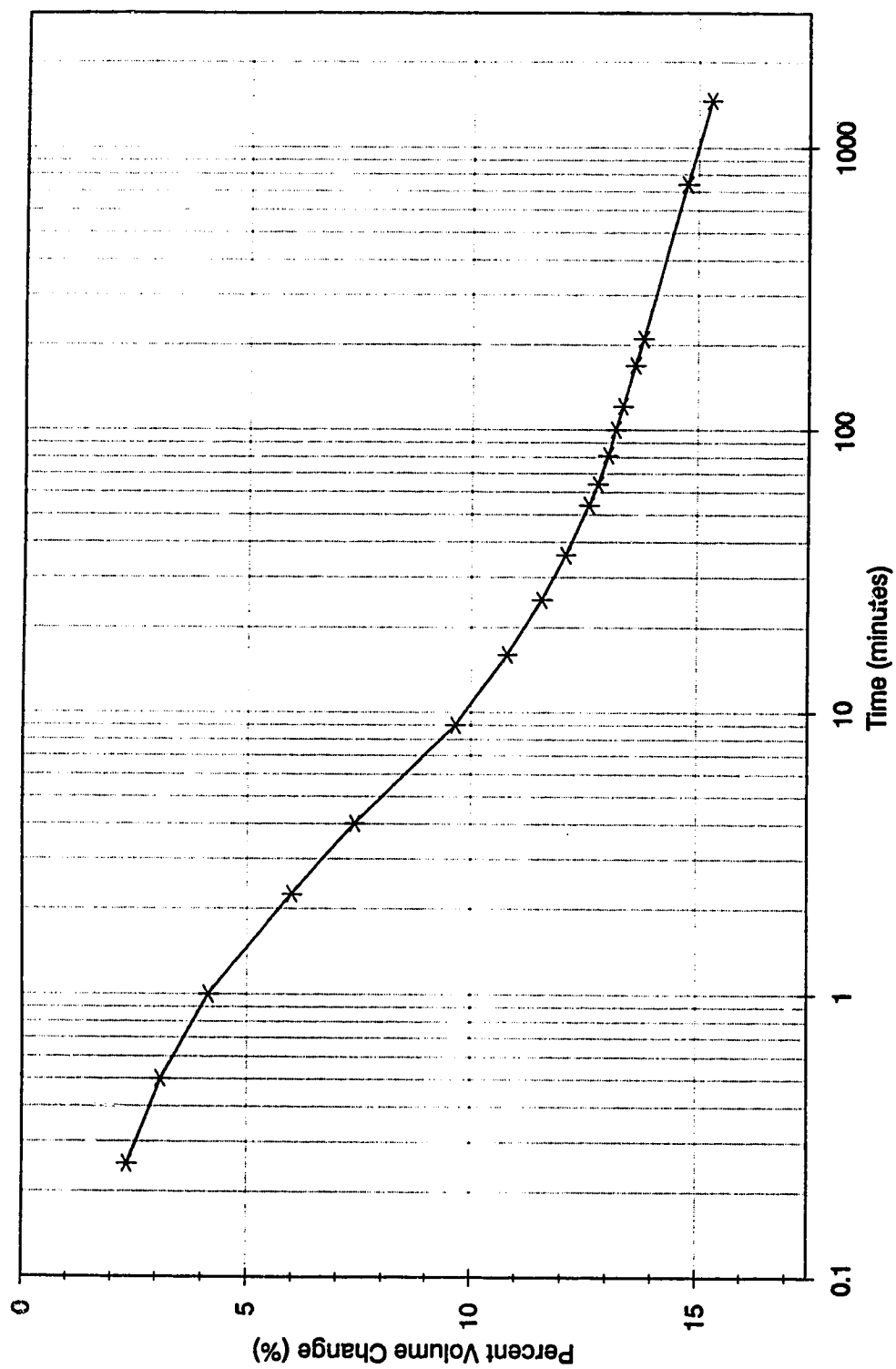
Figure B14 Consolidation/Softening - Test PWA15 Series 3
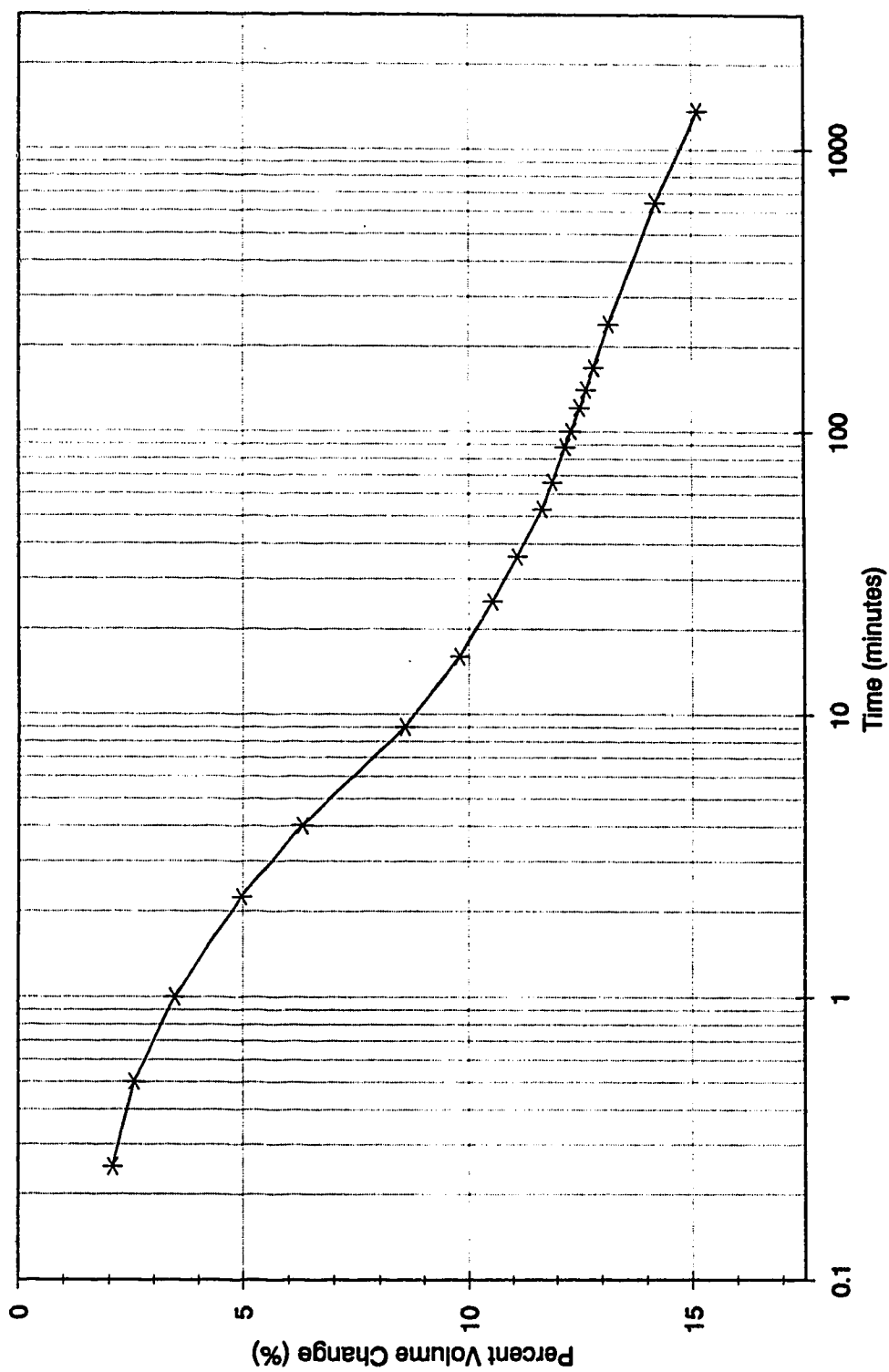
Figure B15 Consolidation/Softening - Test PWA16 Series 3
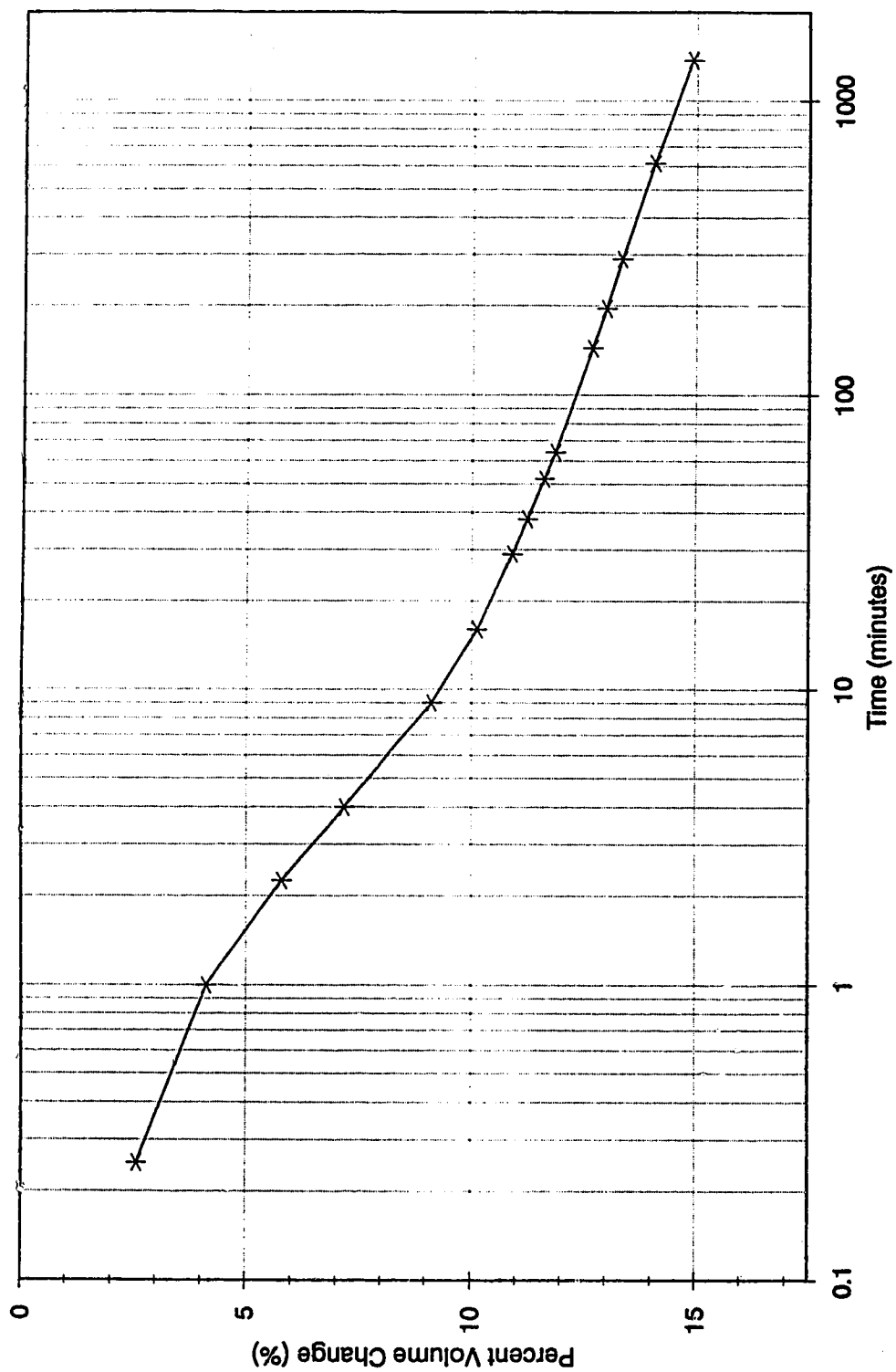
Figure B16 Consolidation/Softening - Test PWA1A Series 4
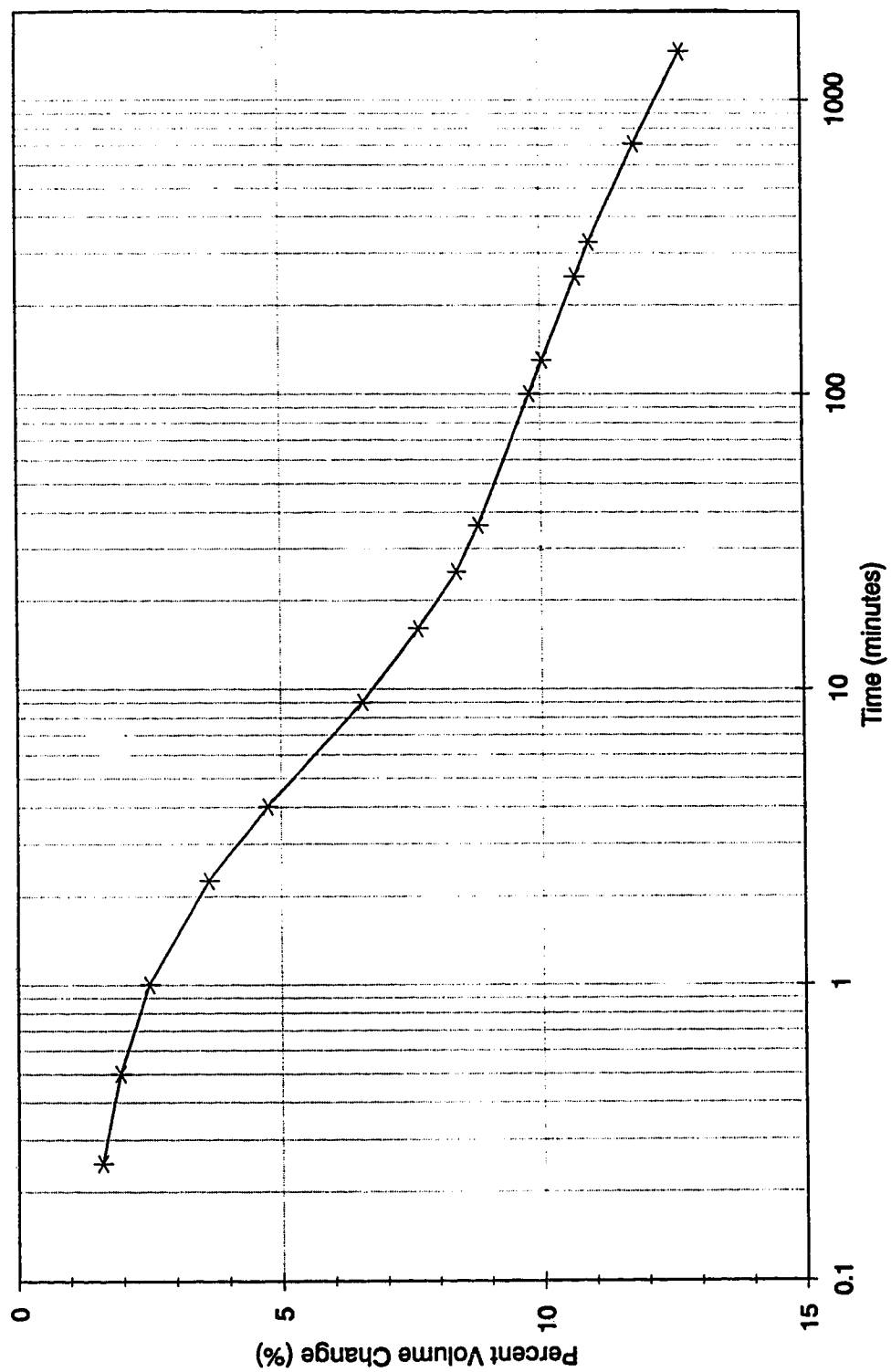
Figure B17 Consolidation/Softening - Test PWA2A Series 4
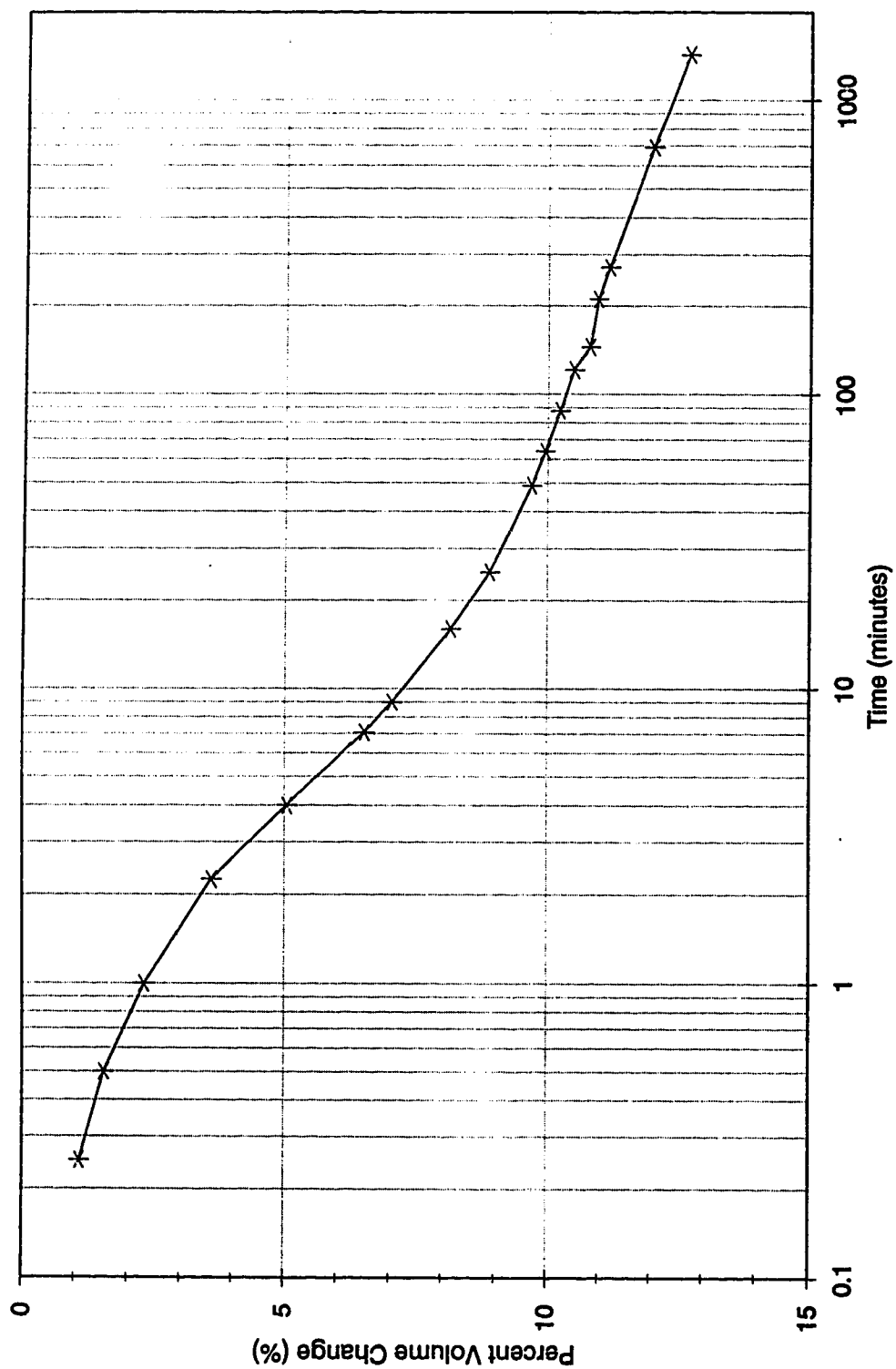
Figure B18   Consolidation/Softening - Test PWA3A   Series 4
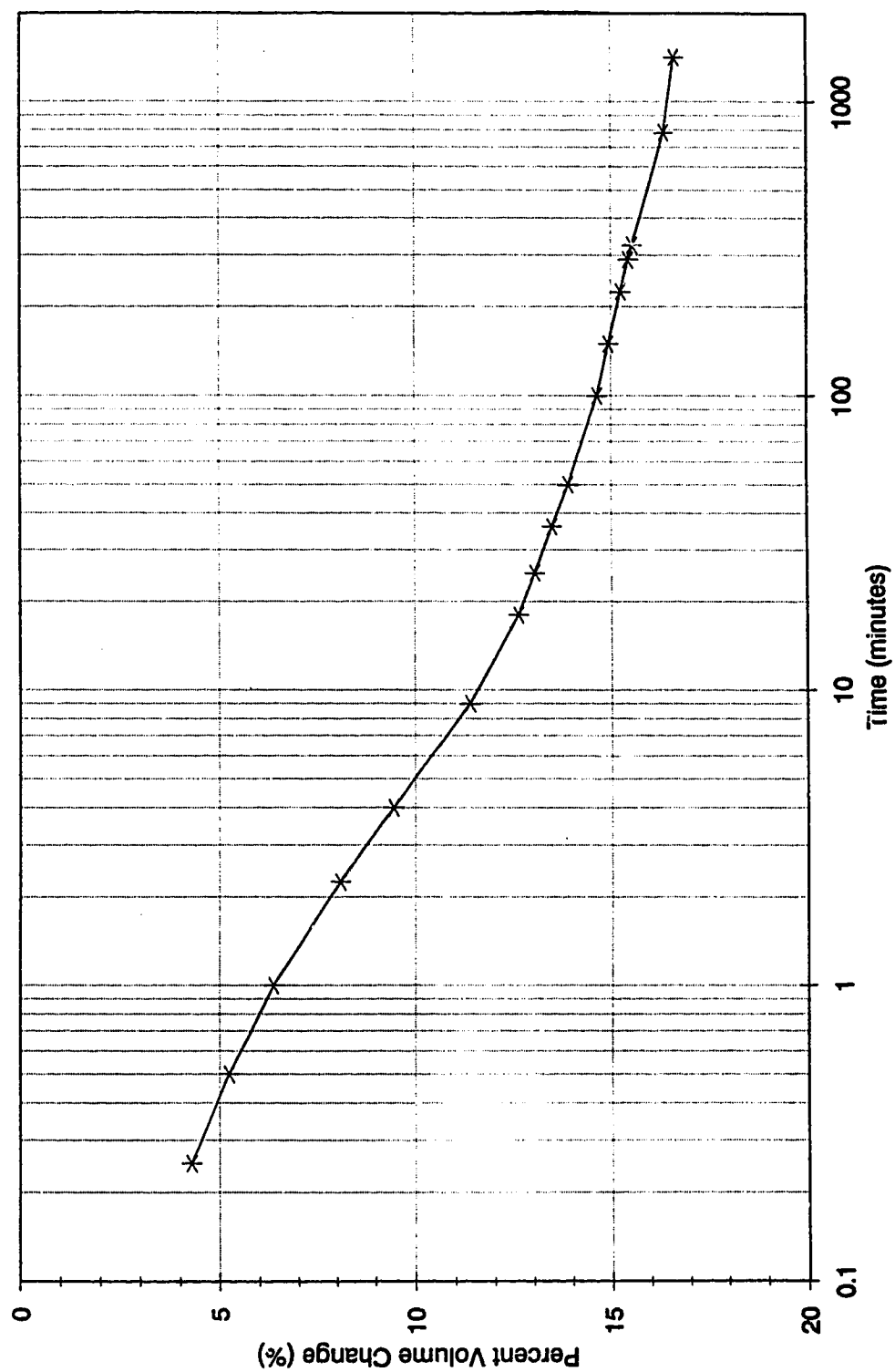
Figure B19 Consolidation/Softening - Test PWA4A Series 4

192
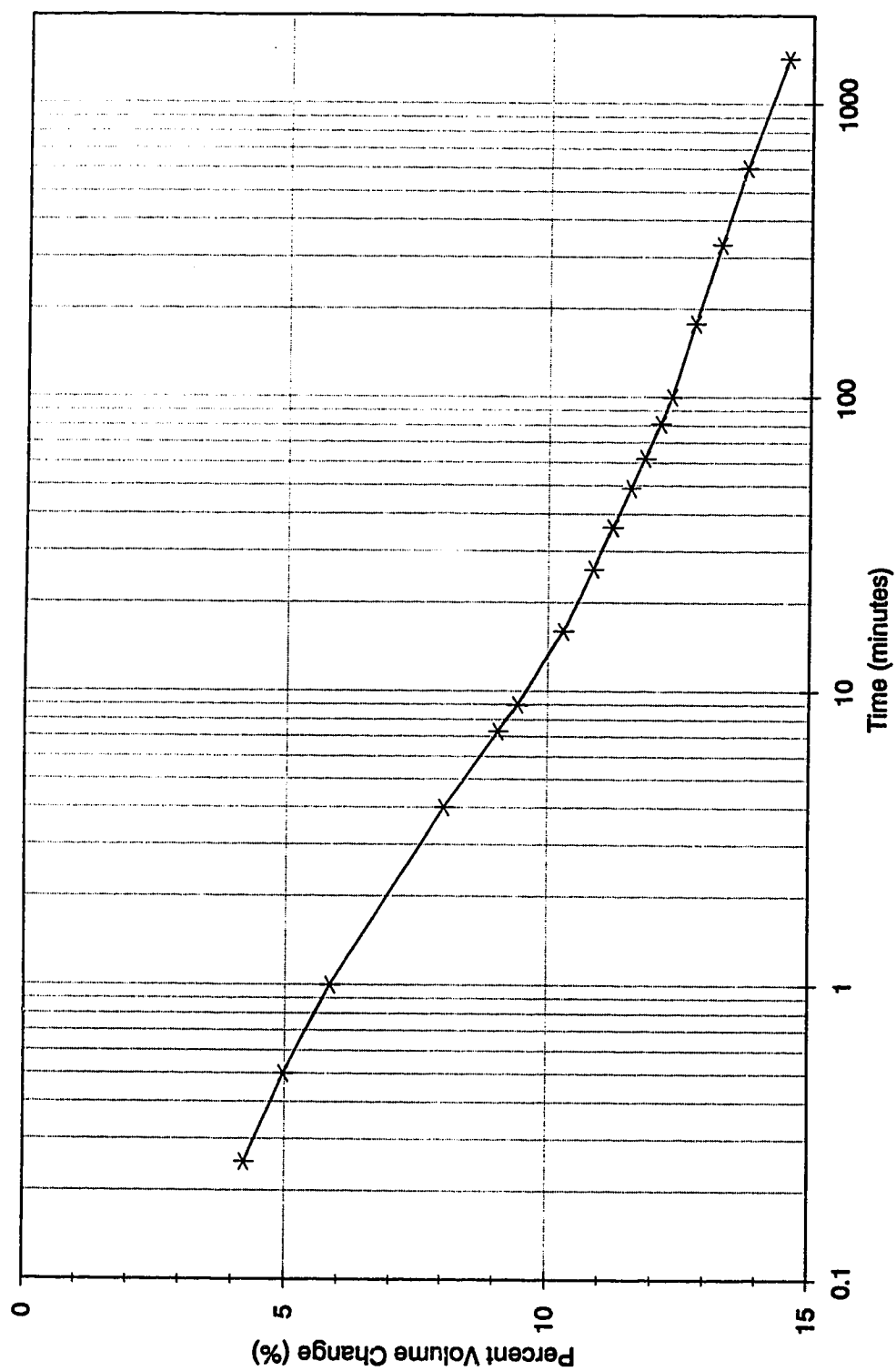
Figure B20 Consolidation/Softening - Test PWA5A Series 4
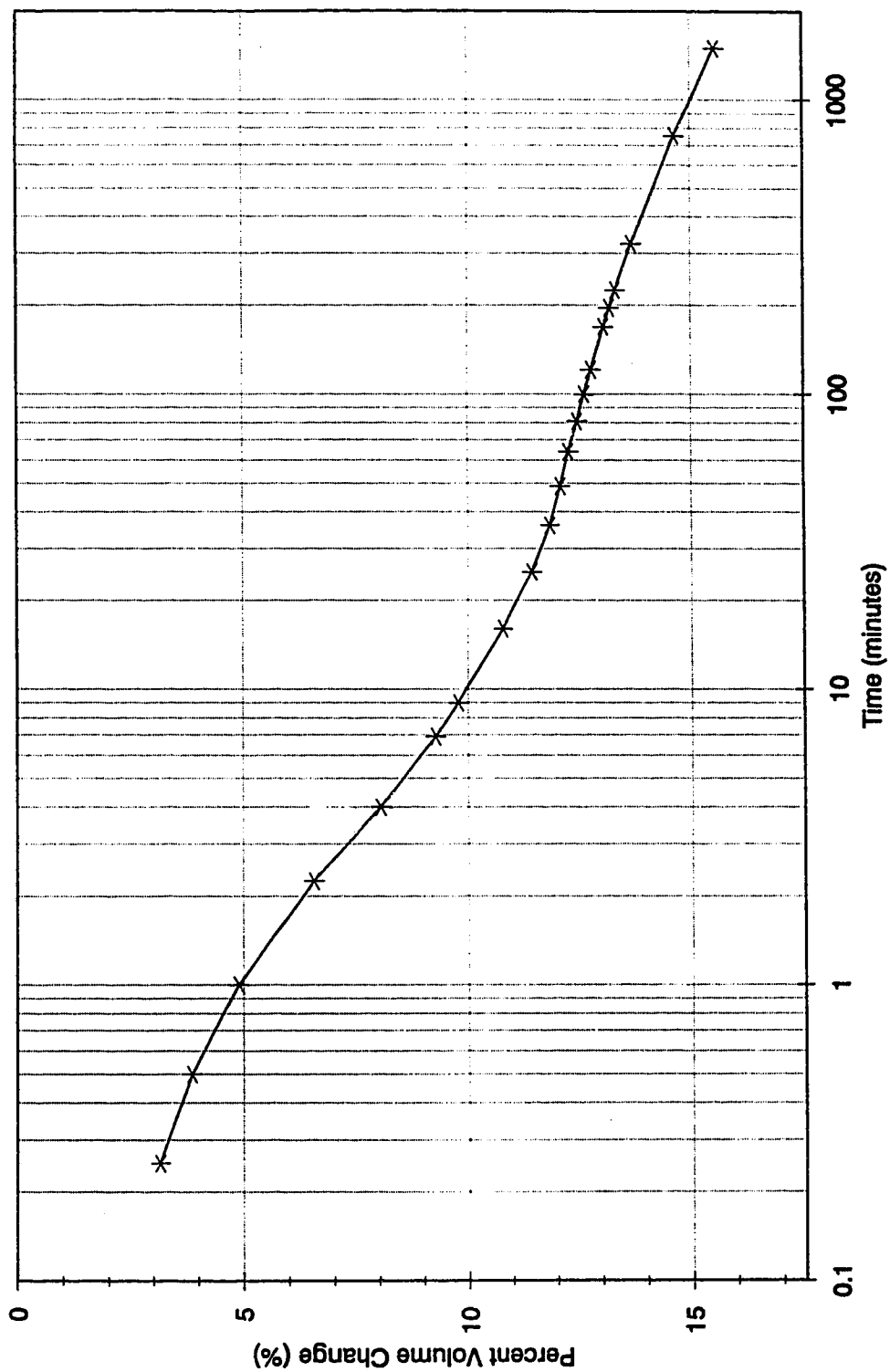
Figure B21 Consolidation/Softening – Test PW/A6A Series 4
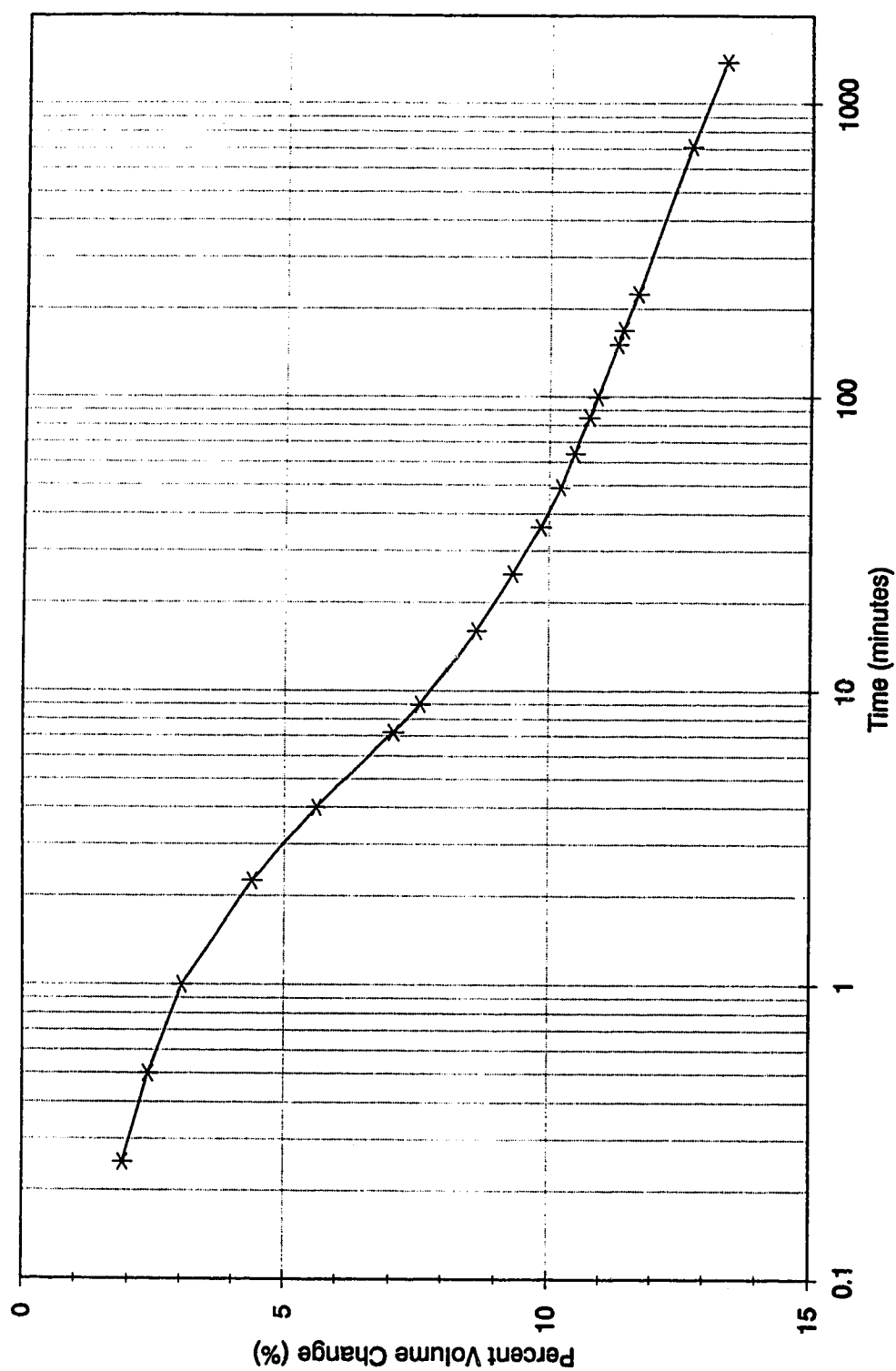
Figure B22 Consolidation/Softening - Test PWA7A Series 4
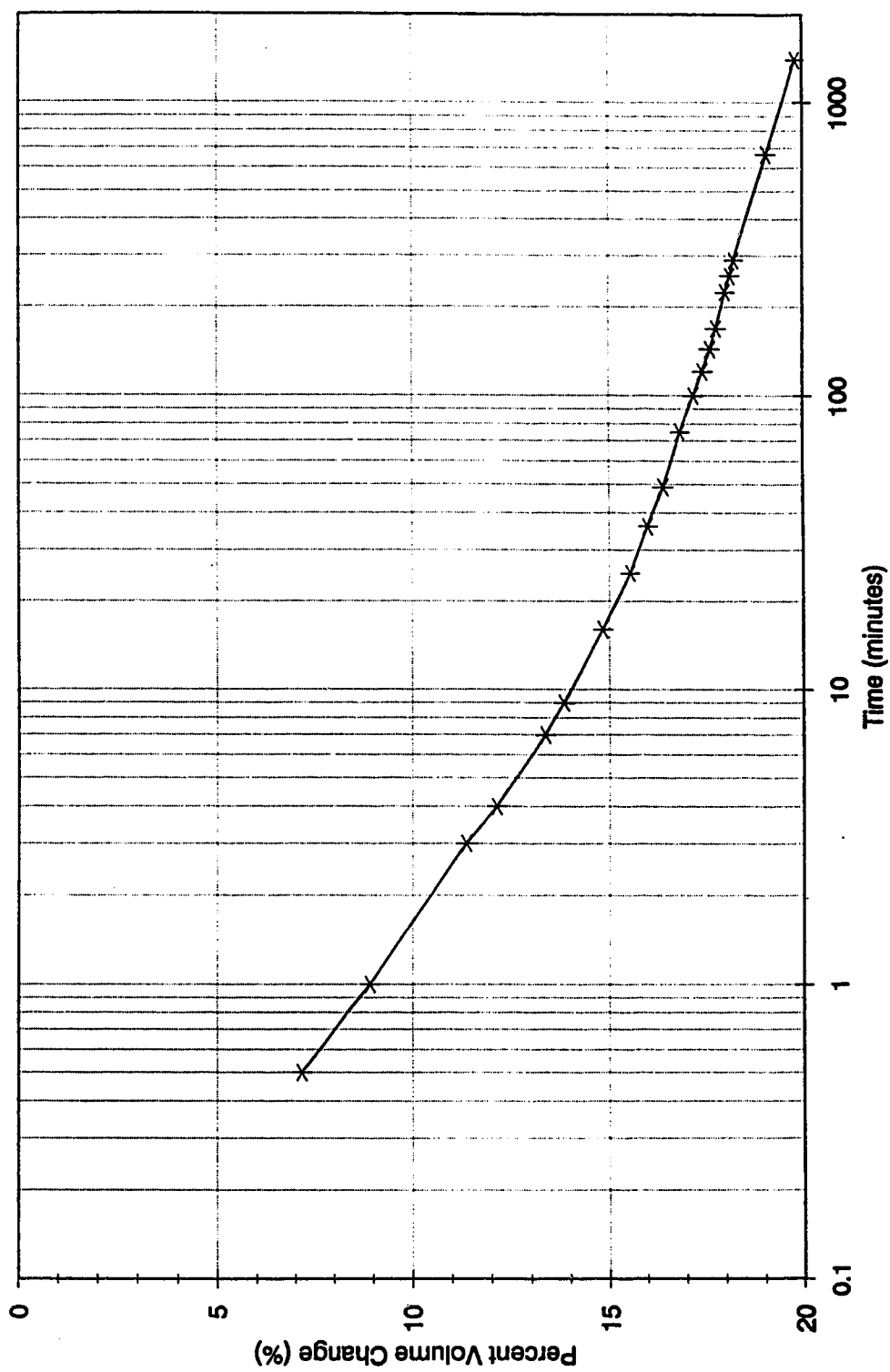
Figure B23 Consolidation/Softening - Test PWA8A Series 4

197
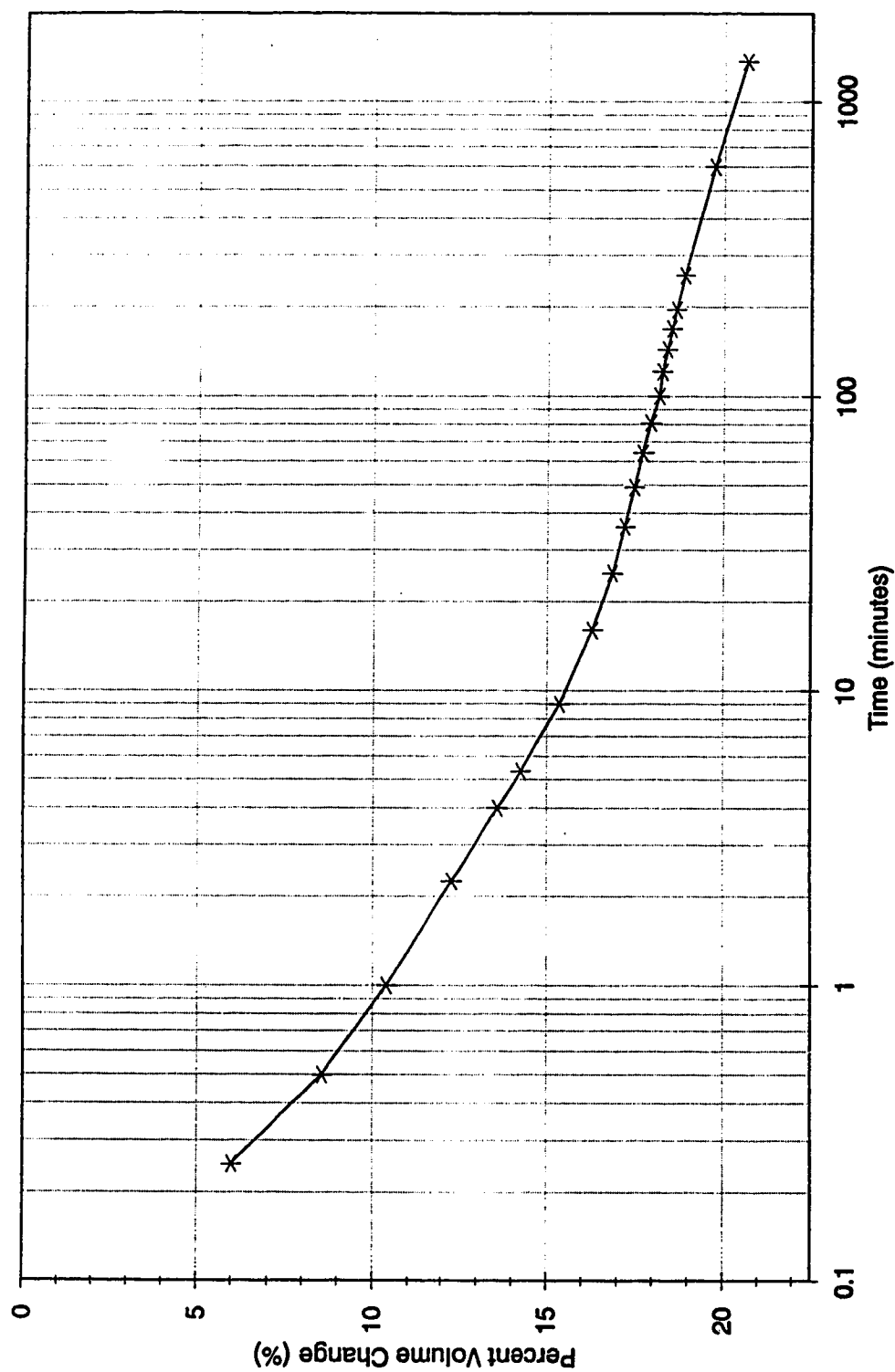
Figure B24 Consolidation/Softening - Test PWA9A Series 4
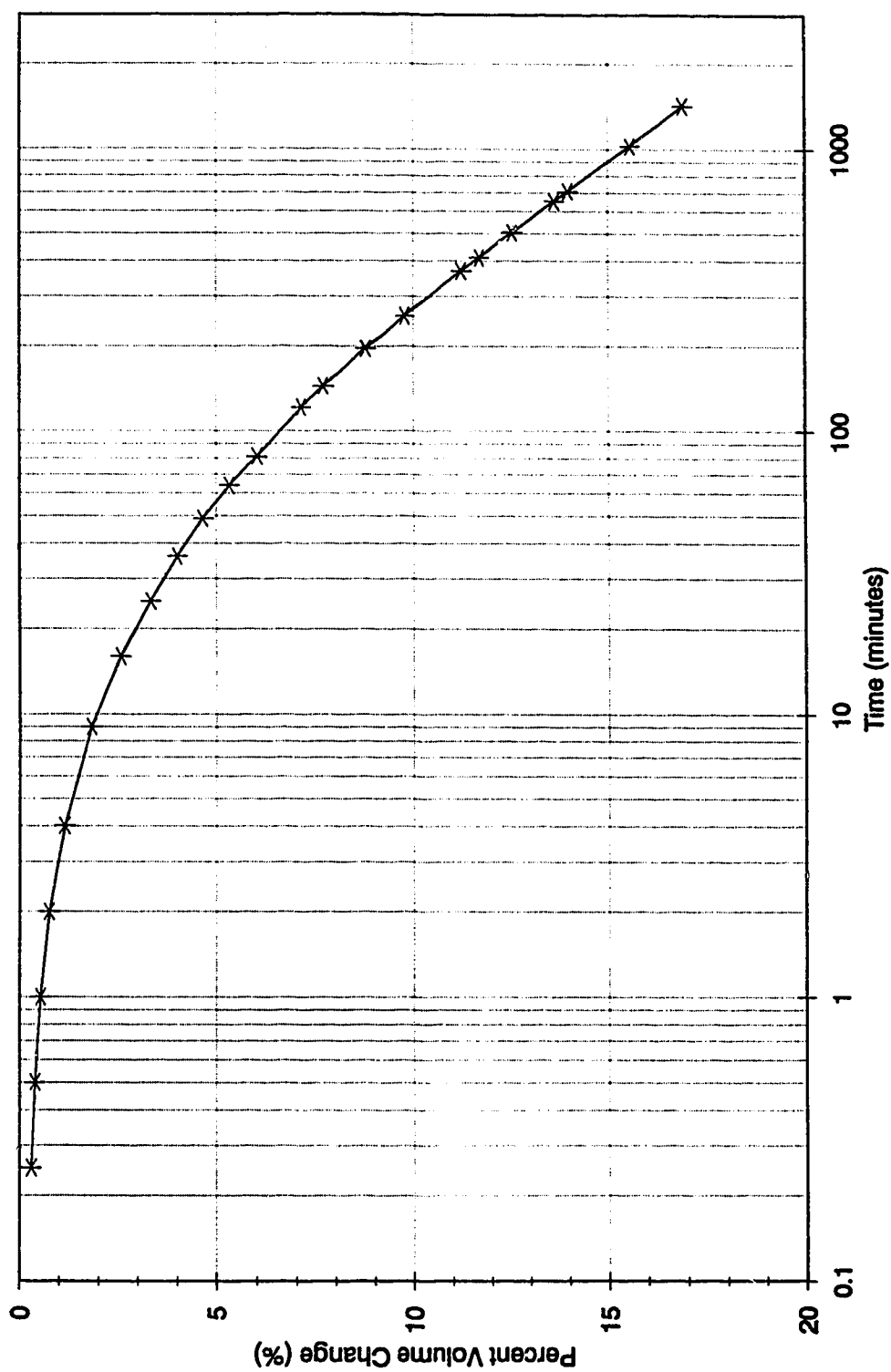
Figure B25 Consolidation/Softening - Test PSA1 Series 5
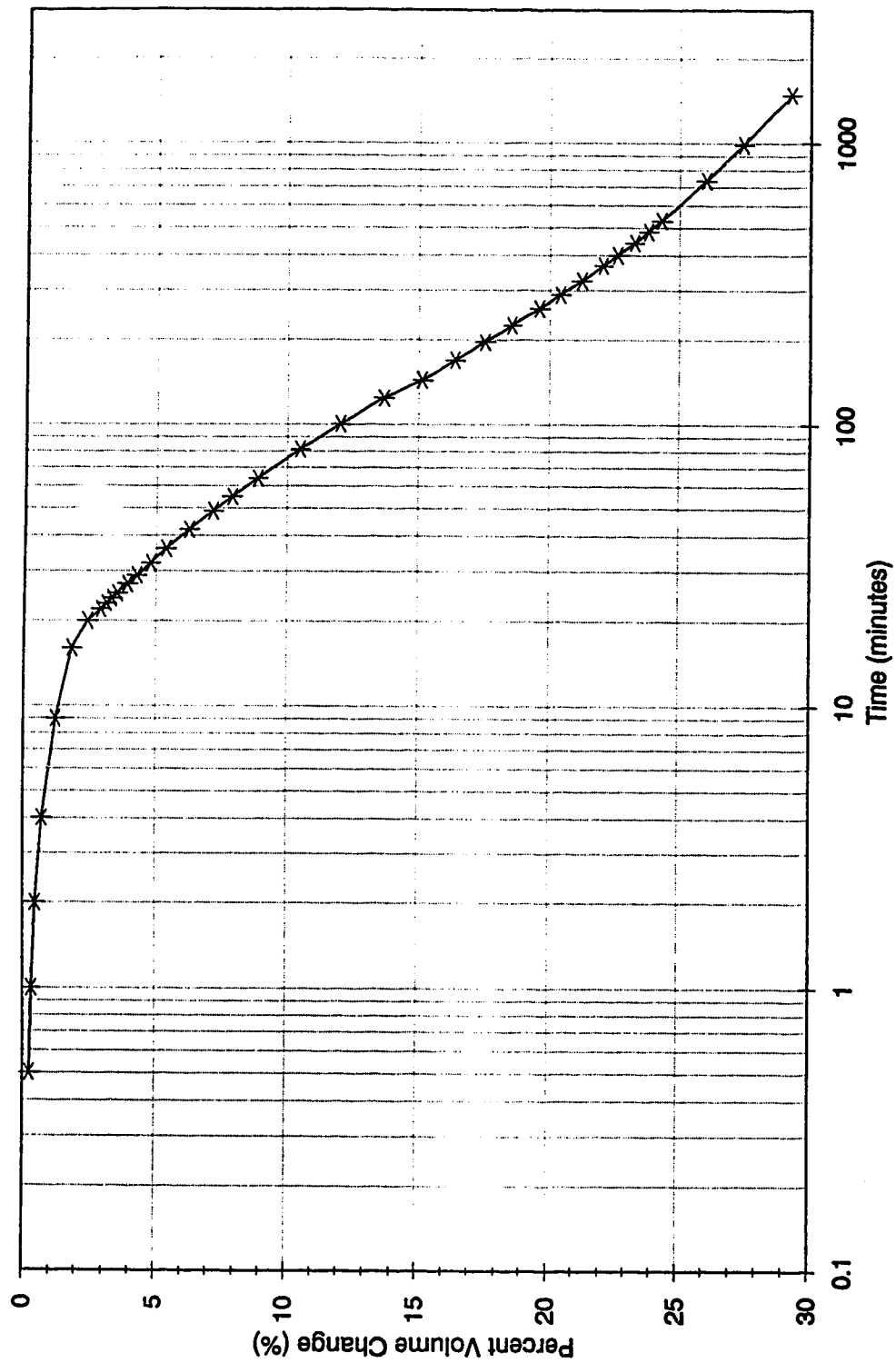
Figure B26   Consolidation/Softening - Test PSA2 Series 5
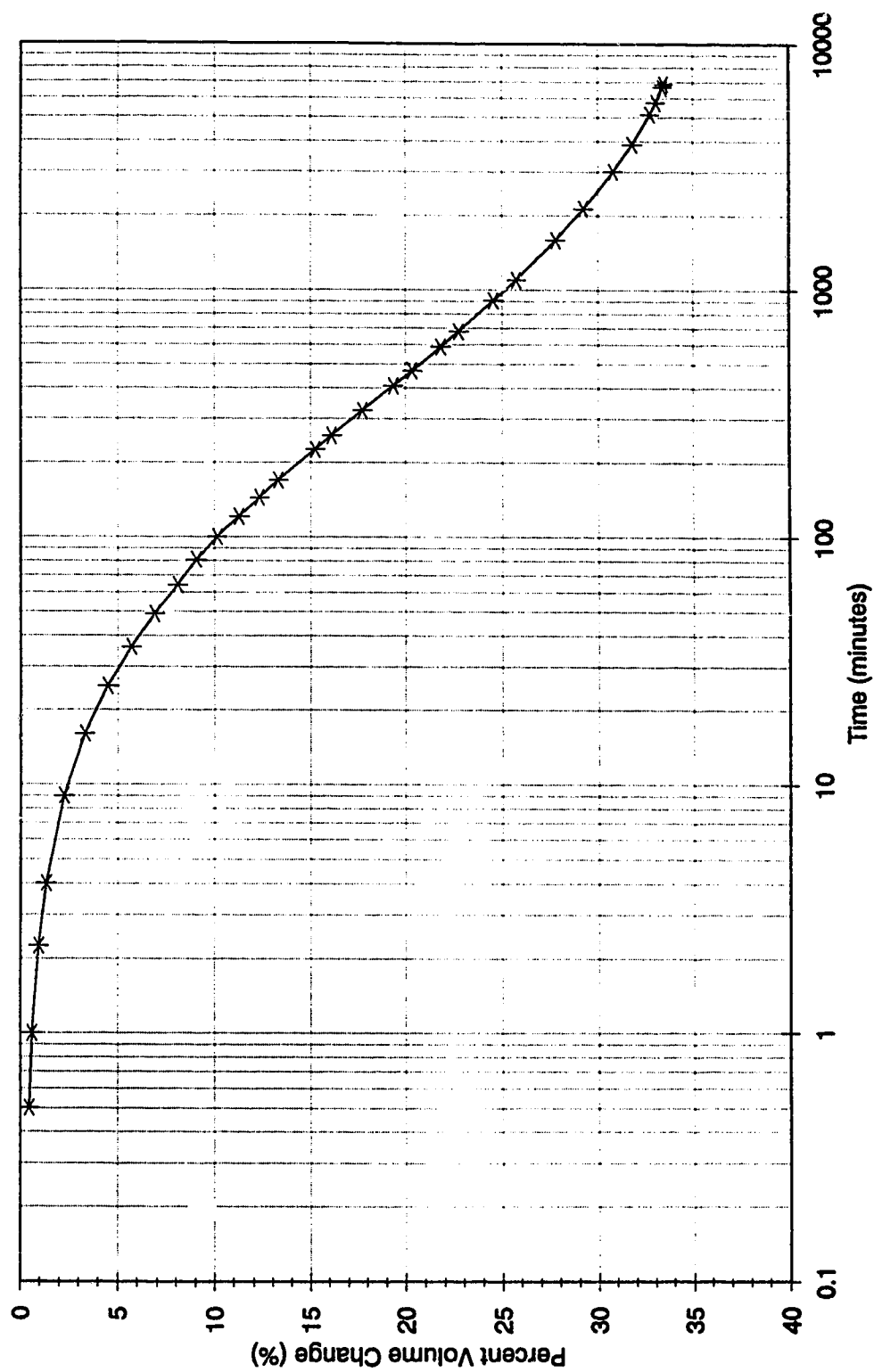
Figure B27 Consolidation/Softening - Test PSA3 Series 5

200
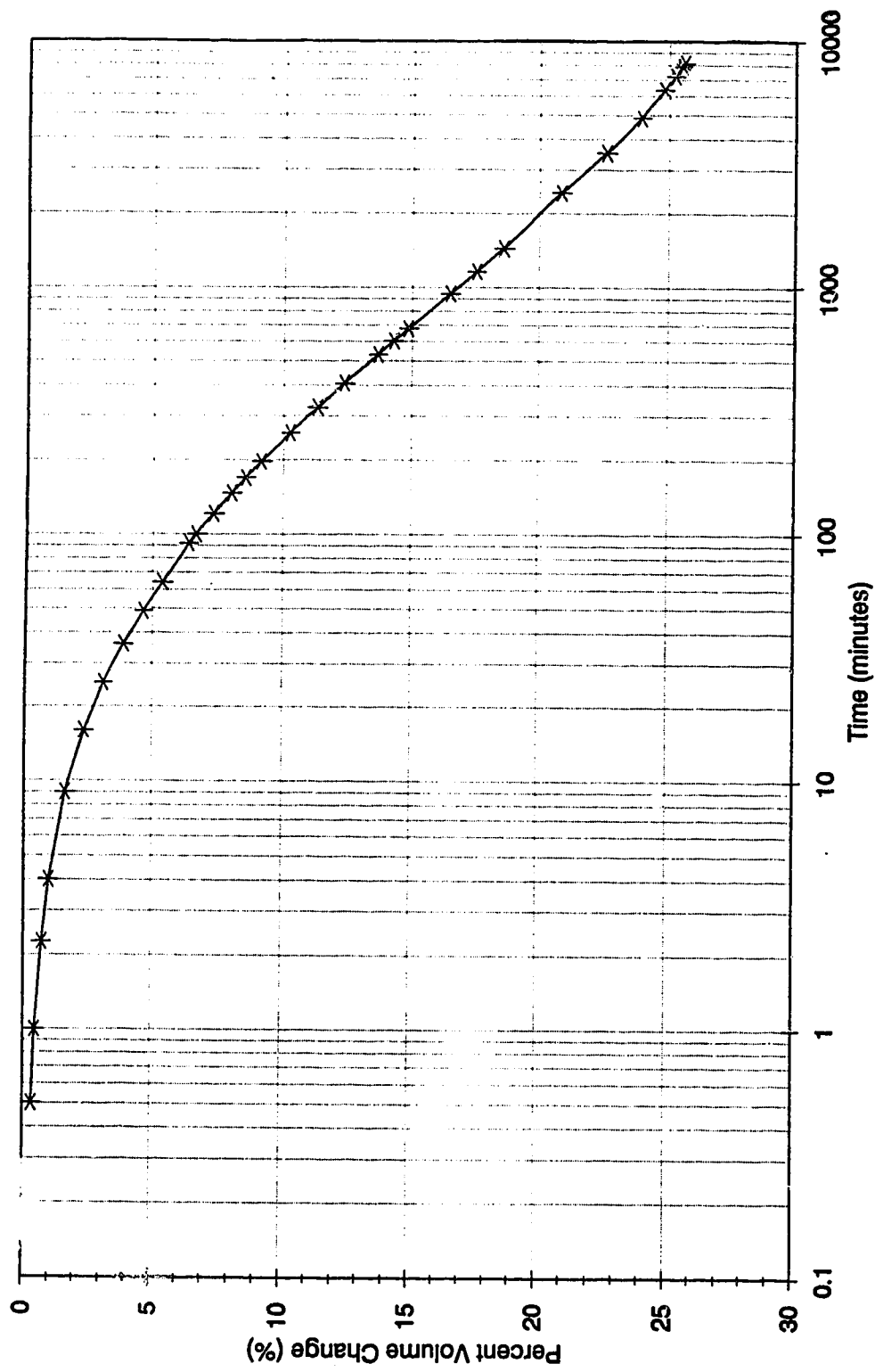
Figure B28 Consolidation/Softening - Test PSA4 Series 5

201
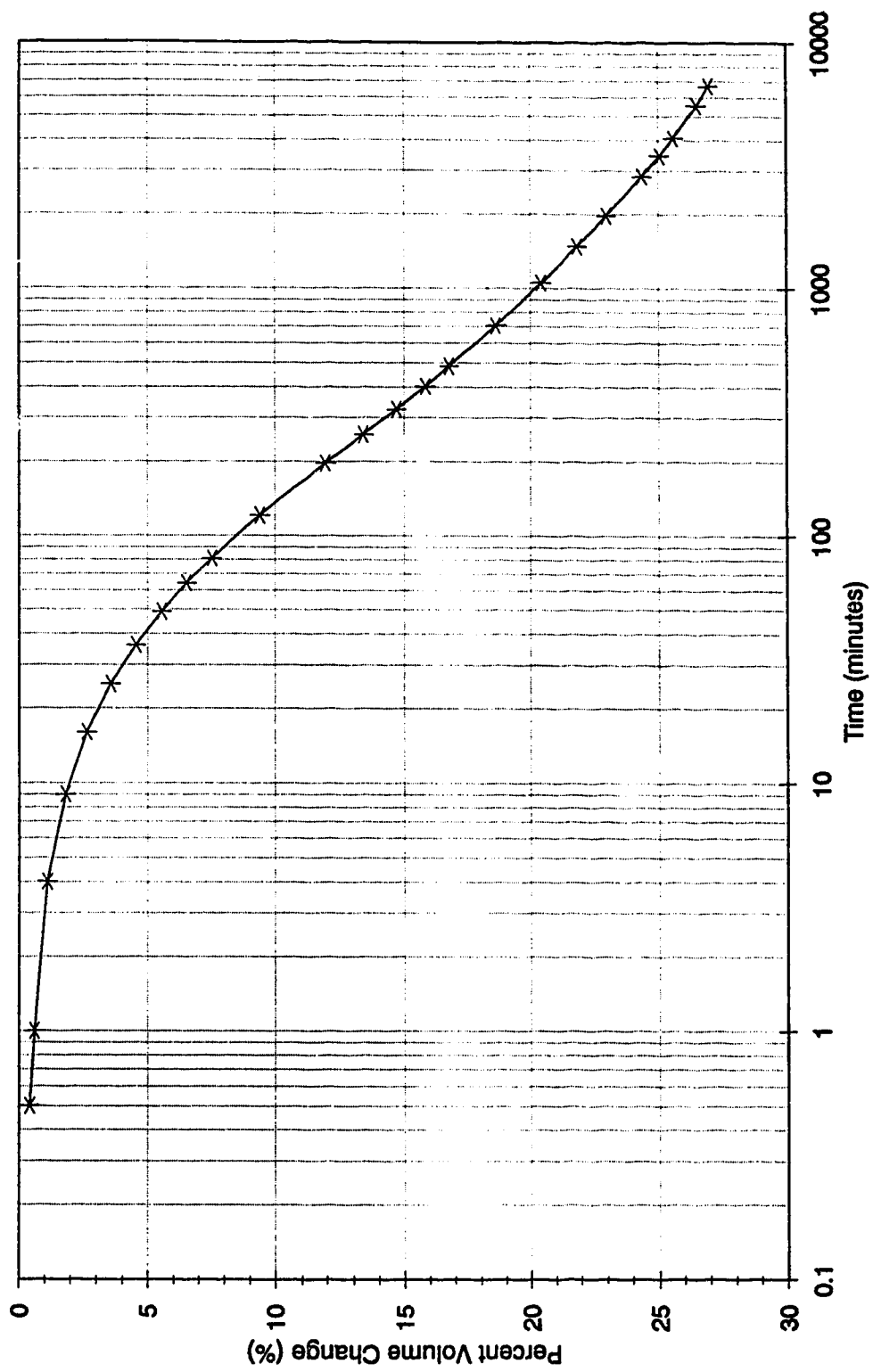
Figure B29 Consolidation/Softening - Test PSA5 Series 5

202
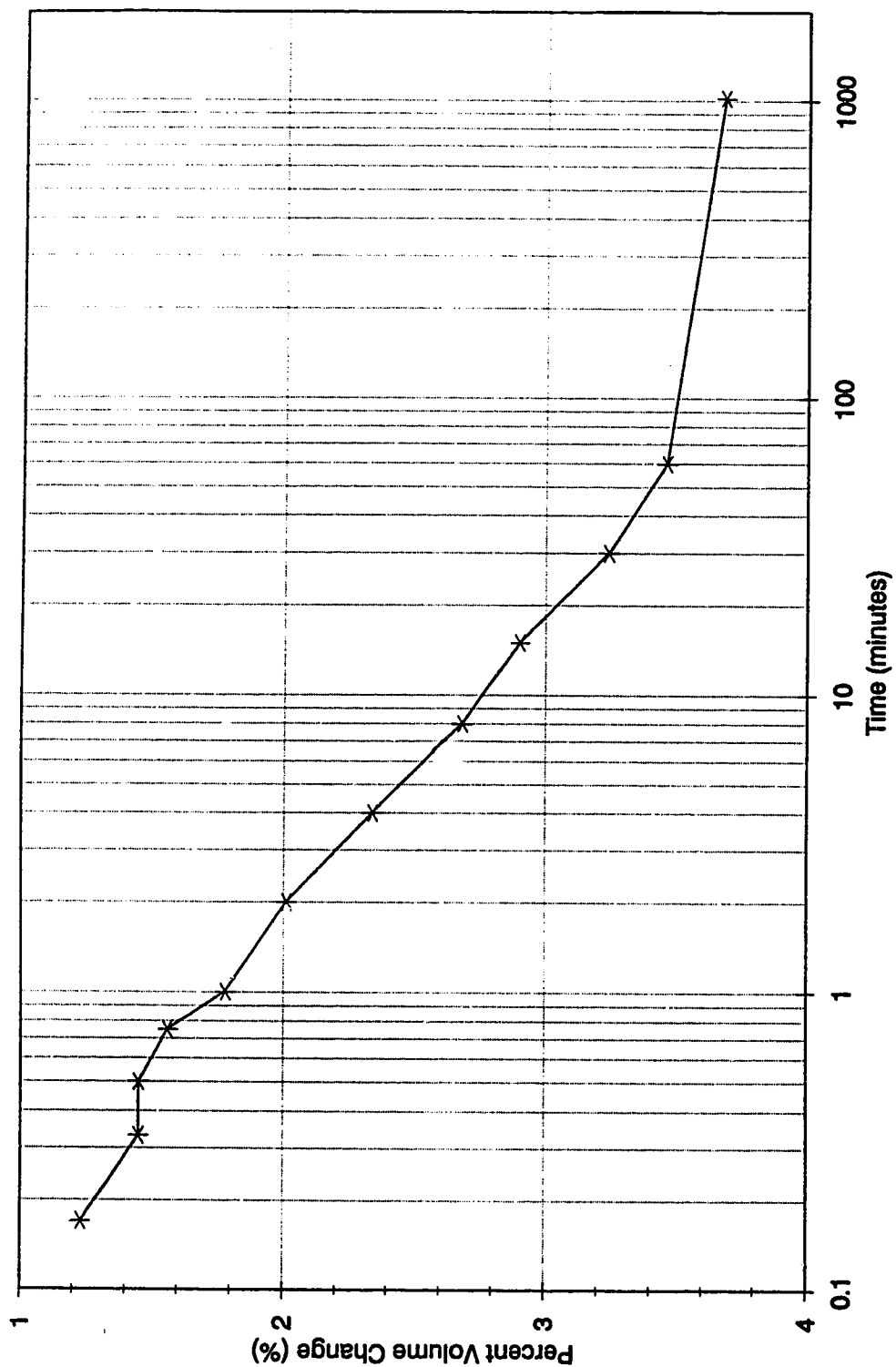
Figure B30 Consolidation/Softening - Test PWMS1 Series 6
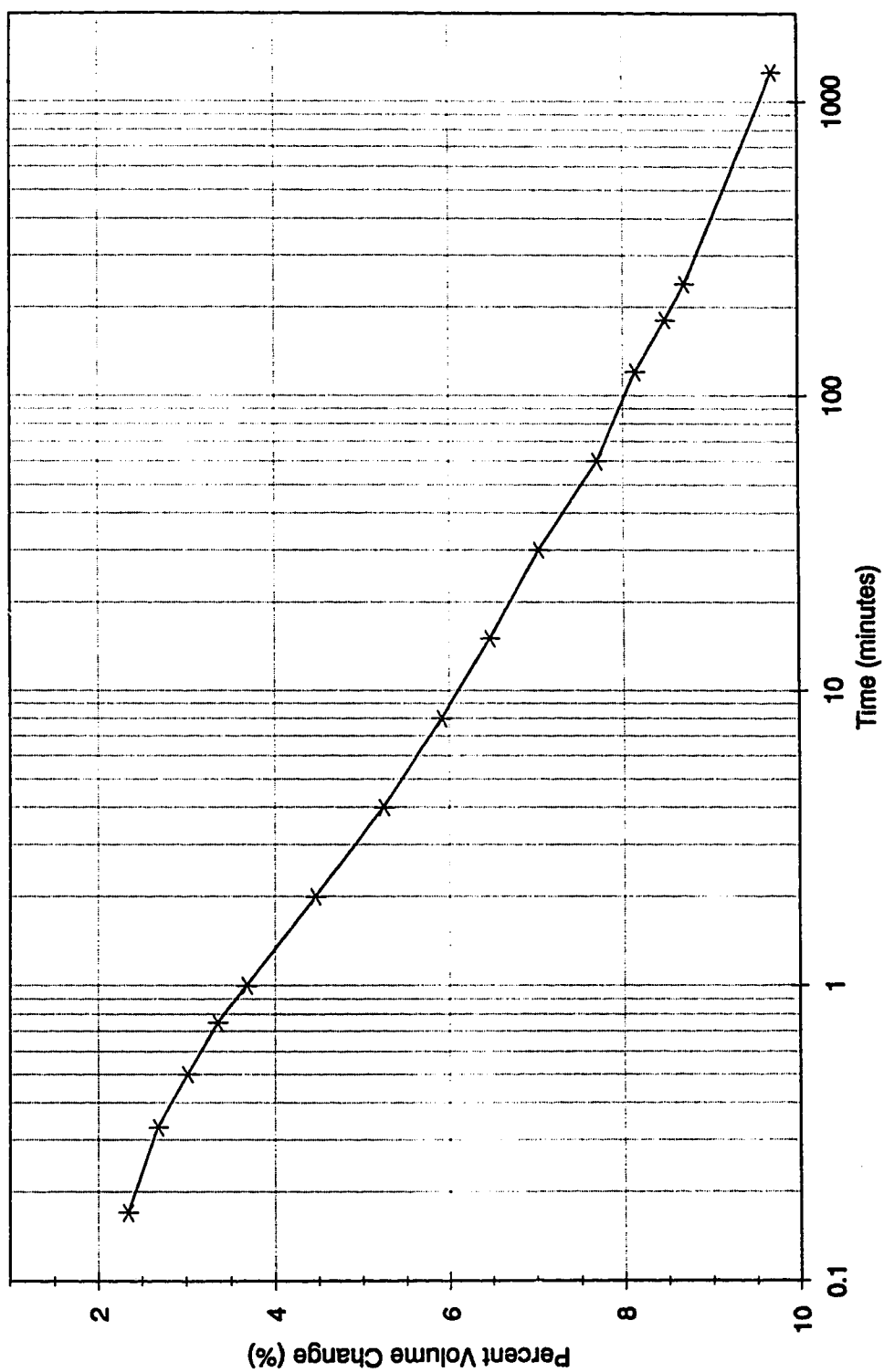
Figure B31 Consolidation/Softening - Test PWMS2 Series 6
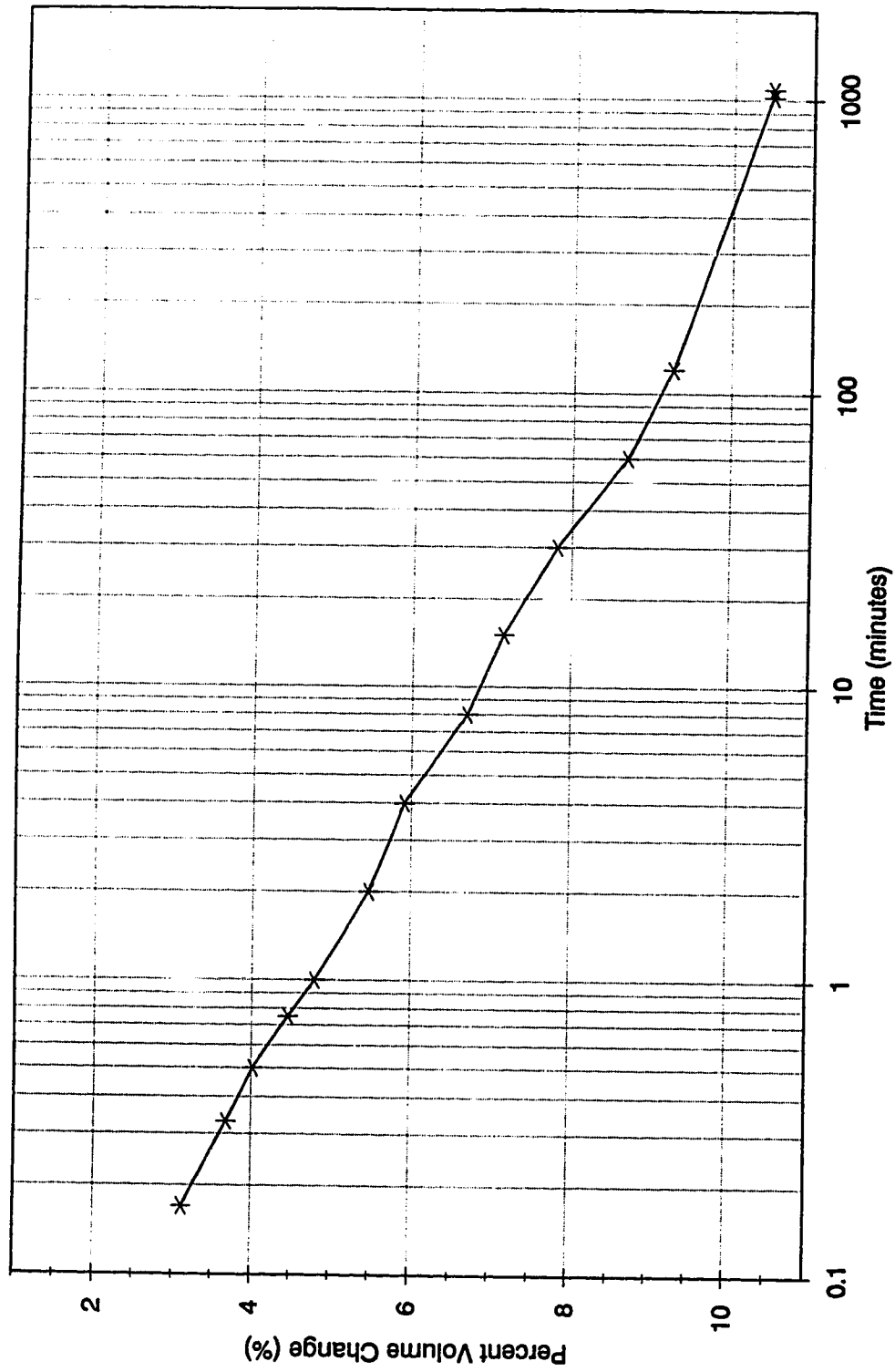
Figure B32 Consolidation/Softening - Test PWMS3 Series 6
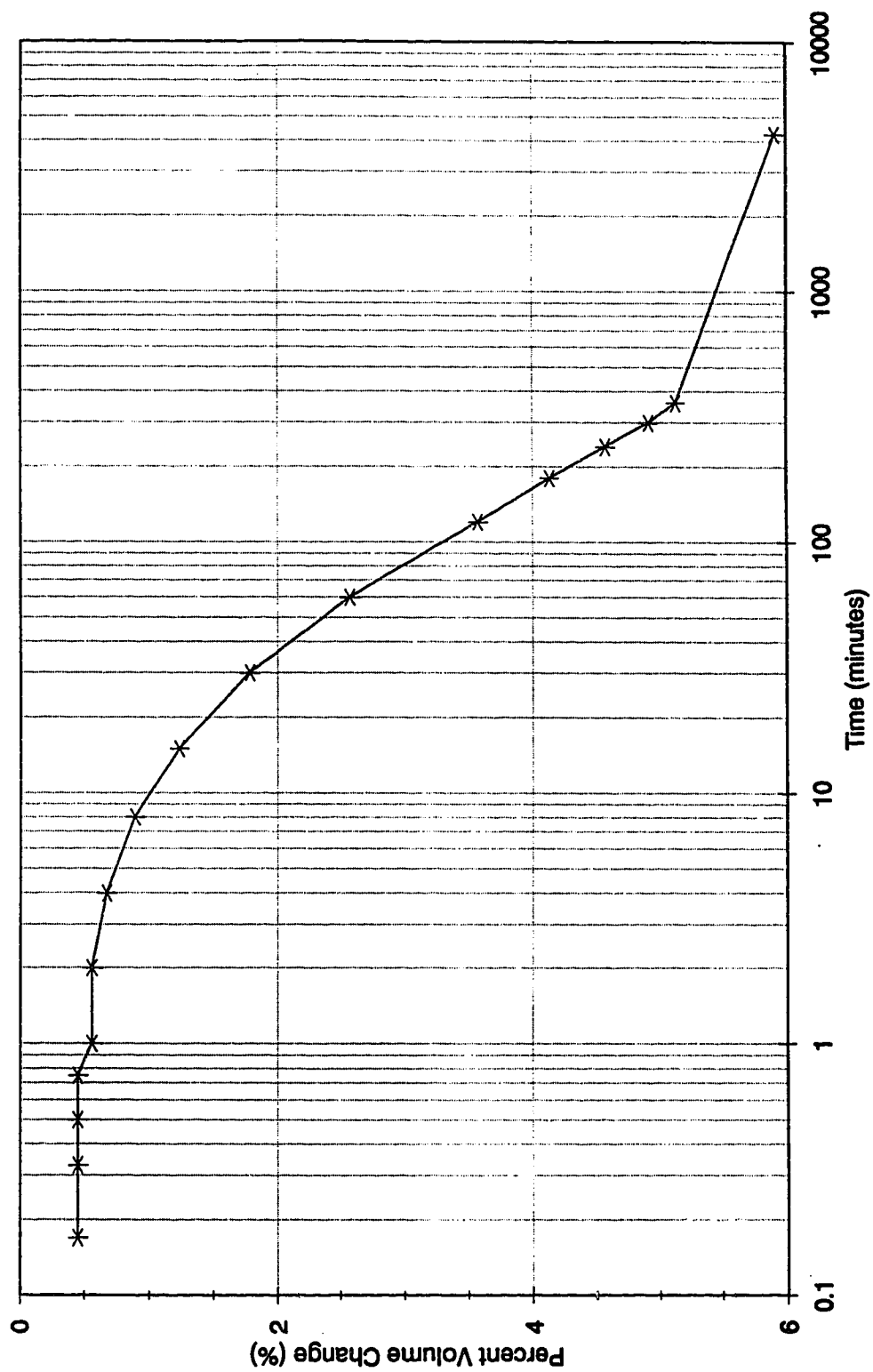
Figure B33 Consolidation/Softening - Test PWMS4 Series 6

206
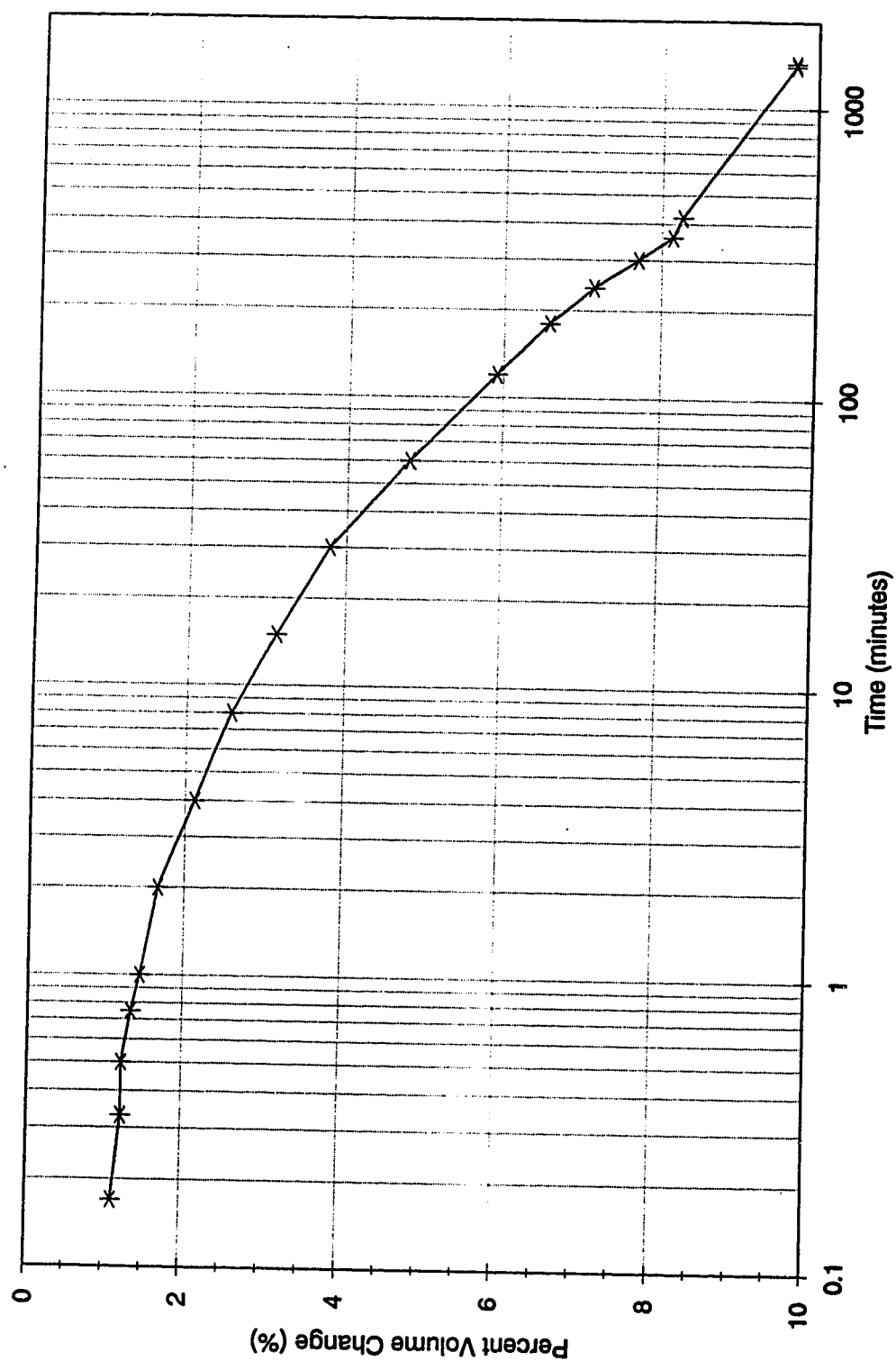
Figure B34 Consolidation/Softening - Test PWMS5 Series 6
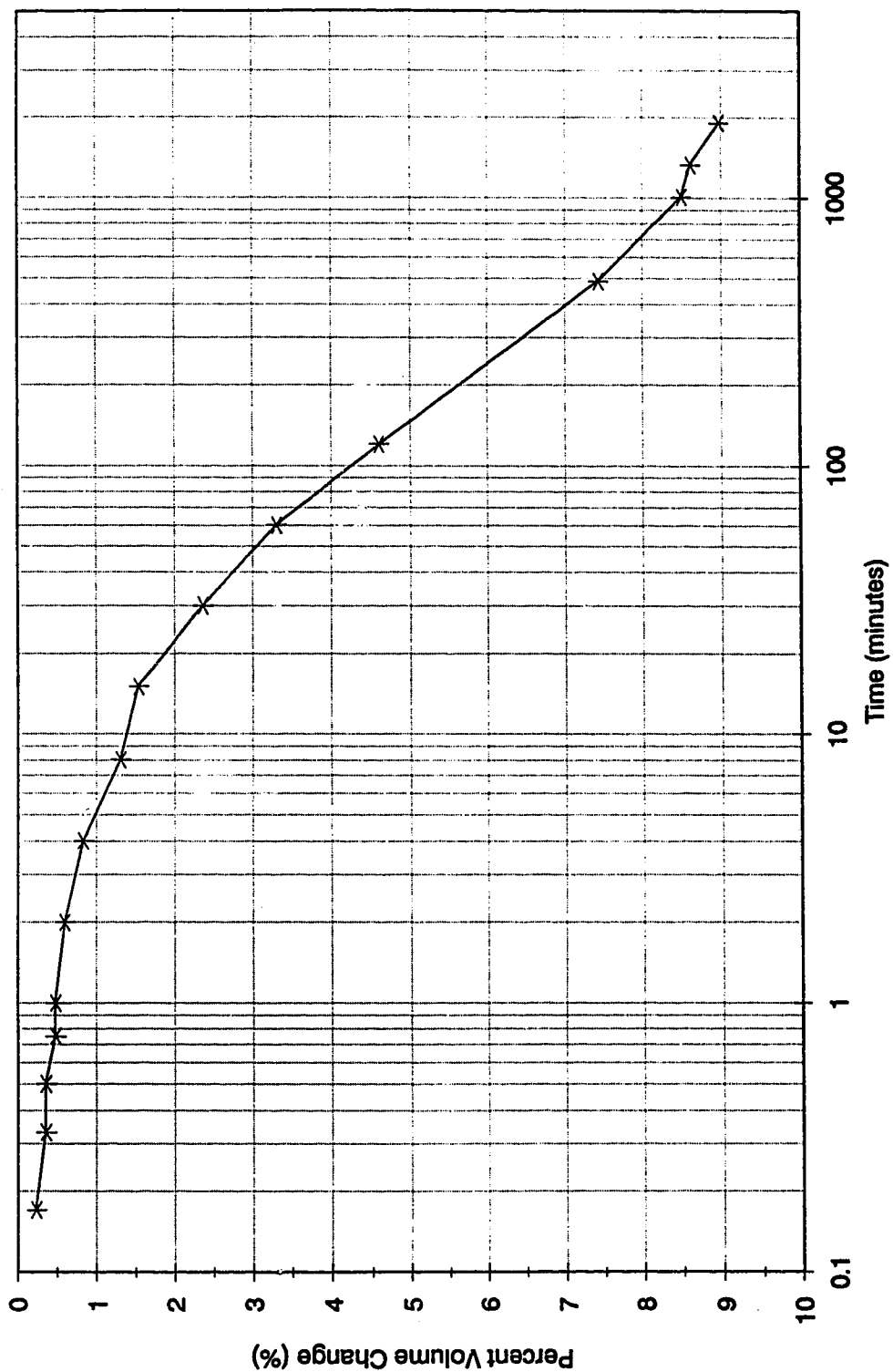
Figure B35 Consolidation/Softening - Test PWMS6 Series 6A

208
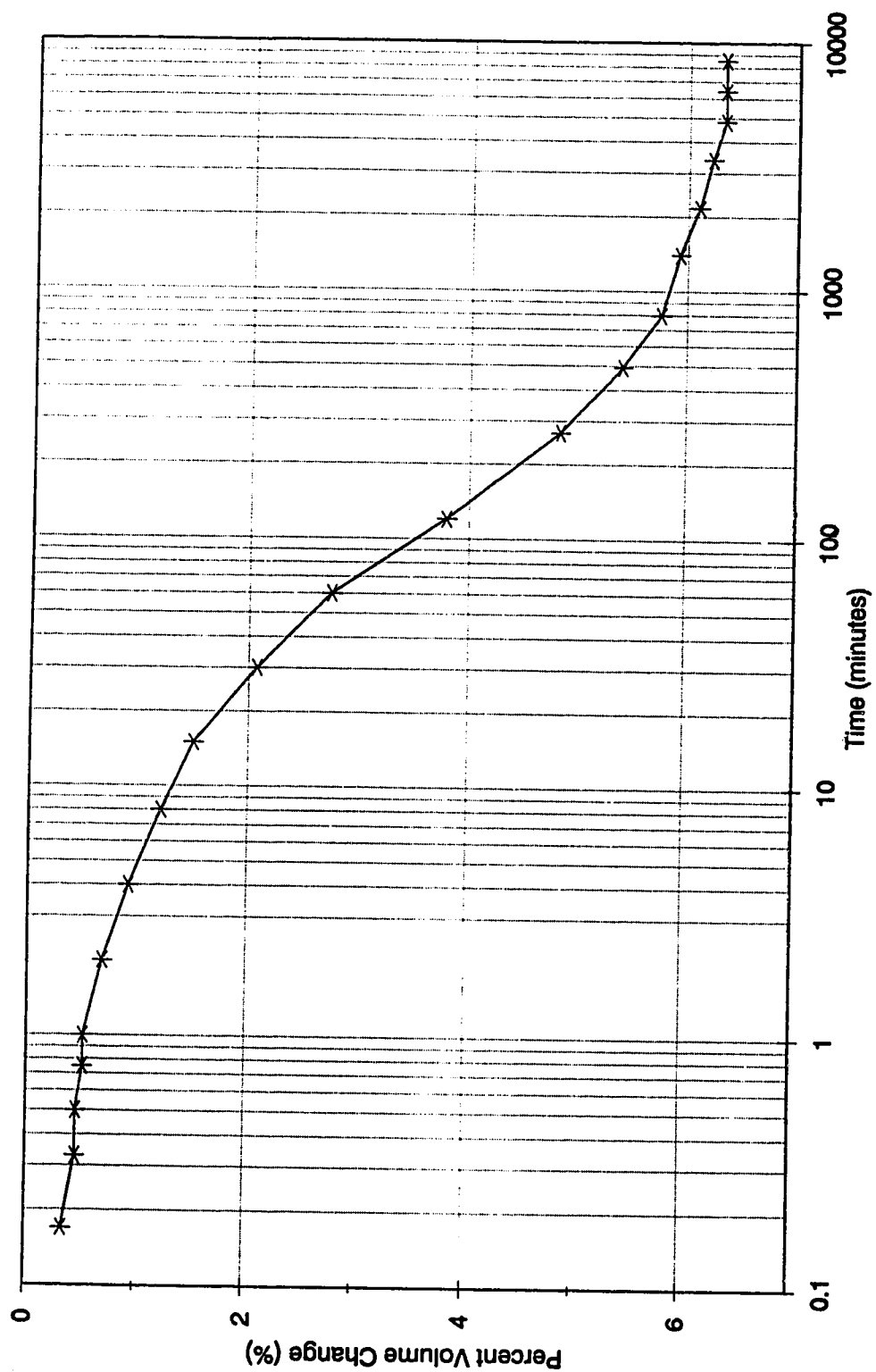
Figure B36 Consolidation/Softening - Test PWMS7 Series 6A

209
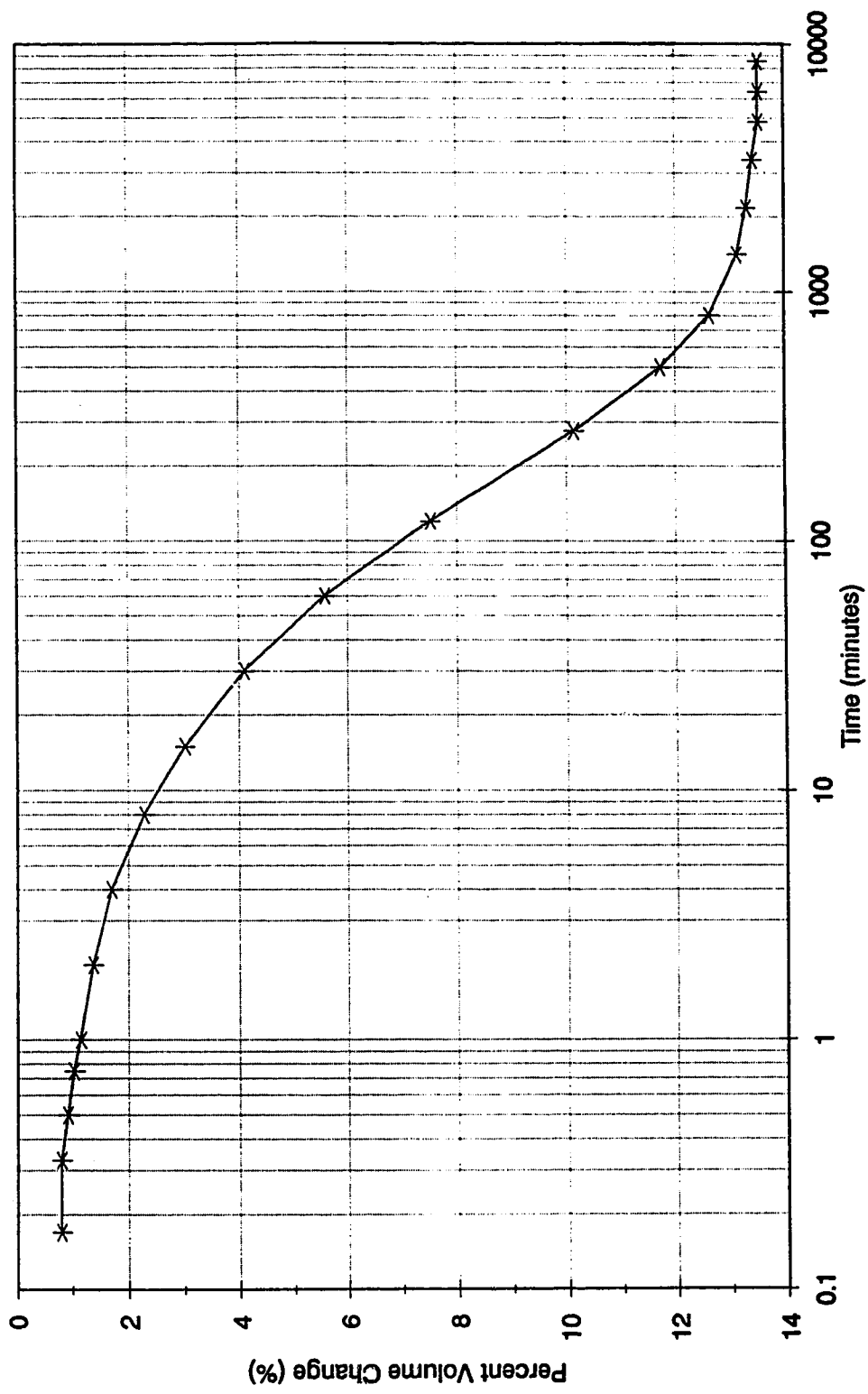
Figure B37 Consolidation/Softening - Test PWMS8 Series 6A 210
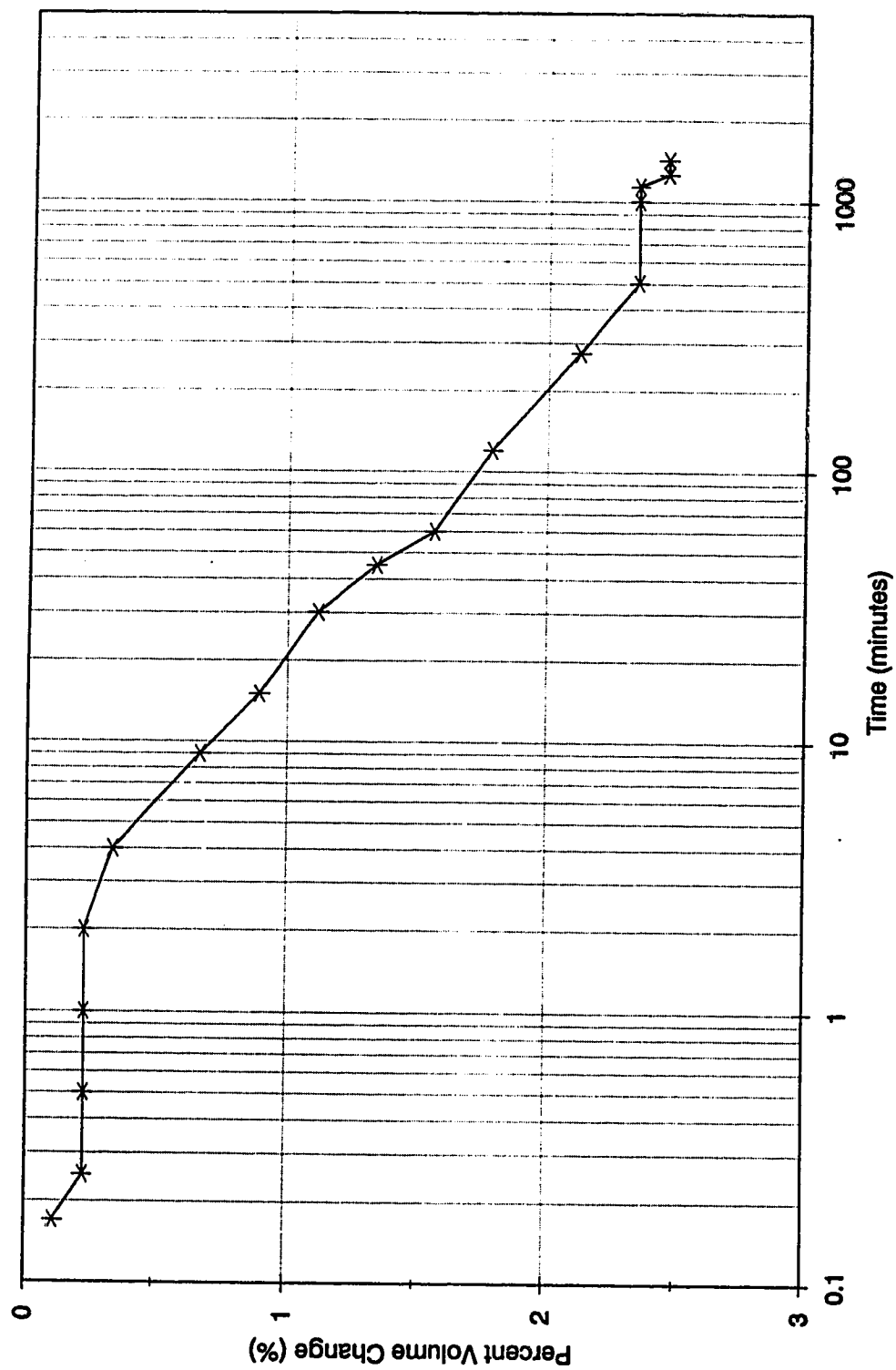
Figure B38 Consolidation/Softening - Test PSMS1 Series 7

211
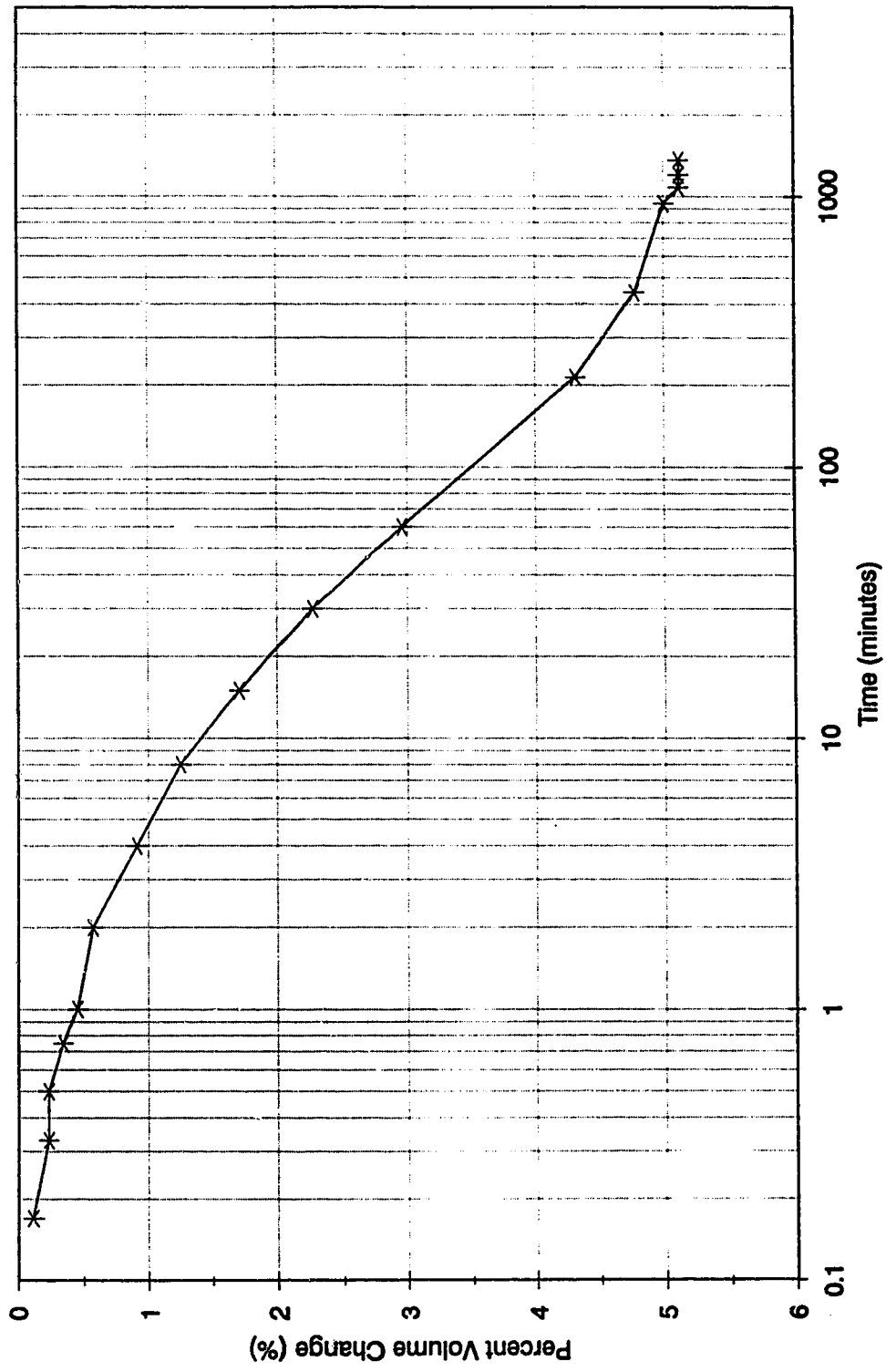
Figure B39 Consolidation/Softening - Test PSMS2 Series 7
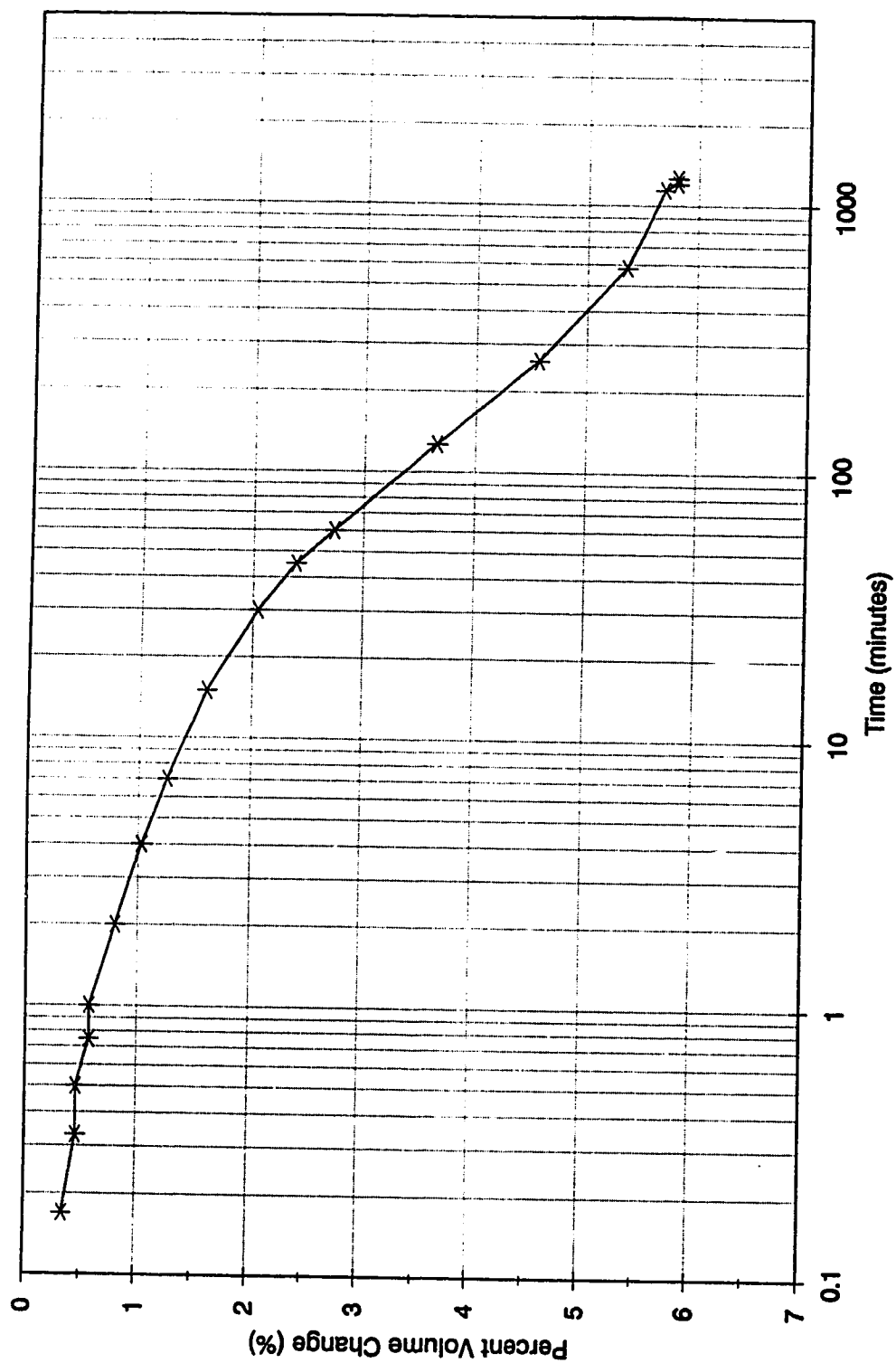
Figure B40 Consolidation/Softening - Test PSMS3 Series 7
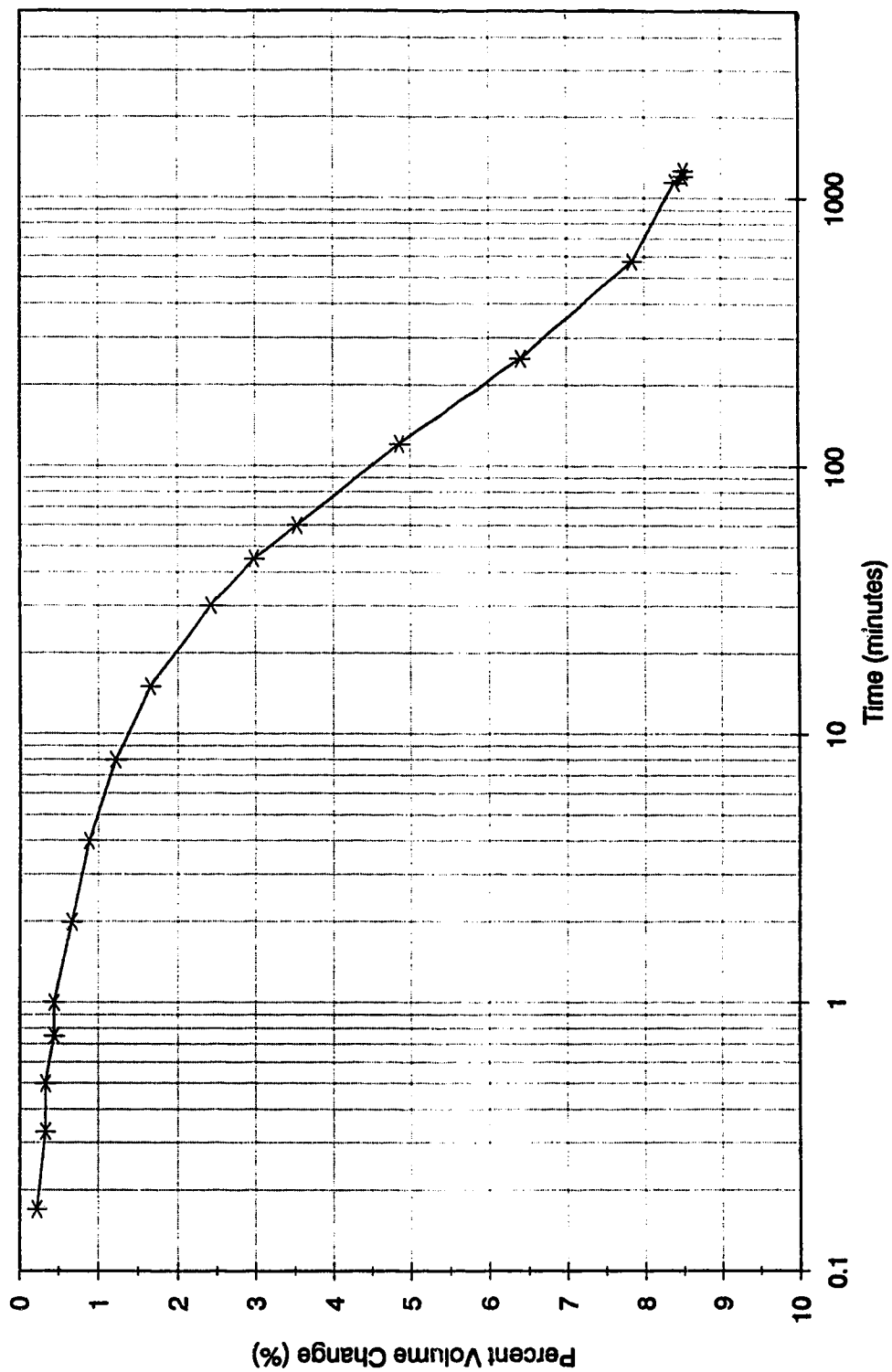
Figure B41   Consolidation/Softening - Test PSMS4   Series 7

214
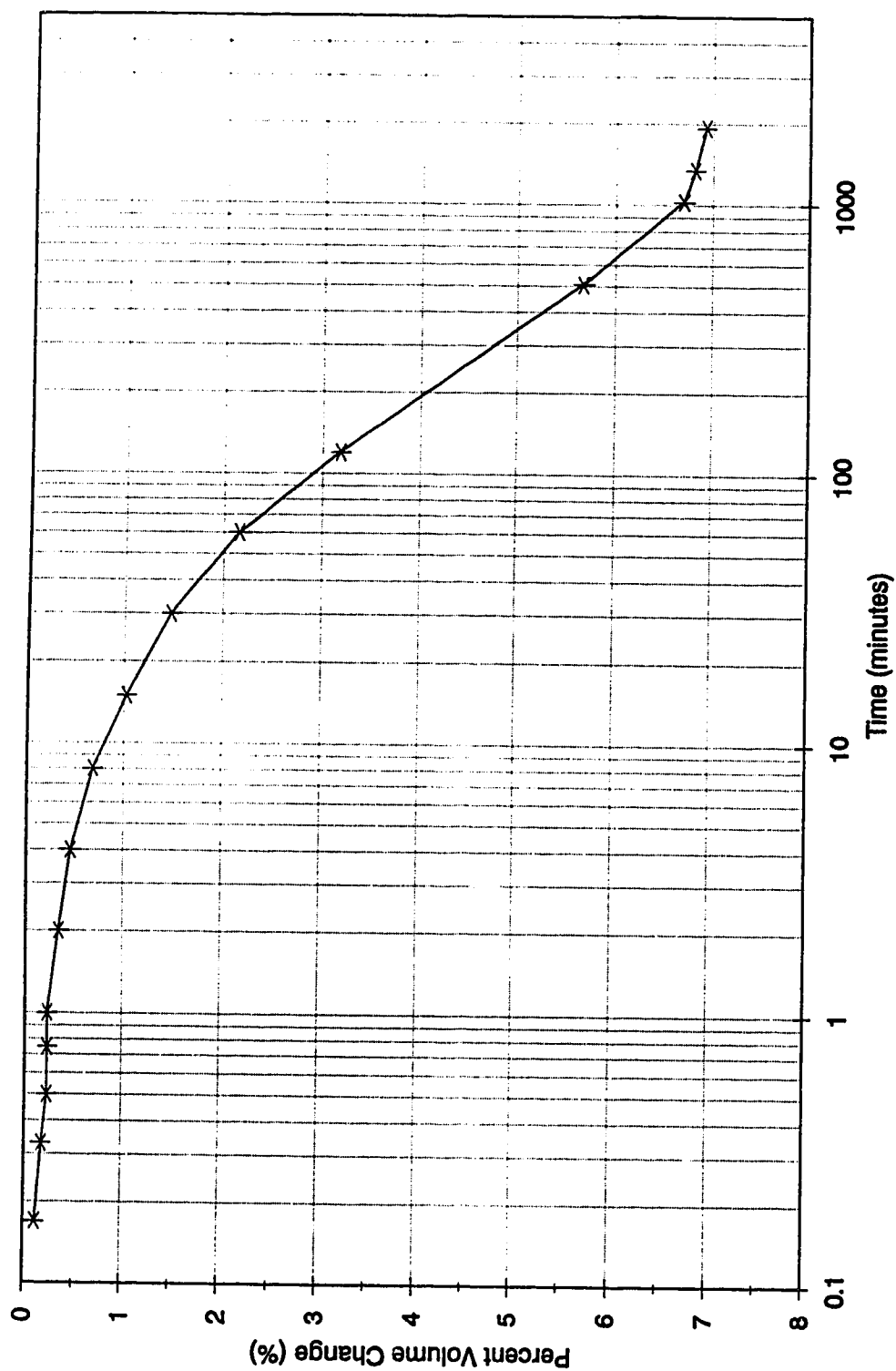
Figure B42 Consolidation/Softening – Test PSMS5 Series 7
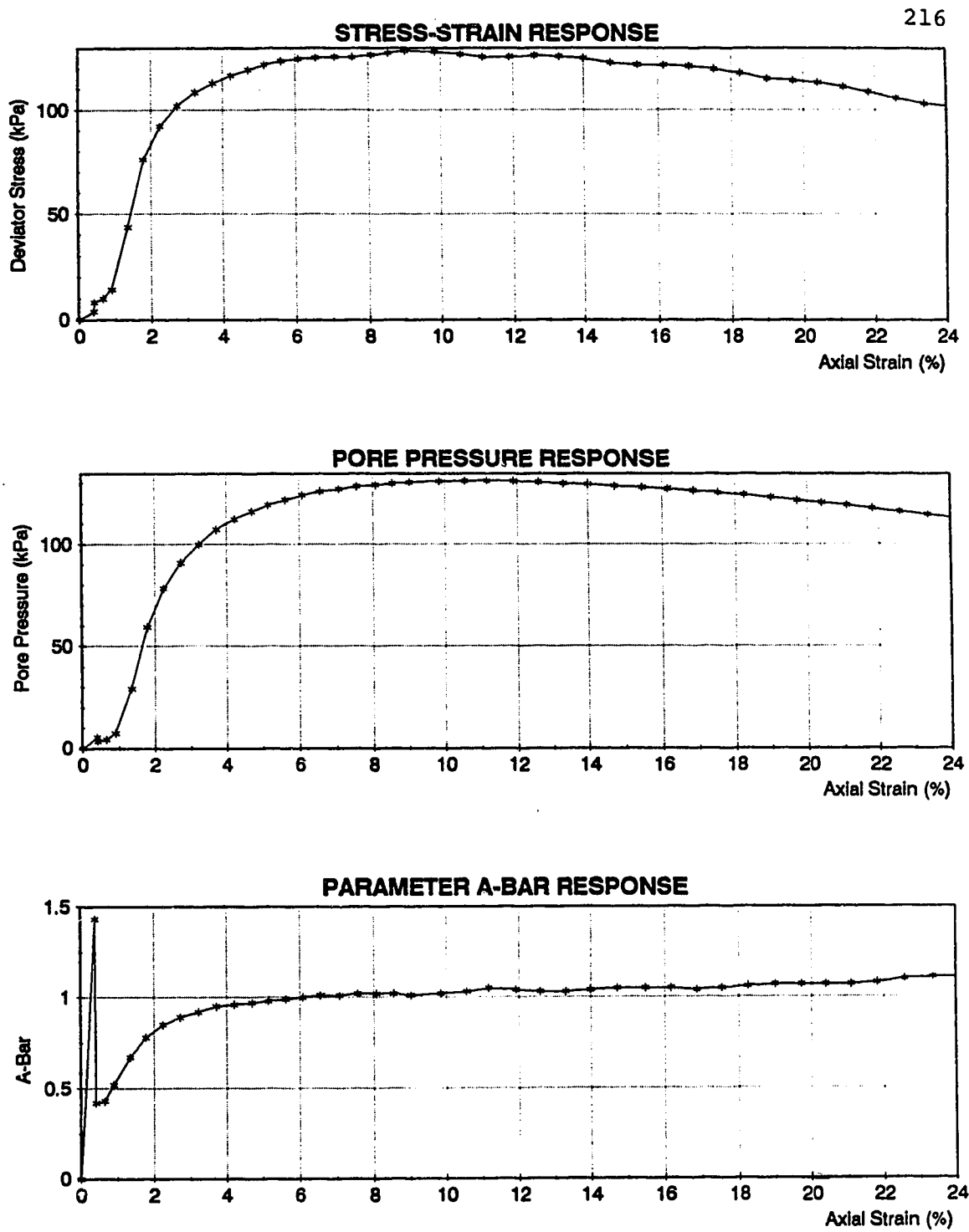
Figure B43   Triaxial Test PWA2   Series 1

STRESS-STRAIN RESPONSE

Deviator Stress (kPa)

Axial Strain (%)

PORE PRESSURE RESPONSE

Pore Pressure (kPa)

Axial Strain (%)

PARAMETER A-BAR RESPONSE

A-Bar

Axial Strain
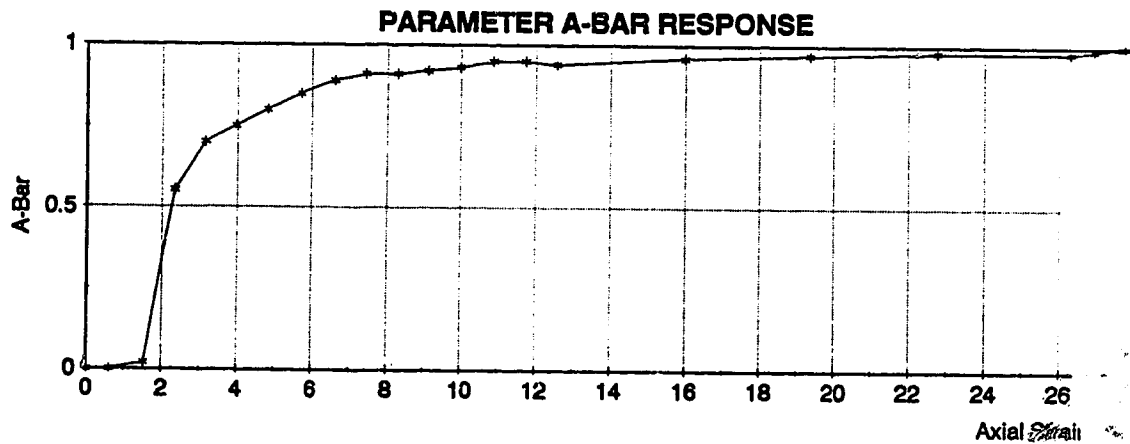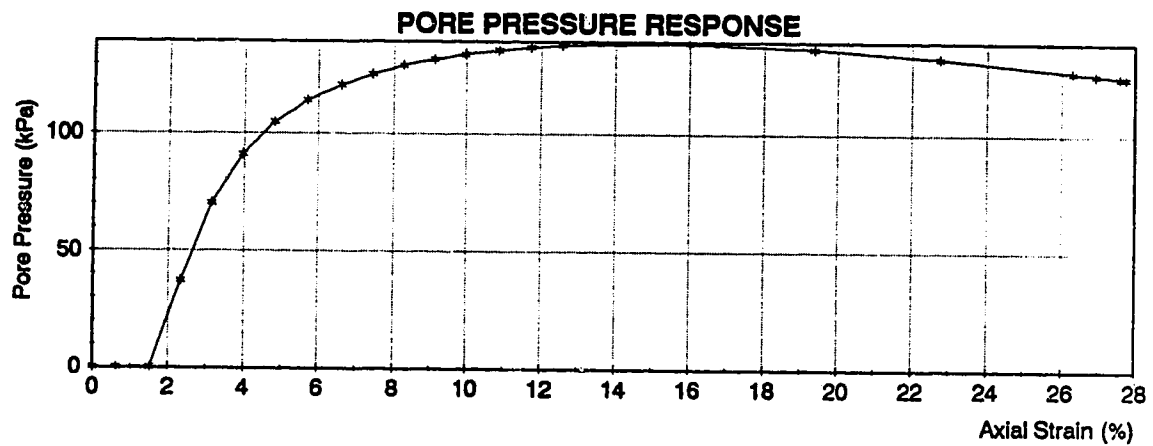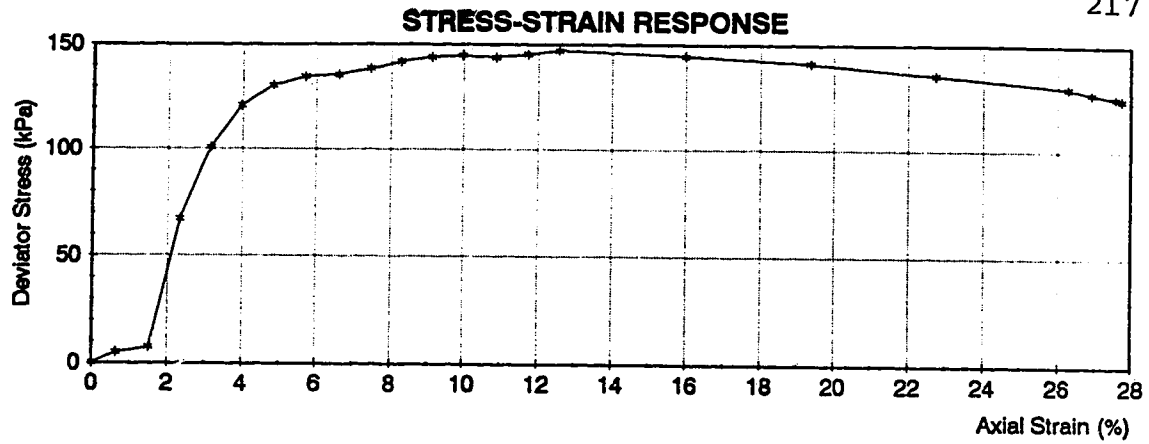
Figure B44   Triaxial Test PWA3   Series

STRESS-STRAIN RESPONSE

PORE PRESSURE RESPONSE

PARAMETER A-BAR RESPONSE
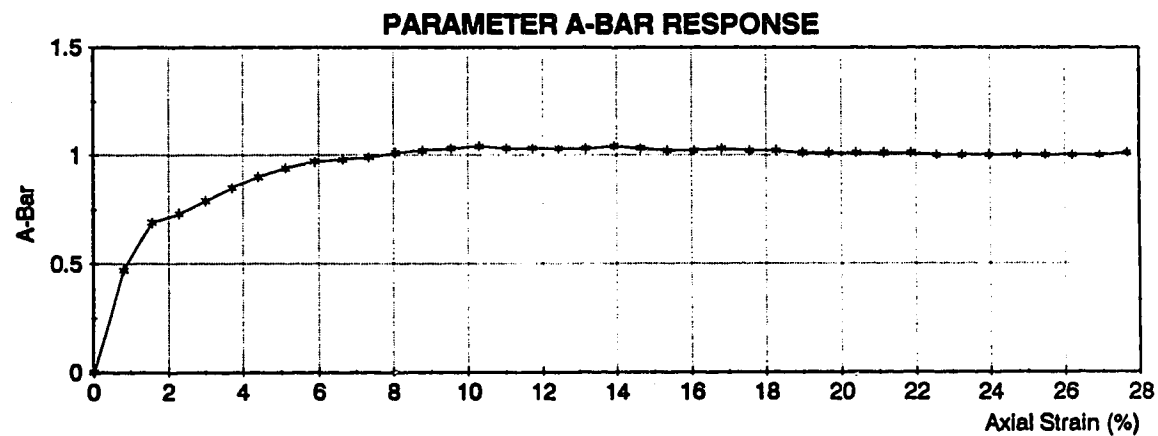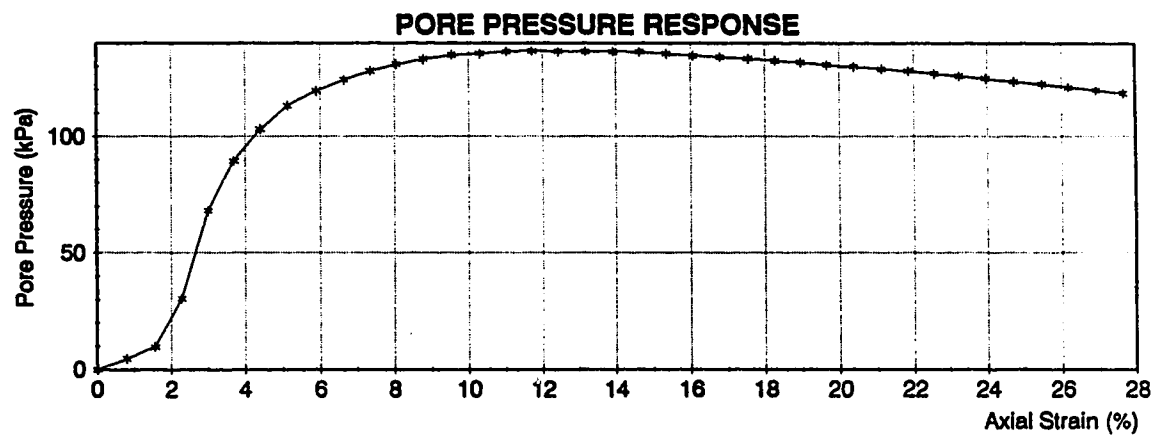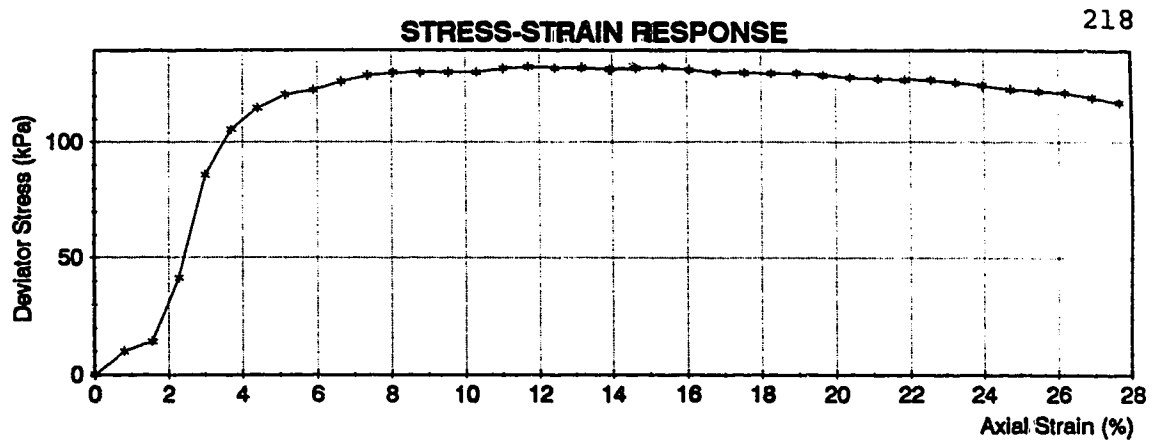
Figure B45 Triaxial Test PWA4 Series 1

STRESS-STRAIN RESPONSE

PORE PRESSURE RESPONSE

PARAMETER A-BAR RESPONSE
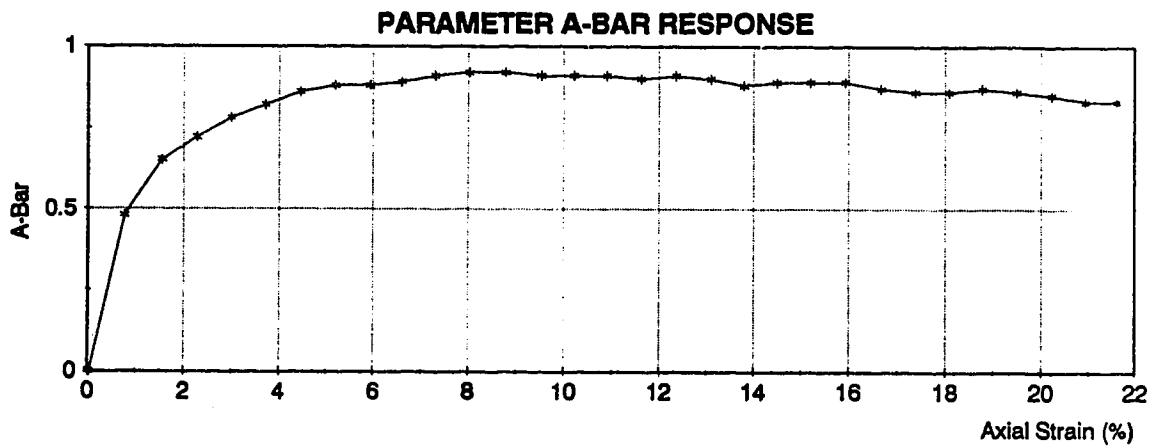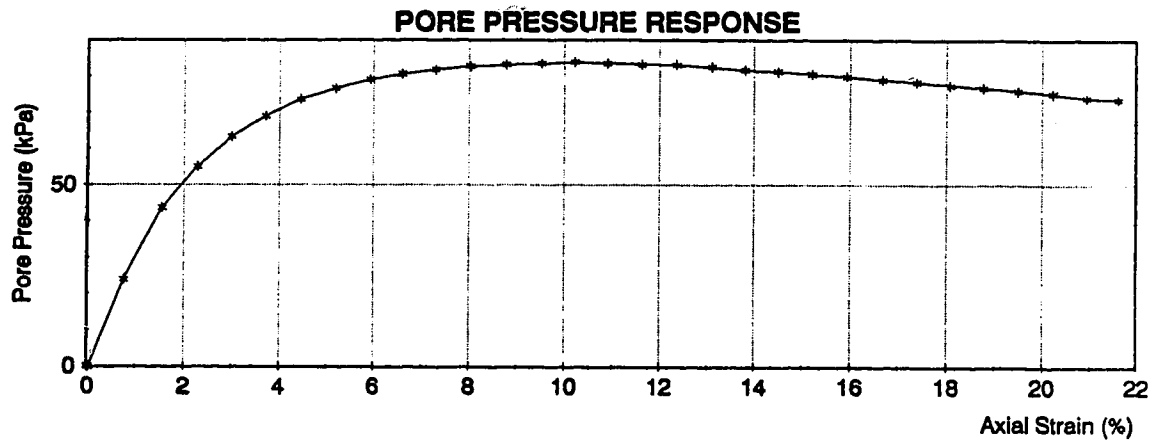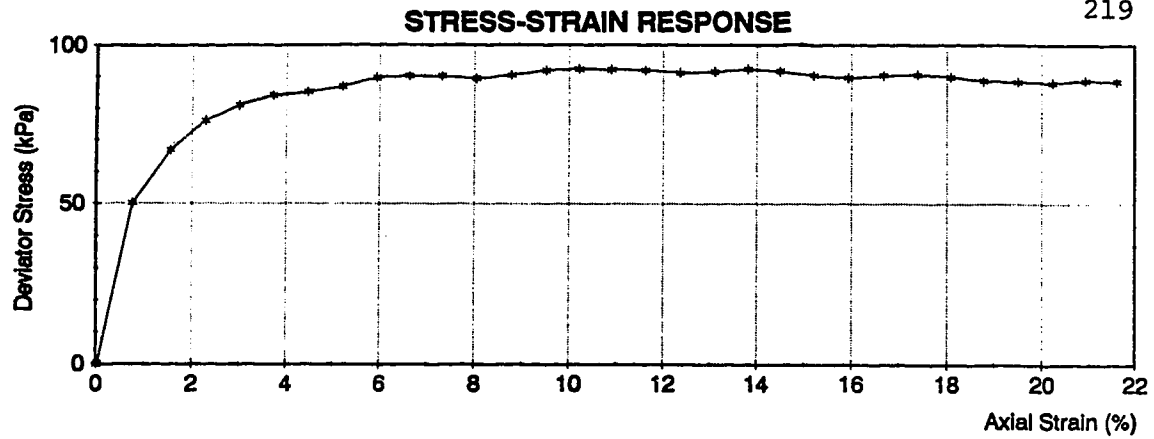
Figure B46   Triaxial Test PWA5   Series 1

STRESS-STRAIN RESPONSE

PORE PRESSURE RESPONSE

PARAMETER A-BAR RESPONSE
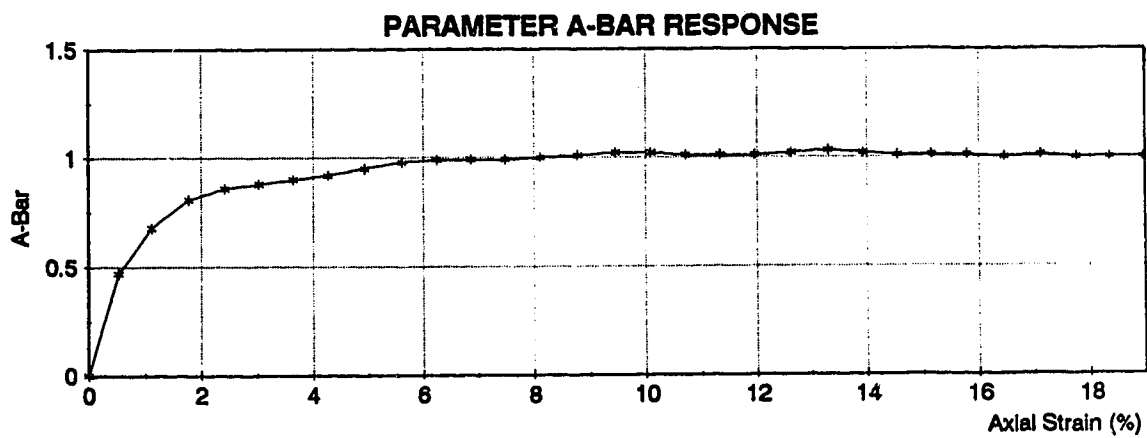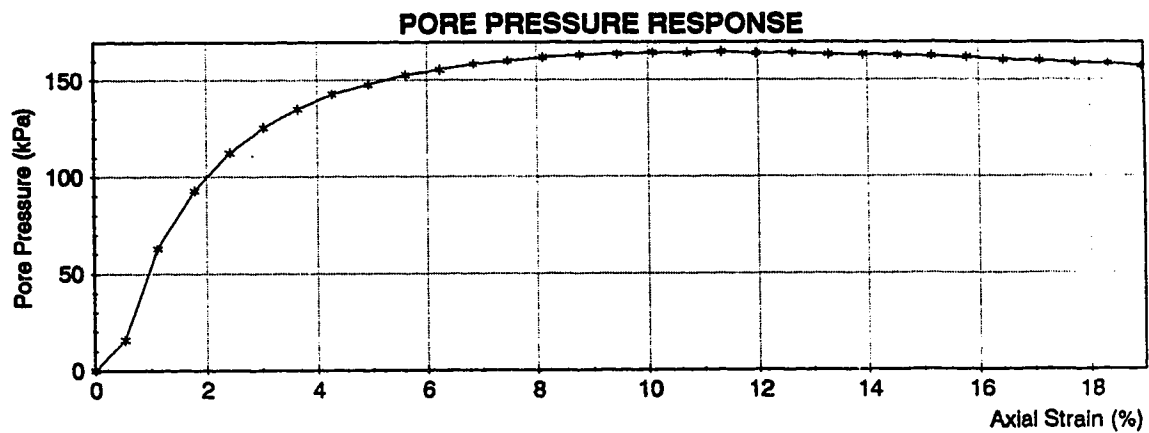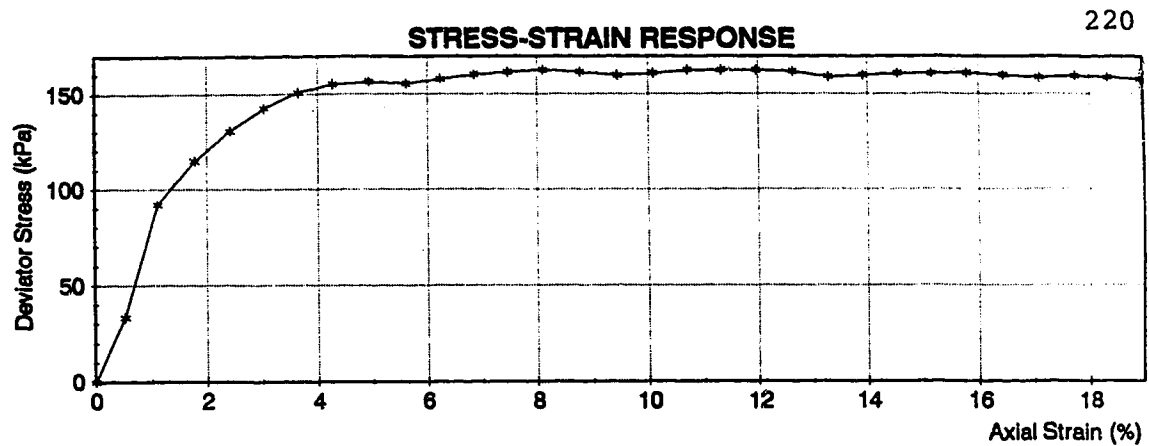
Figure B47   Triaxial Test PWA6   Series 1
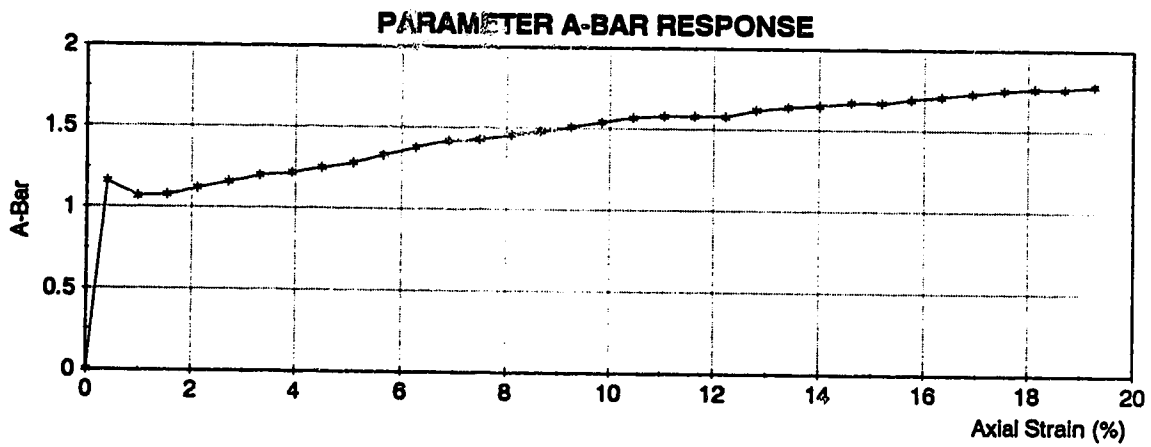
STRESS-STRAIN RESPONSE

PORE PRESSURE RESPONSE

PARAMETER A-BAR RESPONSE
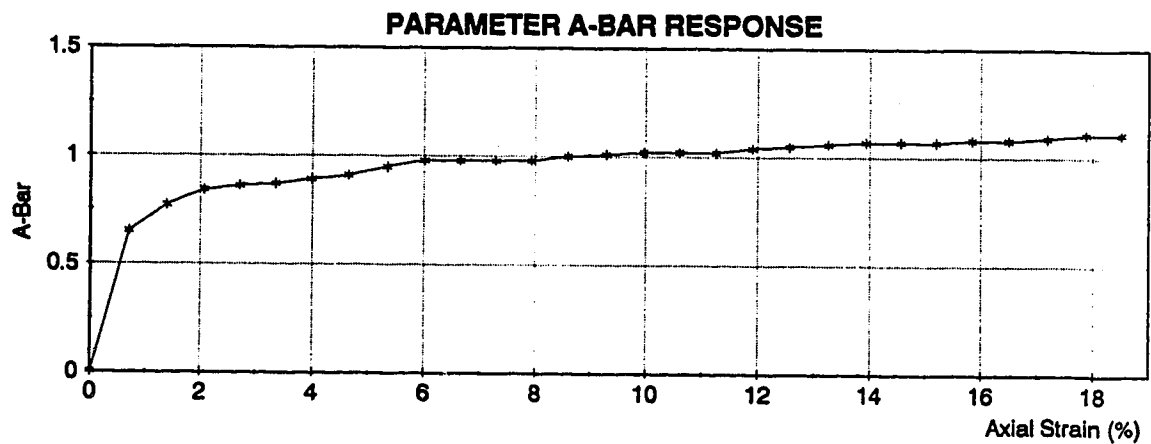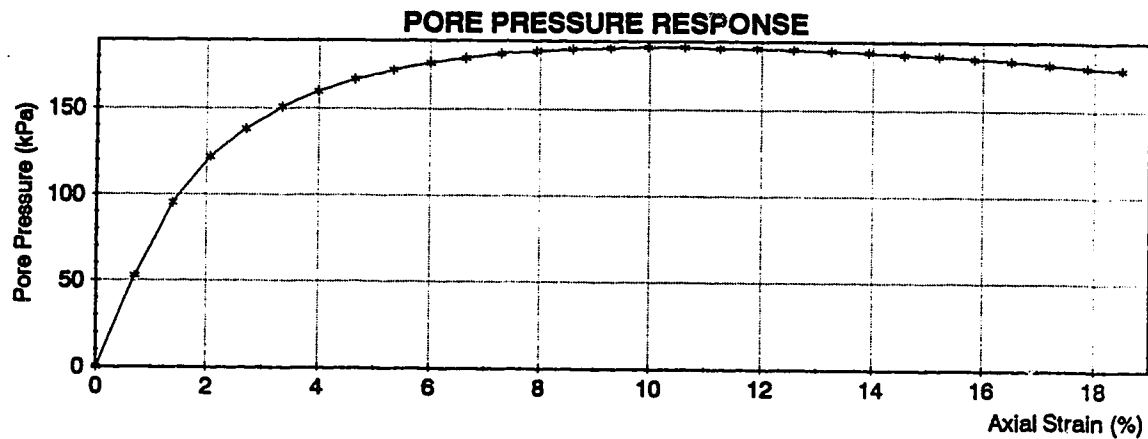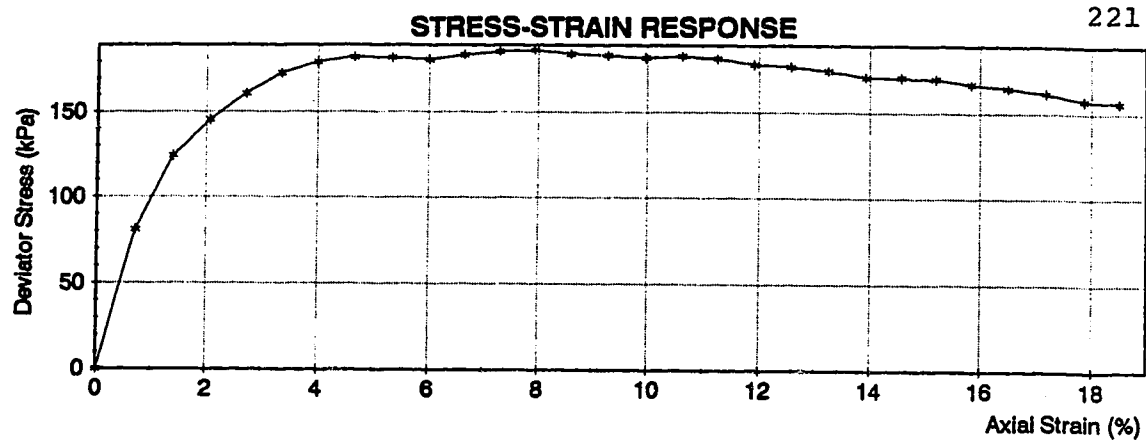
Figure B48   Triaxial Test PWA7   Series 2

STRESS-STRAIN RESPONSE

PORE PRESSURE RESPONSE

PARAMETER A-BAR RESPONSE
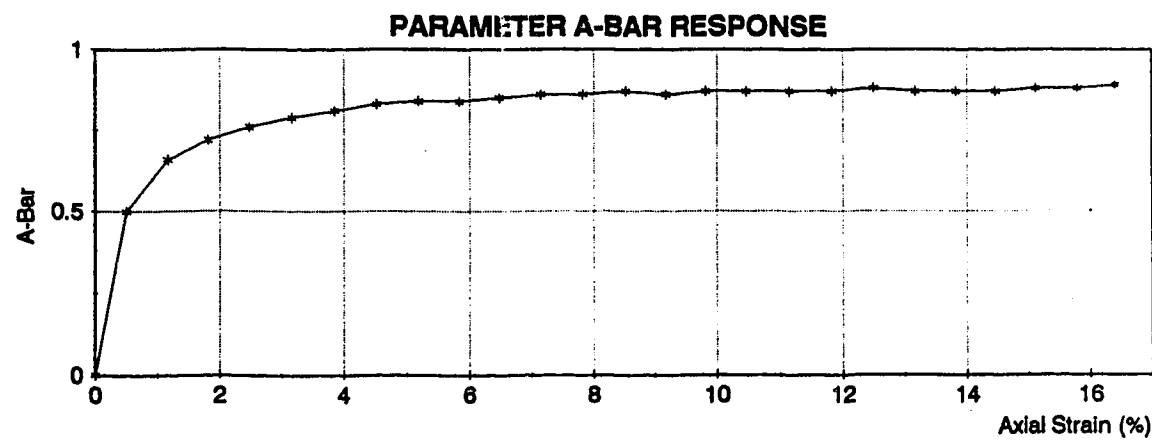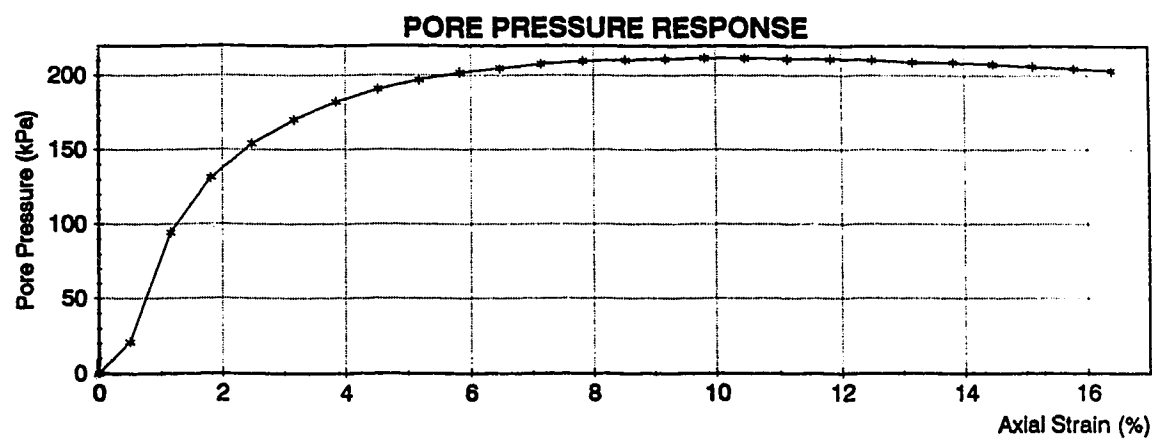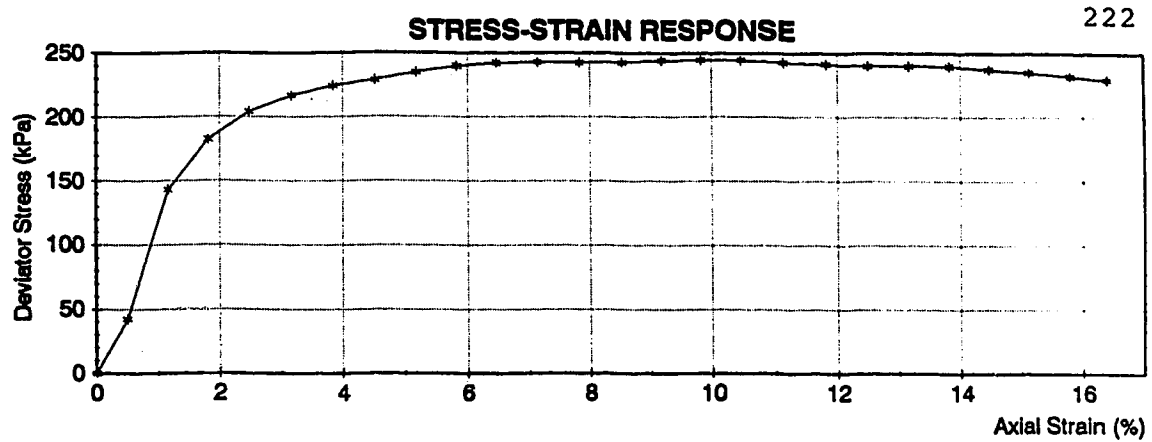
Figure B49   Triaxial Test PWA8   Series 2

STRESS-STRAIN RESPONSE

PORE PRESSURE RESPONSE

PARAMETER A-BAR RESPONSE
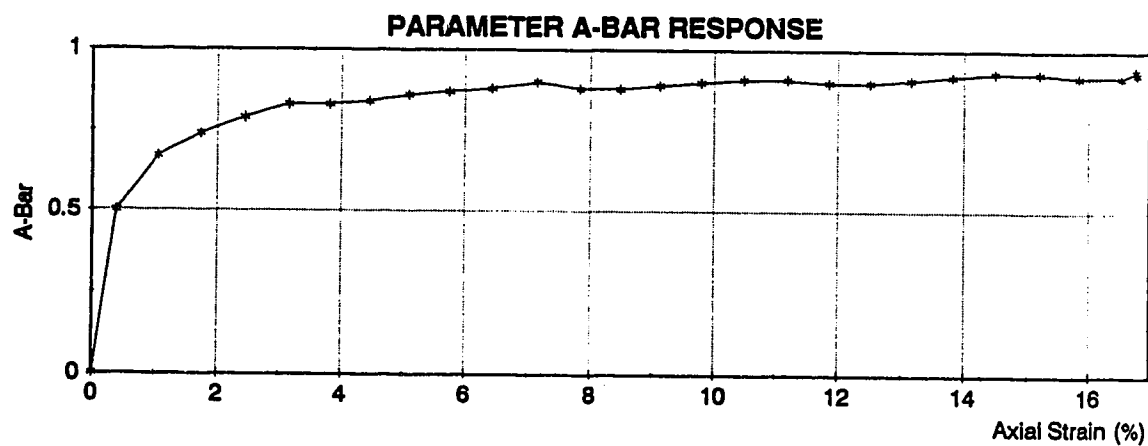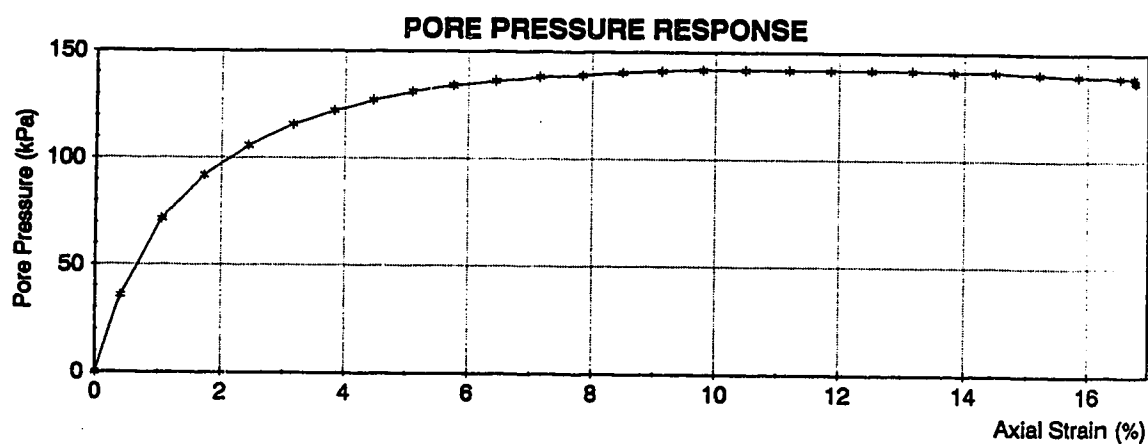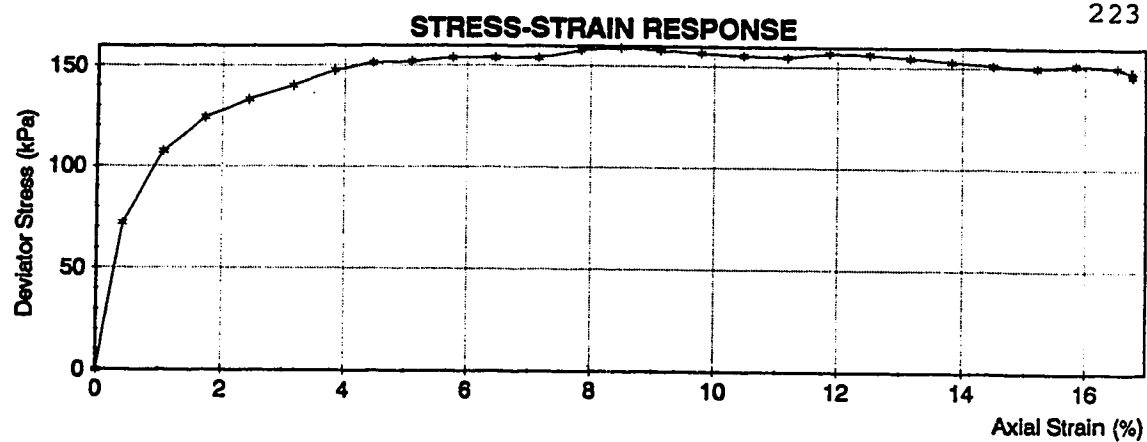
Figure B50   Triaxial Test PWA9   Series 2

STRESS-STRAIN RESPONSE

PORE PRESSURE RESPONSE

PARAMETER A-BAR RESPONSE
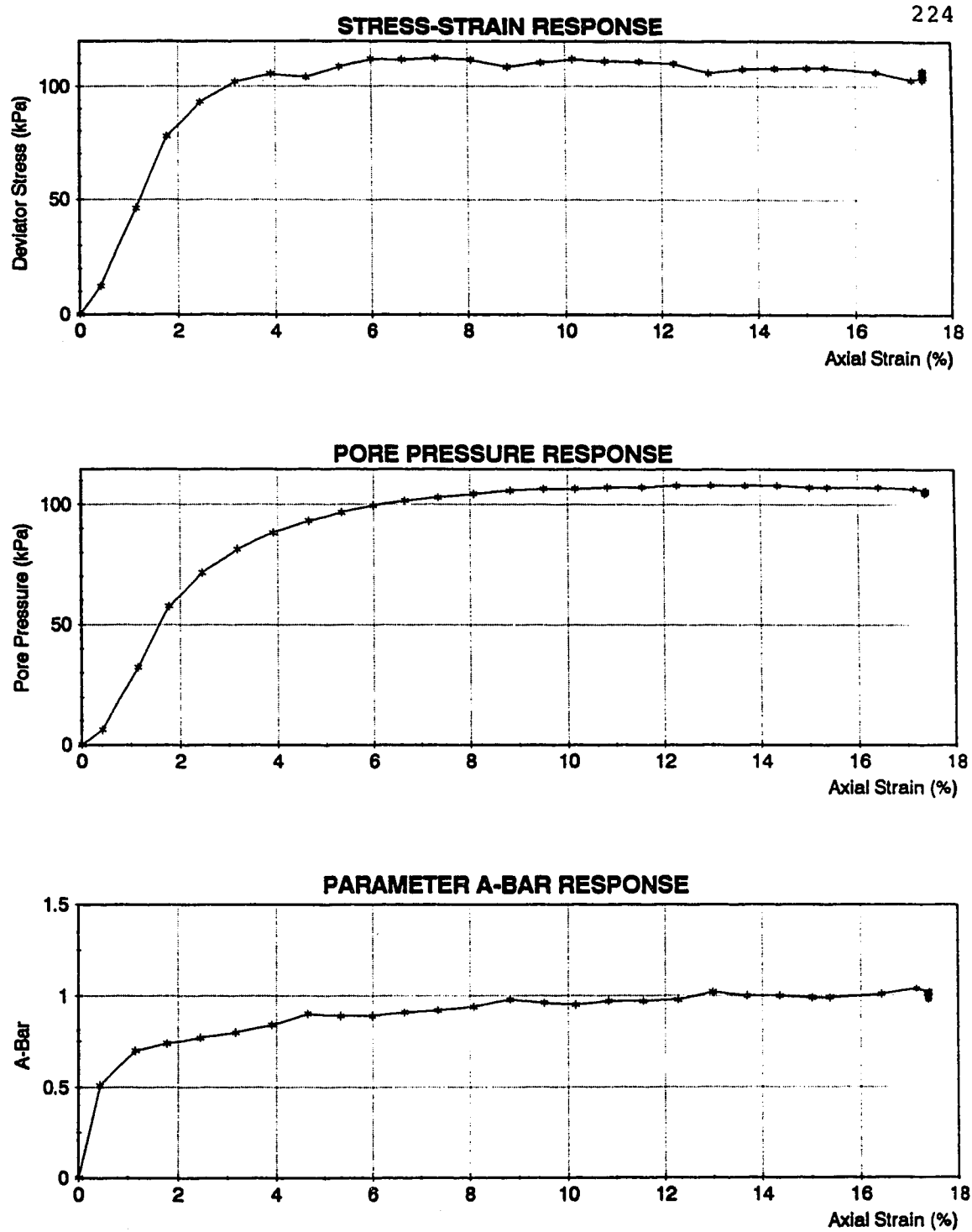
Figure B51   Triaxial Test PWA10 Series 2

STRESS-STRAIN RESPONSE

PORE PRESSURE RESPONSE

PARAMETER A-BAR RESPONSE
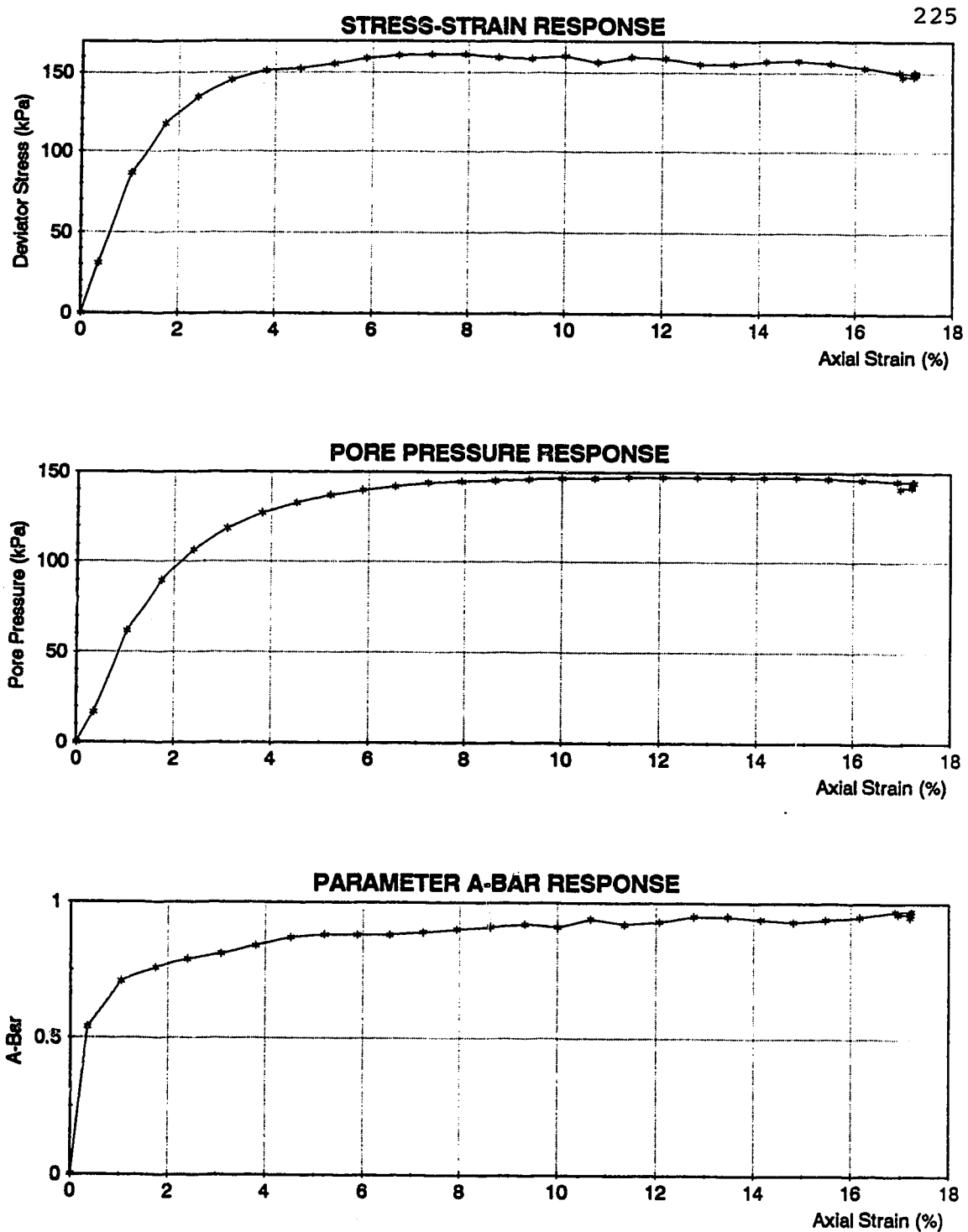
Figure B52   Triaxial Test PWA11   Series 2
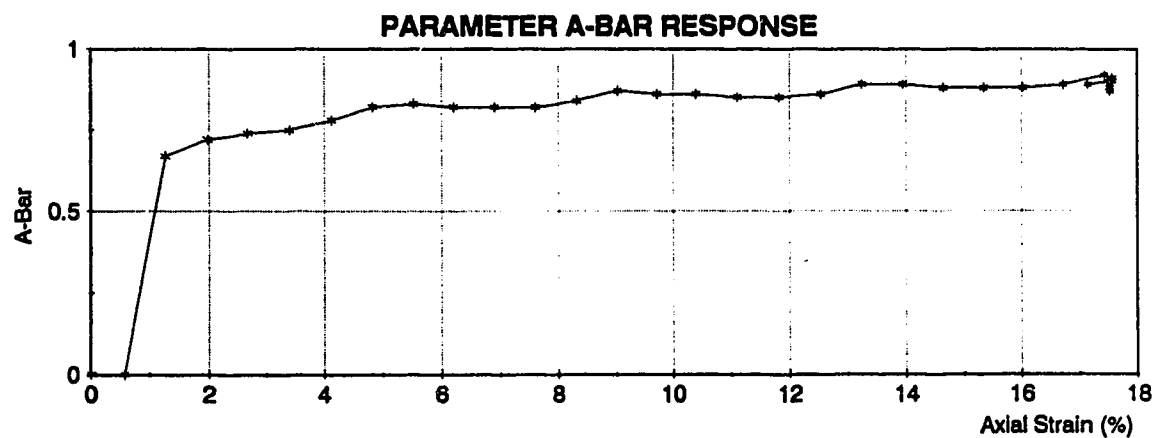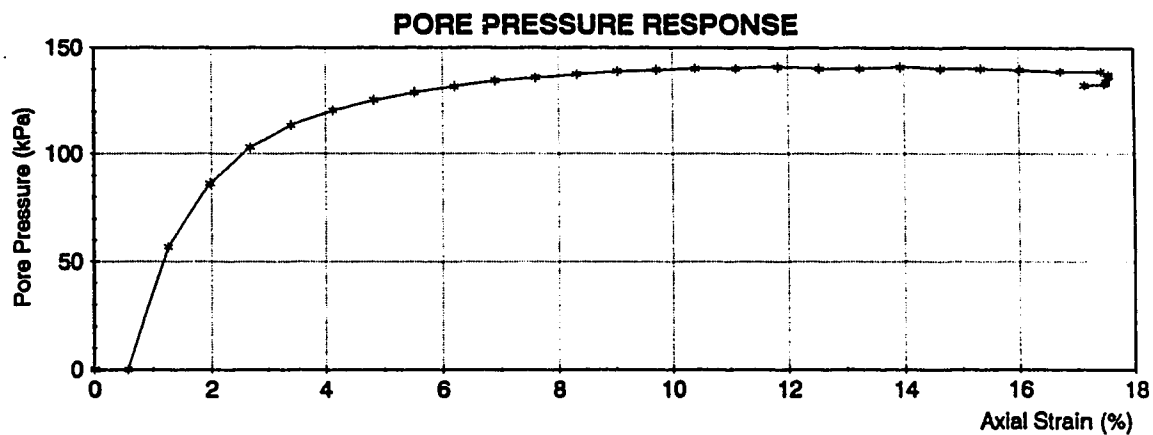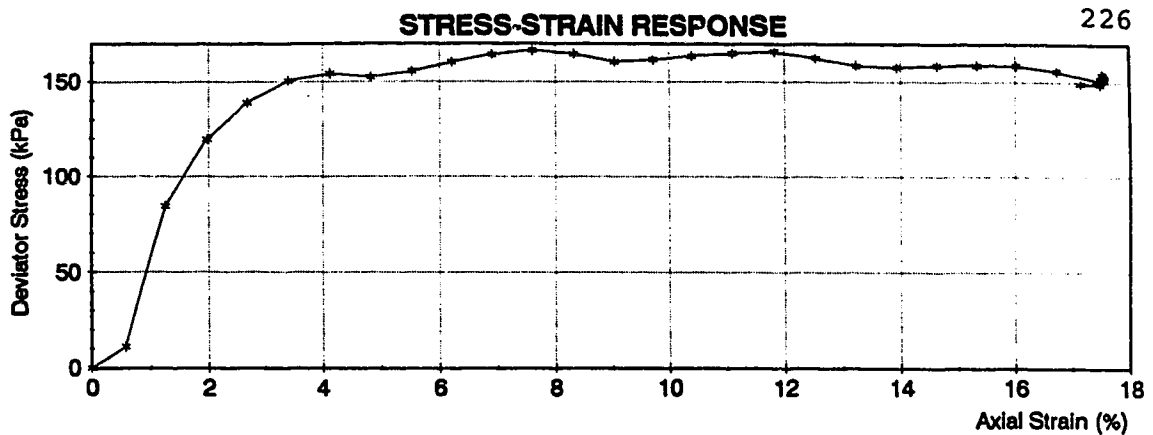
Figure B53   Triaxial Test PWA12 Series 2

STRESS-STRAIN RESPONSE

PORE PRESSURE RESPONSE

PARAMETER A-BAR RESPONSE
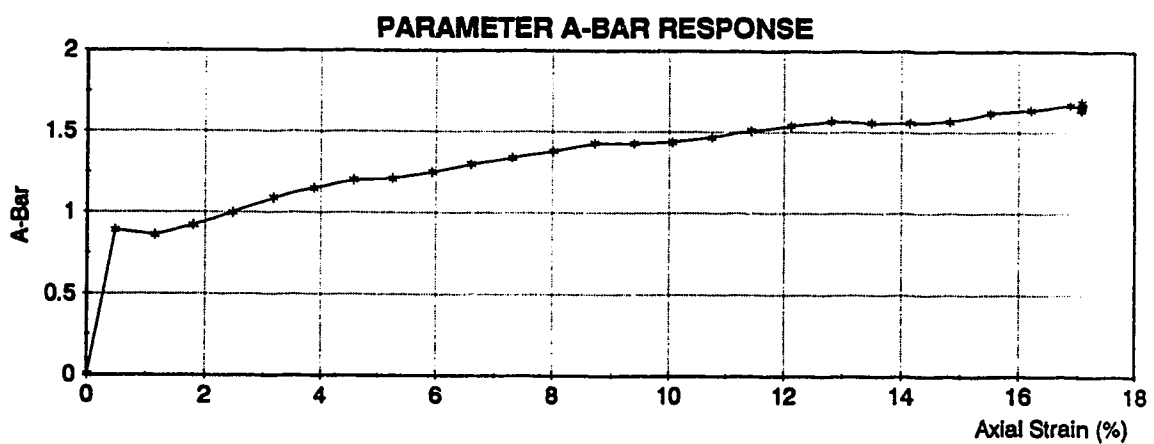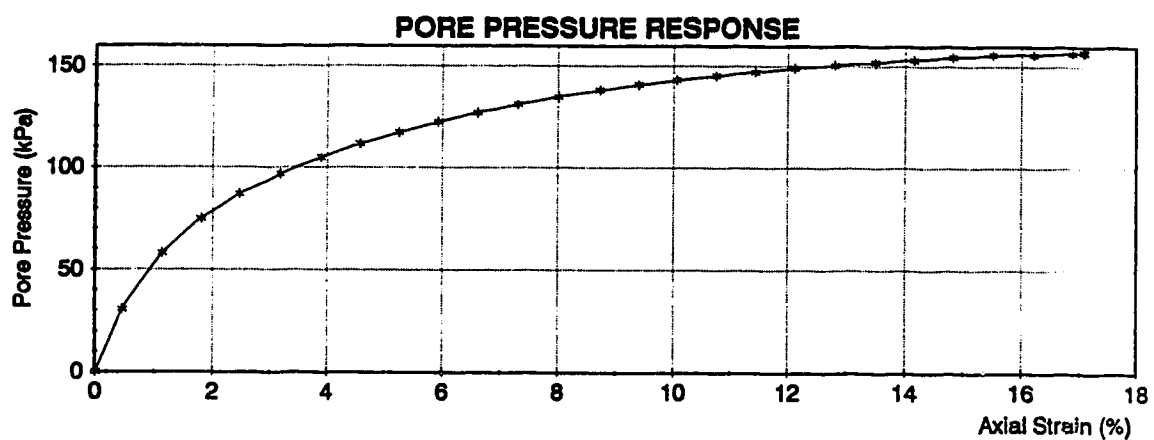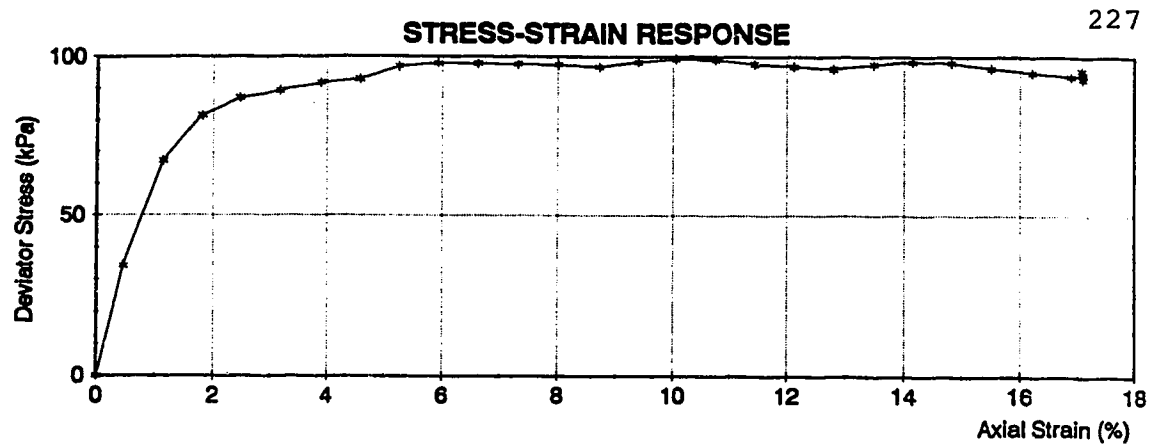
Figure B54 Triaxial Test PWA13 Series 3

STRESS-STRAIN RESPONSE

PORE PRESSURE RESPONSE

PARAMETER A-BAR RESPONSE
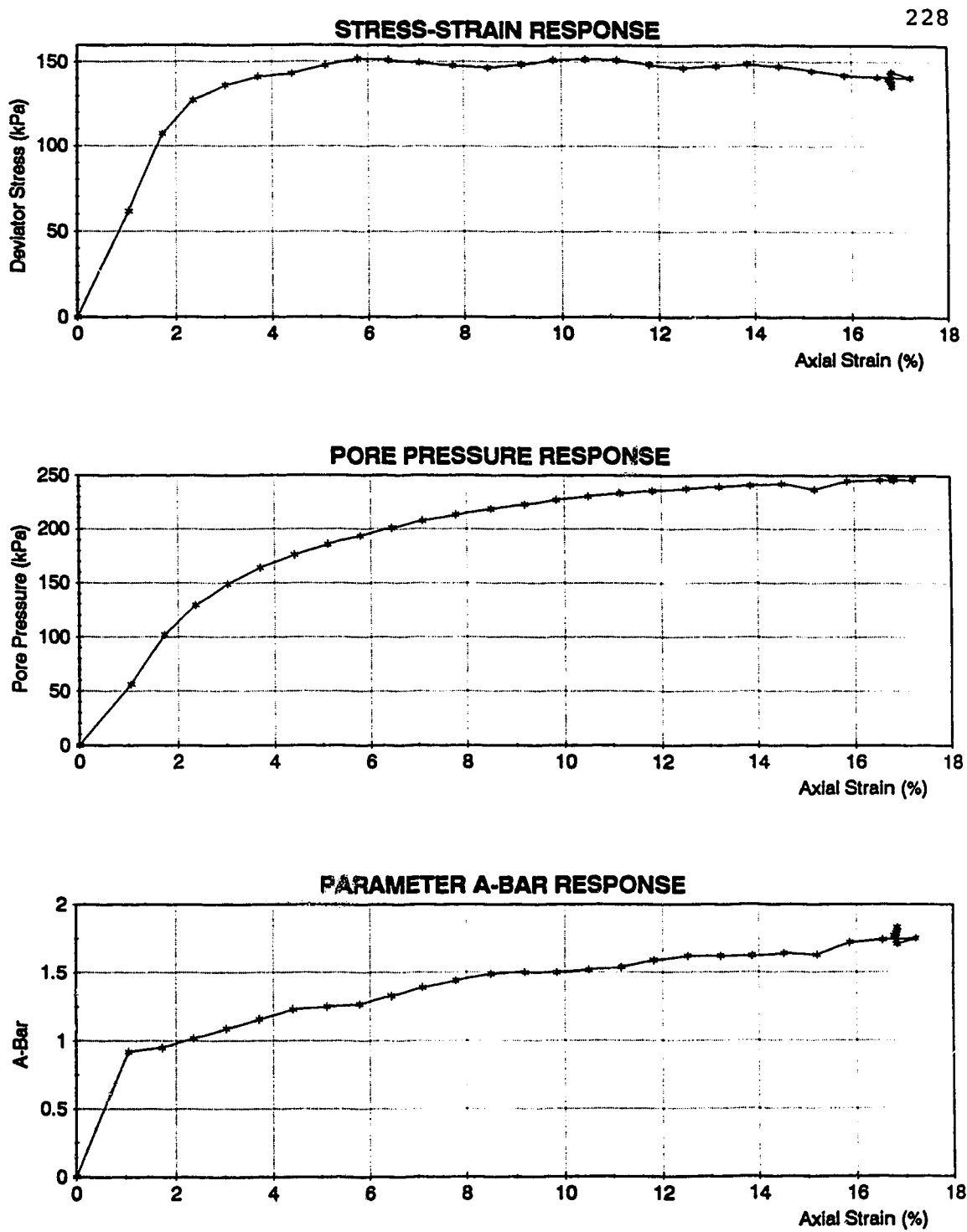
Figure B55   Triaxial Test PWA14   Series 3

STRESS-STRAIN RESPONSE
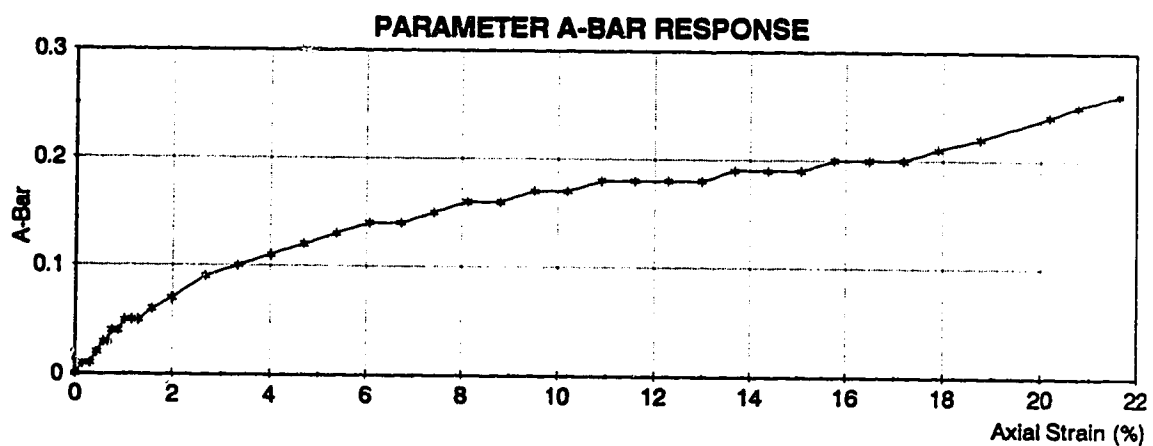

PORE PRESSURE RESPONSE

PARAMETER A-BAR RESPONSE
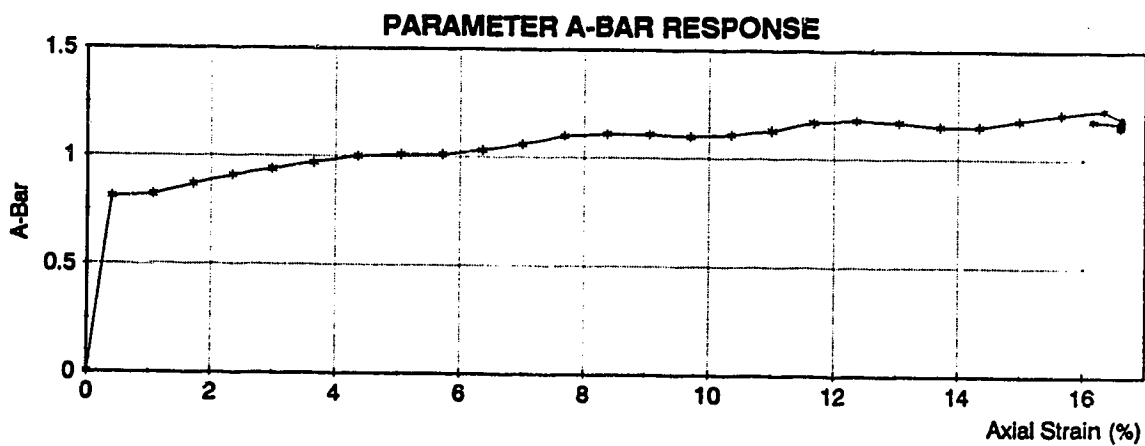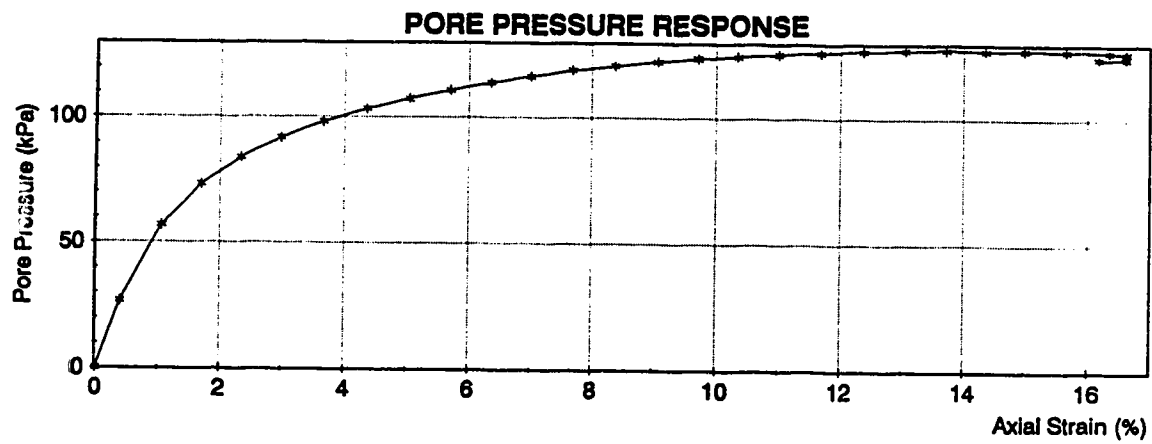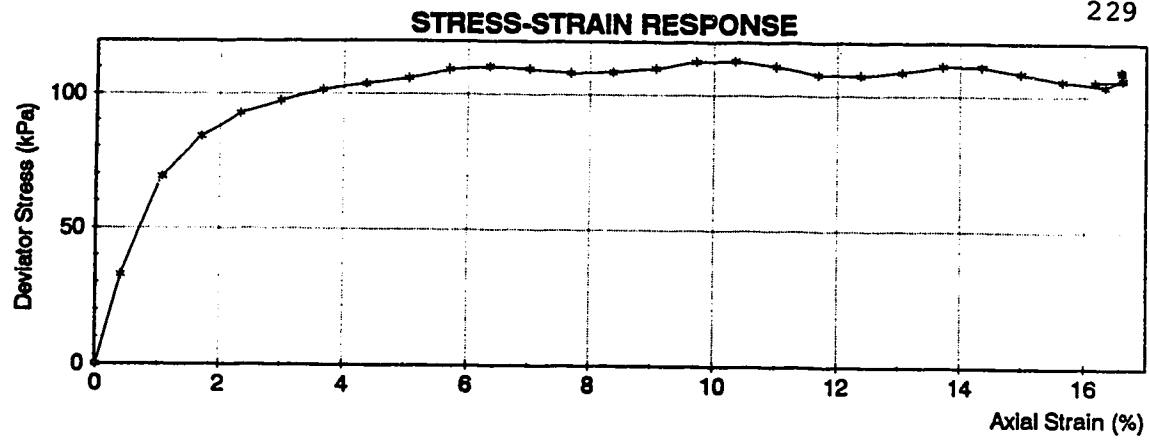
Figure B56   Triaxial Test PWA15 Series 3

STRESS-STRAIN RESPONSE

PORE PRESSURE RESPONSE

PARAMETER A-BAR RESPONSE
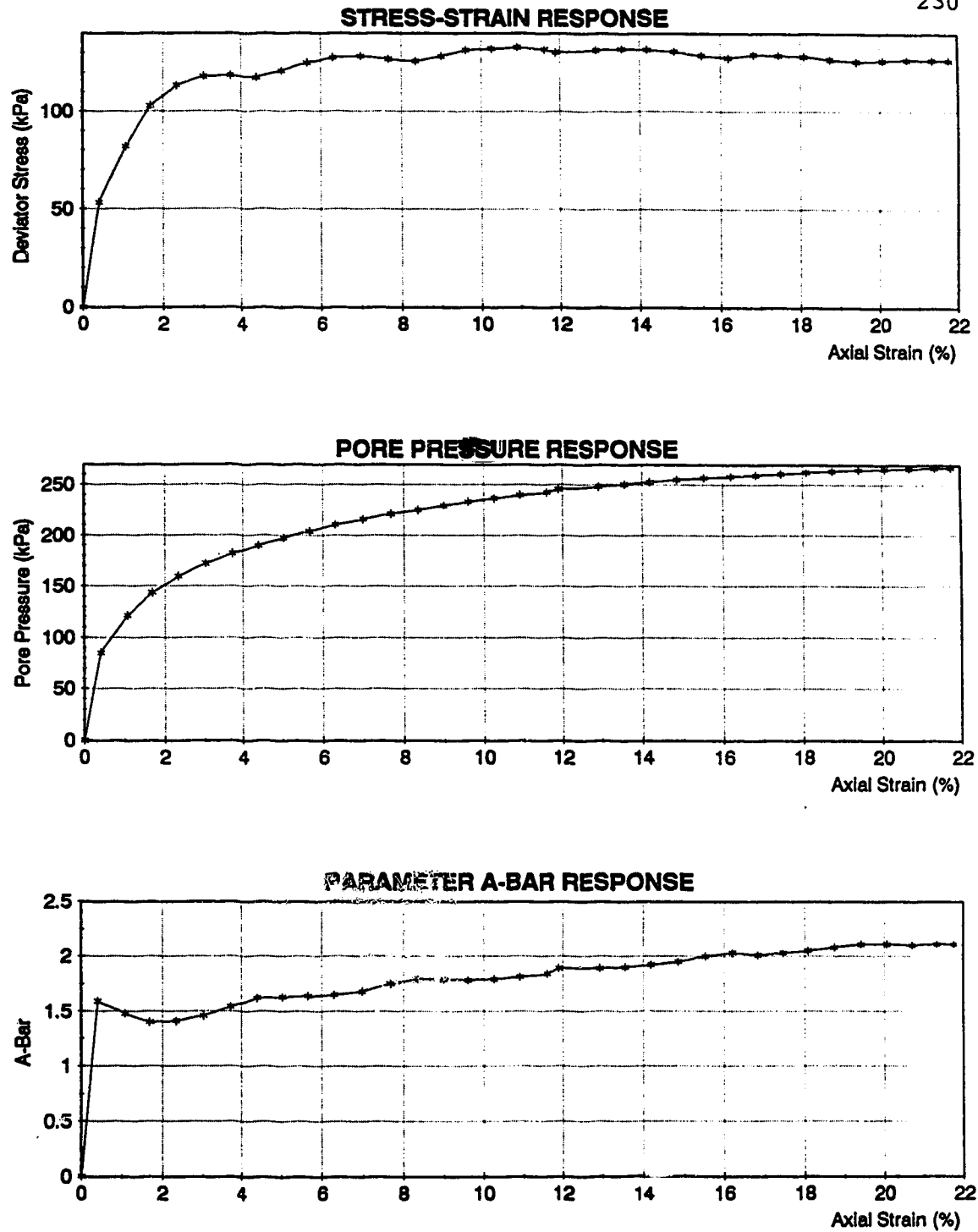
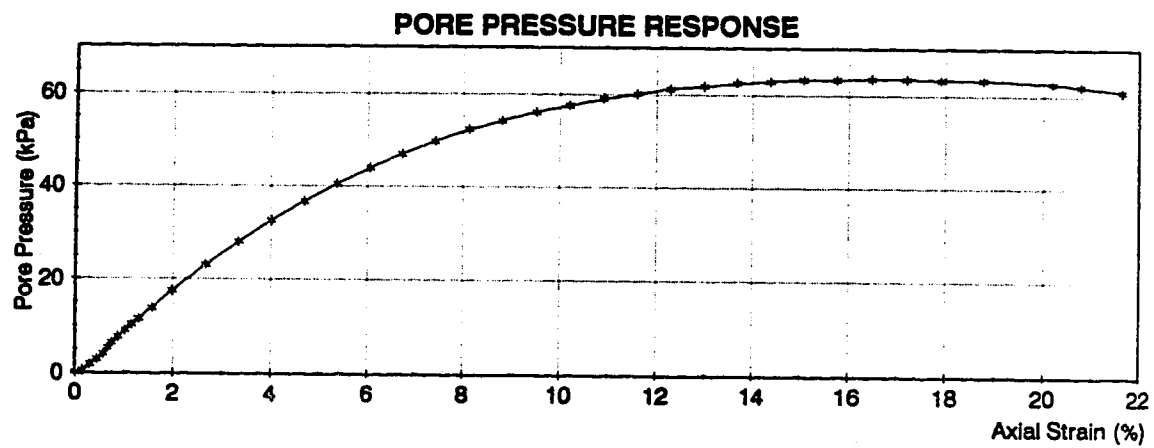# Figure B57   Triaxial Test PWA16 Series 3

231

STRESS-STRAIN RESPONSE

PORE PRESSURE RESPONSE

PARAMETER A-BAR RESPONSE
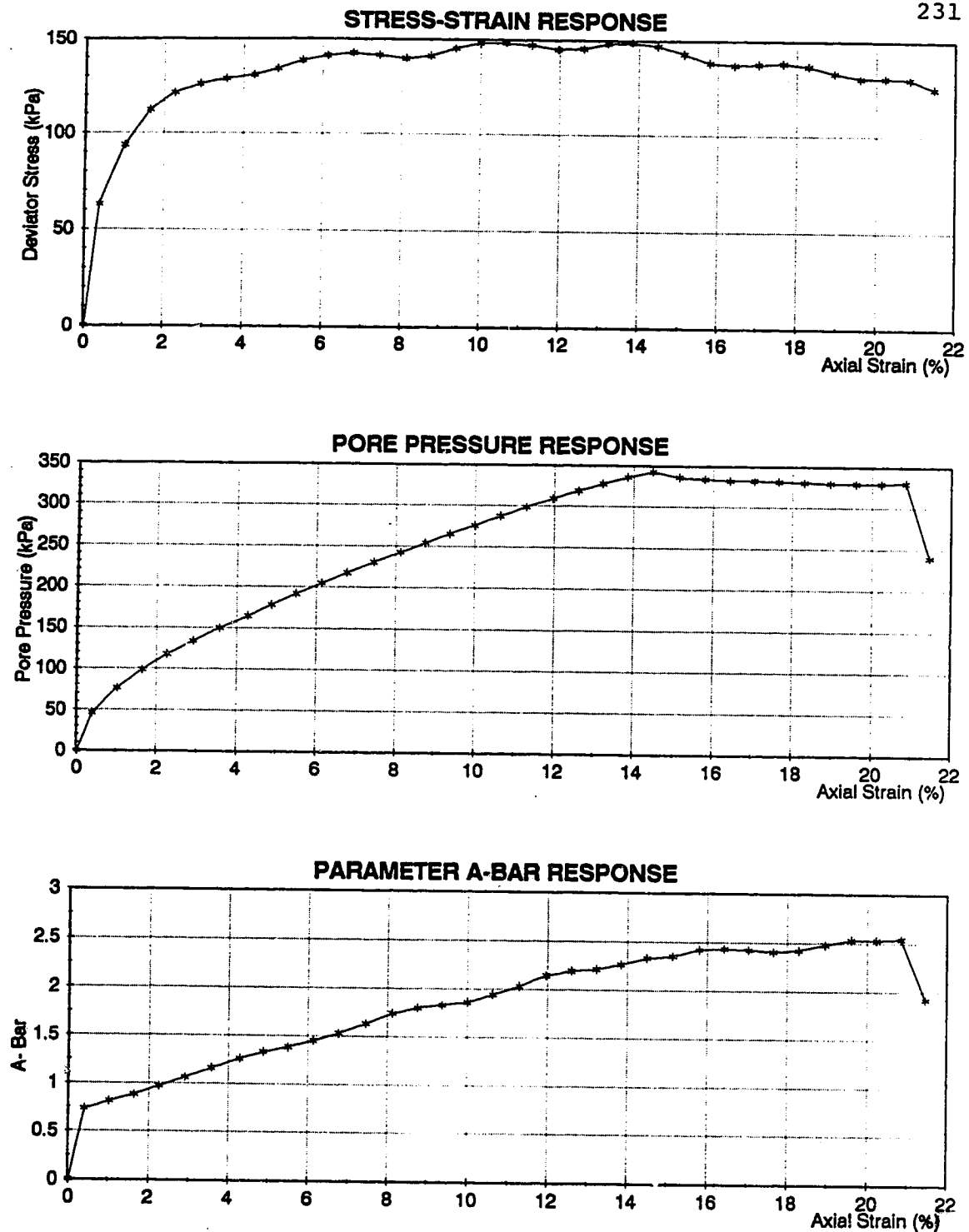
Figure B58   Triaxial Test PWA1A Series 4

STRESS-STRAIN RESPONSE

PORE PRESSURE RESPONSE

PARAMETER A-BAR RESPONSE
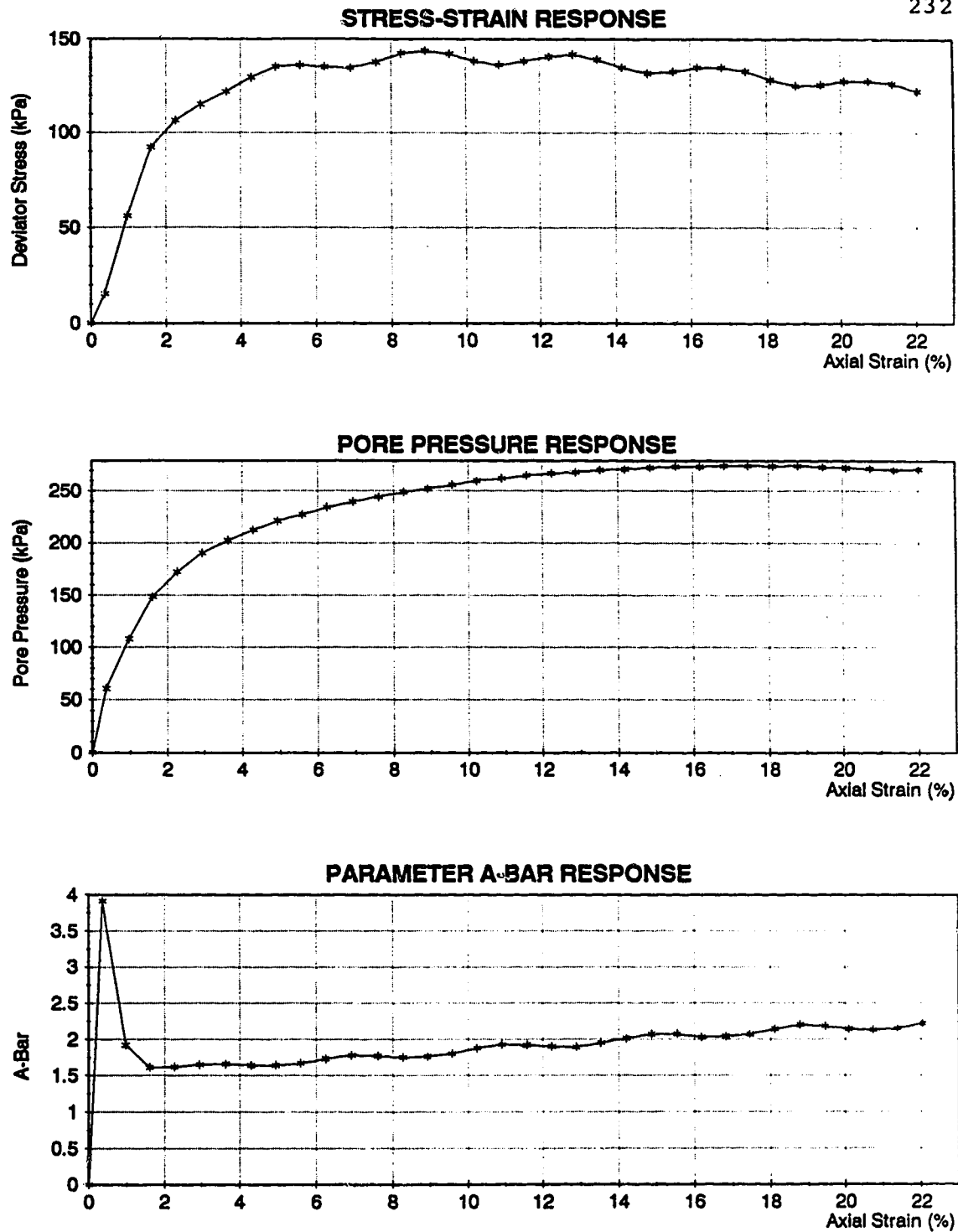
Figure B59   Triaxial Test PWA2A Series 4

STRESS-STRAIN RESPONSE

PORE PRESSURE RESPONSE

PARAMETER A-BAR RESPONSE
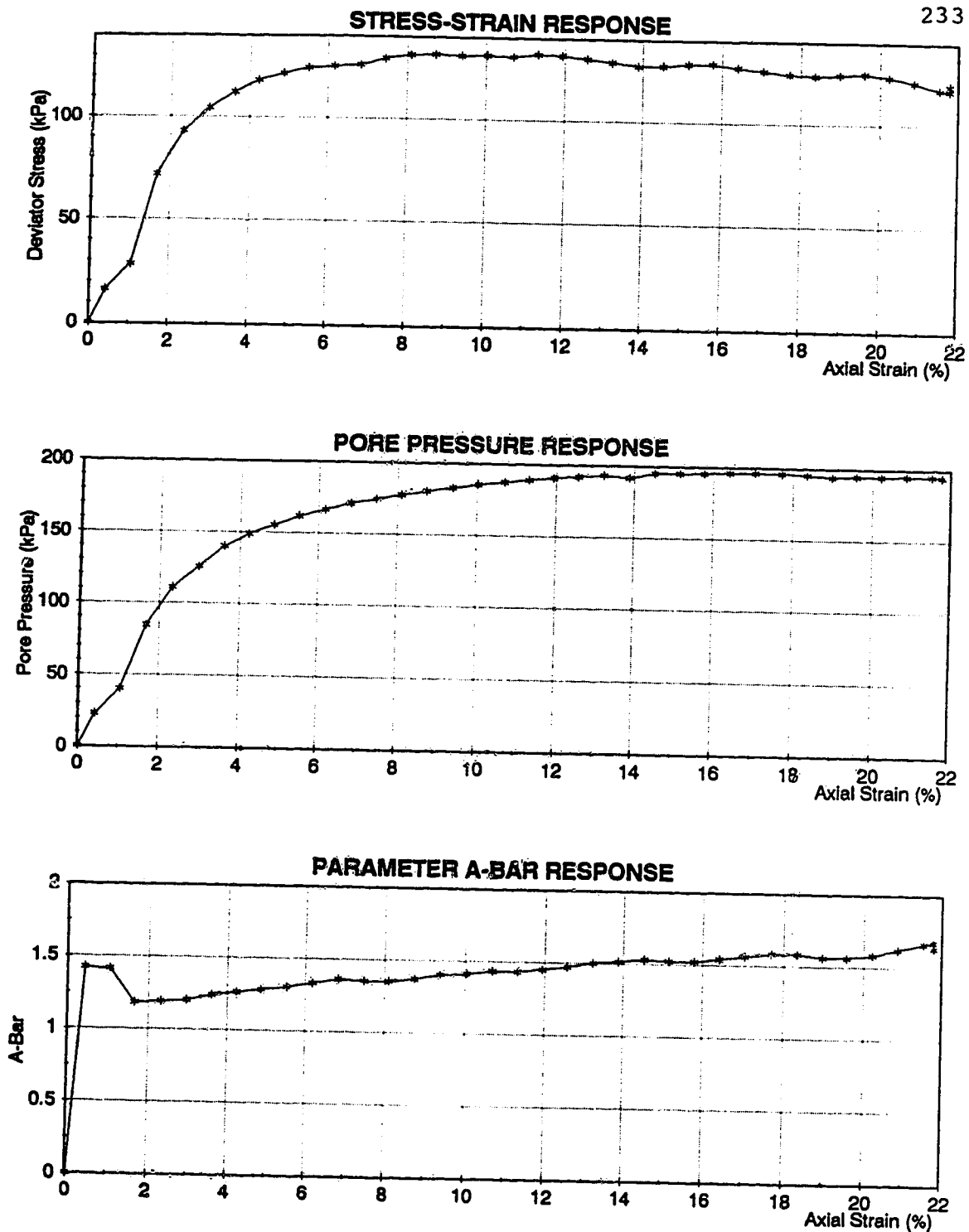
Figure B60   Triaxial Test PWA3A Series 4

STRESS-STRAIN RESPONSE

PORE PRESSURE RESPONSE

PARAMETER A-BAR RESPONSE
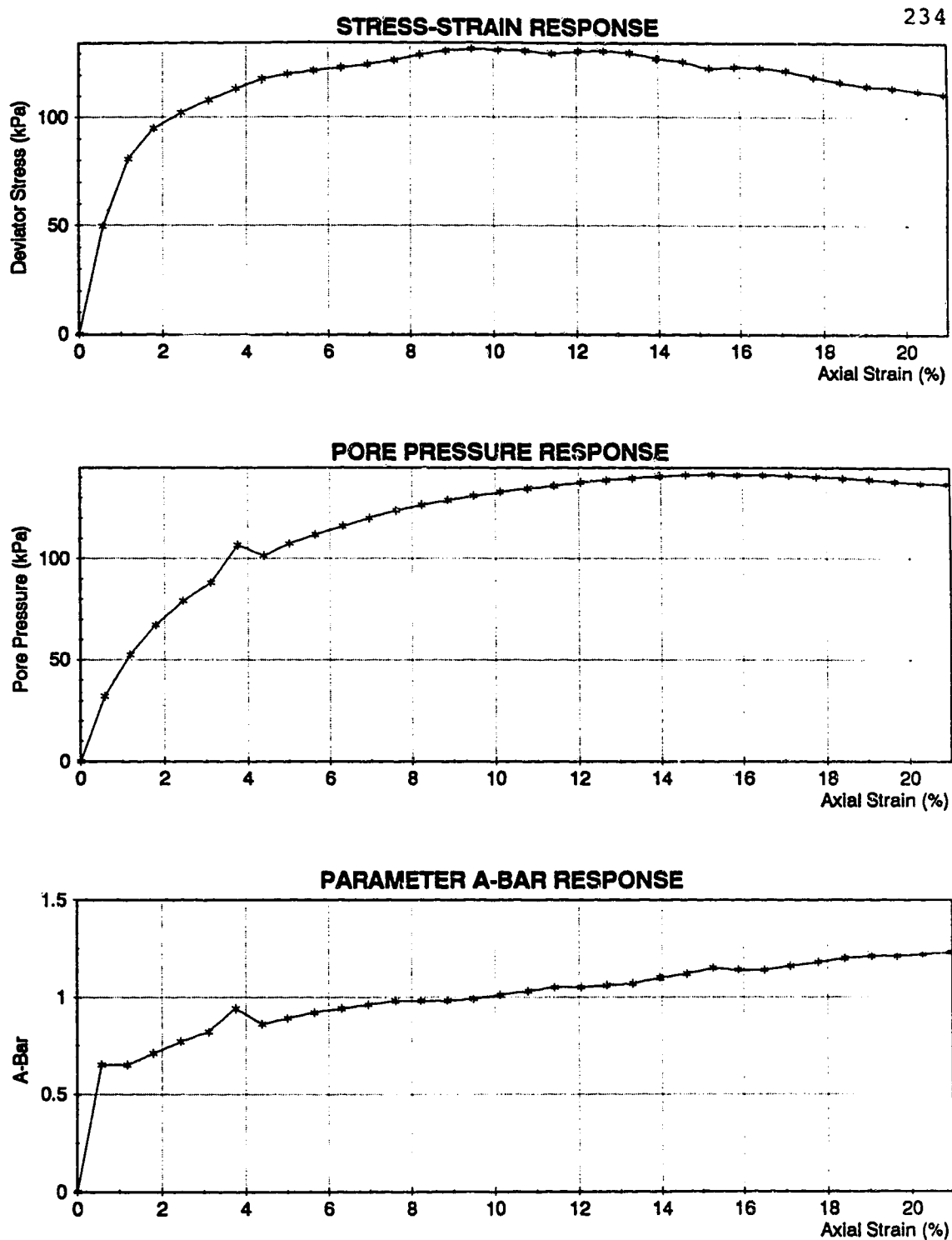
Figure B61   Triaxial Test PWA4A Series 4
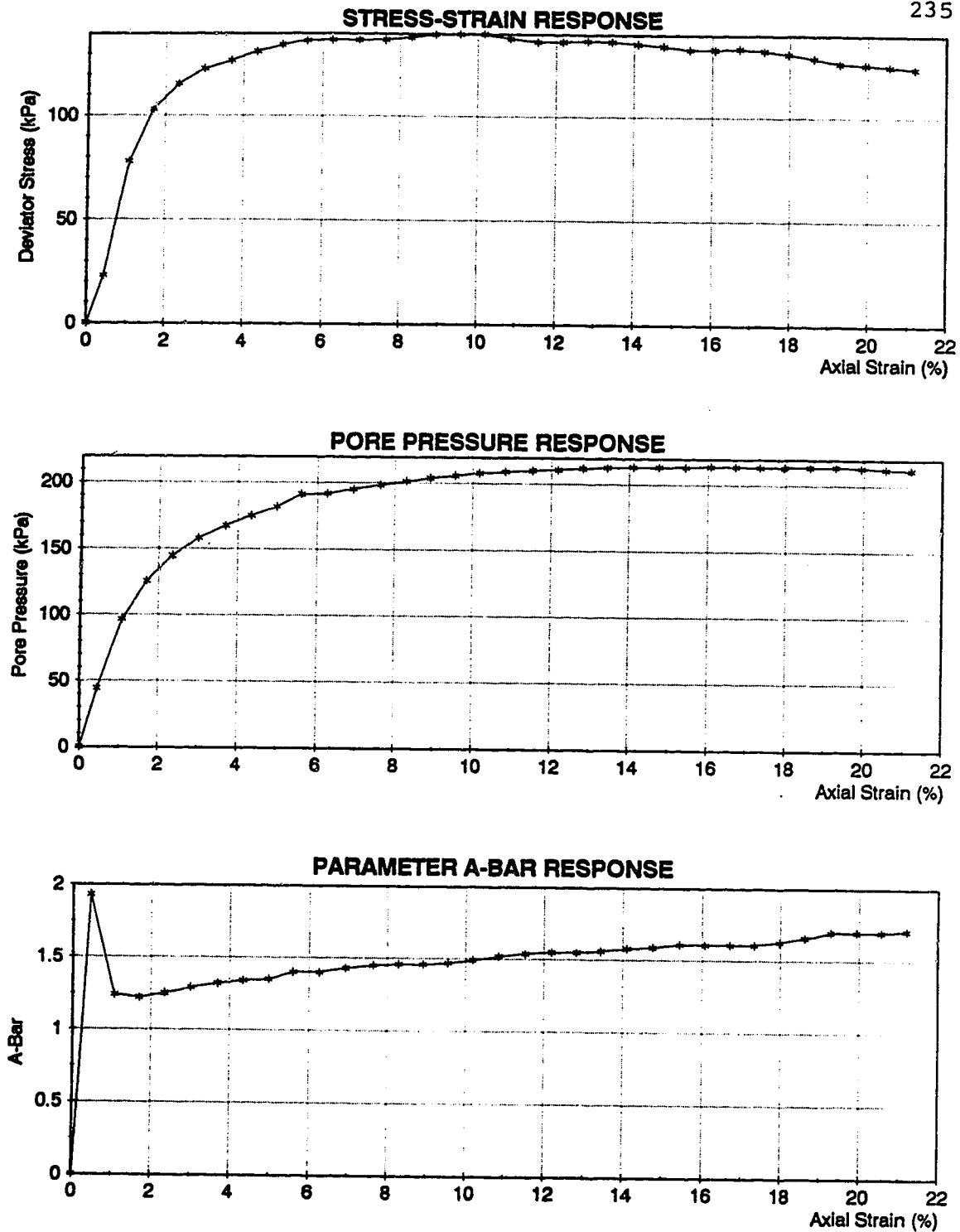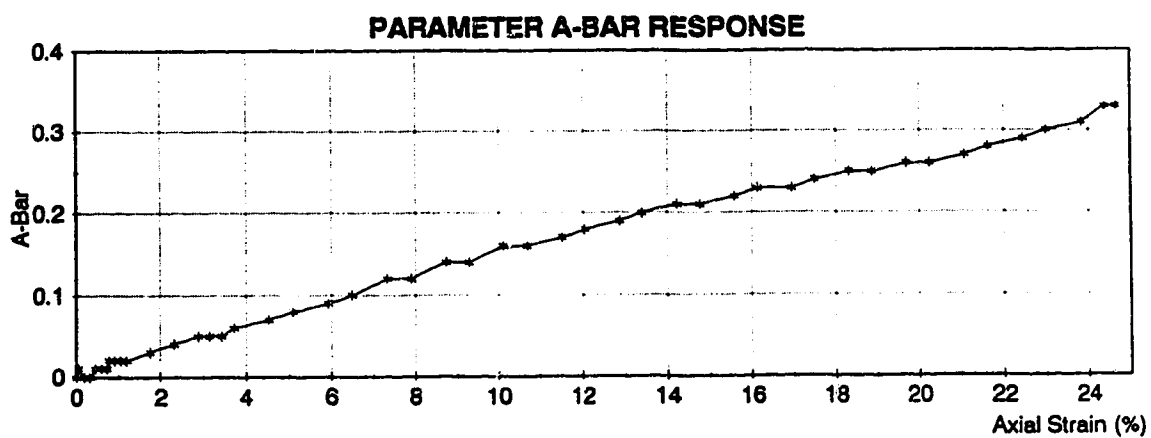
Figure B62   Triaxial Test PWA5A Series 4

STRESS-STRAIN RESPONSE

PORE PRESSURE RESPONSE

PARAMETER A-BAR RESPONSE
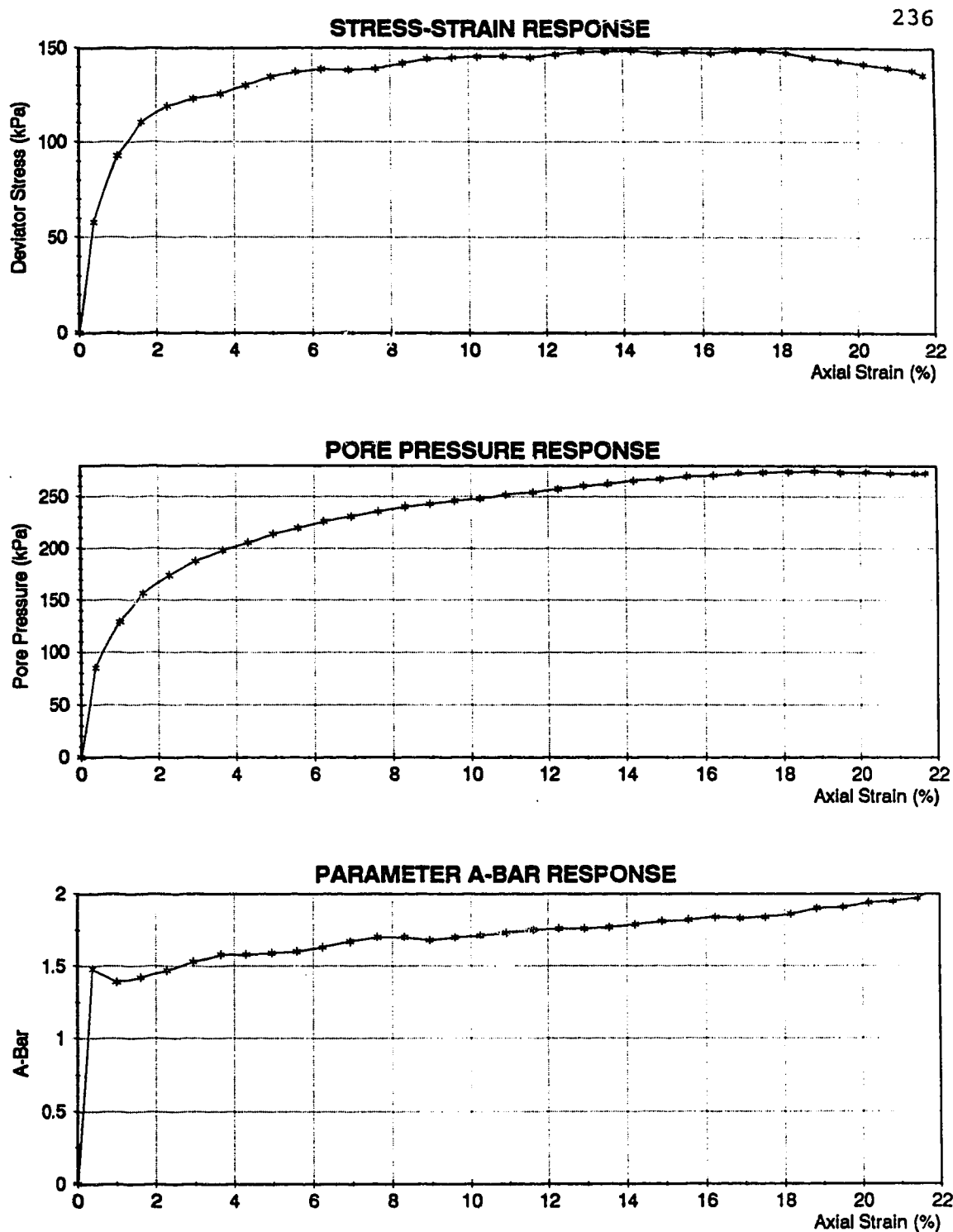
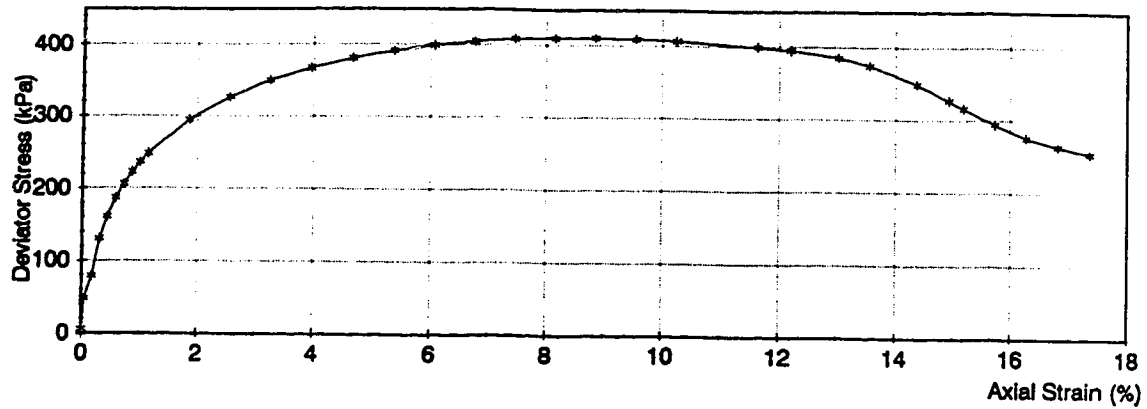# Figure B63   Triaxial Test PWA6A Series 4
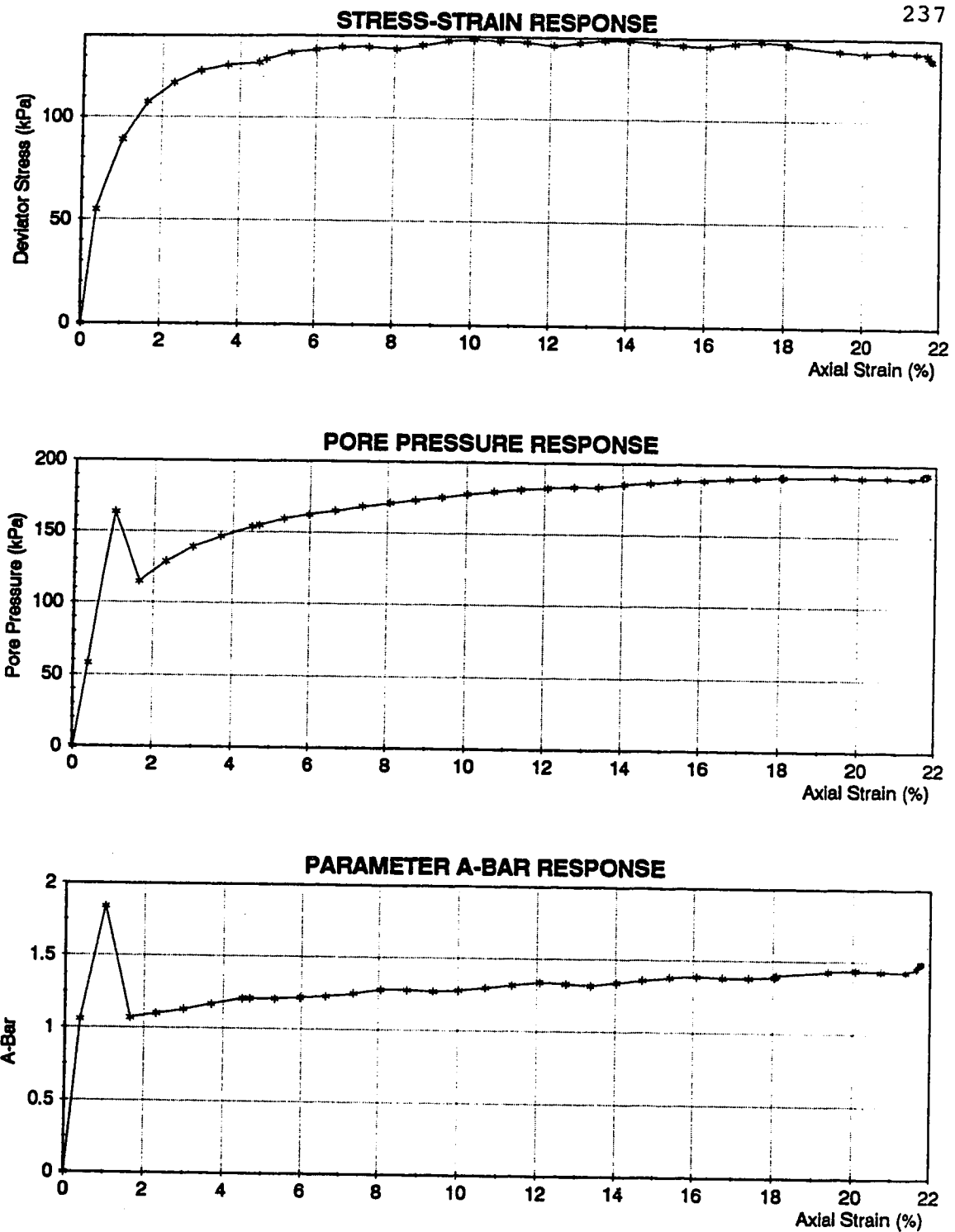
Figure B64 Triaxial Test PWA7A Series 4

STRESS-STRAIN RESPONSE

**PORE PRESSURE RESPONSE**

PARAMETER A-BAR RESPONSE
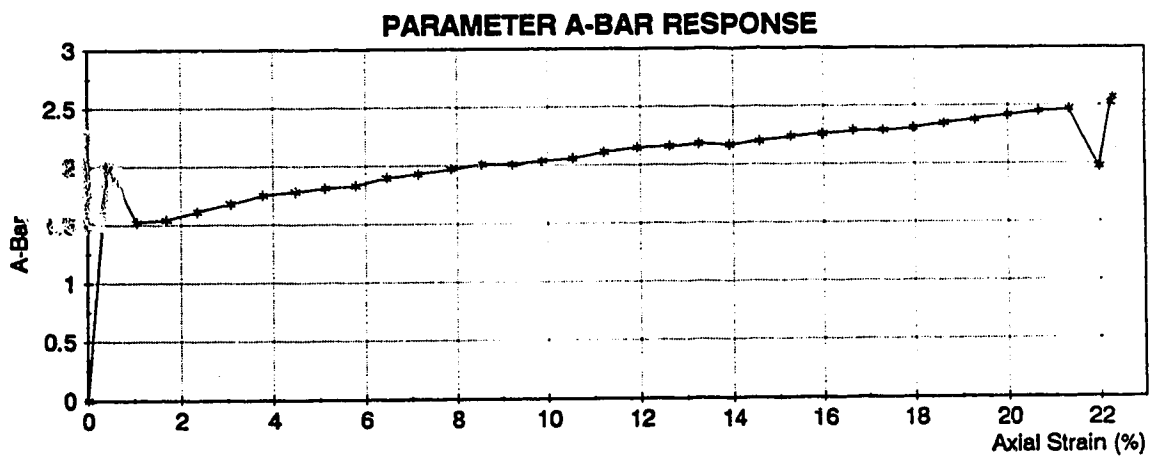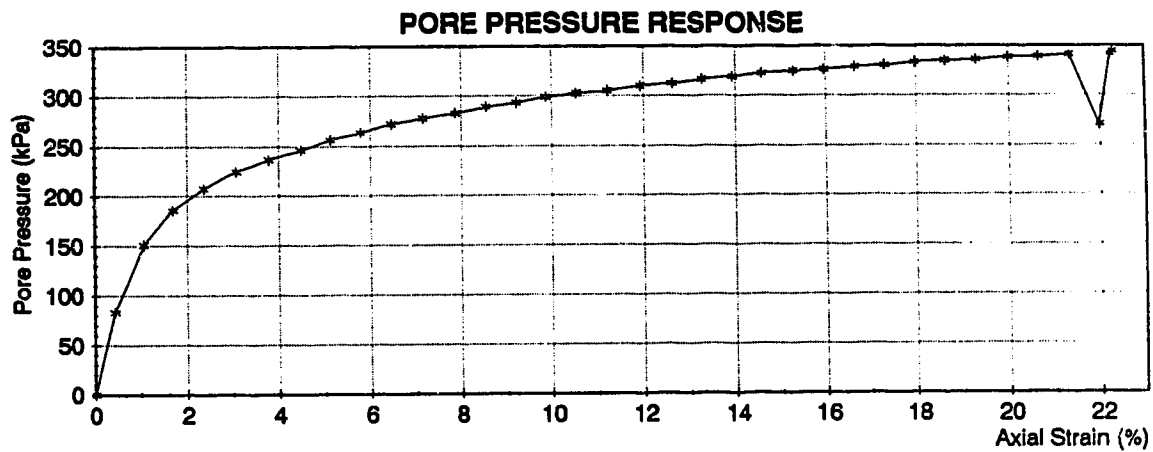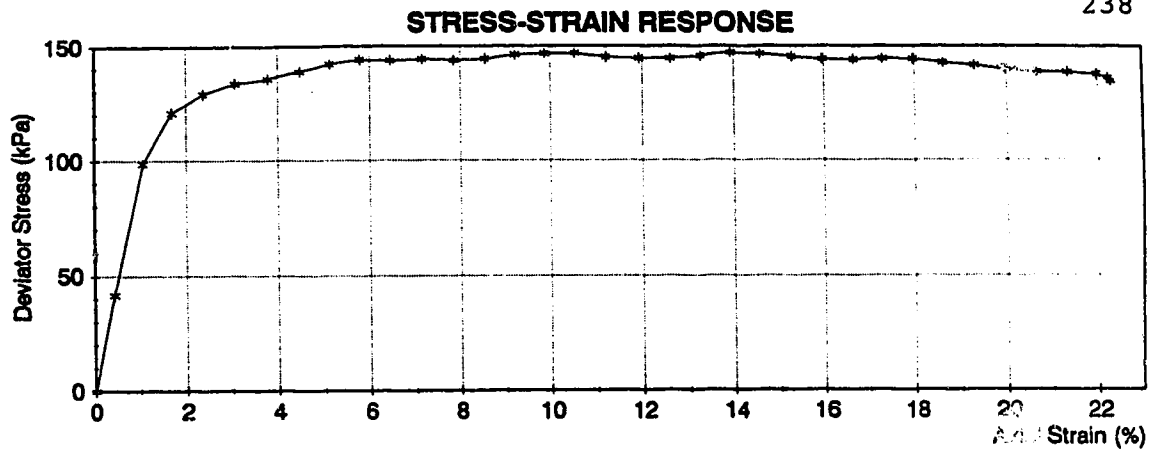
Figure B65   Triaxial Test PWA8A Series 4

STRESS-STRAIN RESPONSE


PORE PRESSURE RESPONSE

PARAMETER A-BAR RESPONSE
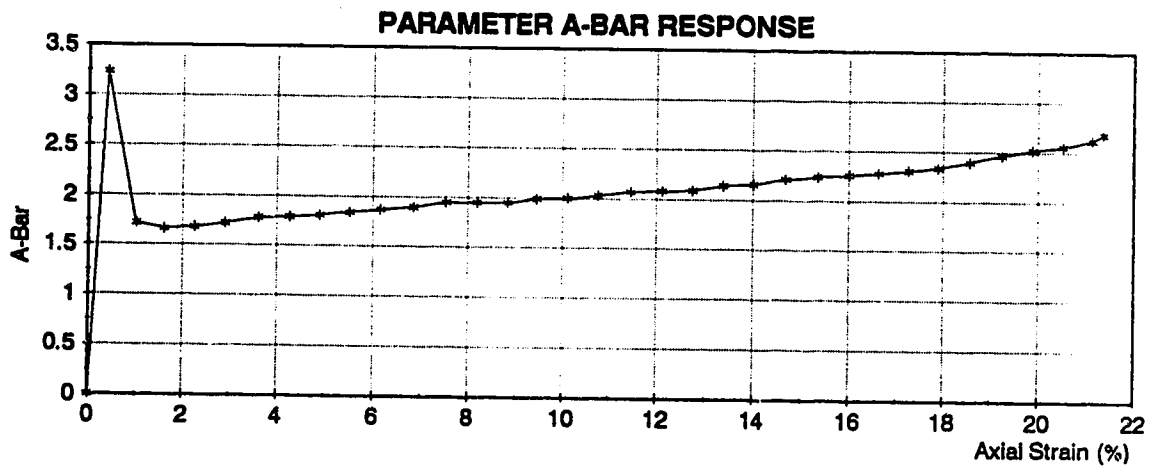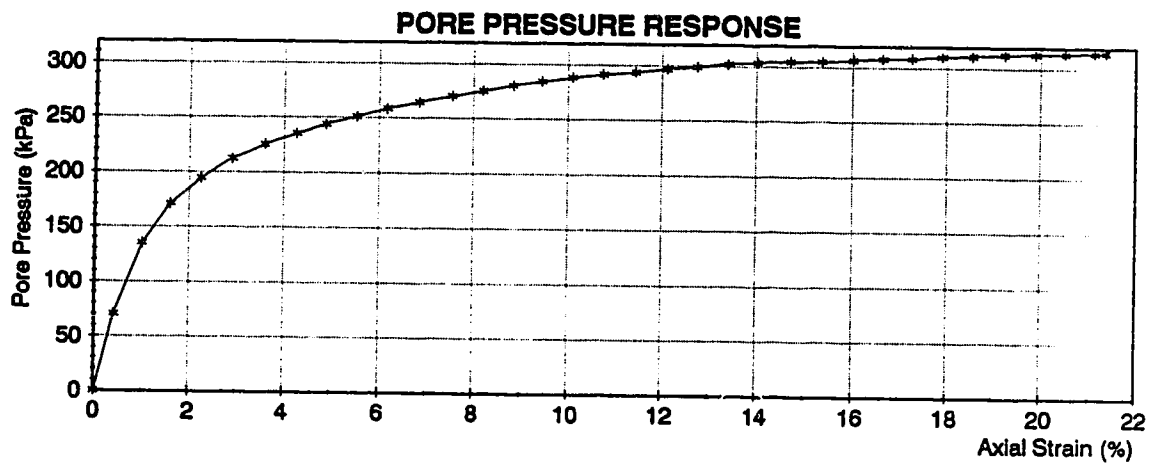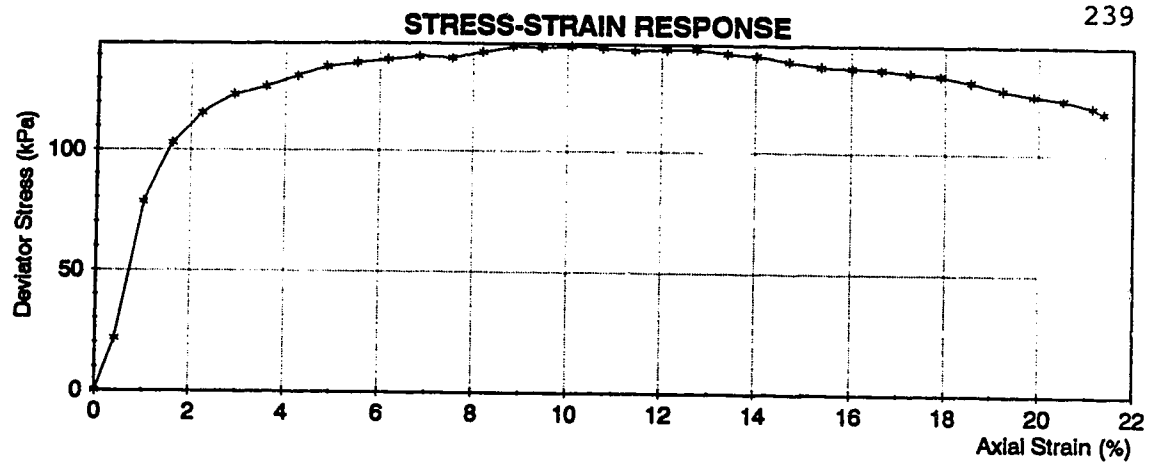
Figure B66   Triaxial Test PWA9A Series 4

STRESS-STRAIN RESPONSE

PORE PRESSURE RESPONSE

PARAMETER A-BAR RESPONSE
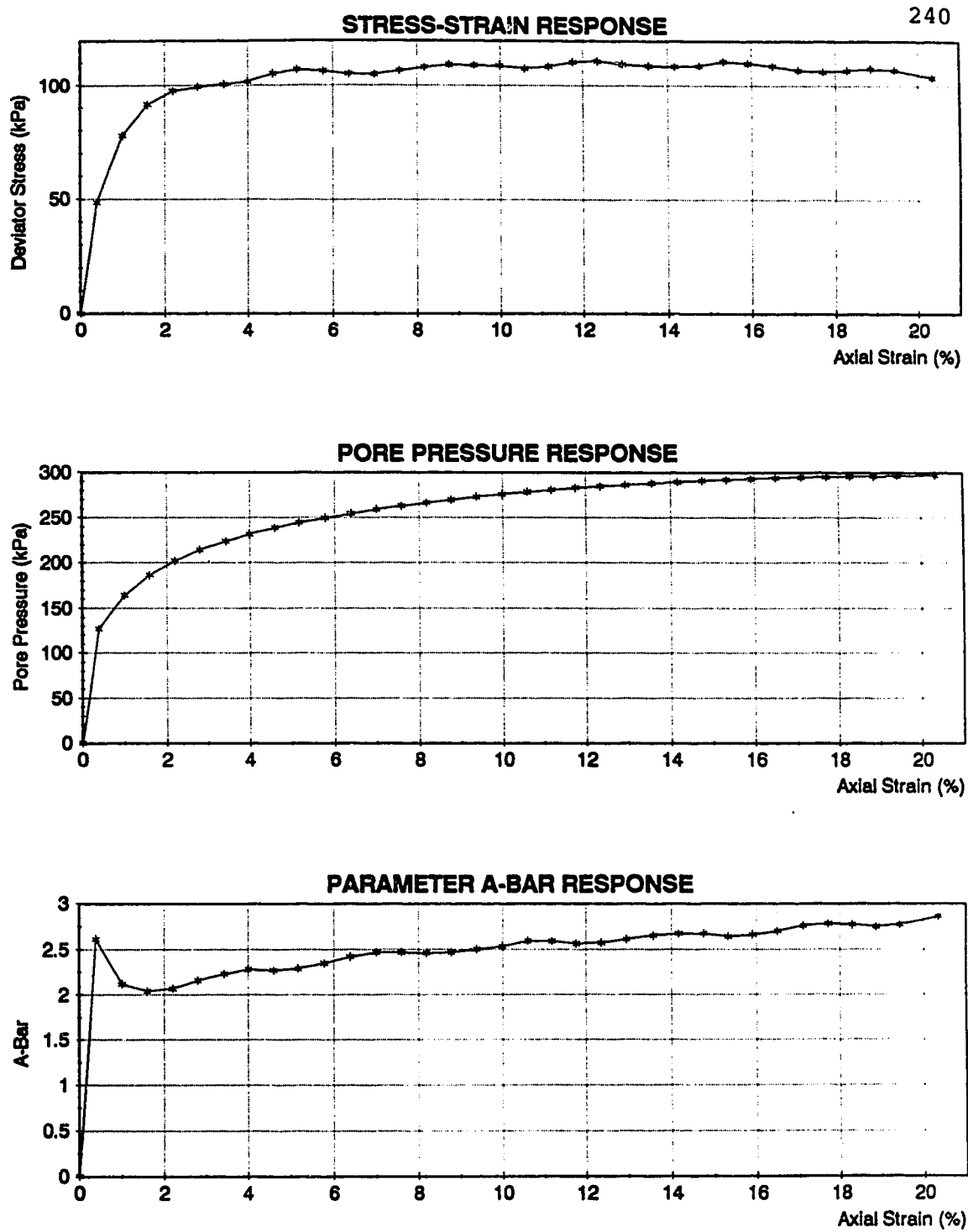
Figure B67   Triaxial Test PSA1 Series 5

241

STRESS-STRAIN RESPONSE
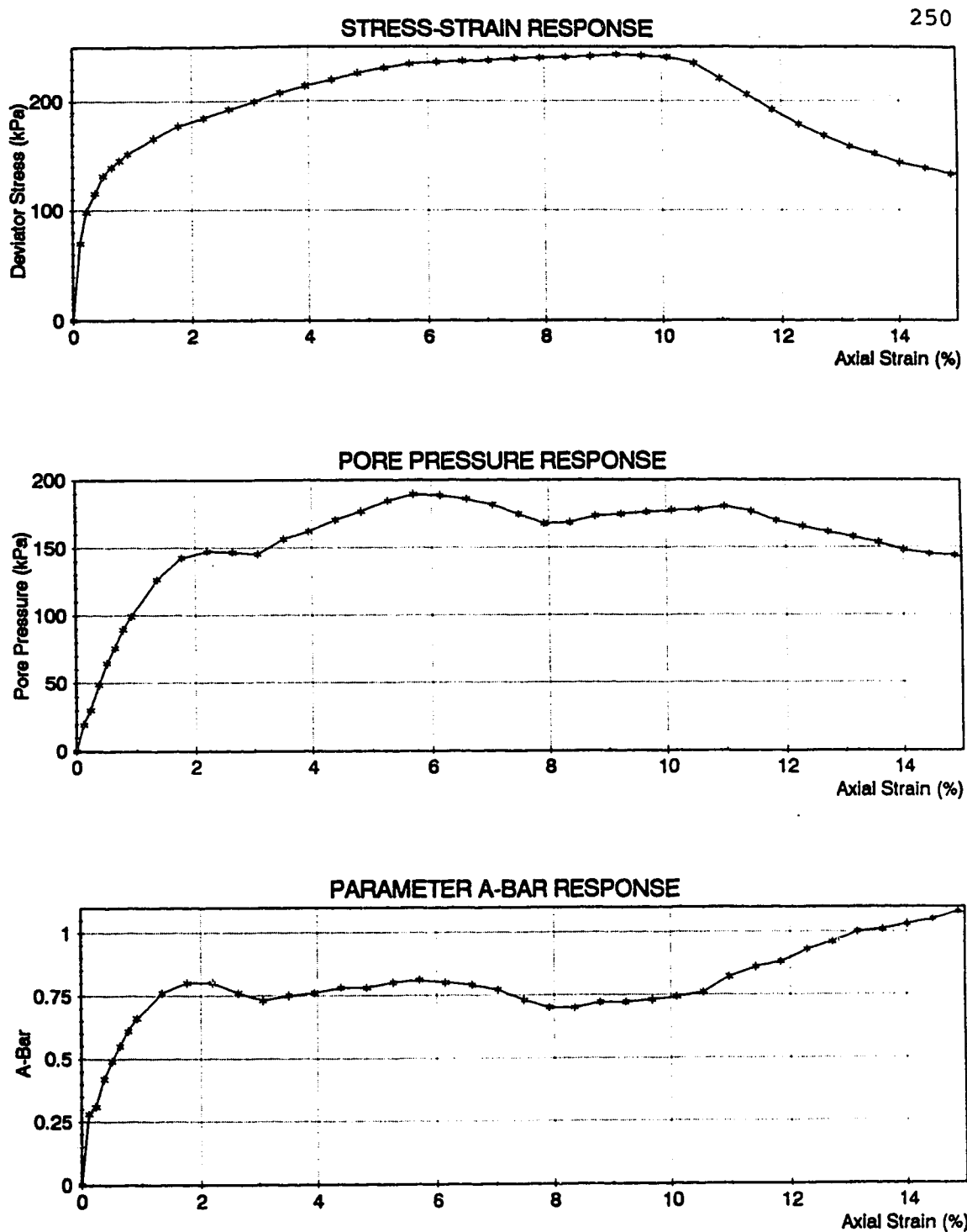

PORE PRESSURE RESPONSE

PARAMETER A-BAR RESPONSE
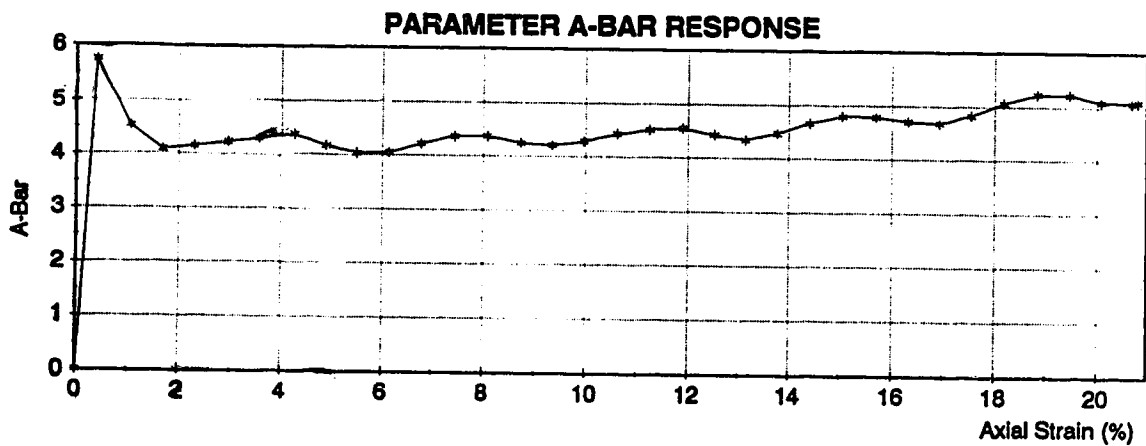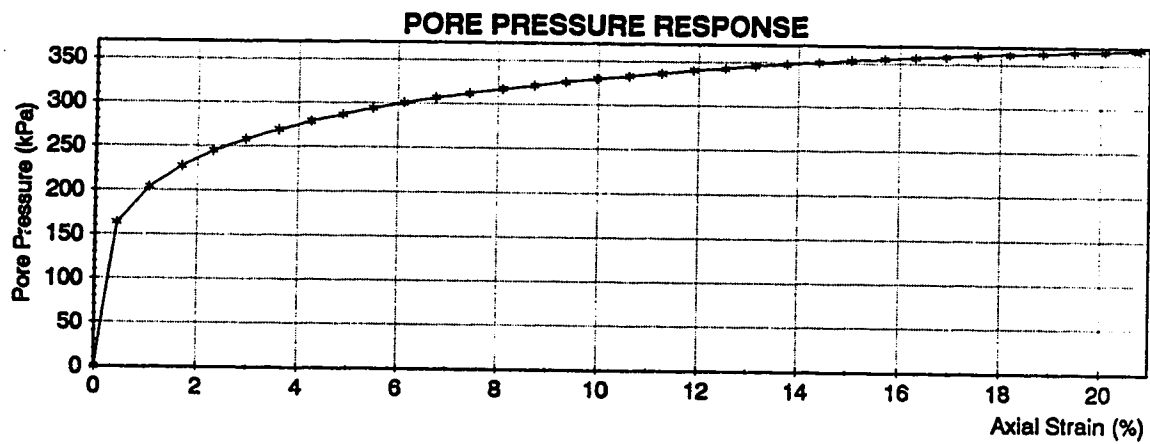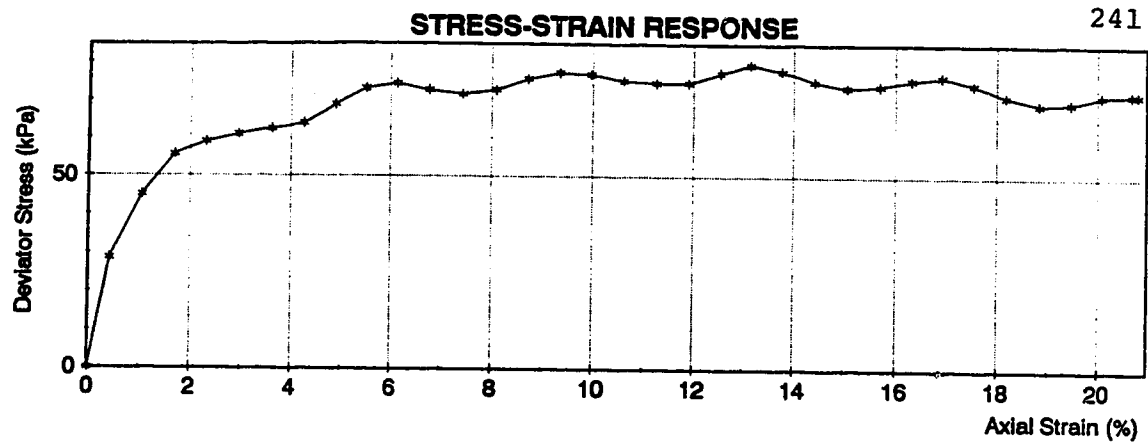
Figure B68 **Triaxial Test PSA2 Series 5**

STRESS-STRAIN RESPONSE

PORE PRESSURE RESPONSE

PARAMETER A-BAR RESPONSE
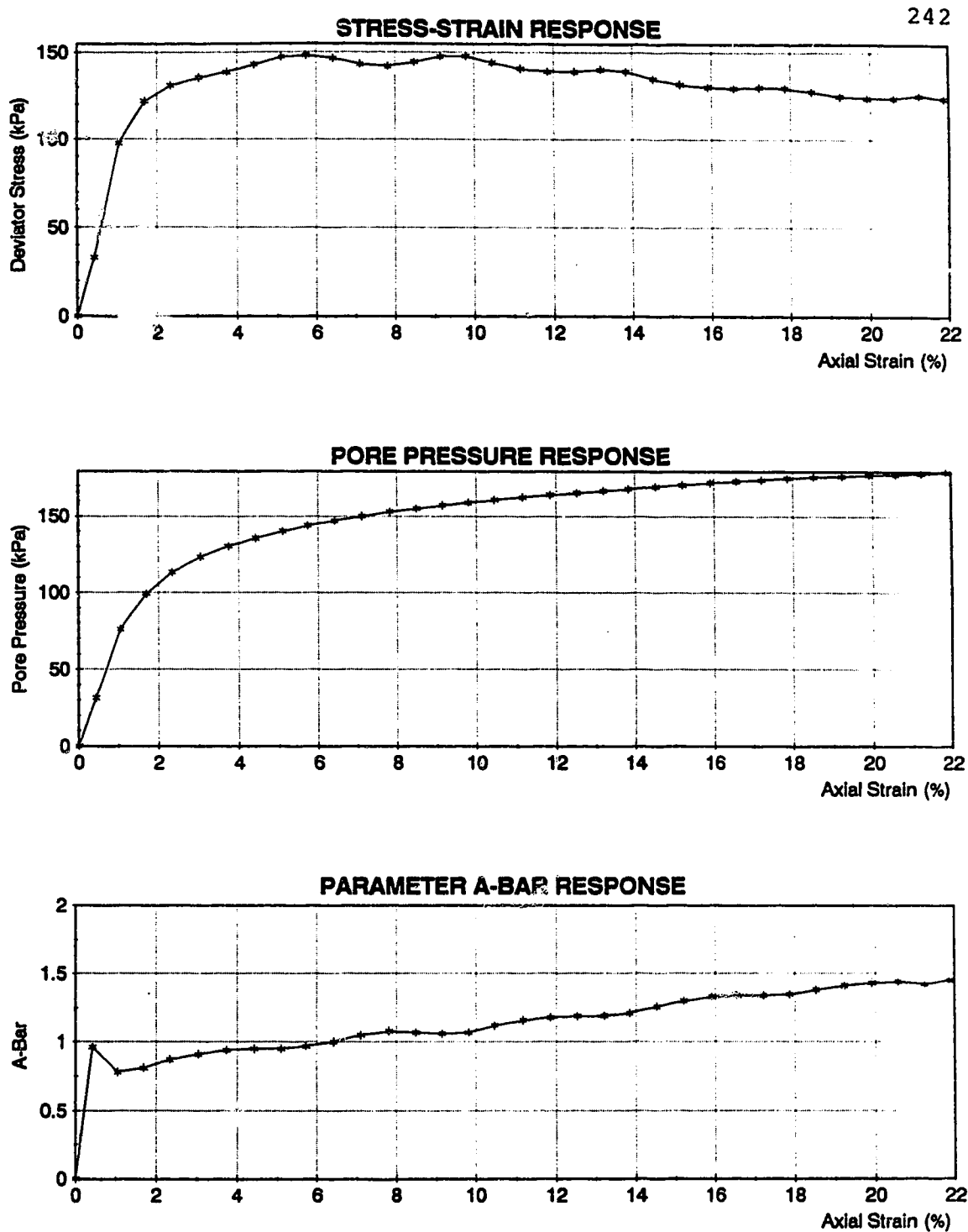
Figure B69   Triaxial Test PSA3 Series 5

STRESS-STRAIN RESPONSE

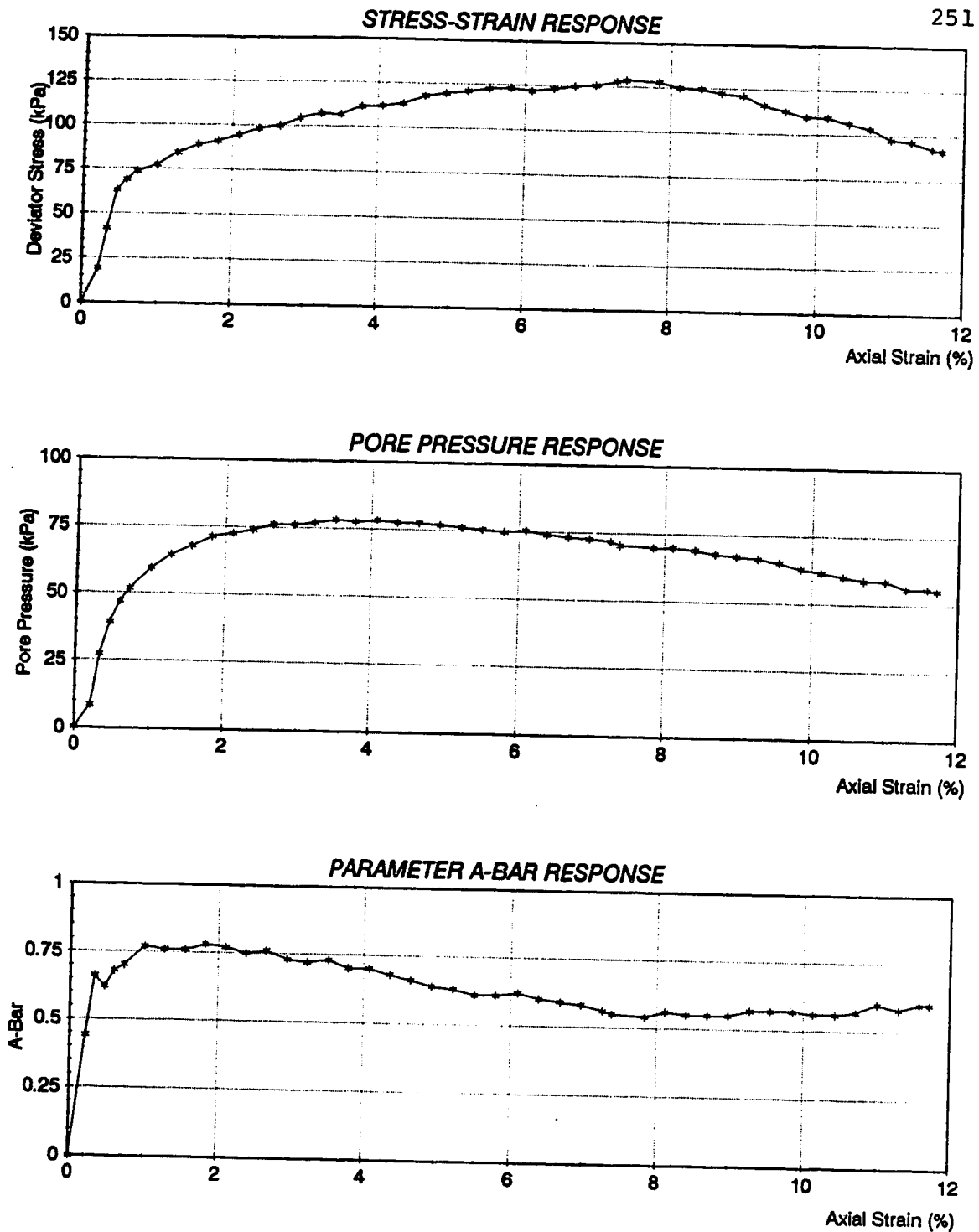## PORE PRESSURE RESPONSE

PARAMETER A-BAR RESPONSE
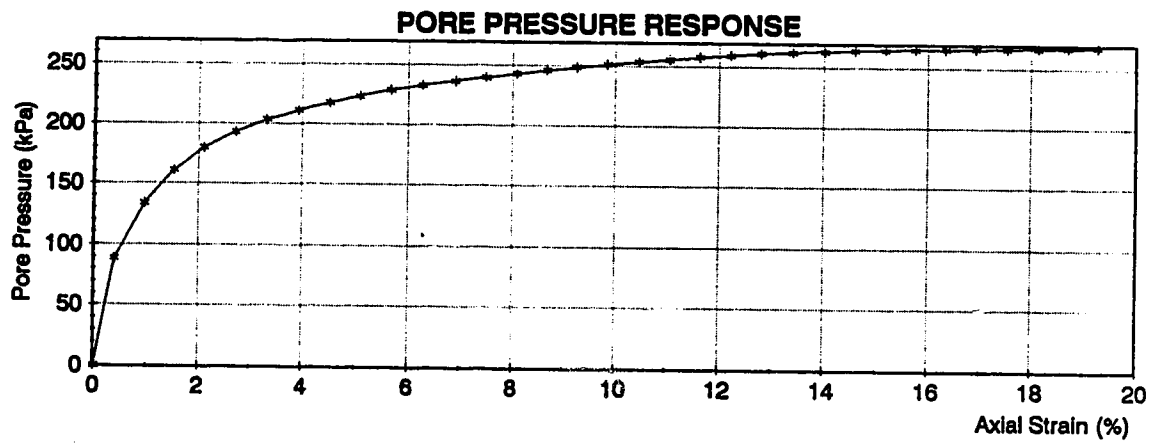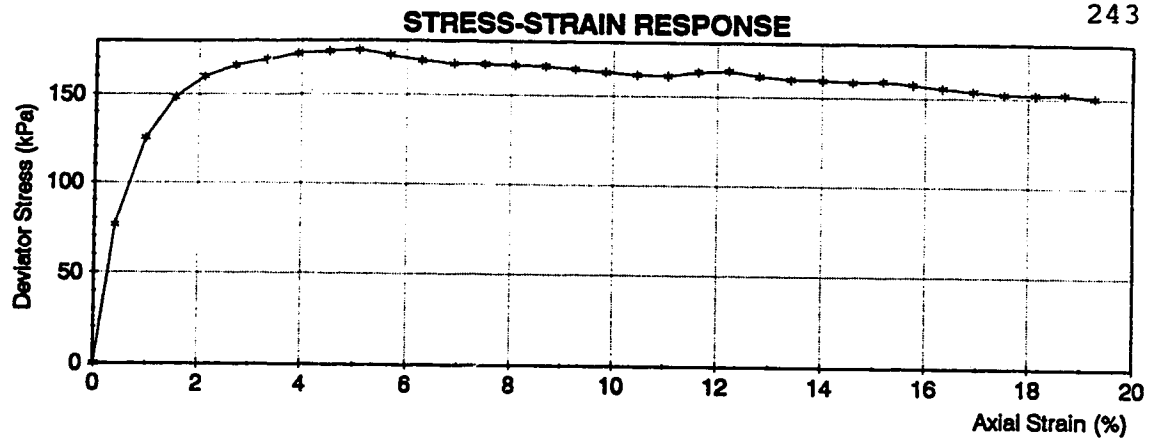
Figure B70   Triaxial Test PSA4 Series 5
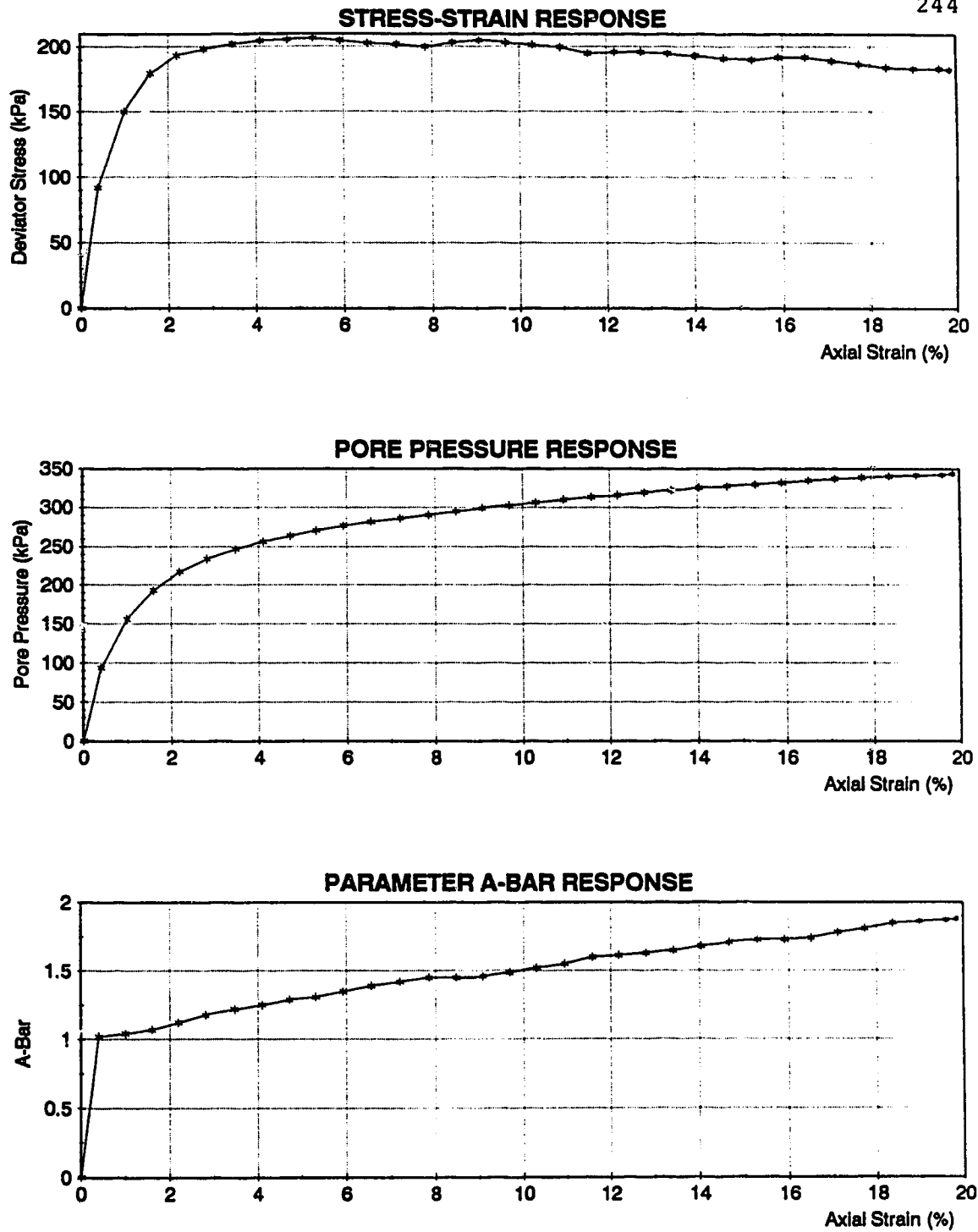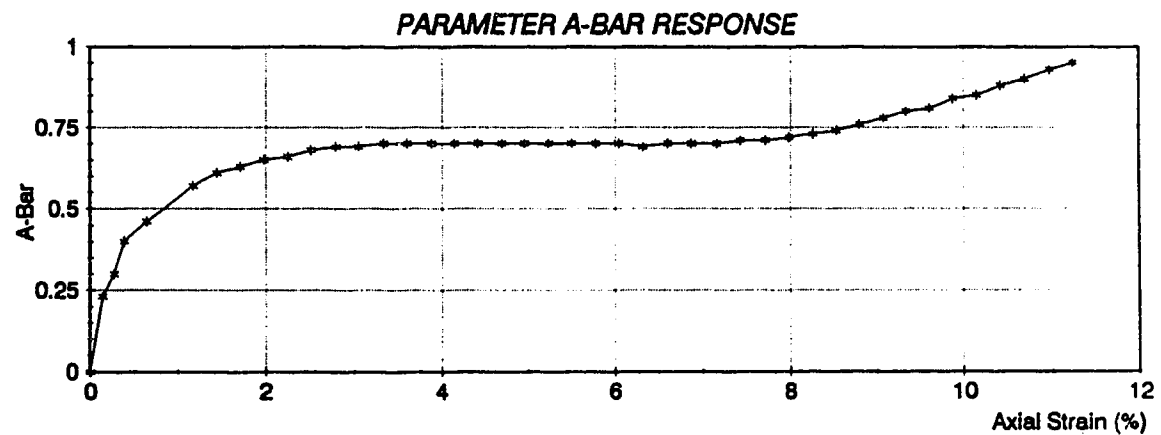
Figure B71   Triaxial Test PSA5 Series 5

STRESS-STRAIN RESPONSE

PORE PRESSURE RESPONSE

PARAMETER A-BAR RESPONSE
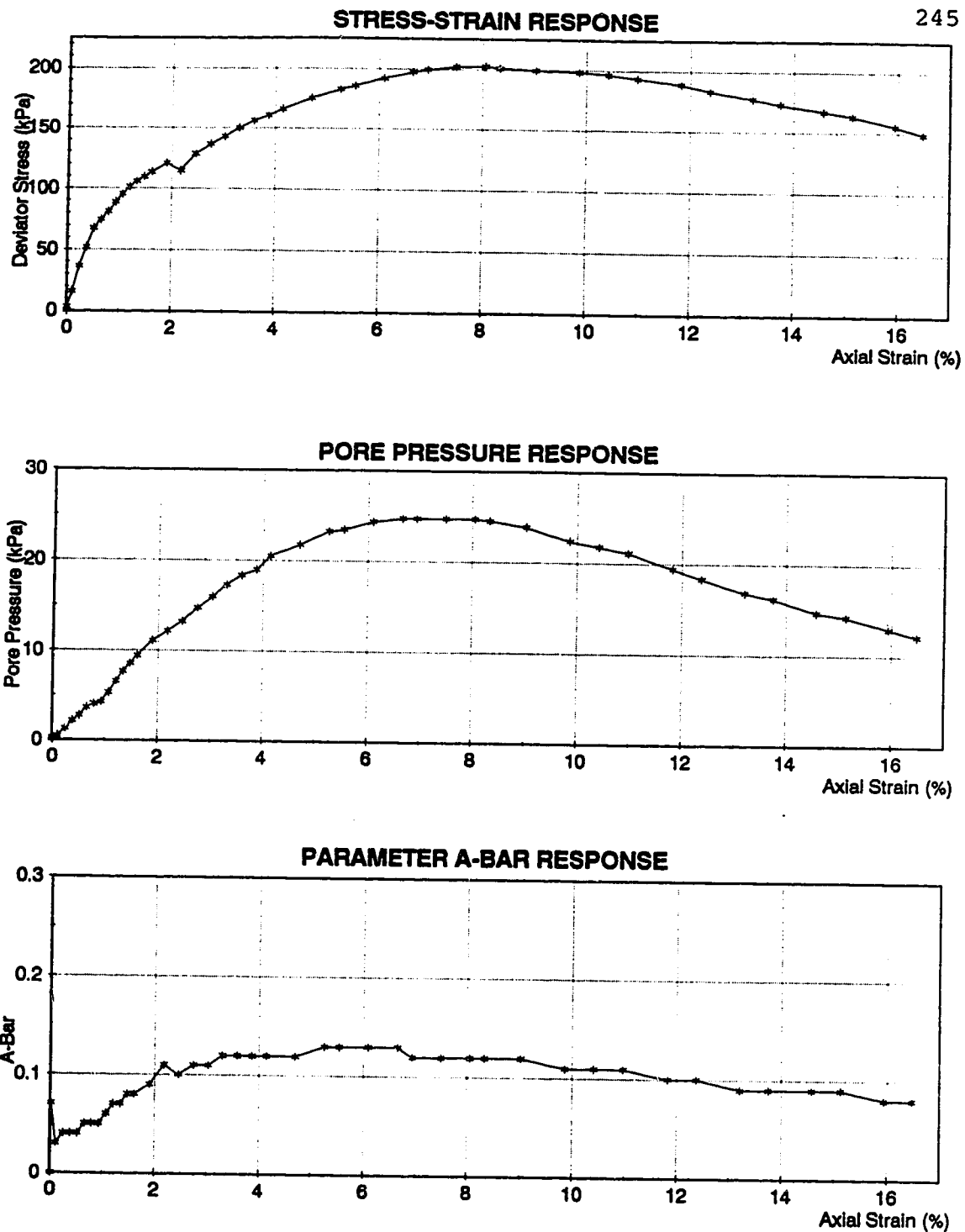
Figure B72   Triaxial Test PWMS1   Series 6
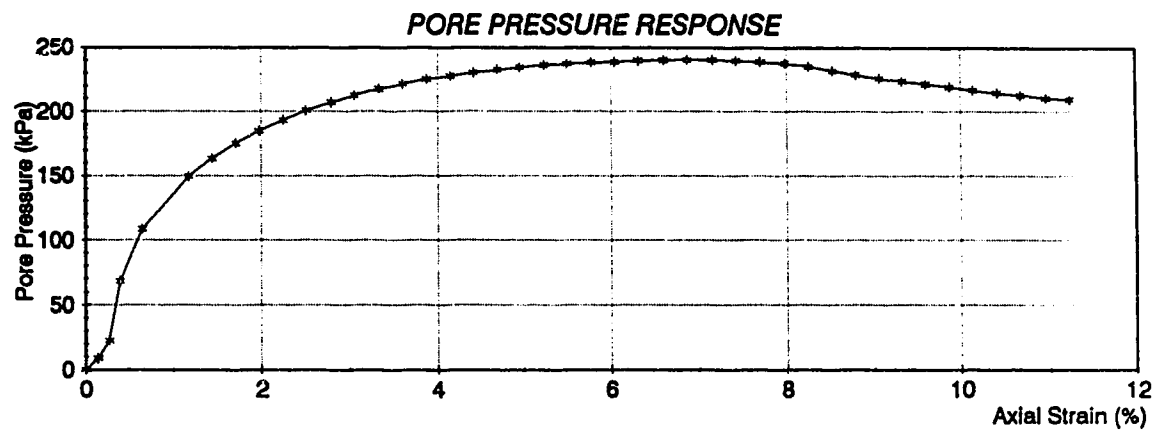
STRESS-STRAIN RESPONSE

PORE PRESSURE RESPONSE

PARAMETER A-BAR RESPONSE
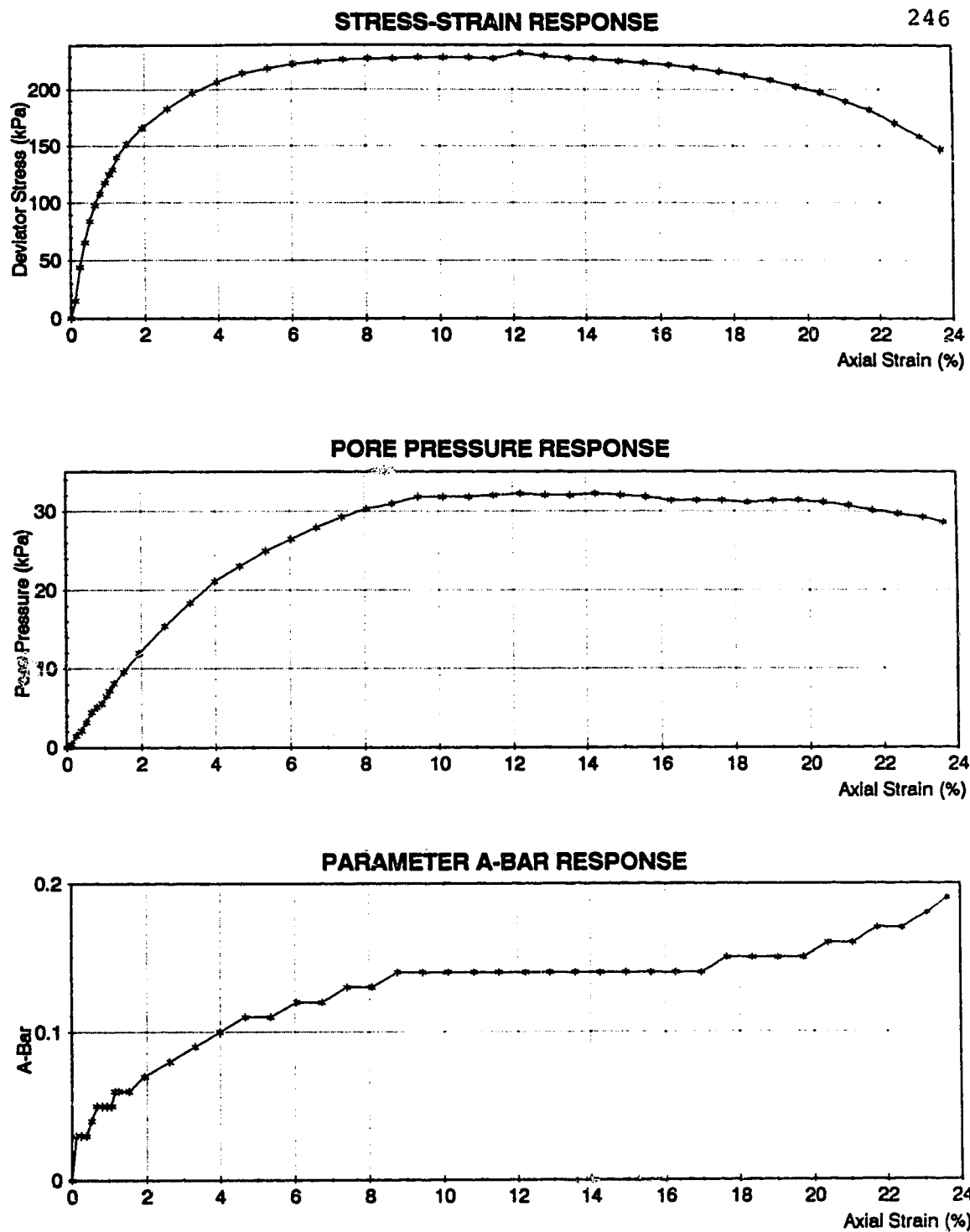
Figure B73   Triaxial Test PWMS2 Series 6

STRESS-STRAIN RESPONSE

PORE PRESSURE RESPONSE

PARAMETER A-BAR RESPONSE
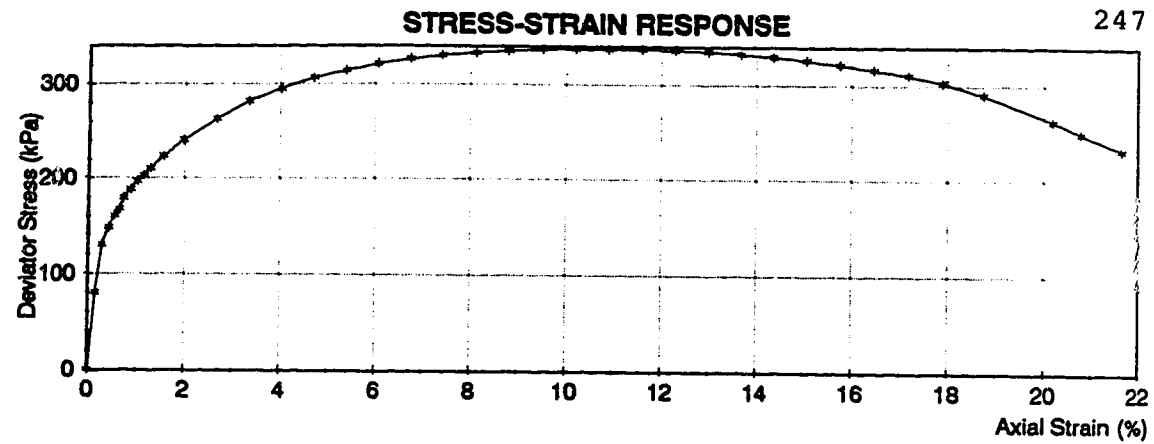
Figure B74   Triaxial Test PWMS3   Series 6

STRESS-STRAIN RESPONSE

PORE PRESSURE RESPONSE

PARAMETER A-BAR RESPONSE
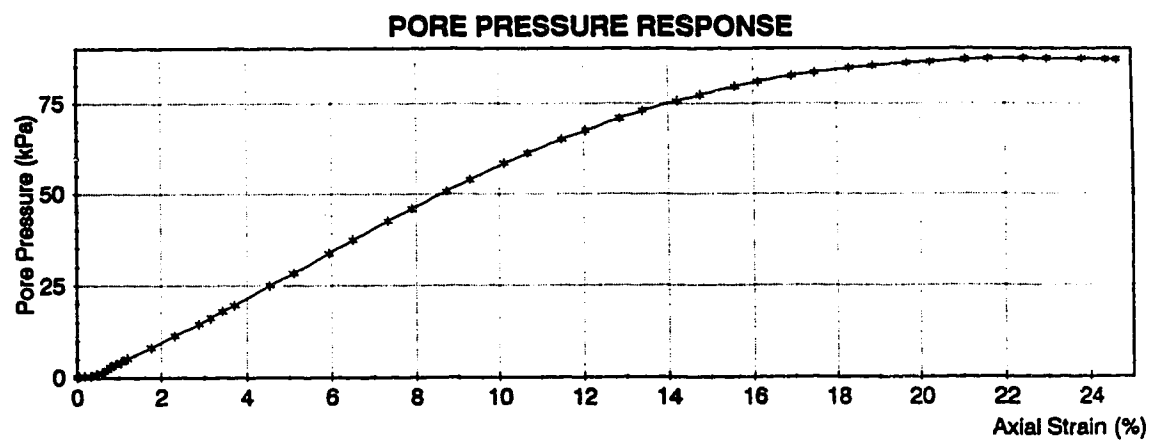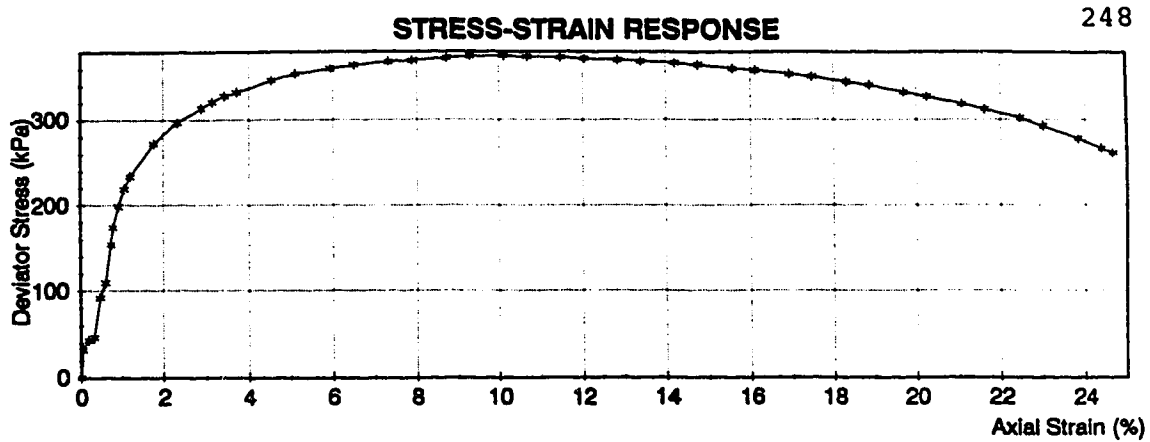
Figure B75   Triaxial Test PWMS4   Series 6

STRESS-STRAIN RESPONSE

PORE PRESSURE RESPONSE
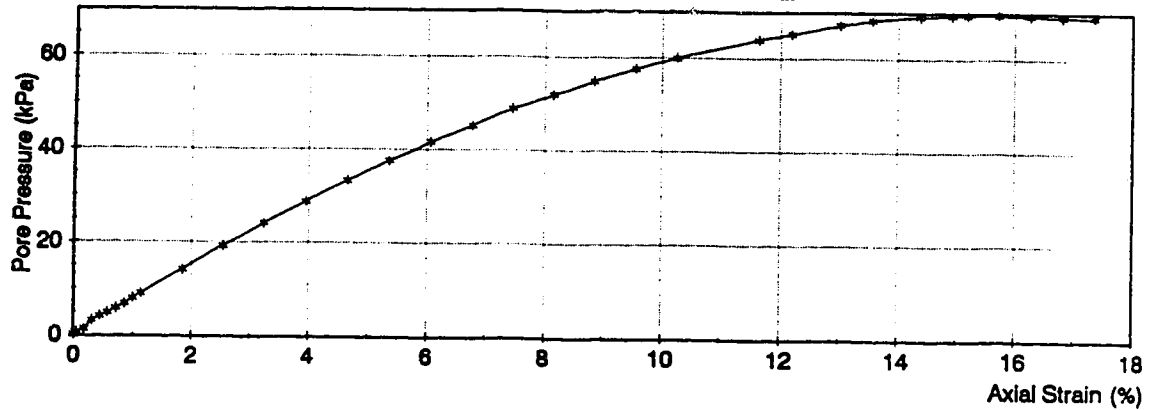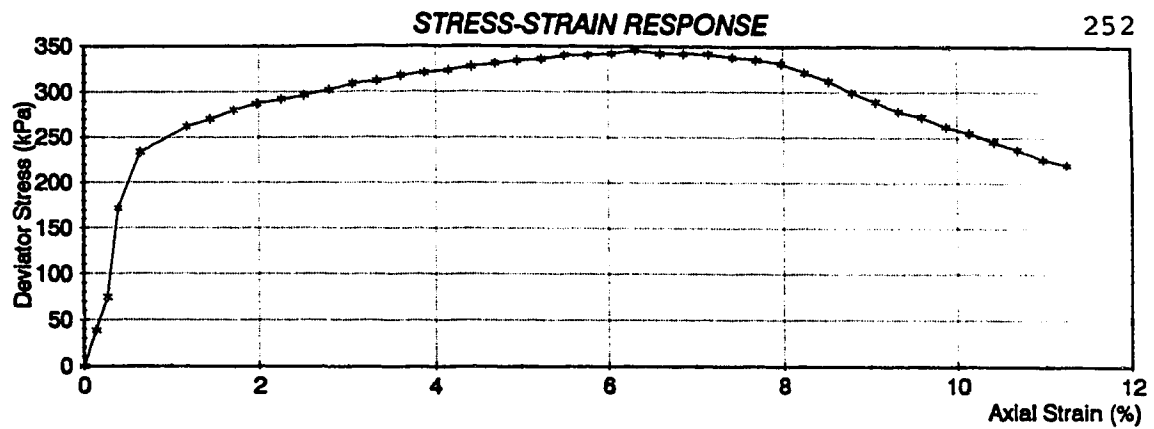

PARAMETER A-BAR RESPONSE
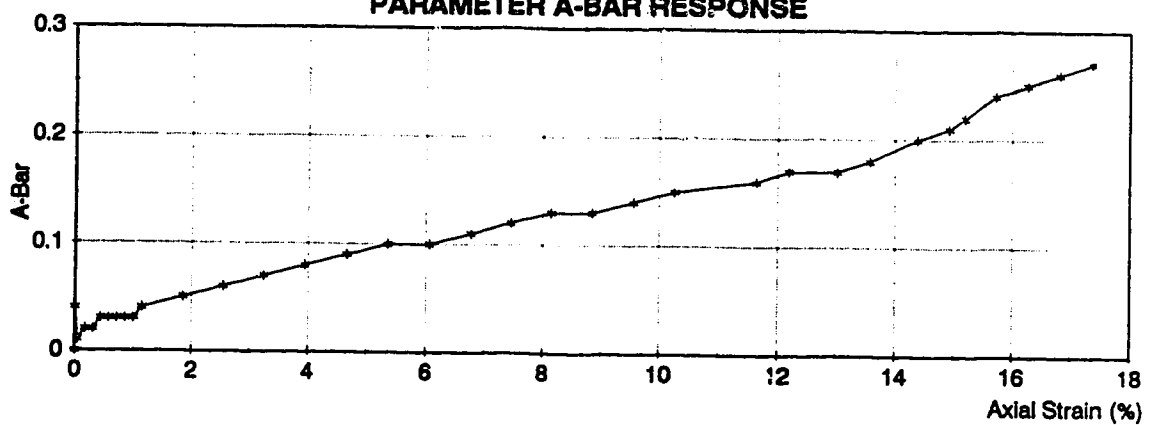
Figure B76   Triaxial Test PWMS5 Series 6

Figure B77 Triaxial Test PWMS6 Series 6A

STRESS-STRAIN RESPONSE

PORE PRESSURE RESPONSE

PARAMETER A-BAR RESPONSE

Figure B78 Triaxial Test PWMS7 Series 6A

STRESS-STRAIN RESPONSE

PORE PRESSURE RESPONSE

PARAMETER A-BAR RESPONSE

Figure B79 Triaxial Test PWMS8 Series 6A

STRESS-STRAIN RESPONSE

PORE PRESSURE RESPONSE

PARAMETER A-BAR RESPONSE
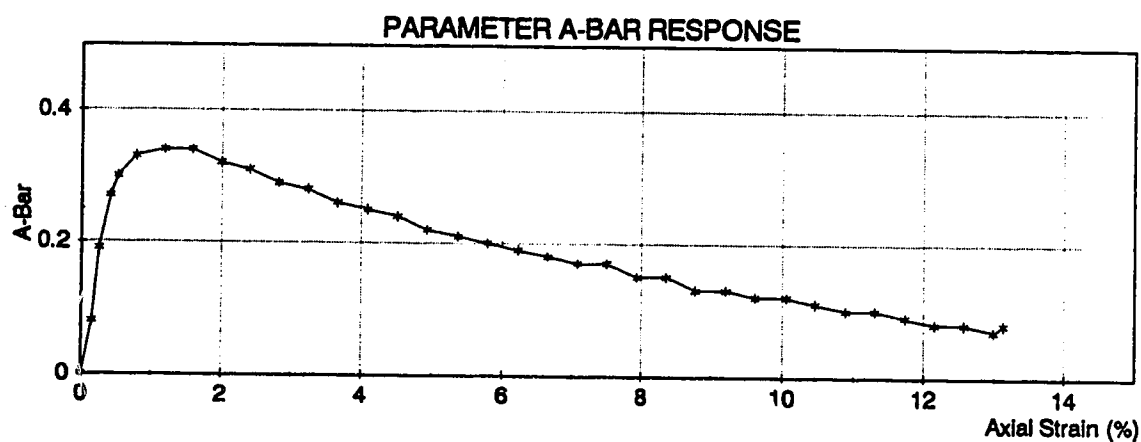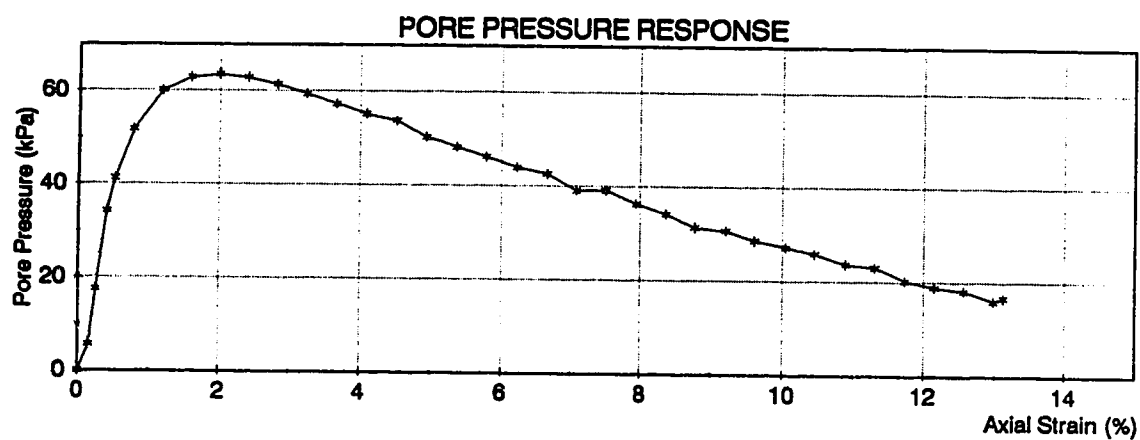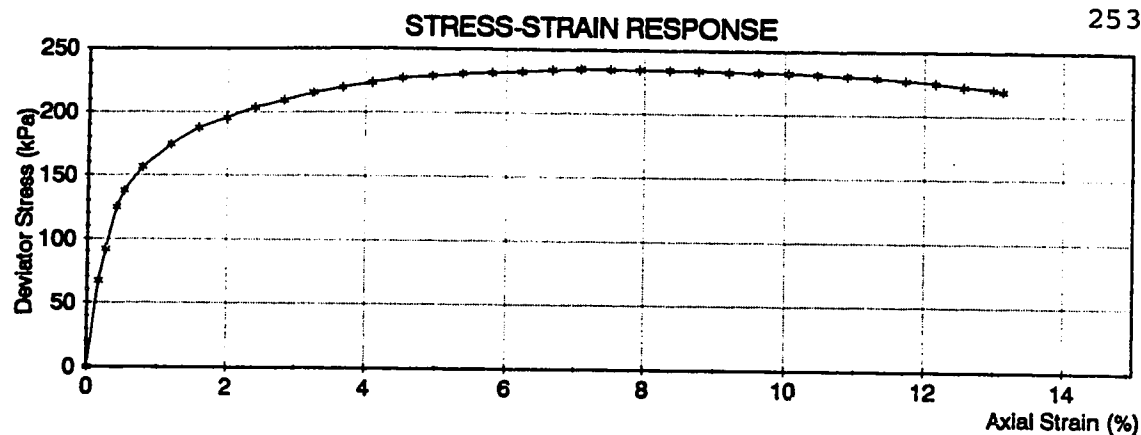
Figure B80   Triaxial Test PSMS1   Series 7

STRESS-STRAIN RESPONSE

PORE PRESSURE RESPONSE

PARAMETER A-BAR RESPONSE
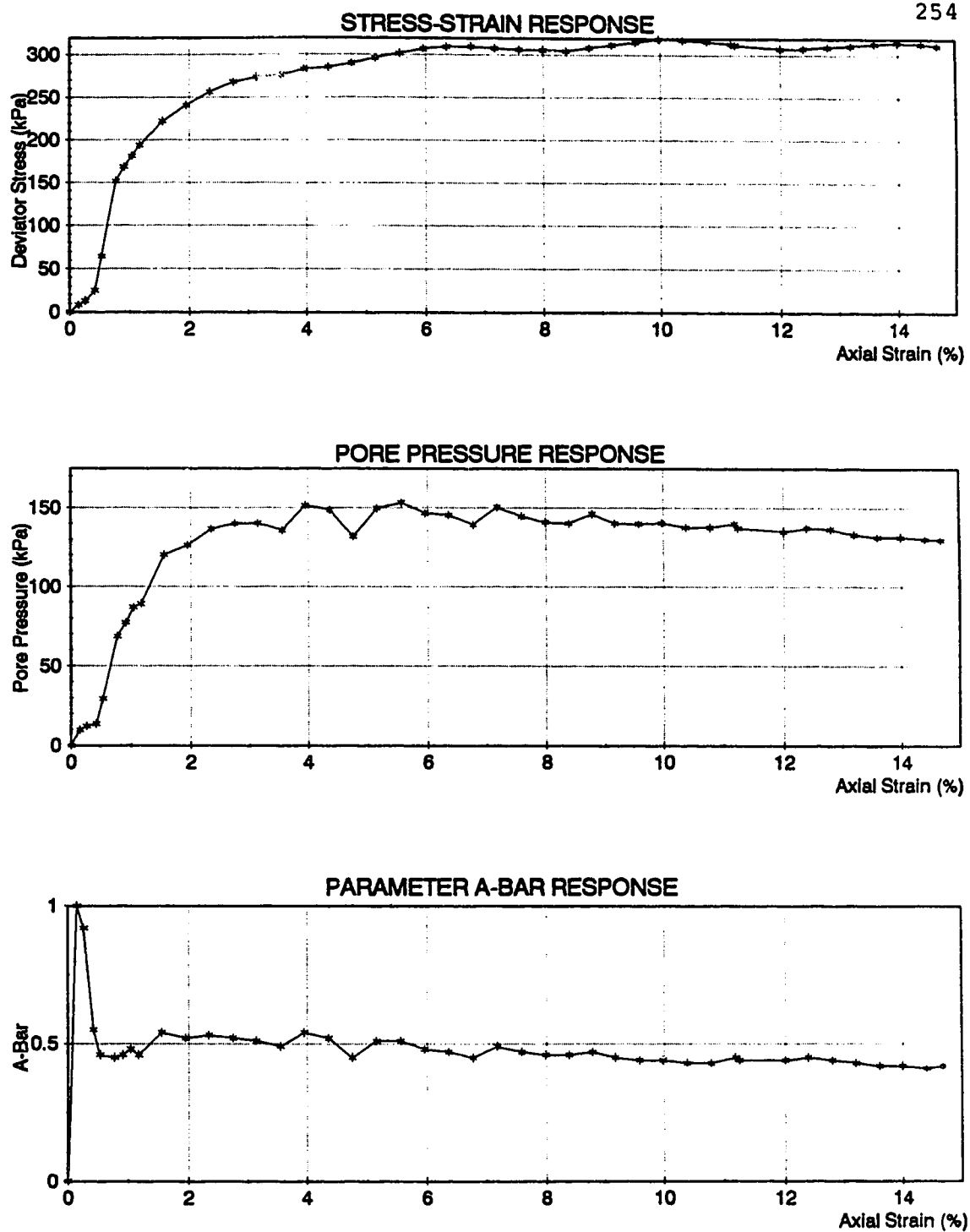
Figure B81   Triaxial Test PSMS2 Series 7
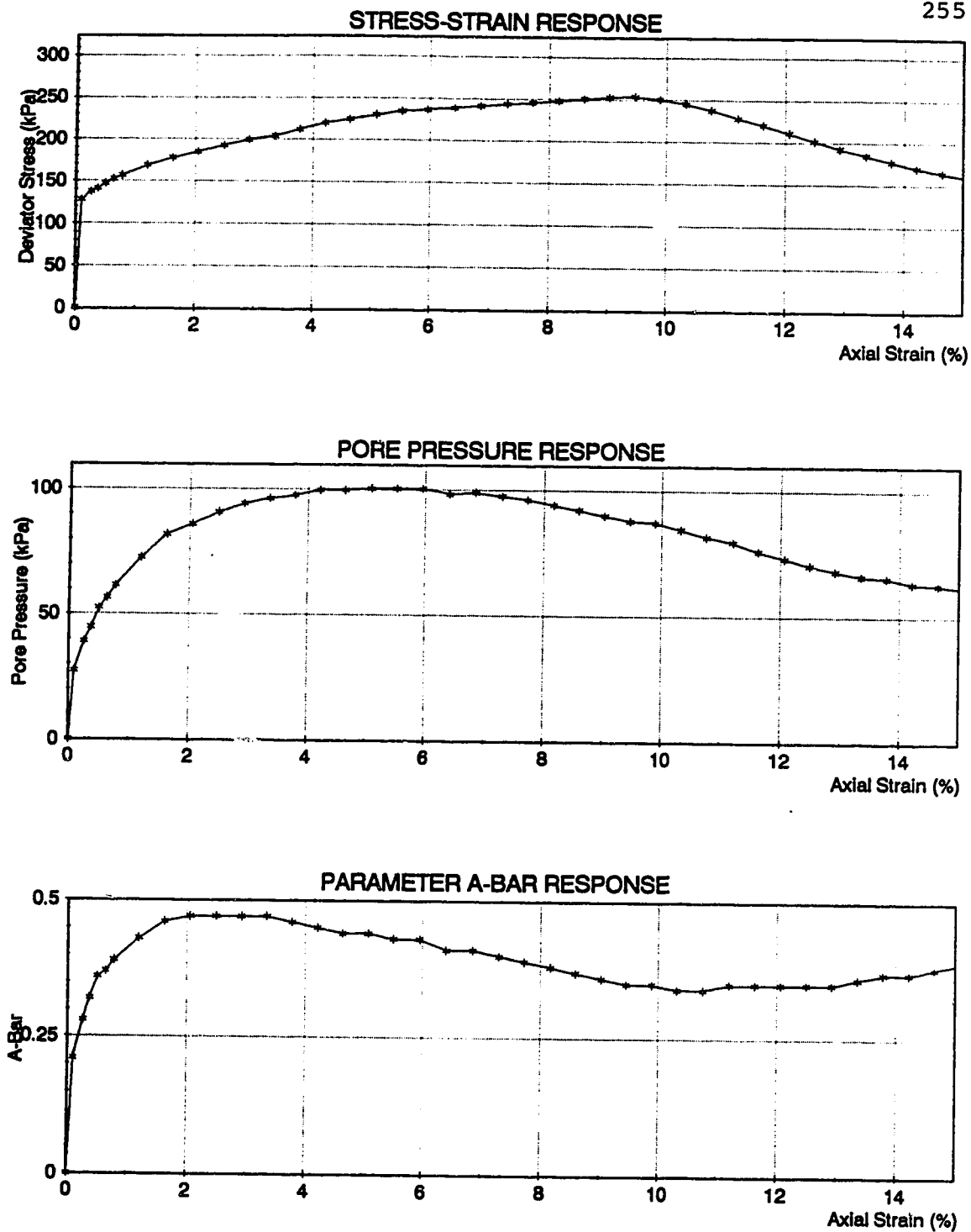
Figure B82   Triaxial Test PSMS3   Series 7

STRESS-STRAIN RESPONSE

PORE PRESSURE RESPONSE

PARAMETER A-BAR RESPONSE
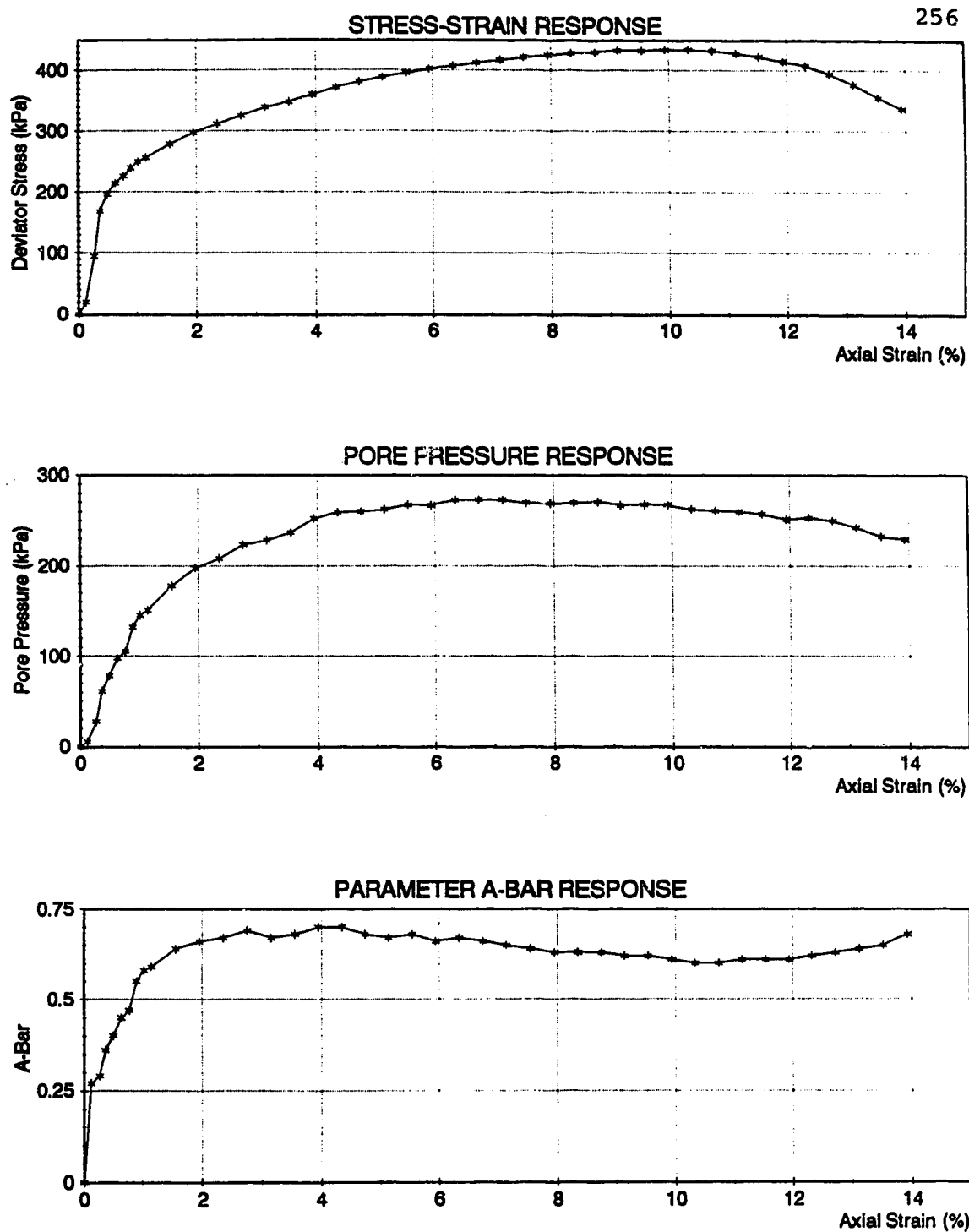
Figure B83   Triaxial Test PSMS4   Series 7

STRESS-STRAIN RESPONSE

PORE PRESSURE RESPONSE

PARAMETER A-BAR RESPONSE
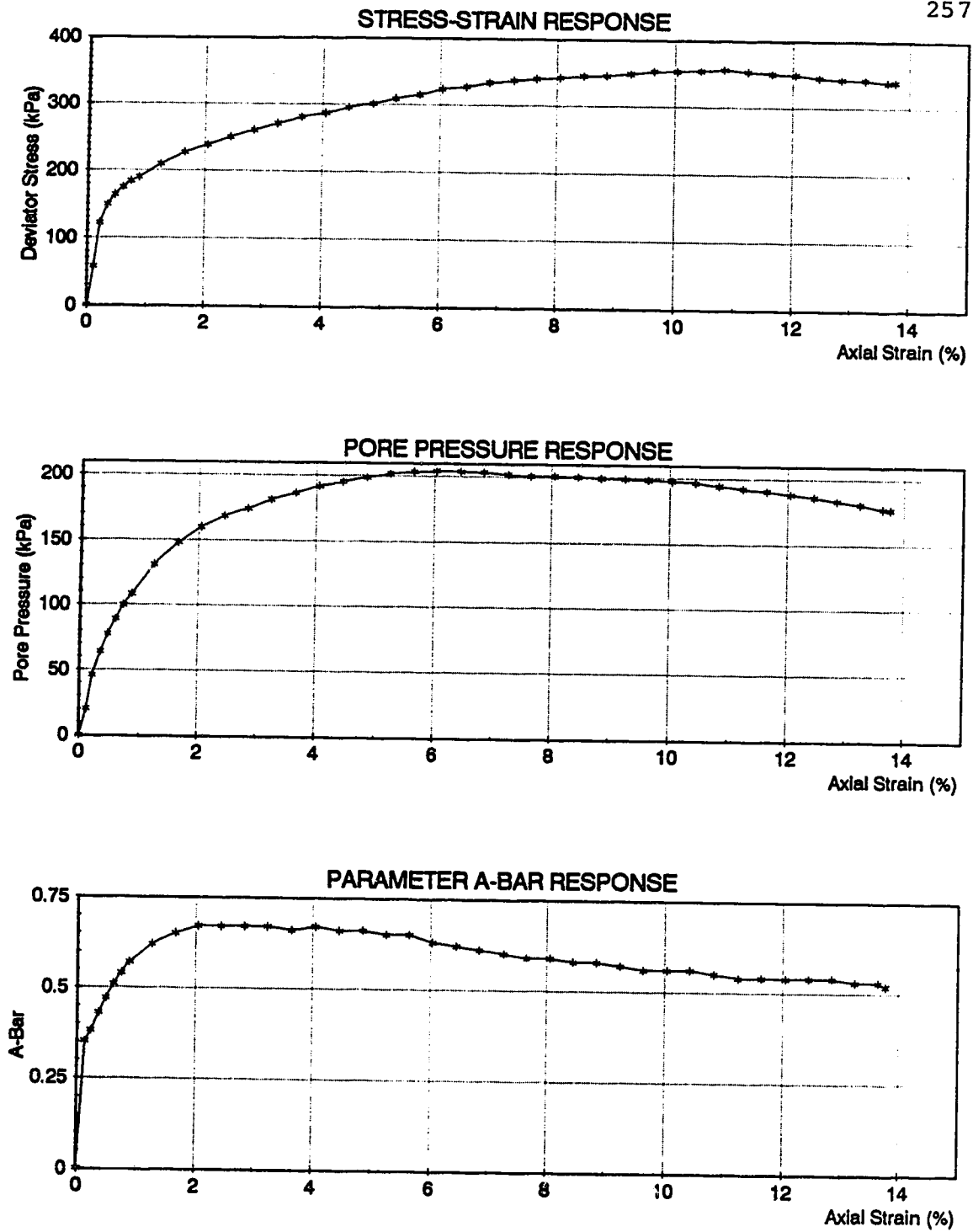
Figure B84   Triaxial Test PSMS5 Series 7